Improving host resistance to Fusarium head blight in wheat (*Triticum aestivum* L.) and Gibberella ear rot in maize (*Zea mays* L.)

Dissertation to obtain the doctoral degree of Agricultural Sciences
(Dr. sc. agr.)

Faculty of Agricultural Sciences

University of Hohenheim

State Plant Breeding Institute

Submitted by

Félicien Akohoue

from Kemondji, Benin

2023

This thesis was accepted as a doctoral dissertation in fulfilment of the regulations for the doctoral degree “Doktor der Agrarwissenschaften” (Dr. sc. agr. / PhD. in Agricultural Sciences) by the Faculty of Agricultural Sciences at the University of Hohenheim on 12th July, 2023.

Date of the oral examination: 27.10.2023

Examination Committee:

Chairperson of the oral examination:	Prof. Dr. Uwe Ludewig
Supervisor and Reviewer:	apl. Prof. Dr. Thomas Miedaner
Co-Reviewer:	Prof. Dr. Hermann Bürstmayr
Additional examiner:	Prof. Dr. Hans-Peter Piepho

Table of Contents

[1]Akohoue, F., Koch, S., Plieske, J., and Miedaner, T. (2022). Separation of the effects of two reduced height (*Rht*) genes and genomic background to select for less Fusarium head blight of short-strawed winter wheat (*Triticum aestivum* L.) varieties. *Theor Appl Genet*. doi: 10.1007/s00122-022-04219-4.

[2]Akohoue, F., and Miedaner, T. (2022). Meta-analysis and co-expression analysis revealed stable QTL and candidate genes conferring resistances to Fusarium and Gibberella ear rots while reducing mycotoxin contamination in maize. *Front Plant Sci* 13**,** 1050891. doi: 10.3389/fpls.2022.1050891.

[3]Akohoue F., Koch S., Lieberherr B., Kessel B., Presterl T., Miedaner T. (2023). Effectiveness of introgression of resistance loci for Gibberella ear rot from two European flint landraces into adapted elite maize (*Zea mays* L.). *PLoS ONE* 18(9): e0292095. https://doi.org/10.1371/journal.pone.0292095.

[4]Akohoue, F., Gaikpa, D.S., Kessel, B., Presterl, T., and Miedaner, T. (2021). Variance components and correlations between doubled haploid lines from two European flint landraces and their corresponding testcrosses for Gibberella ear rot resistance, silking time, and plant height in maize. *Agronomy* 11(6). doi: 10.3390/agronomy11061039.

Abbreviations

AR	Anther retention
BLUEs	Best Linear Unbiased Estimations
CRISPR	Clustered regularly interspaced short palindromic repeats
DNA	Deoxyribonucleic acid
DH	Doubled haploid technology
DON	Deoxynivalenol
EL	Ear length
FER	Fusarium ear rot
FGSC	*Fusarium graminearum* species complex
FHB	Fusarium head blight
GB	Genomic background
GEBV	Genomic estimated breeding values
GER	Gibberella ear rot
GG	Genotypic group
GWAS	Genome-wide association study
KE	Kemater Landmais Gelb
KR	Kernel resistance
LP	Landrace-derived population
MAS	Marker-assisted selection
Mbp	Mega base pairs
MQTL	Meta-quantitative trait loci
MT-GWAS	Multi-trait genome-wide association study

NIV	Nivalenol
NS	Number of spikelets per ear
PE	Petkuser Ferdinand Rot
PH	Plant height
PVE	Phenotypic variance explained
QTL	Quantitative trait loci
RAPD	Random amplified polymorphic DNA
RFLP	Restriction fragment length polymorphisms
Rht	Reduced height gene
RIL	Recombinant inbred line
RNA-seq	Ribonucleic acid sequencing
SNP	Single nucleotide polymorphisms
SR	Silk (channel) resistance
SSR	Single sequence repeats
ST-GWAS	Single-trait genome-wide association study
USA	United states of America
ZON	Zearalenone

List of Tables

List of Figures

Chapter 1: General introduction

Impact of Fusarium diseases on wheat and maize production

The global agricultural productivity is negatively affected by increasing temperature averages, uncertainty in rainfall patterns, frequent drought events and higher pressure of abiotic and biotic stressors (Raza and Bebber, 2022). Comprehensive research and development efforts are required to produce enough quality food and feed for guaranteed food and nutritional security to the growing populations. Wheat (*Triticum aestivum* L.) and maize (*Zea mays* L.) are two major cereal crops cultivated worldwide based on production areas and grain production as well as their utilizations globally. In developed countries, wheat is cultivated for consumption and feeding, whereas maize is cultivated for feeding and ethanol production. Both crops are largely cultivated for human consumption across developing countries, including sub-Saharan African countries (Grote et al., 2021).

Despite their importance as staple food crops, wheat and maize production is hindered by several factors, of which the most important is pest and diseases pressure, which is expected to worsen with the changing climate (Miedaner and Juroszek, 2021a; Miedaner and Juroszek, 2021b). This increased plant disease pressure can counteract efforts to increase grain yield (Raza and Bebber, 2022), resulting in high yield gaps across regions. In Northwestern (NW) Europe, for example, considerable yield gaps have been reported for wheat and maize across countries (Figure 1) (Schils et al., 2018).

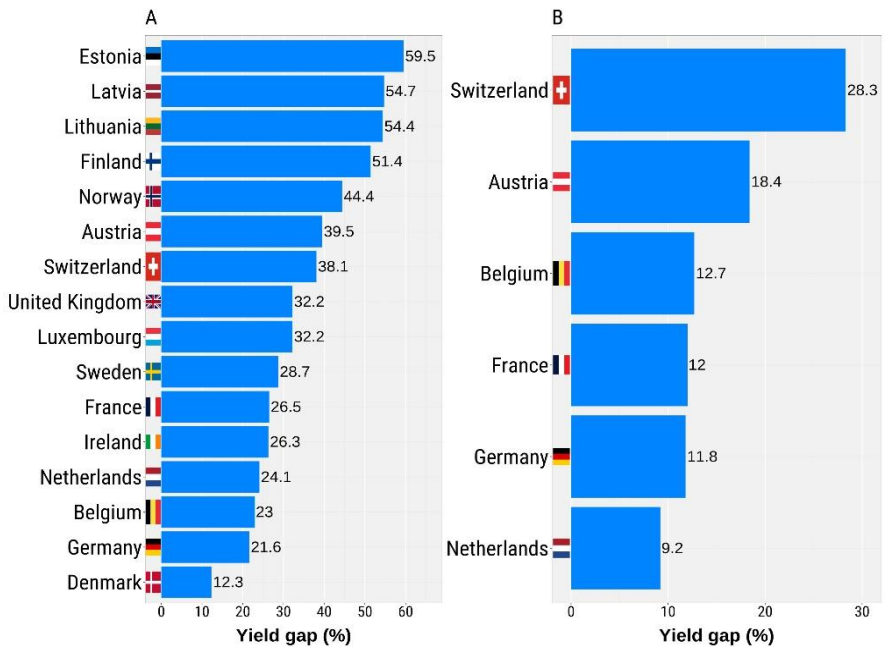

Figure 1: Importance of yield gaps for wheat (A) and maize (B) across Northwestern European countries reported by Global Yield Gap Atlas (Schils et al., 2018)

Among yield- and quality-impacting diseases, Fusarium head blight (FHB) and ear rots are the most important diseases in wheat and maize, respectively. Fusarium head blight, also refered to as "scab", is caused by several toxigenic Fusarium species, of which *Fusarium graminearum* (Schwein.) Petch. is the most important, but several others, *like F. culmorum* (Wm.G.Sm.) Sacc. are often co-occuring across European countries (Bai and Shaner, 2004). The disease severely affects wheat production by contaminating the kernels with mycotoxins and reducing the yield (Figure 2).

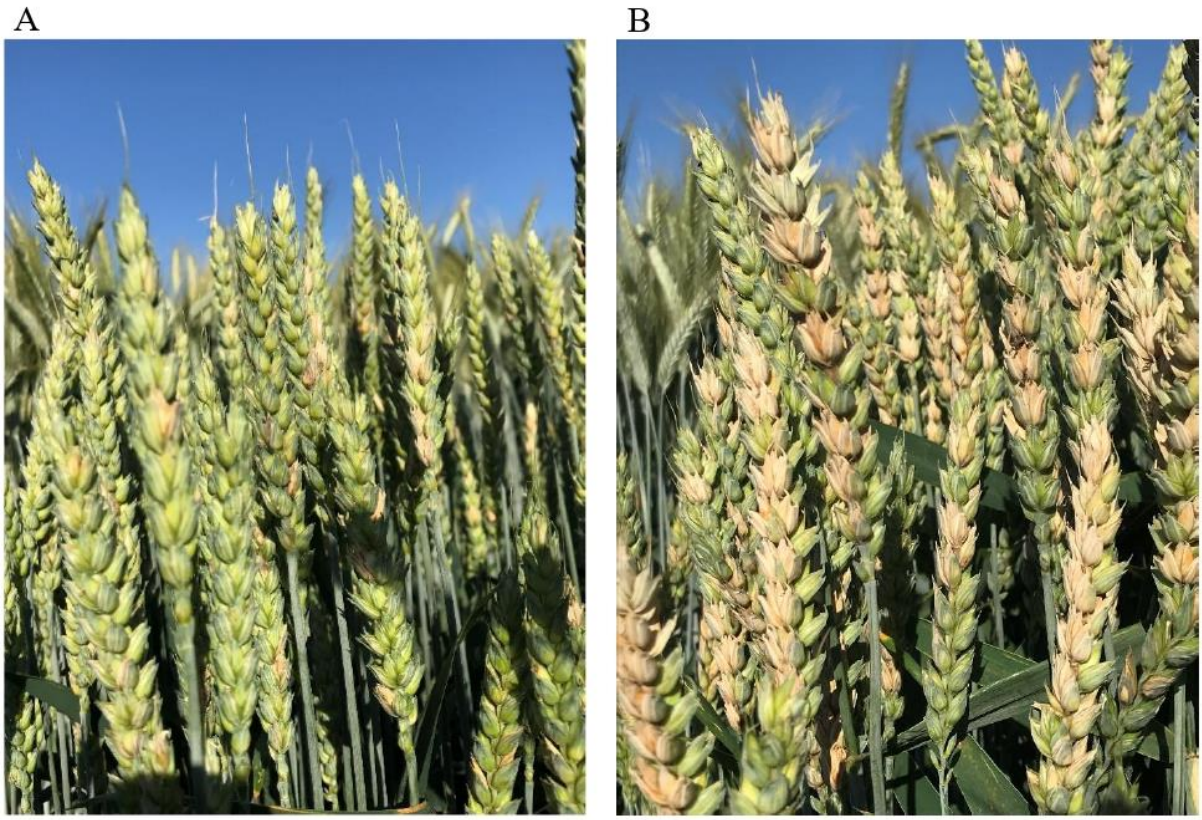

Figure 2: Fusarium head blight (FHB) on resistant (A) vs. susceptible (B) cultivars in Germany. Pictures by Miedaner T.

Gibberella ear rot (GER) or "red ear rot" and Fusarium ear rot (FER), also known as "pink ear rot", are the two most important maize ear rot diseases worldwide. Similar to FHB disease, maize ear rots cause important yield loss, particularly with contamination of kernels with mycotoxins (Figure 3). Recently, Dalla Lana et al. (2022) demonstrated that a GER severity of about 62% in susceptible cultivars leads to more than 50% reduction in grain weight. Moreover, high positive correlations were found between FER and GER diseases, indicating that resistance to FER also implies resistance to GER, and vice-versa (Löffler et al., 2010a; Butrón et al., 2015).

Figure 3: Gibberella ear rot symptoms on a maize line under artificial inoculation in Germany

Fusarium ear rot is mainly caused by *Fusarium verticillioides* (Sacc.) Nirenberg which is more aggressive under warmer climatic conditions. Gibberella ear rot on the other hand is caused by *F. graminearum* species complex (FGSC), with *F. graminearum sensu strictu* Schwabe (teleomorph *Gibberella zeae*) representing the most predominant (Figure 4) (Del Ponte et al., 2021). Despite its presence across all continents (Figure 4), *F. graminearum* infection is considerably higher in cooler geographic regions, like Europe and Canada. Other FGSC pathogens include *F. meriodionale, F. cortaderiae* , *F. bothii, F. asiaticum* and *F. acaciae-mearnsii* which cause GER disease across South America, Africa and Asia (Figure 4) (Beukes et al., 2018; Castañares et al., 2019; Del Ponte et al., 2021; Machado et al., 2022).

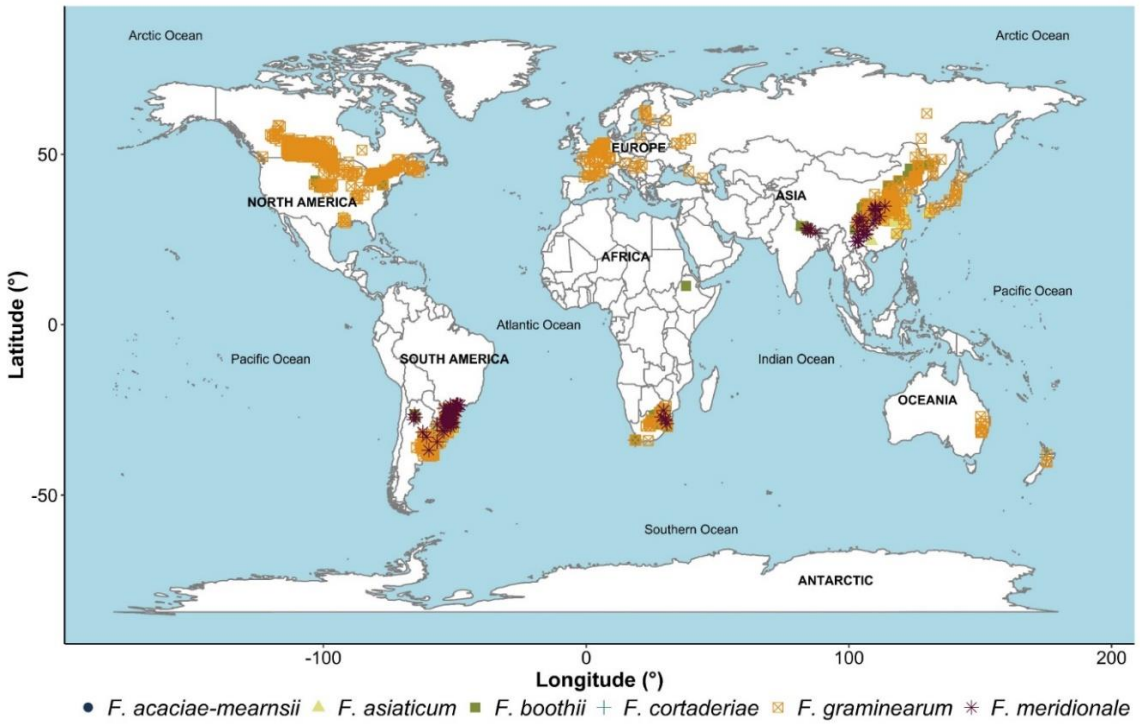

Figure 4: Worldwide distribution of *Fusarium graminearum* species complex (FGSC) isolates on cereal crops. Georeferenced data of the isolates were extracted from FGSC database (Del Ponte et al., 2021)

Fusarium species belong to the *Ascomycota* Phylum, *Sordariomycetes* Class and *Nectriaceae* Family (Leslie and Summerell, 2008). *Fusarium* spp. are ubiquitous in the environment with several plant-pathogenic strains (Arie, 2019). Generally, FHB and GER pathogens have a hemibiotrophic lifestyle with a short biotrophic phase and a ramifying necrotrophic phase. The latter, which is the most important phase, allows the fungi to inhabit crop residues (e.g. corn stalks, wheat straw, and other host plants) which remain in or on the surface of the soil even after harvest (Figure 5). The residues in or on the soil represent the primary inoculum for the next cropping season. On the infected residues, when the conditions become favorable, the fungi produce sexual spores which are dispersed to enable the species survival. Afterwards, asexual spores are produced and spread to other plants through rain-splash and wind to facilitate the infection. The sexual spores are called ascospores, while the asexual spores are called macroconidia whose development is triggered by warm, humid, and wet conditions (Figure 5) (Khan et al., 2020).

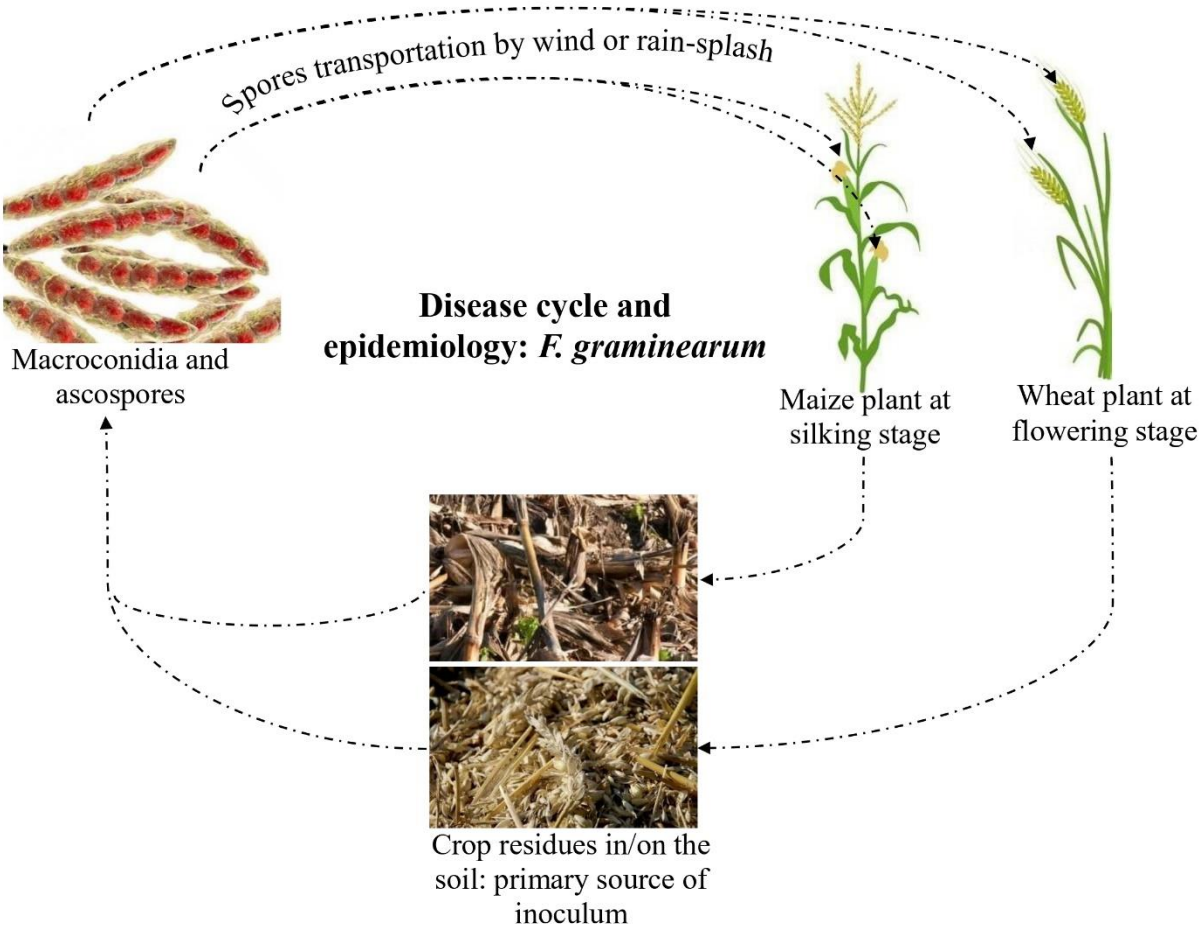

Figure 5: Fusarium diseases cycle and epidemiology. Example of *F. graminearum* on maize and wheat

In wheat, FHB infection occurs when the asexual and/or sexual spores land on extruded wheat anthers during flowering time (Figure 5). Likewise, in maize, GER infection happens when the spores penetrate the cob via silk channel or via wounds created by pests, agricultural tools or machines and hails (Figure 5). FHB and GER infections generally exacerbate when the environment is unfavorable (e.g. drought-prone environments) to the plant growth, making these fungi opportunistic pathogens. The severity of FHB and GER diseases strongly depends on the genetic resistance of the host plant and environmental factors such as precipitation, humidity, temperature as well as their interactions which affects several Fusarium species (Munkvold, 2003; Pfordt et al., 2020).

In both wheat and maize, FHB- and GER-causing pathogens produce various mycotoxins including deoxynivalenol (DON), nivalenol (NIV) and zearalenone (ZON) which are predominantly detected in the kernels (Logrieco et al., 2002; Schaafsma et al., 2008; Dalla Lana et al., 2021; Righetti et al., 2021). These mycotoxins represent a major thread to public health, considering their ability to render kernels toxic for human consumption and animal feeding (Johns et al., 2022). To reduce health problems resulting from mycotoxins in food, the European Union has set maximum safety limits of 1250 µg/kg and 1750 µg/kg DON in wheat and maize, respectively, and 100 µg/kg and 350 µg/kg ZON in wheat and maize, respectively (European Commission, 2017; Johns et al., 2022).

Current FHB and GER disease management strategies include agronomic/cultural practices, biological control as well as chemical control using several fungicides (Wegulo et al., 2015). The use of different plant species as cover crops was also suggested as a strategy to reduce infections by Fusarium species such as *F. verticillioides* in maize (Ray et al., 2022). Agronomic management options include the tillage to bury crop residues after harvest of plant host, crop rotation incorporating non-host plants as well as water management through an appropriate irrigation system during the anthesis (Dill-Macky and Jones, 2000; Wegulo et al., 2015). The biological management strategy lies in the use of biocontrol agents which are bacterial and fungal species exerting an antagonistic activity against the pathogens. Most popular bacterial antagonists include *Bacillus spp.* (Zhao et al., 2014), *Pseudomonas spp.* (Schisler et al., 2006), *Lysobacter enzymogenes* (Jochum et al., 2006), *Streptomyces spp.* (Palazzini et al., 2007), while fungal antagonists are *Cryptococcus spp.*, *Trichoderma spp.* (Matarese et al., 2012), *Clonostachys rosea* (Xue et al., 2014) and *Aureobasidium pullulans* (Wachowska and Głowacka, 2014). However, these management strategies do not provide a full control of FHB and GER diseases. In addition, existing mycotoxins reducing technologies are considerably

expensive and might not have a durable effect on wheat and maize production (Logrieco et al., 2021). Therefore, the sustainable cereal production and reduction of mycotoxin contaminations in kernels require additional strategies focusing on intensive efforts to improve plant host resistance to FHB and ear rot diseases in wheat and maize, respectively.

Resistance to Fusarium head blight disease in wheat

Resistance to FHB disease in wheat was classified by Schroeder and Christensen (1963) into two types, namely: resistance to initial infection referred to as type I resistance, and resistance to spread of symptoms within the spike also referred to as type II resistance. Three other types were later reported including Type III (resistance to DON accumulation), Type IV (resistance to kernel damage) and Type V (tolerance) (Mesterházy et al., 1999). Despite tremendous breeding efforts that have been deployed over the last decades, no significant progress has been achieved in Europe. In Germany, based on 158 winter wheat varieties registered after year 2000, Miedaner et al. (2023) demonstrated an absence of breeding progress for FHB resistance for the last 20 years. Breeding for FHB resistance in wheat is mainly challenged by the complex nature of the trait which is quantitatively inherited, and its complex interactions with the environment and morphological traits, like plant height and anther retention. Extensive investigations have been conducted to demonstrate the existence of moderate to high negative correlations between FHB resistance and plant height (Buerstmayr and Buerstmayr, 2016; Buerstmayr et al., 2020; Ruan et al., 2020). As implication, semi-dwarf wheat genotypes generally exhibit higher FHB severity. This represents a challenge for FHB resistance breeding considering the high proportion of the semi-dwarfing allele *Rht-D1b* within high yielding varieties as reported in Germany and Austria (Miedaner et al., 2023).

Meanwhile, in commercial wheat production, semi-dwarf genotypes are mainly preferred to tall genotypes by farmers because of their lodging resistance, increased fertilizer use efficiency, higher grain yield and land-use efficiency (Loddo and Gooding, 2012; Wang et al., 2021; Zhao et al., 2022). This is mainly evidenced by a global increase in wheat yield after the introduction of reduced height (*Rht*) genes such as *Rht-B1* (formerly known as *Rht-1*) and *Rht-D1* (*Rht-2*) as drivers of the "Green Revolution" of 1960s and 1970s (Hedden, 2003). Considering this opposed interaction between the traits, appropriate breeding strategies are required to improve FHB resistance in commercial wheat cultivars with semi-dwarf alleles.

Resistance to Gibberella ear rot disease in maize

Depending on the infection mode, two types of resistance have been reported including silk or silk channel resistance (fungal spores enters the cob via the silk channel) and kernel resistance (fungal spores penetrates the kernel via wounds on the cob) (Mesterházy et al., 2012). The existence of phenotypic correlations between the two types of resistance was reported by Kebebe et al. (2015) and Chungu et al. (1996). European germplasm resources encompass large genetic variation for GER resistance as shown on Figure 6. As the backbone of resistance breeding, this high genetic variation represents an opportunity which indicates that there is room for improvement of GER resistance as demonstrated by Gaikpa et al. (2021).

Figure 6: Variation of Gibberella ear rot severity (0-100%) among highly resistant to highly susceptible maize lines in Germany

However, high yielding maize varieties with durable resistance to GER disease are not available to farmers to effectively tackle the disease. The European flint landraces have been identified as an important source of resistance genes to GER disease (Han et al., 2018; Gaikpa et al., 2021). Gaikpa et al. (2021) evaluated 500 doubled haploid (DH) lines from two flint landraces, namely “Kemater Landmais Gelb” (KE) and “Petkuser Ferdinand Rot” (PE) across four locations in Germany, and identified lines with moderate to strong resistance to GER disease. In NW Europe, the flint pool represents a major class of maize which is established in production systems across different countries. The transfert of GER resistance genes from these landraces into elite materials could contribute to sustainably improving maize production. The successful introgression of GER resistance genes into elite materials, from non-adapted maize populations, using bi-parental crosses combined with doubled haploid technology, was recently demonstrated by Galiano-Carneiro et al. (2021) for Brazilian landraces. However, this needs to be explored for the European flint landraces

since the success of gene introgression depends on the germplasm and the level of genetic variation within the breeding program (Li et al., 2022).

Genomics-based breeding methods for Fusarium resistance

In wheat, more than 500 quantitative trait loci (QTL) have been reported and recently clustered in 65 meta-QTL with unique and refined genomic regions by Venske et al. (2019). From these QTL, *Fhb1*, *Fhb2* and *Fhb5* have been identified from Chinese germplasms as major genomic loci conferring resistance to FHB disease in wheat. Miedaner et al. (2019) indicated that *Fhb1* and *Fhb5* were able to reduce FHB susceptibility by 6.5 and 11.3 percentage points, respectively, suggesting their potential use in commercial wheat breeding programs.

Fhb1 is extensively used through marker-assisted selection (MAS) in breeding programs outside Europe (Anderson et al., 2001; Anderson et al., 2007; Zhu et al., 2019; Hao et al., 2020). Although these major non-adaptive FHB resistance QTL have been widely used in breeding programs, they only confer partial resistance and attempts for their introgression into foreign germplasms have not been successful across all genetics backgrounds (Brar et al., 2019). In addition, these foreign sources of resistance carry undesirable agronomic traits which are also a major bottleneck to their introgression into susceptible cultivars (Li et al., 2016). Therefore, there is a need to identify locally adapted resistance loci while taking into consideration the complex interactions of FHB resistance with morphological traits as described earlier in this chapter.

Recently, the existence of FHB-neutral *Rht* genes, such as *Rht24* has been revealed by Herter et al. (2018) from a European bi-parental population. In addition, Miedaner et al. (2022) have analysed 420 European wheat cultivars and demonstrated that *Rht24* does not affect FHB resistance. However, given the complex relationships of FHB resistance with morphological traits, it is worth exploring possible effects of *Rht24* on these traits. Moreover, Buerstmayr and Buerstmayr (2022) evaluated near-isogenic lines with contrasting backgrounds and demonstrated that background resistance reduced the negative effect of *Rht-1* gene on FHB resistance. Therefore, understanding the potential applications of genomic background resistance is necessary to ultimately reduce FHB disease in semi-dwarf wheat varieties.

Similarly, GER resistance is a complex polygenic trait which is quantitatively inherited with both additive and dominance gene effects. About 131 QTL for GER resistance have been reported, using low-density technologies such as single sequence repeats (SSR), restriction fragment length polymorphisms (RFLP) and random amplified polymorphic DNA (RAPD),

and high-throughput technologies, like single nucleotide polymorphisms (SNP) (Table 1). However, in their current state, the incorporation of reported QTL by individual studies into breeding programs may not be as effective as expected. A comprehensive analysis of all loci is required to render them more useful and facilitate their integration into breeding strategies. QTL were identified in diverse populations sourced from various geographic origins such as Brazil, Argentina, Canada, USA, China and Europe. Furthermore, for both FHB and GER resistances, given the high number of reported QTL and the polygenic nature of the traits, an appropriate exploitation of these loci requires the application of advanced molecular breeding strategies such as genomic selection as indicated by Miedaner et al. (2020) and Gaikpa and Miedaner (2019).

Table 1: Genomic loci reported for resistance to Gibberella ear rot using diverse mapping populations in maize

Source(s) of resistance	**Origin**	**Number of QTL**	**Range of PVE**	**Reference**
Brazilian tropical line (T3)	Brazil	3	0.04−0.11	Galiano-Carneiro et al. (2021)
LP4637	Argentina	4	0.03−0.13	Giomi et al. (2016)
UH006, UH025	Europe	13	0.02−0.10	Han et al. (2016)
CO441	Canada	10	0.02−0.09	Kebede et al. (2016)
CO441	Canada	10	0.02−0.06	Kebede et al. (2016)
JiV203, Dan598, ZW18, Cheng351	China	22	0.05−0.42	Wen et al. (2020)
IBMSyn10	USA	1	0.33	Yuan et al. (2020)
DH4866	China	11	0.01−0.10	Zhou et al. (2021)
Kemater Landmais Gelb	Europe	8	0.00−0.12	Gaikpa et al. (2021)
UH007 × UH006	Europe	6	0.04−0.13	Martin et al. (2011)
D152 × UH007	Europe	3	0.05−0.06	Martin et al. (2012)
UH009 × UH006	Europe	3	0.08−0.12	Martin et al. (2012)
UH009 × UH007	Europe	8	0.02−0.07	Martin et al. (2012)
CG62 × CO387	Canada	11	0.07−0.33	Ali et al. (2005)
CG62 × CO387	Canada	18	0.07−0.35	Ali et al. (2005)

PVE = phenotypic variance explained, QTL = quantitative trait loci, USA = United States of America

Objectives

Overall objective

This work aims to improve resistance to Fusarium head blight (FHB) and Gibberella ear rot (GER) diseases in wheat and maize, respectively, through the exploitation of an European winter wheat diversity panel from Germany and flint maize landraces from Austria.

Specific objectives

Specifically, the work aims to:

a) Elucidate the complex interaction between FHB resistance and morphological traits such as plant height and anther retention and assess the effect of *Rht24* on traits which are highly correlated with FHB resistance;
b) Assess the contribution of genomic background resistance to reducing FHB severity in semi-dwarf wheat genotypes possessing *Rht-D1b*, and discuss strategies for its application in commercial breeding programs;
c) Conduct a comprehensive meta-analysis of reported quantitative trait loci (QTL) to identify refined and stable QTL harboring candidate genes which confer resistance to ear rot diseases and mycotoxin contaminations in maize;
d) Evaluate the efficiency of the introgression of GER resistance genes from two European flint landraces such as “Kemater Gelb Landmais” (KE) and “Petkuser Ferdinand Rot” (PE) landraces into two susceptible and adapted elite materials;
e) Evaluate the accuracy of the use of line performance as a predictor of hybrid performance for GER resistance, thereby accelerating the development of GER-resistant hybrid maize cultivars.

Research hypotheses

We hypothesized that:

a) FHB resistance is influenced by variations in morphological traits such as plant height and anther retention, and *Rht24* does not affect morphological traits correlated with FHB resistance;
b) Semi-dwarf wheat genotypes possessing *Rht-D1b* allele with higher genomic background resistance have lower FHB severity compared to other semi-dwarf genotypes;

c) Several refined and stable quantitative trait loci harbor promising candidate genes controlling resistance to maize ear rot diseases and mycotoxin contaminations;
d) Bi-parental populations derived from KE and PE landraces have lower GER severity than their corresponding elite lines;
e) Parental line performance is a good predictor of hybrid cultivars for Gibberella ear rot resistance.

Outline of the dissertation

This dissertation is composed of six chapters as presented below:

- **Chapter 1**: is a general introduction to the dissertation. This chapter presents the problem statements, objectives and research hypotheses of the work.
- **Chapter 2**: presents our first publication on "Separation of the effects of two reduced height (*Rht*) genes and genomic background to select for less Fusarium head blight of short-strawed winter wheat (*Triticum aestivum* L.) varieties". It elucidates the complex interactions between FHB resistance and morphological traits including plant height and anther retention, and discusses the effect of *Rht24* on traits correlated with FHB resistance. The chapter also relates to the improvement of FHB resistance in short-strawed wheat genotypes through the exploitation of genomic background resistance and FHB-neutral genes such as *Rht24*.
- **Chapter 3**: relates to our second publication entitled "Meta-analysis and co-expression analysis revealed stable QTL and candidate genes conferring resistances to Fusarium and Gibberella ear rots while reducing mycotoxin contamination in maize". This chapter depicts the molecular basis of maize ear rots resistances using meta-analysis method coupled with co-expression analysis based on publicly available RNA-Seq data. Stable QTL revealed by the meta-analysis were cross-validated by incorporating association mapping studies, and thus depicting the genetic architecture of ear rots resistance. Resistance- and susceptibility-promoting candidate genes were identified for use in ear rots breeding programs.
- **Chapter 4**: is our third publication on "Effectiveness of introgression of resistance loci for Gibberella ear rot from two European flint landraces into adapted elite maize (*Zea mays* L.)". It focuses on the introgression of GER resistance genes from KE and PE landraces into two elite flint materials. Three DH lines from KE and one DH line from PE, with moderate to strong GER resistance were used as donors in bi-parental crosses with the two

GER susceptible flint lines. Effectiveness of the introgression of the two landraces was discussed as well as the genetic advance based on 5% selection intensity.

- **Chapter 5**: presents our fourth publication on "Variance components and correlations between doubled haploid lines from two European flint landraces and their corresponding testcrosses for Gibberella ear rot resistance, silking time, and plant height in maize". This chapter discusses the prediction accuracy of using 76 parental lines from KE and PE landraces to predict performance of testcrosses. The genomic prediction accuracy using parents as training set and testcrosses as validation set was also explored.
- **Chapter 6**: is a general discussion and conclusion of the dissertation. Key findings were discussed in line with our objectives and hypotheses and subsequent implications for improving FHB and GER resistances in breeding programs were highlighted.

Chapter 2: Separation of the effects of two reduced height (*Rht*) genes and genomic background to select for less Fusarium head blight of short-strawed winter wheat (*Triticum aestivum* L.) varieties

Félicien Akohoue[1], Silvia Koch[1], Jörg Plieske[2], Thomas Miedaner[1*]

[1]State Plant Breeding Institute, University of Hohenheim, Stuttgart, Germany;

[2]SGS INSTITUT FRESENIUS GmbH, TraitGenetics Section, Am Schwabeplan 1b, 06466 Seeland OT Gatersleben, Germany

*Correspondence: miedaner@uni-hohenheim.de (T.M.)

ORCID T.M.: https://orcid.org/0000-0002-9541-3726

Published in *Theoretical and Applied Genetics*. 2022; 135, 4303–4326. https://doi.org/10.1007/s00122-022-04219-4.

Submitted: 13 June 2022 / **Accepted**: 08 September 2022 / **Published**: 24 September 2022

Theoretical and Applied Genetics (2022) 135:4303–4326
https://doi.org/10.1007/s00122-022-04219-4

ORIGINAL ARTICLE

Separation of the effects of two reduced height (*Rht*) genes and genomic background to select for less Fusarium head blight of short-strawed winter wheat (*Triticum aestivum* L.) varieties

Félicien Akohoue[1] · Silvia Koch[1] · Jörg Plieske[2] · Thomas Miedaner[1]

Received: 13 June 2022 / Accepted: 8 September 2022 / Published online: 24 September 2022

Abstract

Key message **FHB resistance shared pleiotropic loci with plant height and anther retention. Genomic prediction allows to select for genomic background reducing FHB susceptibility in the presence of the dwarfing allele *Rht-D1b*.**

Abstract With the high interest for semi-dwarf cultivars in wheat, finding locally adapted resistance sources against Fusarium head blight (FHB) and FHB-neutral reduced height (*Rht*) genes is of utmost relevance. In this study, 401 genotypes of European origin without/with dwarfing alleles of *Rht-D1* and/or *Rht24* were analysed across five environments on FHB severity and the morphological traits such as plant height (PH), anther retention (AR), number of spikelets per ear, ear length and ear density. Data were analysed by combined correlation and path analyses, association mapping and coupling single- and multi-trait genome-wide association studies (ST-GWAS and MT-GWAS, respectively) and genomic prediction (GP). All FHB data were corrected for flowering date or heading stage. High genotypic correlation ($r_g = 0.74$) and direct path effect (0.57) were detected between FHB severity and anther retention (AR). Moderate correlation ($r_g = -0.55$) was found between FHB severity and plant height (PH) with a high indirect path via AR (− 0.31). Indirect selection for FHB resistance should concentrate on AR and PH. ST-GWAS identified 25 quantitative trait loci (QTL) for FHB severity, PH and AR, while MT-GWAS detected six QTL across chromosomes 2A, 4D, 5A, 6B and 7B conveying pleiotropic effects on the traits. *Rht-D1b* was associated with high AR and FHB susceptibility. Our study identified a promising positively acting pleiotropic QTL on chromosome 7B which can be utilized to improve FHB resistance while reducing PH and AR. *Rht-D1b* genotypes having a high resistance genomic background exhibited lower FHB severity and AR. The use of GP for estimating the genomic background was more effective than selection of GWAS-detected markers. We demonstrated that GP has a great potential and should be exploited by selecting for semi-dwarf winter wheat genotypes with higher FHB resistance due to their genomic background.

Introduction

Wheat (*Triticum aestivum* L.) is one of the most cultivated cereal crops worldwide and serves as a staple food for millions of people. However, the production of wheat is hampered by several diseases, including Fusarium head blight (FHB) caused by numerous *Fusarium* species, with *Fusarium graminearum* Schwabe and *F. culmorum* (W.G. Smith) Sacc. being the most predominant in Central Europe. FHB causes severe yield losses and contaminates the grains with several mycotoxins including deoxynivalenol (DON) which is one of the most frequently detected in wheat (Righetti et al. 2021; Topi et al. 2021). DON makes the grain unsuitable for flour and malt and is also toxic for non-ruminant animals (Windels 2000). Damages due to FHB in wheat are likely to increase with the rising temperatures and higher atmospheric carbon dioxide (CO_2) caused by climate change (Timmusk et al. 2020; Miedaner and Juroszek 2021; Hay et al. 2022). Fungicides and DON-reducing technologies used as traditional measures to control FHB disease increase production costs, with no significant positive return on grain yield (Wilson et al. 2018). Most effective

Communicated by Hermann Buerstmayr.

✉ Thomas Miedaner
miedaner@uni-hohenheim.de

[1] State Plant Breeding Institute, University of Hohenheim, Stuttgart, Germany

[2] SGS INSTITUT FRESENIUS GmbH, TraitGenetics Section, Am Schwabeplan 1b, 06466 Seeland OT Gatersleben, Germany

and environmentally friendly strategies integrate appropriate agronomic practices and enhanced host resistance.

Breeding for resistance against FHB in European winter wheat faces several challenges related to the complex genetic architecture of the trait (Jiang et al. 2015; Ruan et al. 2020) and requires intensive breeding effort and accurate breeding strategies (Buerstmayr et al. 2020). FHB resistance is controlled by multiple medium- and small-effect quantitative trait loci (QTL) which are vulnerable to the changing environmental conditions due to QTL-environment interactions (Miedaner and Juroszek 2021). To date, more than 500 QTL have been reported for FHB from different breeding populations and were further clustered into 65 QTL with unique physical positions through a recent meta-analysis by Venske et al. (2019). Additionally, morphological traits such as plant height and anther retention or extrusion were shown to passively contribute to FHB resistance (Mesterházy 1995; Buerstmayr et al. 2020; Xu et al. 2020), and relationships between FHB resistance and morphological traits have been extensively reported using correlation coefficients (Buerstmayr and Buerstmayr 2015; Steiner et al. 2019b; Ruan et al. 2020; Xu et al. 2020). Although correlation analysis helps measure the degree of association between two traits, it does not explain causes and effects of the relationship (Dewey and Lu 1959; Ozukum et al. 2019). In addition, the existence of strong correlation between two traits might be due to the presence of one or many other traits which strengthen the complexity of the interactions. Understanding the complex interactions between FHB resistance and morphological traits requires the use of appropriate statistical approaches like path analysis, also referred to as structural equation modelling (SEM) or covariance structural equation modelling (CSEM).

Path analysis is a causal multivariate modelling approach which complements simple correlation analysis by unravelling the nature and magnitude of the observed relationships among traits (Wright 1934). It exploits observed correlations to estimate standardized direct and indirect effects contrary to the standard multivariate modelling which ignores causal relationships among variables and combines all effects together (Valente et al. 2013). Path effects estimated using correlations are unitless and interpreted as standardized regression slopes, allowing for comparison of the relative importance of different variables (Stage et al. 2010). Therefore, a direct path effect of a particular morphological trait on FHB resistance would indicate how much an increase of one unit in the standard deviation of that trait directly changes the standard deviation of FHB resistance. On the contrary, an indirect path effect would indicate how much a particular morphological trait changes the standard deviation of FHB resistance depending on the presence of other morphological traits. The selection for FHB resistance using the indirect path of a trait requires the simultaneous integration of one or several other traits. Based on comparison between the two types of effect, the breeder can decide which paths and morphological traits are more important to be considered for improving FHB resistance using correlated traits for higher genetic progress. Hence, a combined correlation and path analysis has several advantages including setting reliable criteria for multiple-trait selection, minimizing risks of components compensation and guiding in planning of experiments (Usman et al. 2017; Khan et al. 2022). Path analysis was used by researchers to depict complex associations among yield and related traits in several crop species including wheat (Baye et al. 2020; Hinson et al. 2022) and maize (Toebe and Cargnelutti 2013).

Plant height in wheat is controlled by at least 150 QTL scattered across the whole wheat genome (Mao et al. 2010), and 25 *Rht* genes with more than 30 dwarfing alleles are reported (Sanchez-Garcia and Bentley 2019). They became very popular after their introduction during 1960s and 1970s to initiate the "Green Revolution" in developing countries (Hedden 2003) but also to breed short-strawed wheat in industrial countries. Major *Rht* genes are *Rht-B1* (syn. *Rht1*), *Rht-D1* (syn. *Rht2*) and *Rht24*, located on chromosomes 4B, 4D and 6A, respectively (Würschum et al. 2017; Tian et al. 2022). The wild type is named "a" and the height-reducing mutant "b". *Rht-D1b* and *Rht24b* were more frequently found in Central European wheat germplasm than *Rht-B1b*. *Rht* genes have been widely used in commercial wheat breeding to develop semi-dwarf varieties which are preferred to tall genotypes because of their lodging resistance, higher nitrogen fertilizer use efficiency, increased tillers, higher harvest index and grain yield (Zhao et al. 2022).

Unfortunately, *Rht-B1b* and *Rht-D1b* were associated with FHB susceptibility and lower anther extrusion (Lu et al. 2013; Hales et al. 2020). Miedaner et al. (2019) and Zhang et al. (2021) suggested the use of major FHB-resistant QTL through marker-assisted introgression to counterbalance the negative FHB effect of semi-dwarf genotypes. Meanwhile, it has also been demonstrated that major non-adapted FHB resistance QTL (*Fhb1*, *Fhb2*, *Fhb5*) provide only a partial resistance (Su et al. 2019), and their introgression was not equally effective across different backgrounds (Brar et al. 2019) and requires considerable breeding efforts. Breeders must also consider a larger number of medium- and small-effect QTL in locally adapted cultivars for all traits analysed here, so-called genomic background (Brar et al. 2019) in order to aim for local, short-strawed wheat cultivars with higher FHB resistance. The genomic background refers to all locally adapted genes which are likely to influence the phenotype controlled by a particular gene of interest (Yoshiki and Moriwaki 2006). In wheat, all genes of a genotype which are capable of influencing the reduction effect of major *Rht* genes on plant height can be considered as genomic background for the plant height in that genotype and similarly

for FHB resistance and AR. Numerous medium- and small-effect loci have been reported for FHB resistance and anther retention, but their potential to counterbalance the negative effect major *Rht* genes such as *Rht-D1* and possible exploitation in practical breeding have been poorly investigated.

Herter et al. (2018) evaluated segregating materials derived from a biparental cross between two German winter wheat cultivars, "Solitär x Bussard", and demonstrated that *Rht24b* was not associated with FHB resistance. This was recently confirmed in a large European winter wheat germplasm by Miedaner et al. (2022) who also found that *Rht24b* did not affect FHB resistance. Therefore, strategies to develop FHB-resistant varieties with semi-dwarfing alleles should reconsider the choice of such *Rht* genes. This gives the opportunity to develop marker arrays and strategies to facilitate the exploitation of FHB-neutral *Rht* genes in breeding programmes. However, given the complex interactions among morphological traits and their passive contribution to FHB resistance (Buerstmayr et al. 2020), a clear understanding of the effect of *Rht24b* on morphological traits, like anther retention or extrusion, is required. Furthermore, the choice of *Rht* genes could also be driven by breeding objectives and the extent to which FHB-neutral *Rht* genes reduces the plant height compared with other genes.

In this study, we aimed to (i) describe the nature and magnitude of the complex interactions between FHB resistance and morphological traits, including plant height, anther retention, number of spikelets per ear, ear length and ear density using combined correlation and path analyses; (ii) dissect the genetic architecture of FHB severity, plant height and anther retention, thus uncovering the genetic basis of the complex interactions among these traits through a joint implementation of single- and multi-trait genome-wide association study (GWAS), and genomic prediction (GP); and (iii) separate for each trait, the effects of *Rht* genes and genomic background (GB), evaluating the potential of GB in selecting FHB-resistant genotypes with short *Rht* alleles based on the single-trait GWAS and genetic estimated breeding values (GEBV) from the GP. GB refers to all QTL affecting the traits, except those associated with plant height on chromosomes 4D and 6A corresponding to *Rht-D1* and *Rht24* genes, respectively.

Materials and methods

Plant materials and field experiments

The materials consisted of 401 winter wheat cultivars from European origin (Table S1). These cultivars were evaluated in Germany at three locations in 2020 and two in 2021, resulting in five environments (location × year combinations) in total. In 2020, the cultivars were evaluated in Hohenheim (HOH) near Stuttgart (9.12° E, 48.42° N; 400 m above sea level [a.s.l]), Oberer Lindenhof (OLI) near Reutlingen (9.18° E, 48.28° N; 700 m a.s.l), and Wohlde (WOH) near Bergen (9.98° E, 52.80° N; 80 m a.s.l). In 2021, field experiments were conducted in HOH and OLI only. At each location, the cultivars were randomized using an incomplete lattice design with two replicates. Experimental units were planted in double rows of 0.9 m length in WOH and single rows of 1.2 m length in HOH and OLI. Experiments were sown with a density of 40 kernels/row in WOH and 60 kernels/row in HOH and OLI.

Artificial inoculations

Inoculum of the highly aggressive single-spore isolate FC46 (IPO 39-01) of *F. culmorum* (Snijders and Perkowski 1990) was produced on autoclaved wheat kernels as described in detail by Miedaner et al. (1995, 1996). Prior to inoculation, the Fusarium suspension was diluted to a concentration of 2×10^5 spores mL^{-1}. Approximately 100 mL m^{-2} of the diluted inoculum was applied using an adapted agricultural sprayer (Hege 75, Waldenbuch, Germany). Inoculations were repeated four to five times at intervals of two to three days to inoculate each genotype at least once during mid-anthesis. The first inoculations were done when early cultivars started flowering.

Phenotypic data collection

Eight traits were recorded: Fusarium head blight severity (FHB severity, %), plant height (PH, cm), anther retention (AR, %), ear length (EL, cm), number of spikelets per ear (NS, spikelets ear^{-1}), ear density (ED, spikelets cm^{-1}), days to flowering (DTF, days) and heading stage (HS). Days to flowering, the number of days when 75% of heads showed extruded anthers after May 1, was assessed in all environments except in WOH. Heading stage (1–9) was recorded on one a single day (different dates in different environments) and is equal to BBCH stage 51–59 (Meier 2001). Plant height was recorded for each plot after flowering. FHB severity was rated as the percentage of infected spikelets (0–100%) of each head, averaged across all plants of a plot. The first rating started at the onset of symptom development about 15–20 days after inoculation and was repeated in intervals of three to five days until the first signs of ripening. We rated each time the total number of infected spikelets per plot. This rating approach at different stages in the development of the plants under field conditions helped to evaluate the combination of both type I (incidence) and type II (symptom development) FHB resistance in one number (Nannuru et al. 2022). Anther retention was assessed as percentage of retained anthers per spike according to Atashi-Rang and Lucken (1978). Five spikes per plot were harvested five to

seven days after flowering and frozen in paper bags to do the assessment in off-season. Retained anthers of two lateral florets of eight central spikelets were counted on each of the five spikes. In contrast to Atashi-Rang and Lucken (1978), anthers located between the lemma and palea, and partially extruded, were counted as retained. From the same spikes, the number of spikelets per ear (NS_i) was counted and ear (spike) length (EL_i, cm) was measured. Ear density ED_i was calculated as the number of spikelets per centimetre:

$$ED_i = \frac{NS_i}{EL_i} \quad (1)$$

AR, EL and ED were estimated plot-wise by averaging values over the five spikes.

Genotyping and molecular analysis

DNA isolation and genotyping were done by SGS Institut Fresenius, TraitGenetics Section (https://traitgenetics.com/index.php/contact, Gatersleben, Germany) from seed samples of the 401 genotypes. Genotyping was done using an Illumina 25 K Infinium single-nucleotide polymorphism (SNP) array which produced a total of 24,145 SNP markers. About 58 and 14% of the markers overlapped, respectively, with 90 K iSelect and 820 K Axiom® arrays, which are publicly available at CerealsDB (http://www.cerealsdb.uk.net/cerealgenomics/CerealsDB) (Wilkinson et al. 2020). SNPs were filtered by removing markers with minor allele frequency (MAF) < 0.05 and call rate < 80%. This narrowed down the marker data to 19,969 polymorphic and high-quality SNPs with a total of 0.7% of missing data. SNPs were coded as − 1, 0 and 1 corresponding to AA, Aa and aa. A represented the major allele, while a denoted the minor allele. Heterozygous loci were replaced with missing values, and the data were imputed using the Wright's equilibrium approach (Wright 1922). SNPs filtering, coding and imputation were conducted using the *raw.data* function in the snpReady R package (Granato et al. 2018). Start and end physical positions (Table S6) of the markers sequences were obtained by blasting against the International Wheat Genome Sequencing Consortium (IWGSC) reference sequence (IWGSC RefSeq) v.2.1 which is accessible at the Research Unit in Genomics-Info (URGI) of the French National Institute for Agriculture, Food and Environment (INRAE) (https://wheat-urgi.versailles.inra.fr/Seq-Repository/Assemblies) (Zhu et al. 2021).

Phenotypic data analysis

For each plot, arithmetic mean of repeated ratings of FHB severity was calculated and included in the statistical analysis as described by Mesterházy (1995). Estimated individual value was validated when the corresponding coefficient of variation of error was below 5%. Outliers were removed from the data using the Bonferroni–Holm method (Bernal-Vasquez et al. 2016). Variance components, genetic coefficient of variation, broad-sense heritability and best linear unbiased estimations (BLUEs) were calculated for each of the eight traits, based on a mixed linear model:

$$y_{ijkl} = g_i + e_j + b_{jlk} + r_{jl} + ge_{ij} + \varepsilon_{ijkl} \quad (2)$$

where y_{ijkl} is the phenotype of the ith genotype in the jth environment within the kth block of the lth replicate; g_i is the effect of the ith genotype; e_j is the effect of the jth environment; ge_{ij} is the effect of the interaction between the genotype and the jth environment; b_{jlk} is the effect of the kth block; r_{jl} is the effect of the lth replicate; and ε_{ijkl} is the residual error on the phenotype of the ith genotype in the jth environment within the kth block of the lth replicate. To adjust for the impact of repeated artificial inoculations on early flowering genotypes (higher inoculum dose after flowering), days to flowering was added as a cofactor (fixed effect) to the mixed linear model for calculating FHB severity. Because days to flowering was not assessed in WOH, the model was further extended by adding heading stage as a second cofac-tor in order to correct FHB severity. This correction reduced the correlation coefficient between FHB severity and days to flowering from − 0.32 to − 0.16. Similarly, the correlation between FHB severity and heading stage was reduced from 0.29 to 0.11. The genotype was treated as fixed effect, while block, replicate, environment and genotype-environment interaction were included as random effects. Variance components were firstly estimated for all genotypes as one group. Secondly, genotypes were grouped based on *Rht* genes and variances components were estimated to describe the extend of genetic variation within each group for PH, FHB severity and AR. Prior to genotypes grouping, a single-trait genome-wide association study was conducted on each trait to identify significant markers associated with PH on chromosomes 4D and 6A, which correspond to *Rht-D1* and *Rht24* genes. Based on the presence/absence of *Rht-D1b* and *Rht24b*, genotypes were categorized into four *Rht* groups, namely NoRht, *Rht24b*, *Rht-D1b* and *Rht24b* + *Rht-D1b*. NoRht was composed of genotypes with tall alleles of both genes. *Rht24b* included genotypes carrying *Rht24b* only, while *Rht-D1b* was constituted of genotypes with *Rht-D1b* only. Similarly, *Rht24b* + *Rht-D1b* included genotypes possessing semi-dwarfing alleles of both genes. Dummy variables (0, 1) as described by Piepho et al. (2006) were created to separate genotypes, and genotype-dummy interaction was added to the model to estimate variance components within each *Rht* group. For dummy = 1, the interaction between genotype and dummy estimates variance components within the respective group. Significance of variance components

was calculated using a likelihood ratio test (LRT) based on factor-wise comparisons of a model with all factors and a model without the respective factor (Stram and Lee 1994; Morrell 1998). Environment-specific (heterogeneous) variances were fitted for replicate, block and residual effects. Harmonic means of environment-specific residual variances were calculated and reported. The mixed linear models were fitted using the ASReml-R package v.4.1.0 (Gilmour et al. 2015). Only adjusted means (BLUEs) of the corrected FHB severity and other traits across the five environments (location × year combinations) were considered for further analyses (Table S1).

Broad-sense heritability (H^2) was estimated for each trait following the procedure described by Piepho and Möhring (2007):

$$H^2 = \frac{\sigma_G^2}{\sigma_G^2 + \frac{\bar{v}_{\Delta\ldots}^{\mathrm{BLUE}}}{2}} \tag{3}$$

where σ_G^2 is the genotypic variance and $\bar{v}_{\Delta\ldots}^{\mathrm{BLUE}}$ is the mean variance of the difference of two adjusted means (BLUEs). The genetic coefficient of variation (CV_G) was calculated for each trait as follows:

$$\mathrm{CV}_G = \frac{\sqrt{\sigma_G^2}}{\bar{x}} \tag{4}$$

where σ_G^2 is the genotypic variance and $\bar{x}$ is the mean of BLUEs of the trait. Coefficient of variation of error (CV_ε) was also calculated for each trait by replacing the genotypic variance by the residual variance (σ_ε^2) in Eq. (4). All analyses were performed in R software, v.4.1.3 (R Core Team 2021).

Correlation and path analysis

Genotypic correlations were calculated between pairs of traits by fitting a bivariate mixed linear model as follows:

$$\begin{bmatrix} y_{ijkl} \\ y'_{ijkl} \end{bmatrix} = g_i + e_j + b_{jlk} + r_{jl} + ge_{ij} + \varepsilon_{ijkl} \tag{5}$$

where y_{ijkl} is the phenotypic value of the first trait; y'_{ijkl} is the phenotypic value of the second trait; g_i is the effect of the ith genotype; e_j is the effect of the jth environment; ge_{ij} is the effect of the interaction between the ith genotype and the jth environment; b_{jlk} is the effect of the kth block; r_{jl} is the effect of the lth replicate; and ε_{ijkl} is the residual error. Bivariate models were fitted with unstructured variance–covariance using the *corh-option* for the genotype, environment and genotype by environment interaction and diagonal variance–covariance for replicate and blocks. In addition to genotypic correlations, Pearson's product-moment correlations analysis was performed based BLUEs and the results plotted using the GGally package v.2.1.2. Correlation coefficients were classified and interpreted as described by Zou et al. (2003).

The genotypic correlations were used to perform path analysis between FHB severity, as response variable, and morphological traits such as PH, AR, EL and NS included as explanatory variables in agricolae R package v.1.3–5 (De Mendiburu 2016). The analysis was based on standardized partial regressions which used observed genotypic correlations to estimate direct and indirect path effects as illustrated diagrammatically in detail in Fig. 1 (Wright 1918, 1934; Dewey and Lu 1959). For simplicity, PH, AR, EL and NS were coded as 1, 2, 3, and 4, respectively. The path model was fitted as follows:

$$Y = \hat{\beta} X + \varepsilon \tag{6}$$

where $\hat{\beta}$ is the standardized regression slope, representing the direct effect estimators; Y is the vector of genotypic correlations between FHB severity and morphological traits; X is the genotypic correlation matrix among morphological traits; and ε is a vector of residual errors. To estimate the direct effect of each exploratory variable on FHB severity, we minimized the residual least squares and took its derivative with respect to $\hat{\beta}$, creating a system of normal equations as described by Toebe and Cargnelutti (2013):

$$\hat{\beta} = \left[X'X\right]^{-1} X'Y = \begin{bmatrix} p_{15} \\ p_{25} \\ p_{35} \\ p_{45} \end{bmatrix} \tag{7}$$

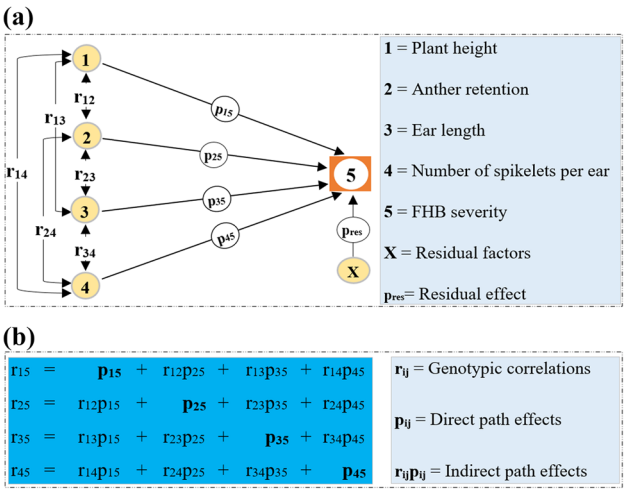

Fig. 1 Representation of the nature of the interactions among traits. **a** = path diagram illustrating direct and indirect effects; **b** = simultaneous structured equations matrix showing relationships between correlations and path coefficients. Double-arrowed lines indicate mutual association as measured by genotypic correlations (r_{ij}), and single-arrowed lines represent direct path effects (p_{ij})

where X' and X^{-1} are the transpose and inverse of the correlation matrix X, respectively; p_{15}, p_{25}, p_{35} and p_{45} are the direct path effects of PH, AR, EL and NS on FHB severity, respectively. Afterwards, the indirect path effects were estimated using structured equations (Dewey and Lu 1959) linking the correlation coefficients and the direct path effects as follows:

$$r_{i5} = p_{i5} + \sum r_{ik}p_{k5} \tag{8}$$

where r_{i5} is the genotypic correlation coefficient between the ith trait and FHB severity; p_{i5} is the direct path effect of the ith trait on FHB severity; and $\sum r_{ik}p_{k5}$ is the summation of indirect path effects of the ith trait on FHB severity via all other k traits. We obtained four structured and simultaneous equations which defined a matrix of direct (diagonal elements) and indirect path (off-diagonal elements) effects of morphological traits on FHB severity (Fig. 1b). Coefficient of determination (R^2) of the path model was estimated as:

$$R^2 = r_{15}p_{15} + r_{25}p_{25} + r_{35}p_{35} + r_{45}p_{45} \tag{9}$$

where r_{15}, r_{25}, r_{35} and r_{45} are the genotypic correlations between FHB severity and PH, AR, EL and NS, respectively. The direct effect (p_{res}) of the residual factors was calculated as the part of the variation of FHB severity which was not explained by PH, AR, EL and NS (Toebe and Cargnelutti 2013). That is,

$$p_{\text{res}} = \sqrt{1 - R^2} \tag{10}$$

The residual factors referred to all other variables which contribute to the variation of FHB severity and were not included in the path model. Similar to the standard multivariate modelling, the existence of high multicollinearity among exploratory variables can lead to significant biases in the estimates of path effects and result in a wrong interpretation of existing causal relationships among the variables (Stage et al. 2010; Toebe and Cargnelutti 2013). Therefore, we investigated the multicollinearity among exploratory variables by calculating the variance inflation factor (VIF). In doing this, a linear regression was fitted for each variable on other variables, and the respective multiple R^2 (R^2_{mult}) was used to calculate VIF as:

$$\text{VIF} = \frac{1}{1 - R^2_{\text{mult}}} \tag{11}$$

Multicollinearity was considered as high, if VIF > 5 (Olivoto et al. 2017).

Population structure and genome-wide association studies

Polymorphic and high-quality SNP markers obtained after the filtering were used to investigate the population structure of the 401 genotypes, using the *snpdgsPCA()* function available in SNPRelate R package v.1.26 (Zheng 2015). Scatter plots illustrating the structure of the population were built for the first two principal coordinates using the ggplot2 package v.3.3.5 (Wickham et al. 2021).

To dissect the genetic architecture of FHB severity, PH and AR, single genome-wide association study (ST-GWAS) analysis was performed based on all 19,969 SNP markers with MAF ≥ 0.05 to identify significant marker–traits associations (MTAs), using the Bayesian-information and Linkage-disequilibrium Iteratively Nested Keyway (BLINK) method available in the Genomic Association and Prediction Integrated Tool (GAPIT) R package v.3.1.0 (Wang and Zhang 2021). BLINK is a multi-locus GWAS method which was demonstrated to outperform in both speed and statistical power other methods such as the fixed and random model circulating probability unification (FarmCPU) and mixed linear model (MLM) (Huang et al. 2019; Wang and Zhang 2021). In contrary to FarmCPU, BLINK works directly on the markers instead of bins, thereby removing the assumption that causal loci are evenly distributed across the genome. BLINK includes two fixed effects models (FEM_1 and FEM_2) and one filtering process, which are performed iteratively (Huang et al. 2019). The filtering process consists in sorting all markers and selecting the first t most significant markers referred to as pseudo-quantitative trait nucleotides (QTNs) (based on indicated threshold) that are not in linkage disequilibrium (Pearson's correlation < 0.7) as covariates. Based on this, the two FEMs can be written as follows:

$$\text{FEM}_1 : y_i = S_{i1}b_1 + S_{i2}b_2 + S_{i3}b_3 + \ldots + S_{ik}b_k + S_{ij}d_j + \varepsilon_i \tag{12}$$

$$\text{FEM}_2 : y_i = S_{i1}b_1 + S_{i2}b_2 + S_{i3}b_3 + \ldots + S_{ik}b_k + \varepsilon_i \tag{13}$$

where y_i is the BLUE across environments of the ith genotype; S_{i1}, S_{i2}, …, S_{ik} are the genotype scores of k pseudo-QTNs, initiated as an empty set; b_1, b_2, …, b_k are the respective effects of the pseudo-QTNs; S_{ij} is the genotype score of the ith genotype and jth marker; d_j is the corresponding effect of the jth marker; and e_i is the residual with $e_i \sim N(0, \sigma^2_\varepsilon)$. In FEM_1, $S_{ij}d_j$ represents a testing markers term where all remaining markers are tested one at a time. In FEM_2, all t pseudo-QTNs selected after the filtering are re-examined together using the Bayesian information content (BIC) as an optimization criterion. Afterwards, k out of the t pseudo-QTNs with the best BIC values are selected and included in FEM_1 as covariates to test the remaining markers.

As BLINK method does not automatically make a clear separation between major- and small-effect QTL (pseudo-QTNs selected are retested together and some are also removed in FEM_2), we implemented two ST-GWAS analyses ($ST\text{-}GWAS_1$ and $ST\text{-}GWAS_2$) on each of the trait. In $ST\text{-}GWAS_1$, all markers were included in the analysis, while in $ST\text{-}GWAS_2$ significant MTAs identified on chromosomes 4D (*Rht-D1*) and 6A (*Rht24*) from $ST\text{-}GWAS_1$ were used as covariate variable to increase the detection of small-effect markers. In wheat, the use of *Rht* markers as covariate variables in BLINK was reported to increase the number of significant markers (Merrick et al. 2022). Significant MTAs were identified based an exploratory threshold of $-\log10$ (p value) = 6 and a Bonferroni-corrected threshold of $-\log10$ (p value) = 6.30. The corrected Bonferroni threshold (p value) was determined as follows:

$$p \text{ value} = \frac{\alpha}{\text{Me}} \tag{14}$$

where $\alpha = 0.01$ is the type 1 error and Me is the number of markers included in the analysis. The total proportion of genetic variation (p_G) explained by significant markers for each trait was determined as follows (Utz et al. 2000):

$$p_G = \frac{R^2_{\text{adj}}}{H^2} \tag{15}$$

where R^2_{adj} is the adjusted R^2 and H^2 is the broad-sense heritability of the trait. The adjusted R^2 was estimated by fitting a multiple linear regression model as follows:

$$y = \text{snp}_i + \text{snp}_j + \ldots + \text{snp}_k + \varepsilon \tag{16}$$

where y is the BLUEs and snp_i, snp_j, and snp_k are the SNP markers identified by ST-GWAS with threshold of $\text{snp}_i > \text{snp}_j > \ldots > \text{snp}_k$ (Gaikpa et al. 2020). Individual p_G values were calculated using the sum of squares (SS) from the analysis of variance of the linear model (Würschum et al. 2015) as:

$$p_G = \frac{\text{SS}_{\text{snp}}}{\text{SS}_{\text{total}} \times H^2} \times 100 \tag{17}$$

where SS_{snp} is the sum of squares of individual SNP and SS_{total} is the total sum of squares of the model. The sum of squares was estimated using the SS type II to avoid changes in the estimates due to SNPs order in the model. Additive effects were estimated by fitting individual SNP in the linear model one at a time as described by Gaikpa et al. (2020).

Additionally, pleiotropic loci between FHB severity, PH and AR were investigated by performing a multi-trait GWAS (MT-GWAS) using the multi-trait mixed-model (MTMM) method proposed by Korte et al. (2012). MT-GWAS was implemented in ASRemL-R package v.4.1.0 between FHB severity and PH (FHB vs PH), FHB severity and AR (FHB vs AR) and PH and AR (PH vs AR). For each pair of traits, the MTMM was:

$$\begin{bmatrix} y_1 \\ y_2 \end{bmatrix} = \sum_{i=1}^{2} S_i \mu_i + X\beta + (X + S_i)\alpha + \upsilon \tag{18}$$

where y_1 and y_2 are the phenotypes of the first and second traits, respectively; S_i is a vector of 1 for all values belonging to the ith trait; μ_i is a vector of fixed effects including the mean of the ith trait; X is the vector of SNP markers; β is the vector of common effects between the two traits; α is the vector of interaction effects; and υ is a random variable capturing both the error and genetic random effects such as the kinship matrix (K). To identify causal loci with common effects (COM) as well as opposite/interaction effects (IE) on each pair of traits, we performed three generalized least squares (GLS) F tests (Korte et al. 2012). Firstly, the full model was tested against a null model where $\beta = 0$ and $\alpha = 0$ in order to identify the combination of both COM and IE loci. Secondly, COM loci were detected by testing the model with $\alpha = 0$ against the null model. Thirdly, the model with $\beta = 0$ was tested against the full model to identify IE loci. Significant effects were identified based on the same exploratory and Bonferroni-corrected threshold used in ST-GWAS. This helped to further reduce potential false positives due to inflation of p values from F tests as found by Merrick et al. (2022). The genotypic correlation between traits pertaining to each pleiotropic locus (r_{snp}) was estimated by fitting the significant markers as fixed effects in the bivariate model described in Eq. (5). Markers were fitted consecutively one after the other starting from the highest p value to the lowest; that is, threshold of $\text{snp}_i > \text{snp}_j > \ldots > \text{snp}_k$. In that order, the genetic correlation attributable to the jth SNP was the difference between the correlation of the model after fitting the ith SNP and the one detected after the jth SNP. Furthermore, the proportion of genetic correlation explained by each pleiotropic locus was calculated as:

$$p_{Ci} = \frac{r_{\text{snpi}}}{r_g} \times 100 \tag{19}$$

where p_{Ci} is the proportion of genotypic correlation explained by the ith SNP and r_g is the total genotypic correlation obtained from Eq. (5).

For both ST-GWAS and MT-GWAS, the genomic relationship matrix was estimated using the kinship algorithm, VanRaden (2008) in GAPIT v.3.1.0. The kinship matrix (K) was fitted as covariate variable in each GWAS model. Quantile–quantile (Q–Q) plots were used to evaluate the power of the model in controlling false positives and negatives. Q–Q plots having a straight line, close to 1:1 on the diagonal, with a sharp upward deviated tail, indicate

a good control of both false positives and negatives by the model and confirm the existence of true MTAs (Kaler et al. 2020). Q–Q and Manhattan plots were drawn using the R package CMplot v.4.0.0 (Yin et al. 2021). Moreover, linkage disequilibrium (LD) patterns were also investigated by calculating R^2 values between pairs of significant markers to identify chromosomal positions of unmapped SNP markers. Markers were considered to be in LD when $R^2 \geq 0.70$.

Genomic prediction and marker-assisted selection

Genomic prediction analysis was performed using the mixed linear ridge regression model in the rrBLUP package v.4.6.1 (Endelman 2011). The model (GP_1) included all markers as random effects and was fitted as follows:

$$Y = \beta + \mathrm{Zu} + \varepsilon \tag{20}$$

where Y is the vector of BLUEs; β is a vector of fixed effect such as the grand mean; Z is the design matrix; $u \sim N(0, A\,\sigma_\varepsilon^2)$ is the vector of random markers effects; A is a relationship matrix and the residuals are normal with constant variance; and ε is a vector of residual errors. GP_1 model was validated using the fivefold cross-validation approach where the training and validation sets were constituted by splitting the phenotypic and genotypic data into five sets, consisting of 80–81 genotypes each (Gaire et al. 2022). Sampling was repeated 50 times, and GP_1 model was run for each set to determine the genomic prediction ability (r_{MG}) and accuracy ($r_{MG/H}$) for each of the traits. Genomic prediction ability was the Pearson correlation coefficient between predicted and observed phenotypes for each of the five validation sets (Ould Estaghvirou et al. 2013). Moreover, the prediction accuracy was determined for each validation set as described by Ould Estaghvirou et al. (2013):

$$r_{MG/H} = \frac{r\mathrm{MG}}{\sqrt{H^2}} \tag{21}$$

where H^2 is the broad-sense heritability of the trait. rMG and rMG/H values were averaged over the five validation sets to obtain the prediction ability and accuracy of each GP_1 model. Additionally, we evaluated the potential of marker-assisted selection (MAS) using only significant markers from ST-GWAS which explained at least 5% of the genetic variation. MAS prediction was done based on the markers effects deducted from the GP_1 model, and the prediction accuracy was calculated.

Estimation of genomic background effect for PH, FHB severity and AR and selection of resistant genotypes with *Rht-D1b*

Based on the ST-GWAS, we evaluated the contribution of GB to FHB severity, PH and AR using the additive effects and estimates of total genetic variation (p_G values) explained by GB and *Rht* markers. p_G values were estimated separately for GB and *Rht* markers by fitting a linear regression model and using the adjusted R^2 as described in Eq. (15). In addition, a second genomic prediction model (GP_2) was built and the prediction ability (r_{MG}) and accuracy ($r_{MG/H}$) were evaluated following the fivefold approach. Training and validation sets were the same as described for GP_1. In GP_2, significant MTAs for PH on chromosomes 4D and 6A were used as covariates, and the prediction accuracy was estimated for each trait based on small-effect markers only. GP_2 was fitted as follows:

$$Y = X\beta + \mathrm{Zu} + \varepsilon \tag{22}$$

where Y is the vector of BLUEs; β is the vector of fixed effects of the covariates; X and Z are the design matrices; $u \sim N(0, A\,\sigma_\varepsilon^2)$ is the vector of random markers effects; A is a relationship matrix and the residuals are normal with constant variance; and ε is a vector of residual errors. Furthermore, we selected the ten best genotypes with low FHB severity and *Rht-D1b* allele based on the calculation of genetic estimated breeding values (GEBV) using the effects of random markers from the GP_2 model as:

$$Y_0 = Z_0 u \tag{23}$$

where Y_0 and Z_0 are the vectors of GEBV and design matrix of the genotypes, respectively. The correlation between the GEBV-based approach and stacking of additive effects (SAE) of GB markers from ST-GWAS was also determined in order to check the relative effectiveness of GWAS for exploiting genomic background. SAE was calculated only for GB markers which explained at least 5% of genetic variation.

Results

Considerable genetic variation was found for FHB severity and morphological traits

Genetic coefficients of variation (CV_G) were low for DTF, HS, EL, NS and ED and moderate to high for PH, FHB severity and AR (Table 1). The higher CV_G observed for AR was due to the considerable existing genetic variation among the genotypes. The coefficient of variation due to

Table 1 Descriptive statistics, variance components and broad-sense heritability estimates for all traits

Trait	Unit	Mean	Range	CV_G (%)	CV_ε (%)	Variance components			H^2
						σ^2_G	σ^2_{GE}	σ^2_ε	
PH	cm	91.40	52.42	10.80	3.31	97.40	5.89	9.13	0.97
FHB	%	37.78	58.29	29.53	11.81	124.43	35.58	19.90	0.92
DTF	Days	43.58	7.60	3.49	1.56	2.31	0.31	0.46	0.91
HS	BBCH stage	53.41	12.64	4.93	2.26	6.94	1.41	1.46	0.94
AR	%	55.72	89.10	39.70	11.41	489.39	80.70	40.43	0.95
EL	cm	10.55	5.40	8.26	3.79	0.76	0.06	0.16	0.95
NS	Spikelets ear^{-1}	22.46	8.39	6.30	1.99	2.00	0.09	0.20	0.97
ED	Spikelets cm^{-1}	2.15	1.28	8.06	0.00	0.03	0.02	0.00	0.96

PH plant height, *FHB* Fusarium head blight severity, *DTF* days to flowering, *HS* heading stage, *AR* anther retention, EL ear length, NS number of spikelets per ear, *ED* ear density, CV_G, CV_ε genetic and error coefficient of variation, respectively, σ^2_G, σ^2_{GE} and σ^2_ε refer to genotypic and genotype × environment interaction and residual variances, respectively, H^2 = broad-sense heritability. All variance components were significant at $p < 0.001$

error (CV_ε) was low for all traits (Table 1). Genetic variances ranged from 0.03 to 6.9 for DTF, HS, EL, NS and ED and were higher (97.4–489.4) for PH, FHB and AR. The genotype–environment interaction (GEI) was significant and generally lower than the genetic variance. Depending on the trait, GEI variance was 1.5–22.2-fold lower than the genetic variance. Broad-sense heritability estimates were very high (> 0.9) for all traits.

Correlations and path coefficients depict the contribution of morphological traits to FHB severity

Density plots of BLUEs across environments showed nearly normal distribution for all traits (Fig. 2). Linear relationships with significant phenotypic correlations were observed among traits. FHB severity was positively and highly correlated with AR ($r_p = 0.70$) and negatively and moderately correlated with PH ($r_p = -0.62$). The outlying point in the scatter plot FHB severity/AR belongs to the cleistogamic cultivar "Anapolis" that has a very high AR (99.6%) and a low FHB severity (20.9%).

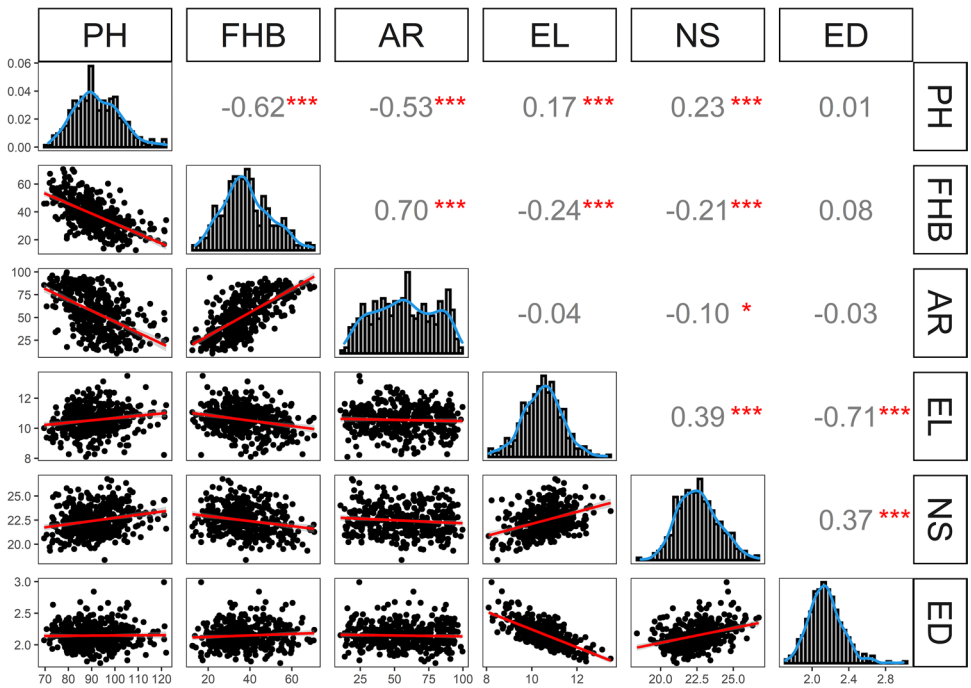

Fig. 2 Pearson's product-moment correlation analysis among traits *, **, ***significant at $p < 0.05$, 0.01 and 0.001, respectively. PH = plant height, FHB = FHB severity, AR = anther retention, EL = ear length, NS = number of spikelets per ear, ED = ear density.

PH was negatively and moderately correlated with AR ($r_p = -0.53$), while NS showed positive and low correlation with EL ($r_p = 0.39$) and ED ($r_p = 0.37$). Highly negative phenotypic correlations were detected between EL and ED ($r_p = -0.71$) (Fig. 2). Phenotypic correlations between FHB severity and EL and NS were significant, but low. At the genetic level, the correlations were negative and moderate between FHB severity and PH ($r_g = -0.64$), PH and AR ($r_g = -0.55$) and negatively high between ED and EL ($r_g = -0.70$). Genotypic correlations were positively high between FHB severity and AR ($r_g = 0.74$) and low between NS with EL ($r_p = 0.38$) and ED ($r_p = 0.37$) (Table 2).

The causal system formed by PH, AR, EL and NS explained 67.04% of the variation of FHB severity (Table 3). Path effect due to residual factors was 0.56. The direct effect of AR (0.57) was 3.3-fold higher than its indirect paths and similar to the residual effect. The indirect effect of PH via AR (− 0.31) was slightly higher than its direct effect (− 0.28), but both effects were lower than the residual effect. Direct and indirect effects of EL were considerably lower than the residual effect, while effects of NS were not significant. Inflation due to multicollinearity among PH, AR, EL and NS was negligible (VIF < 2), showing that estimates of direct and indirect effects and coefficient of determination were accurate (Table 3).

Several marker-trait associations (MTAs) were detected by genome-wide association (GWA) studies

The first two principal coordinates (PCs) indicated that the 401 genotypes included in the study were not structured (Fig. S1). Therefore, we corrected in the GWAS for relatedness among genotypes using the kinship matrix and did not include PCs. The ST-GWAS was performed to depict the genetic architecture of FHB severity, PH and AR (Table S2). Considering all traits, a total of 25 significant MTAs were identified, of which seven were specific to ST-GWAS$_1$, seven to ST-GWAS$_2$ and eleven common to both models (Fig. 3a, b). The use of *Rht* markers as covariate variables in ST-GWAS$_2$ identified additional small-effect MTAs for all traits. Particularly, the number of small-effect MTAs increased from four to seven for AR, while two new MTAs were identified for FHB severity. In total, eight, eleven and nine MTAs were identified for PH, FHB severity and AR, respectively (Table S2). One MTA was common to PH and FHB severity, one to PH and AR and two to FHB severity and AR. MTAs explained 69.7, 60.7 and 44.2% of total genetic variation for PH, FHB severity and AR, respectively. Markers *rs20873* on chromosome 4D linked to *Rht-D1* and *rs10110* on chromosome 6A linked to *Rht24* were major MTAs for PH (Fig. 3a, b), which explained 45.2 and 10.8% of genetic variation, respectively. In addition, *rs20873* conveyed the largest reduction effect of − 7.02 cm on PH. For FHB severity, major MTAs were *rs20873*, *rs5192* on chromosome 7B and *rs3647* on chromosome 5A. Likewise, *rs20873*

Table 2 Genotypic correlation coefficients among traits, excluding days to flowering and heading stages that both were used as covariates (r_g, above diagonal), and corresponding standard errors (SE, below diagonal)

Traits	FHB severity	PH	AR	EL	NS	ED
FHB severity		− 0.64	0.74	− 0.30	− 0.24	0.09
PH	0.03		− 0.55	0.18	0.24	0.02
AR	0.02	0.04		− 0.05	− 0.11	− 0.03
EL	0.05	0.05	0.05		0.38	− 0.70
NS	0.05	0.04	0.05	0.04		0.37
ED	0.05	0.05	0.05	0.02	0.04	

PH plant height, *FHB* Fusarium head blight, *AR* anther retention, *EL* ear length, *NS* number of spikelets per ear, *ED* ear density. All correlation coefficients were significant at $p < 0.001$

Table 3 Direct and indirect path effects of morphological traits on FHB severity

Traits	r_g	VIF	Direct effects	Indirect effects			
				PH	AR	EL	NS
PH	− 0.64	1.47	− 0.28**		− 0.31	− 0.04	− 0.01
AR	0.74	1.40	0.57***	0.15		0.01	0.01
EL	− 0.30	1.19	− 0.21*	− 0.05	− 0.03		− 0.01
NS	− 0.24	1.21	− 0.03	− 0.07	− 0.06	− 0.08	
Residual effect (β_{res}) = 0.56				Coefficient of determination (R^2) = 0.67			

PH plant height, *AR* anther retention, *EL* ear length, *NS* number of spikelets per ear, *FHB* Fusarium head blight; r_g genotypic correlation, *VIF* variance inflation factor

*, **, ***Significant at $p < 0.05$, 0.01 and 0.001, respectively

was the major MTA identified for AR, explaining 22.7% of genetic variation. *rs20873* increased FHB severity and AR by about 6 and 12%, respectively. The false discovery rates were very low (FDR < 0.05) for identified MTAs.

The MT-GWAS identified a total of six pleiotropic loci distributed on chromosomes 2A, 4D, 5A, 6B and 7B. All six were detected between FHB severity and PH (Table 4a), four between FHB and AR (Table 4b) and three between PH and AR (Table 4c). In comparison with the ST-GWAS from BLINK, the marginal trait from the MT-GWAS identified three additional MTAs on chromosomes 4D, 6B and 5A for FHB severity, one on chromosome 5A for PH and one on chromosome 4D for AR. However, the MT-GWAS identified three MTAs for FHB severity, one for PH and three for AR, which were also detected by ST-GWAS. Three out of the six MTAs detected for FHB versus PH exhibited positive contribution to the genotypic correlation and thus exerted common effects on FHB severity and PH (Table 4a). Inversely, the remaining three MTAs showed negative genotypic correlations, revealing their opposite effects on both traits. Marker *rs9660* on chromosome 4D was associated with FHB severity only, but it exerted an opposite effect on the two traits. Similarly, all common effects MTAs were associated with FHB severity only. Common effect MTAs explained 6.3–26.6% of the genotypic correlation between FHB severity and PH, while 3.1–6.3% of the correlation was attributable to interaction effects MTAs (Table 4a). For FHB versus AR, all four MTAs identified by the full model had common effects with 1.4–14.9% of the genotypic correlation explained between FHB severity and AR (Table 4b). Although marker rs5192 on chromosome 7B was specific to FHB severity, it had a common effect on both traits. For PH versus AR, two out of the three MTAs identified by the full model had opposite effects with 5.5–56.4% of the genotypic correlation explained between the two traits (Table 4c). Marker rs7788 that was specific to AR had a common effect on both PH and AR with 10.9% of the genotypic correlation explained.

In both ST-GWAS and MT-GWAS, the inspection of Q–Q plots of the two GWAS revealed a good control of false positives and negatives, demonstrating the existence of true MTAs controlling the genetic architecture of each trait as well as their interactions (Figs. S2–S5). The linkage disequilibrium analysis revealed strong linkage ($R^2 = 0.9$) between markers *rs19377* and *rs13973* located on chromosome 5B for PH (Fig. S6). Very low R^2 values were observed among all other MTAs.

Significant differences were observed among groups of genotypes

NoRht, *Rht24b*, *Rht-D1b* and *Rht24b* + *Rht-D1b* represented, respectively, 23.7, 27.7, 14.9 and 33.7% of our materials (Table 5). Furthermore, considerable genetic variation was observed within each group for PH, FHB severity and AR (Table 5). For PH, the genetic variance was 2.5–6.1-fold higher in NoRht compared with other groups. The lowest genetic variance was observed in *Rht-D1b* for PH. However, in FHB severity, the genetic variance was 1.3–1.3-fold higher in *Rht-D1b* than in NoRht and *Rht24b*. The genetic variance was also 1.5–1.6-fold higher in *Rht24b* + *Rht-D1b* compared with NoRht and *Rht24b* which had similar variation for FHB severity. Genetic variance was high and similar among groups for AR. Genotype–environment interactions were significant and relatively low for the three traits in all groups. Comparative analysis among the four groups revealed statistically significant differences for all traits (Fig. 4). Genotypes were on average shorter in *Rht24b* + *Rht-D1b* and taller in NoRht. In *Rht24b*, genotypes were taller than those in *Rht-D1b* and *Rht24b* + *Rht-D1b*. Contrary to PH, FHB severity was on average lower in NoRht and *Rht24b* than in *Rht-D1b* and *Rht24b* + *Rht-D1b*. FHB severity was statistically identical between NoRht and *Rht24b*, and *Rht-D1b* and *Rht24b* + *Rht-D1b*, respectively. Similar to FHB severity, the average AR was lower in NoRht and *Rht24b* compared with *Rht-D1b* and *Rht24b* + *Rht-D1b*, respectively. No significant difference was found for AR between NoRht and *Rht24b*, as well as *Rht-D1b* and *Rht24b* + *Rht-D1b*. The reduction effect of *Rht* alleles on PH was moderately correlated with FHB severity and AR. Highly negative reduction effect was associated with high FHB severity and AR.

Genomic prediction (GP) exhibited high prediction ability (rMG) and accuracy (rMG/H) for FHB severity, PH and AR

Genomic prediction ability and accuracy averaged over the five validation sets were greater than 0.7 depending on the trait (Table S3). FHB severity and AR showed similar and lower prediction accuracy than PH. Genotypes with *Rht-D1b* and *Rht24b* alleles were distributed across all the validation sets, showing a good representation of the genetic variation in each set (Table S4). This guaranteed the accurate estimation of both r_{MG} and $r_{MG/H}$, resulting in low standard errors of the estimates across validation sets (Table S3). In contrary, the prediction accuracy of marker-assisted selection based on SNP markers with $p_G \geq 5\%$ was moderate for all traits, with the lowest value (0.4) observed in AR (Fig. 5). GP_1 including all available markers increased the prediction accuracy by about 0.2, 0.3 and 0.2 for FHB severity, AR and PH, respectively.

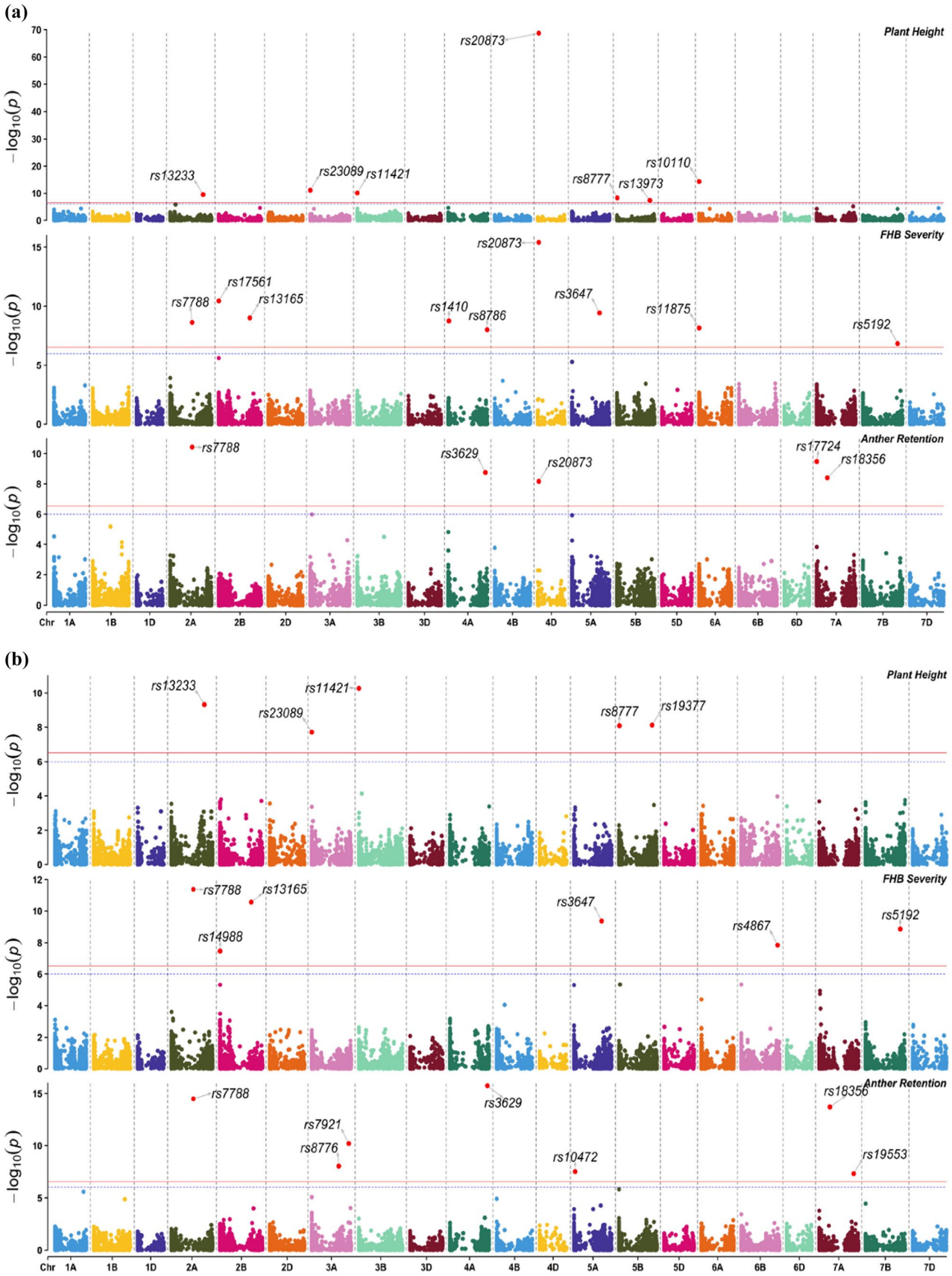
(a)
Plant Height
rs20873
rs13233
rs23089
rs11421
rs8777
rs13973
rs10110
FHB Severity
rs20873
rs7788
rs17561
rs13165
rs1410
rs8786
rs3647
rs11875
rs5192
Anther Retention
rs7788
rs3629
rs20873
rs17724
rs18356
−log10(p)
Chr 1A 1B 1D 2A 2B 2D 3A 3B 3D 4A 4B 4D 5A 5B 5D 6A 6B 6D 7A 7B 7D
(b)
Plant Height
rs13233
rs11421
rs23089
rs8777
rs19377
FHB Severity
rs7788
rs13165
rs14988
rs3647
rs4867
rs5192
Anther Retention
rs7788
rs3629
rs18356
rs7921
rs8776
rs10472
rs19553
−log10(p)
Chr 1A 1B 1D 2A 2B 2D 3A 3B 3D 4A 4B 4D 5A 5B 5D 6A 6B 6D 7A 7B 7D

◂**Fig. 3** Manhattan plots highlighting significant marker–trait associations (MTAs) for single-trait genome-wide association studies (ST-GWAS): **a** = ST-GWAS$_1$ including all markers and **b** = ST-GWAS$_2$ without markers linked to plant height on chromosomes 4D (*Rht-D1*) and 6A (*Rht24*). The blue dotted line corresponds to an exploratory threshold of − Log 10(p) = 6, while the red plain line represents the Bonferroni-corrected threshold cut-off of alpha = 0.01 (color figure online)

Genomic background affects PH, FHB severity and AR

The contribution of GB to the genetic variation was different among the three traits (Fig. 6). The total proportion of genetic variation explained by GB markers was higher for FHB severity than PH and AR (Fig. 6a). Contrary to PH, GB markers had higher contribution to the genetic variation of FHB severity and AR than *Rht* markers (Fig. 6a). Ten, eight and six GB markers were found for FHB severity, AR and PH, respectively (Fig. 6b). Non-*Rht* markers which explained at least 5% of the genetic variation were *rs5192*, *rs3647* and *rs13165* for FHB severity, *rs3629* and *rs8776* for AR and *rs13233* for PH (Fig. 6b). Reduction effects exerted by GB markers were relatively high for all traits (Fig. 7a–c). The cumulative reduction effect (CRE) calculated from markers with $p_G \geq 5\%$ was − 5.7 cm, − 11.2% and − 14.3% for PH (Fig. 7a), FHB severity (Fig. 7b) and AR (Fig. 7c), respectively. CRE was about twofold lower than the additive effects of *Rht* markers for PH. Inversely, the CRE exerted by GB markers on FHB severity and AR was 1.3–1.9-fold higher than the increase effect of *Rht* markers (Fig. 7b, c). Results of the second genomic prediction (GP$_2$) implemented using *Rht* markers as covariates showed moderate prediction accuracy for the three traits (Table S5). This showed that the estimated contribution of GB was higher in the three traits with GP$_2$ compared with GWAS. The highest accuracy was observed for AR, while the lowest value was obtained in PH, confirming the trend revealed by the GWAS. Standard errors were also low for GP$_2$, indicating a high consistency of the prediction accuracy among the five validation sets.

Genotypes with low FHB severity in the presence of *Rht-D1b* were selected using genomic background

Depending on *Rht* groups, GEBV from GP was positively correlated (r = 0.64–0.77) with stacking of additive effects (SAE) of GB markers with $p_G \geq 5\%$ (Fig. 8). However, several genotypes with same SAE (i.e. − 14.42) exhibited different GEBV. The phenotypic performances of the ten best genotypes selected based on GEBV from the genomic prediction (GP$_2$) in *Rht-D1b* and *Rht24b* + *Rht-D1b* groups are summarized in Table 6. The negativity and size of the effects of GB markers as measured by GEBV describe the degree of resistance GB for FHB severity. Thus, highly negative GEBV for FHB severity indicates higher resistance GB, whereas positive GEBV indicates low GB or susceptibility GB. Genotypes with the lowest observed FHB severity exhibited negatively high GEBV for FHB severity carrying *Rht-D1b* allele only (e.g. Faktor and Anapolis), or the combination *Rht24b* + *Rht-D1b* alleles (e.g. Kranich and Kamerad) (Table 6). More resistant genotypes within each *Rht* group also showed negatively high GEBV with lower observed AR, except Anapolis which had a highly positive GEBV for AR and the highest observed AR at all. Taller genotypes had positive GEBV for PH.

Discussion

Through a combined correlation and path analysis, we provided a first insight into the nature and magnitude of the complex interactions between FHB resistance and morphological traits including plant height and anther retention. ST-GWAS, MT-GWAS and genomic prediction were implemented to depict the genetic architecture of FHB severity, anther retention and plant height and understand the effect of alternative *Rht* genes on FHB resistance. Additionally, multi-trait GWAS was conducted to identify positively and negatively pleiotropic loci controlling complex interactions among traits. The ST-GWAS and genomic prediction helped to evaluate for the first time the contribution of genomic background to each trait and its potential to improve FHB resistance in wheat genotypes with semi-dwarfing allele *Rht-D1b*.

Existence of high path effects set criteria for effective indirect selection for FHB resistance

FHB severity exhibited high positive correlation with anther retention and moderate negative correlation with plant height at both phenotypic and genotypic levels. Similar observations were reported by Buerstmayr and Buerstmayr (2015); Steiner et al. (2019b) and Ruan et al. (2020). Buerstmayr and Buerstmayr (2015) reported that FHB severity was positively correlated with anther retention (0.63) and negatively with plant height (− 0.39). Previous investigations on anther extrusion, the opposite of anther retention, also highlighted negative correlation of − 0.45 to − 0.64 (Lu et al. 2013) and − 0.55 to − 0.74 (Xu et al. 2020). Recently, Nannuru et al. (2022) also reported negative moderate correlations between FHB severity with anther extrusion (− 0.48) and plant height (− 0.43) in Nordic spring wheat. Our results confirmed that anther retention was negatively correlated with plant height, indicating the existence of shared genetic control between the two traits in winter wheat in contrary to Nannuru et al.

Table 4 SNP markers associated with common (COM), interaction effects (IE) and the full model (FULL) on plant height (PH), FHB severity and anther retention (AR) from MT-GWAS

Marker	Chr	Pos	UA/FA	FAF	COM	IE	FULL	Y_1	Y_2	r_{snp}	p_C (%)
a. FHB severity (Y_1) versus PH (Y_2)											
rs20873	4D	19.19	G/T	0.49	2.00	**29.08**	**29.37**	**30.21**	**16.75**	− 0.17	26.56
rs9660	4D	195.24	G/A	0.15	0.75	**9.13**	**8.40**	**7.92**	1.20	− 0.04	6.25
rs9869	6B	459.72	T/G	0.22	**7.09**	2.52	**8.15**	**6.92**	0.02	0.04	6.25
rs22296	5A	681.46	T/C	0.40	1.45	**6.47**	**6.61**	**7.45**	**7.01**	− 0.05	7.81
rs5192	7B	661.18	A/G	0.66	**6.00**	1.54	**6.00**	**7.00**	2.44	0.02	3.12
rs7788	2A	419.17	A/G	0.36	**6.39**	0.72	**6.00**	**10.82**	2.50	0.04	6.25
b. FHB severity (Y1) versus AR (Y_2)											
rs20873	4D	19.19	G/T	0.49	**17.60**	0.47	**16.75**	**16.75**	**12.62**	0.11	14.86
rs9660	4D	195.24	G/A	0.15	**8.38**	0.34	**7.62**	**7.92**	**6.08**	0.03	4.05
rs7788	2A	419.17	A/G	0.36	**6.00**	0.57	**6.55**	**7.19**	**7.19**	0.01	1.35
rs5192	7B	661.18	A/G	0.66	**7.00**	2.71	**6.20**	**6.44**	0.70	0.03	4.05
c. PH (Y_1) versus AR (Y_2)											
rs20873	4D	19.19	G/T	0.49	2.65	**30.42**	**31.31**	**30.21**	**12.62**	− 0.31	56.36
rs22296	5A	681.46	T/C	0.40	1.67	**6.50**	**6.83**	**7.45**	2.11	− 0.03	5.45
rs7788	2A	661.18	A/G	0.36	**6.11**	1.31	**6.14**	0.82	**8.19**	0.06	10.91

Chr chromosome, *Pos* physical position on the wheat reference genome RefSeq v.2.1, *UA/FA* unfavourable allele /favourable allele, *FAF* favourable allele frequency, Y_1 = first trait, Y_2 = second trait, FHB = Fusarium head blight, r_{snp} = genotypic correlation between Y_1 and Y_2 pertaining to each marker, p_C = proportion of genotypic correlation explained by each marker. Values highlighted in bold are negative logarithm of *p* value [− Log 10(*p*)] which were higher than the Bonferroni-corrected threshold cut-off of 6

Table 5 Genotype grouping using *Rht* markers and within-group genotypic (σ^2_G) and genotype × environment interaction (σ^2_{GE}) variances

Group	Size	PH (cm)		FHB severity (%)		AR (%)	
		σ^2_G	σ^2_{GE}	σ^2_G	σ^2_{GE}	σ^2_G	σ^2_{GE}
No*Rht*	95	212.55	9.88	103.45	31.44	531.18	96.74
Rht24b	111	84.57	8.63	100.55	34.04	448.51	82.80
Rht-D1b	60	34.65	2.64	131.26	35.69	449.92	80.42
Rht24 + *Rht-D1b*	135	71.96	2.58	160.05	39.66	512.41	67.74

PH plant height, *FHB* Fusarium head blight, *AR* anther retention. All variances were significant at $p < 0.001$

(2022) who found a lower correlation (0.16) between plant height and anther extrusion. The differences in the strength of the correlations across studies are an evidence that interactions among the traits are also affected by environment and breeding material characterized by diverse genetic factors.

The causal system formed by morphological traits including anther retention and plant height explained up to 67% of the phenotypic variation of FHB severity in this study. This confirms the importance of morphological traits in the passive resistance mechanism against FHB disease in winter wheat (Mesterházy 1995; Buerstmayr et al. 2020; Xu et al. 2020). The effect due to residual factors was high (0.56) and can be attributed to specific unshared local genetic factors which had considerable influence on FHB severity. The existence of high direct path of 0.57 between FHB severity and anther retention indicates that any increase by 1% in the standard deviation of anther retention implies a direct increase of 0.57% in the standard deviation of FHB severity independently from other traits. This finding exhibits anther retention as a major indicator trait to be included in multiple-trait breeding strategies to aim for FHB-resistant cultivar development in wheat. Particularly, when the breeder's interest is not in other traits, an indirect selection using anther retention is likely to yield FHB-resistant cultivars (Fernandes et al. 2018; Moreno-Amores et al. 2020). However, path effects between plant height and FHB severity were lower than the residual and the direct effect of anther retention, indicating that plant height as a sole trait does not have considerable contribution to the variation of FHB severity. It is worth noting that the indirect path effect of plant height via anther retention was higher than its direct effect on FHB severity, and this can be explained by the association between plant height and anther retention and underlying genetic factors. A decrease of 1 cm in the standard deviation of plant height in a cultivar would cause a direct increase of 0.28% in the standard deviation of FHB severity

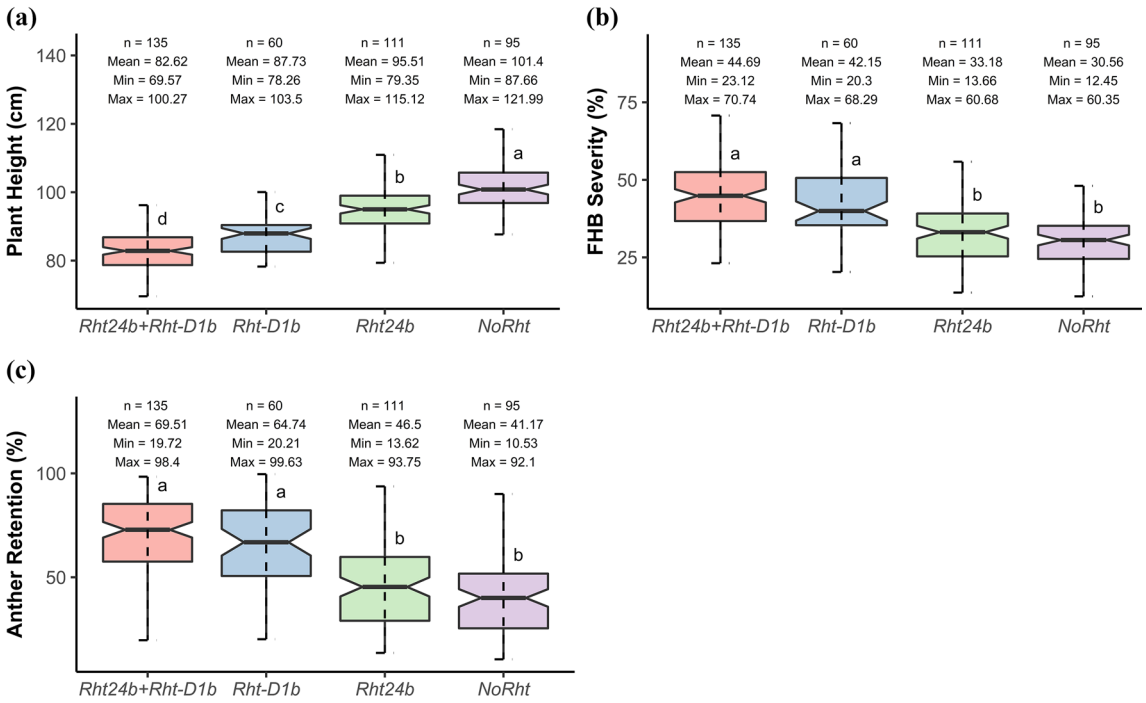

Fig. 4 Boxplots showing variation of traits among *Rht* groups. (**a**) = plant height, (**b**) = FHB severity, and (**c**) = anther retention. n = number of genotypes, Min = minimum, Max = maximum. Boxplots with the same superscripts are statistically not significant at $p < 0.05$

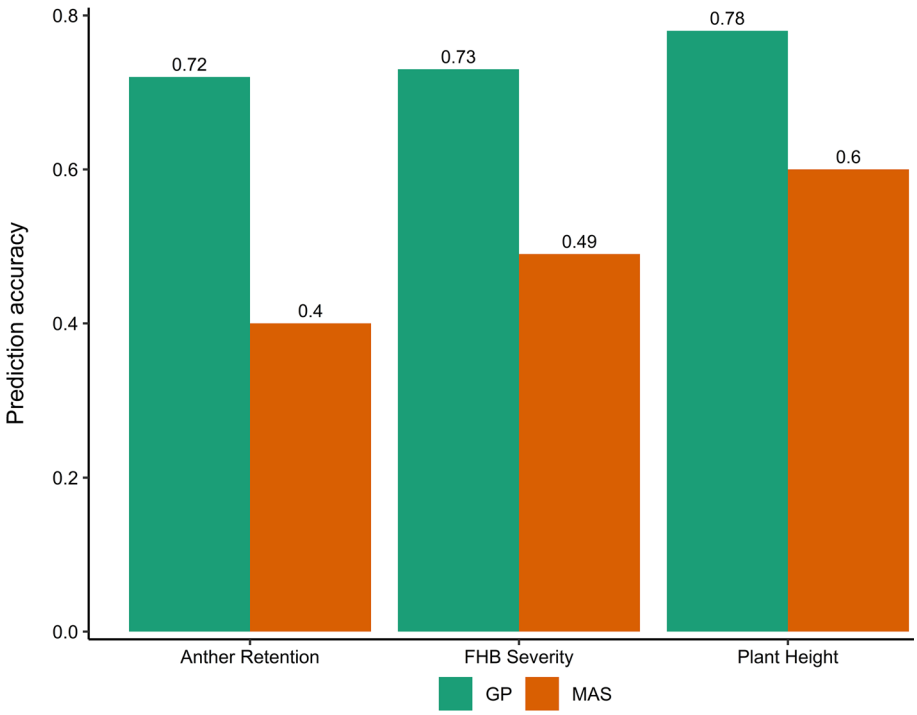

Fig. 5 Comparison of prediction accuracies of genomic prediction (GP) and marker-assisted selection (MAS)

and an indirect increase 0.31% via anther retention. This demonstrates firstly that the moderate correlation detected between plant height and FHB severity was mainly due to anther retention, and secondly that plant height per se has a high impact on FHB severity, even when the experiments are inoculated from above like in this study. As implication, plant height should therefore be considered simultaneously

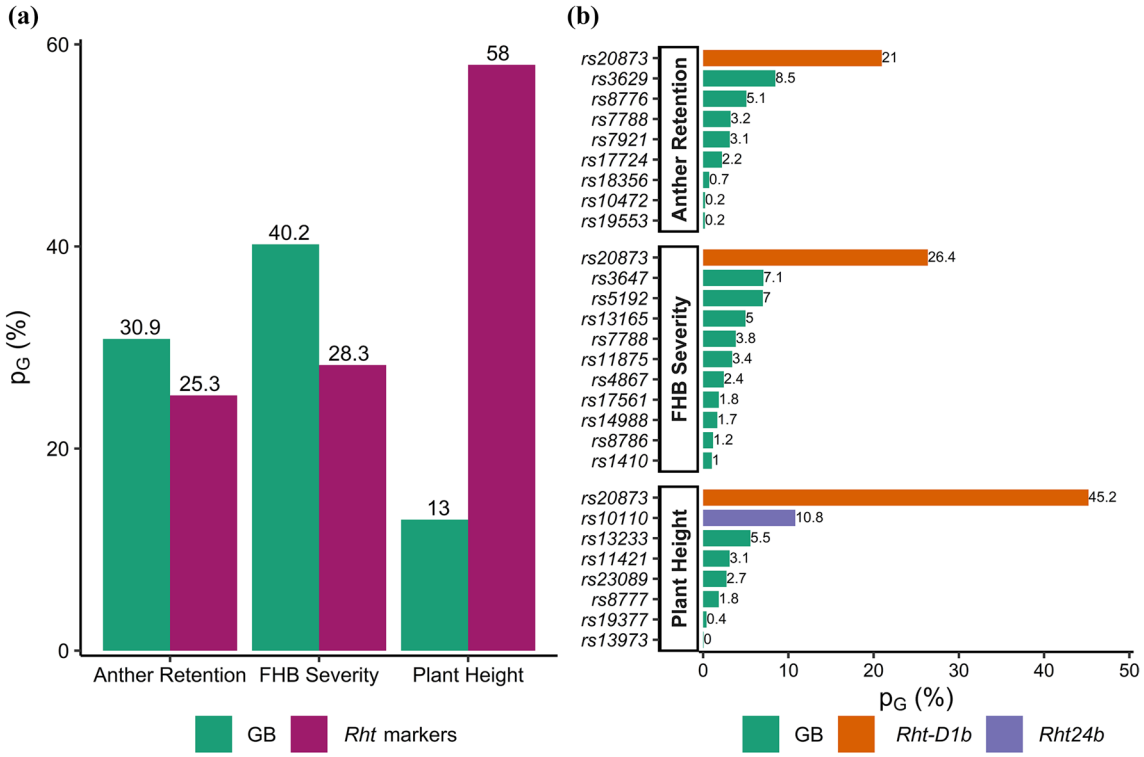

Fig. 6 Contribution of *Rht* genes and genomic background (GB) markers to plant height, FHB severity and anther retention. **a** = total genetic variation explained by groups of markers, and **b** = Genetic variation explained by individual markers

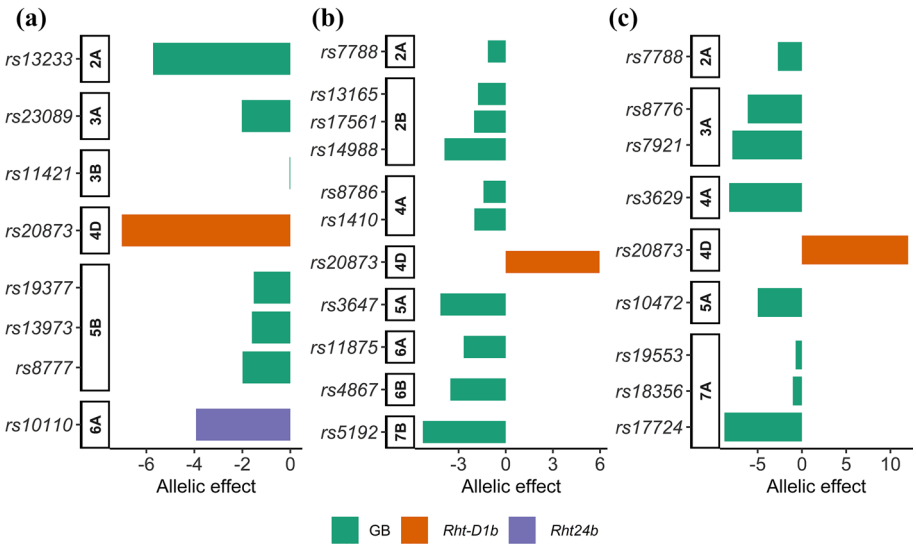

Fig. 7 Comparison of additive effects of *Rht* alleles and reduction effects of alleles by genomic background (GB) markers on: **a** = plant height, **b** = FHB severity and **c** = anther retention

with anther retention in a multiple-trait selection approach for the development of semi-dwarf FHB-resistant cultivars.

Combined ST-GWAS and MT-GWAS revealed two major *Rht* genes and novel pleiotropic loci for plant height, FHB severity and anther retention

Frequency distributions (Fig. 2) already indicated that all traits analysed here were quantitatively inherited, *i.e.* by many loci of varying effects. Indeed, a total of eight loci that control plant height were identified, with corresponding

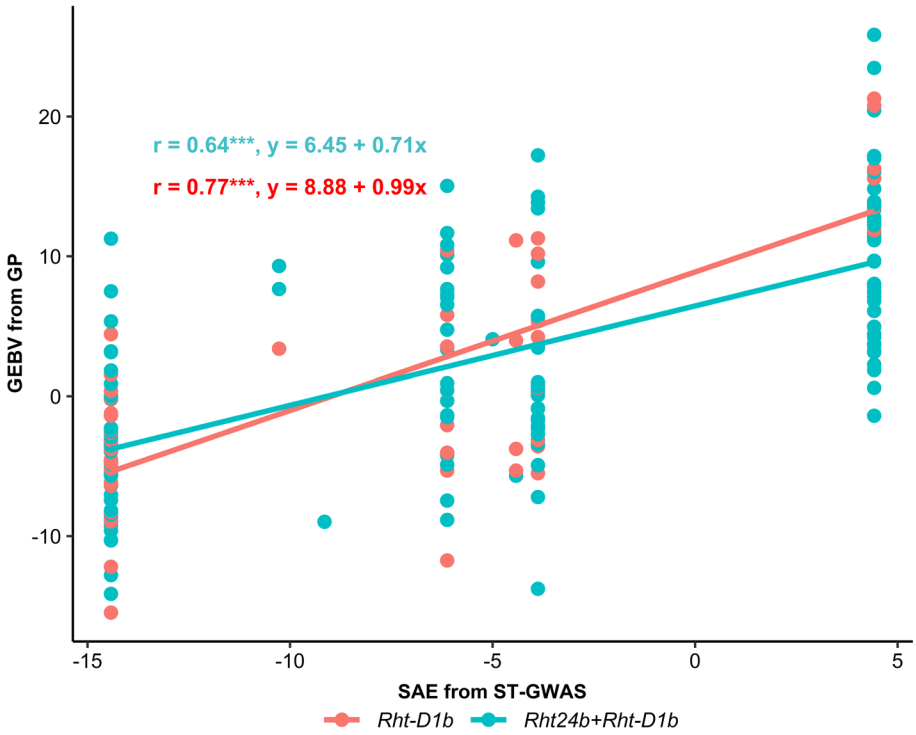

Fig. 8 Scatter plot showing the strength of relationship between stacking of additive effects (SAE) of genomic background (GB) markers from single-trait genome-wide association study (ST-GWAS) and genomic estimated breeding values (GEBV) from genomic prediction (GP). SAE was estimated based on GB markers with $p_G \geq 5\%$. ***significant at $p < 0.001$

Table 6 Ten best semi-dwarf genotypes with the highest resistance genomic background (GB) and low FHB severity

Genotype	*Rht* group	FHB severity (%)		AR (%)		PH (cm)	
		GB	BLUE	GB	BLUE	GB	BLUE
Faktor	*Rht-D1b*	− 15.48	20.30	− 38.98	20.21	10.34	100.05
Anapolis	*Rht-D1b*	− 11.75	20.86	30.82	99.63	− 5.75	79.30
Kranich	*Rht24b* + *Rht-D1b*	− 12.79	23.12	− 11.10	48.67	− 2.28	82.85
Kamerad	*Rht24b* + *Rht-D1b*	− 10.28	25.40	8.32	72.87	− 5.26	80.70
Toras	*Rht24b* + *Rht-D1b*	− 10.01	27.66	− 19.33	48.82	3.16	89.46
Esket	*Rht24b* + *Rht-D1b*	− 9.31	28.09	− 9.35	55.69	2.68	87.22
Opal	*Rht24b* + *Rht-D1b*	− 9.22	28.09	− 9.50	51.86	4.17	88.68
Pamier	*Rht24b* + *Rht-D1b*	− 9.55	29.34	− 5.15	58.25	− 2.63	81.77
Mikon	*Rht-D1b*	− 9.20	29.69	− 34.97	23.39	9.02	92.92
Profilus	*Rht24b* + *Rht-D1b*	− 9.61	30.45	− 1.46	50.52	− 2.07	81.15

AR anther retention, *FHB* Fusarium head blight, *PH* plant height

genomic regions on chromosomes 2A, 3A, 3B, 4D, 5B and 6A. Genomic regions of 4D and 6A were attributed to the presence of *Rht-D1b* and *Rht24b* (Würschum et al. 2015, 2017; Herter et al. 2018; Khadka et al. 2021; Tian et al. 2022), respectively, explaining 45.31% and 10.81% of the total genetic variation of plant height. This supports findings of Würschum et al. (2017), Herter et al. (2018) and Tian et al. (2017), who found that *Rht24* was the second most important *Rht* gene in Central European and worldwide commercial wheat breeding programmes. *Rht-D1* and *Rht24* are, respectively, gibberellin-insensitive (De Velde et al. 2021) and gibberellin-sensitive (Tian et al. 2022) genes responsible for reduced plant height in wheat. The other genomic regions were also enriched with several medium- and small-effect QTL which contribute to plant height. Those small-effect QTL represent the genomic background which explains existing genetic variation of plant height within *Rht* groups.

In addition to *Rht-D1*, a larger number of small-loci controlling FHB severity were identified on other genomic regions such as 2A, 2B, 4A, 5A, 6A, 6B and 7B, which were considered as genomic background contributing the variation of FHB severity among semi-dwarf genotypes. Several FHB resistance QTL were also reported on chromosomes 2A (He et al. 2016a; Gadaleta et al. 2019), 2B (Sari et al. 2018; Ollier et al. 2020), 4A (He et al. 2016a; Zhang et al. 2021; Nannuru et al. 2022), 5A (Steiner et al. 2019a; Ruan

et al. 2020; Sari et al. 2020; Nannuru et al. 2022), 6A (Ruan et al. 2020), 6B (Cuthbert et al. 2007; Ollier et al. 2020) and 7B (Sari et al. 2018; Ollier et al. 2020). In addition, FHB resistance QTL on chromosomes 5A and 7B explained more than 7% of the genetic variation each and can be considered as important locally adapted QTL to improve FHB resistance in European winter wheat. The QTL on chromosome 5A was linked to marker (*AX-158558712*) at position 521 Mbp (Table S6). This falls within the QTL region *Qfhb.nmbu.5A.1* (480–552 Mbp) which was reported through a meta-QTL analysis by Venske et al. (2019) and recently detected in the European wheat panel by Nannuru et al. (2022). For anther retention, in addition to *Rht-D1b*, several medium- and small-effect QTL were detected in genomic regions including chromosomes 2A, 3A, 4A, 5A and 7A. Previous studies also identified QTL for anther retention on chromosomes 3A (Muqaddasi et al. 2019), 4A (Buerstmayr and Buerstmayr 2015) and 5A (Buerstmayr and Buerstmayr 2015; Steiner et al. 2019a; Sari et al. 2020; Xu et al. 2020). These QTL, representing the genomic background, contribute to the adjustments of anther retention, particularly within *Rht* genes groups.

In contrary to *Rht24b*, *Rht-D1b* exerted an opposite or interaction effect on both plant height and FHB severity. *Rht-D1b* explained more than 26% of the observed negative genotypic correlation between the two traits. The linkage disequilibrium analysis revealed an absence of close association between QTL identified for the different traits. This exhibits *Rht-D1* as a major gene conveying a negatively pleiotropic effect on FHB resistance. As indicated by Raherison et al. (2020), alleles of negatively pleiotropic loci exert favourable effects on one trait and unfavourable effects on the other trait depending on the breeding objectives. In commercial wheat breeding, the reduction effect of *Rht-D1b* on plant height represents a favourable effect, while its increase effect on FHB severity or susceptibility is perceived as an unfavourable effect. Several studies also found that *Rht-D1b* was highly associated with FHB susceptibility (Srinivasachary et al. 2008; Mao et al. 2010; Lu et al. 2013; Buerstmayr and Buerstmayr 2016; He et al. 2016b; Prat et al. 2017; Hales et al. 2020; Zhang et al. 2020). Two other interaction effect loci were also identified in other regions of chromosomes 4D and 5A between plant height and FHB severity. The second causal locus on chromosome 4D with linked marker *BobWhite_rep_c48828_217* at position 195 Mbp was associated with FHB severity only, demonstrating the existence of mediated negatively pleiotropic loci that contribute to the negative correlation between FHB resistance and plant height. Mediated pleiotropy as described by Hackinger and Zeggini (2017) represents a situation where a causal locus controls one trait, which in turn causes a second trait, resulting in significant association between the two traits as detected by correlation/covariance analysis. Moreover, our results also revealed that the small-effect loci identified for FHB severity on chromosomes 2A and 7B by the ST-GWAS and another locus on chromosome 6B conveyed a common effect on both FHB resistance and plant height. Although associated with FHB severity only, these QTL exhibited positive contribution to the interactions between the traits with about 16% of the genotypic correlation explained. Ghimire et al. (2022) also reported five stable and pleiotropic QTL associated with FHB resistance and related traits such as DON accumulation and plant height in red winter wheat. Similarly, Schulthess et al. (2017) reported the existence of genomic regions inducing pleiotropic effects on grain yield and related traits in wheat. Our study revealed the existence of positively pleiotropic loci which changes (increase or decrease) FHB severity and plant height in the same direction. These positively pleiotropic QTL can be exploited in breeding programmes to reduce FHB severity (i.e. improve FHB resistance) and plant height simultaneously. Most importantly, the QTL on chromosome 7B linked to marker *AX-158601365* at position 661 Mbp, explaining more than 7% of the genetic variation of FHB severity and exerting a positively pleiotropic effect on both FHB severity and anther retention represents a novel promising QTL which could be integrated into multiple-trait breeding strategy for higher FHB resistance in European winter wheat. Breeder-friendly KASP markers can be developed to facilitate the integration of this QTL into marker-assisted selection.

The high positive correlation and direct path effect observed between FHB severity and anther retention were controlled by the pleiotropic loci identified between FHB severity and plant height, particularly *Rht-D1* and the three QTL distributed on chromosomes 4D, 2A and 7B. All pleiotropic loci exerted common effects on FHB resistance and anther retention with about 24% of genotypic correlation explained in total. This firstly supports the existence of shared small-effect QTL between FHB resistance and anther retention (Lu et al. 2013) and secondly demonstrates that shared QTL may have positively pleiotropic effects on the two traits. Moreover, this positive pleiotropy can be either direct or mediated as the causal pleiotropic locus on chromosome 7B was specific to FHB severity, while others were associated with both traits. Existence of positive pleiotropy between FHB severity and anther retention offers the opportunity of utilizing genomics-assisted breeding to improve both FHB resistance and anther retention in winter wheat. Considering that the identified pleiotropic loci were small-effect QTL, except *Rht-D1*, the efficient exploitation of positive pleiotropy for improving FHB severity and anther retention could be achieved by implementing multi-trait genomic prediction as reported by Gaire et al. (2022) for FHB-related deoxynivalenol accumulation in wheat.

Furthermore, the moderate negative correlation observed between plant height and anther retention was controlled by *Rht-D1* and the two pleiotropic loci on 2A and 5A. *Rht-D1* and QTL on 5A exhibited negatively pleiotropic effects on plant height and anther retention, while the QTL on 2A exerted a mediated positively pleiotropic effect on the two traits. *Rht-D1* explained more than 56% of observed correlation between these traits, indicating that *Rht* genes had a major impact on anther retention and supporting that *Rht-D1b* was associated with high anther retention as recently reported by Buerstmayr and Buerstmayr (2022).

Rht24b has no effect on FHB severity and anther retention

The combination of *Rht-D1b* and *Rht24b* was more frequent in our cultivars as previously reported within European wheat germplasm (Würschum et al. 2017; Tian et al. 2019). The similar FHB severity observed between *Rht24b* and genotypes with tall alleles (NoRht) is an indication that *Rht24b* did not affect FHB resistance (Herter et al. 2018; Miedaner et al. 2022). Similarly, our results also revealed that *Rht24b* did not significantly contribute to anther retention. Accordingly, no marker was found that co-segregates with the other morphological traits (Fig. 3). This offers the possibility of developing semi-dwarf genotypes with improved FHB resistance and low anther retention. However, the effect of *Rht24b* allele (− 3.42 cm) on plant height was about twofold lower than the effect of *Rht-D1b* (− 7.85 cm, Fig. 7a), showing that *Rht24b* exerted a lower reduction effect on plant height compared with other *Rht* genes (Tian et al. 2017; Herter et al. 2018). In addition, the high genetic variation for FHB severity observed among genotypes with *Rht24b* indicates the random existence of FHB-susceptible genotypes within this group. With this, alternative sources of resistance including locally adapted loci could also be explored to develop FHB-resistant genotypes within each *Rht* gene group, depending on breeding objectives.

Genomic background has the potential to improve FHB resistance in genotypes with *Rht-D1b*

Considerable genetic variation was observed for FHB severity and anther retention among genotypes with *Rht-D1b* and *Rht24b* + *Rht-D1b* alleles, demonstrating that there is room for the development of FHB-resistant cultivars with the *Rht-D1b* allele. This large genetic variation in semi-dwarf genotypes can be attributed to the effects of genomic background distributed across several genomic regions. A key implication is that the genomic background has the ability to counterbalance the negative effect of *Rht-D1b* on FHB resistance and anther retention as explained by Buerstmayr and Buerstmayr (2022) who demonstrated by backcrosses with four near-isogenic lines (NILs) that the background resistance of the lines reduced efficiently the effect of semi-dwarfing alleles on FHB severity in spring wheat. Brar et al. (2019) also found that the genomic background and epistatic interactions had a significant impact on the expression of FHB resistance in hard red spring wheat. The more negative the genomic background effect, referring to higher resistance genomic background, the lower the FHB severity and anther retention. This offers a great opportunity to exploit the genomic background for improving FHB resistance in dwarf genotypes.

Effects of the genomic background on FHB severity and anther retention can be efficiently evaluated by calculating the genomic estimated breeding values (GEBV) of genotypes based on the effects of all loci, except *Rht* genes in our case (Bonnett et al. 2022). Several studies have suggested the stacking of additive effects or favourable alleles of QTL from genome-wide association study as an efficient approach to improve FHB resistance and related traits (Miedaner et al. 2006; Sidhu et al. 2020; Ghimire et al. 2022; Nannuru et al. 2022). However, our results showed that despite the existence of moderate to high correlations ($r > 0.6$) between the GEBV-based and stacking of additive effects (SAE) approaches, many genotypes with similar additive effects from GWAS exhibited different GEBV and FHB severity. This shows the limitations of SAE to accurately discriminate among genotypes based on their genomic background contrary to the GEBV-based approach and hence confirms the superiority and efficiency of the genomic prediction over fixed effects selection methods as reported by several previous studies (Juliana et al. 2017, 2022; Sandhu et al. 2021). In addition, the higher accuracy observed for the genomic prediction compared with marker-assisted selection based on the effects of QTL with $p_G \geq 5\%$ from the ST-GWAS (Fig. 5) is another indication that genomic prediction would help to better exploit genomic background than GWAS. This poor performance of GWAS can be explained by the quantitative nature of FHB resistance and anther retention (Liu et al. 2019; Ruan et al. 2020), and that genomic background is constituted of several medium- and small-effect QTL. However, the genome-wide association study (GWAS) can identify only a small number of those minor QTL, not regarding the remaining which are also part of the genomic background and could have together a significant contribution to the phenotype. Moreover, using the GEBV-based approach, the best two genotypes with *Rht-D1b* had a FHB severity of 20.3 and 20.8%, respectively (Table 6). The best two genotypes without dwarfing alleles (Carimulti, Helmond, Table S1) had a FHB severity of 12.4 and 12.8%, respectively. Hence, *Rht-D1b* still has a penalty for FHB resistance of about 40% of increase in disease severity compared to genotypes without this semi-dwarfing allele. This illustrates the necessity to use alternative *Rht* alleles

including *Rht24b*, boosted by a short genomic background or other FHB-neutral *Rht* dwarfing alleles.

Furthermore, the GEBV approach would select Anapolis as one of the best genotypes which exhibited the highest anther retention (99.6%). This is a typical cleistogamous genotype which possesses a structural floral barrier for pathogens, resulting in low FHB severity (Kubo et al. 2010; Tang et al. 2020; Buerstmayr et al. 2021; Zajączkowska et al. 2021). Similar observations were made in barley by Kawada and Kubo (2008) who found that cleistogamous genotypes had high FHB resistance and low mycotoxin accumulation.

Concluding remarks

A clear understanding of the complex interactions between FHB severity and morphological traits and their genetic architecture can significantly contribute to addressing the needs for semi-dwarf wheat genotypes with high FHB resistance. The existence of high direct and indirect path effects between FHB severity and morphological traits demonstrates that multiple indirect trait selection for FHB severity has a great potential and should always integrate anther retention and plant height as important secondary traits. Positively direct and/or mediated pleiotropic loci controlling complex interactions between traits could be integrated into breeding programmes for an efficient multiple-trait selection for higher FHB resistance in wheat. Genomic background (GB) explained a high proportion of the genetic variance of FHB severity and anther retention and has the potential to increase FHB resistance in genotypes with *Rht-D1b*. Depending on the breeding goals, the development of FHB-resistant cultivars should consider *Rht24b* which was not linked to FHB susceptibility and exploit the GB for higher FHB resistance to counterbalance the negative effect of *Rht-D1b*. Similarly, PH could be further reduced in the *Rht24* group by the exploitation of GB. Strategies to efficiently exploit existing interactions among traits and the GB in breeding programmes to develop FHB-resistant cultivars with *Rht-D1b* should include the selection of: (i) taller genotypes within the *Rht-D1b* group as long as they have a high (negative) FHB-related resistance GB (e.g. Faktor, Mikon, Table 6), (ii) genotypes having the lowest anther retention, exploiting the high direct path and positively pleiotropic loci between FHB severity and anther retention, and/or (iii) genotypes with anther retention higher than 95% indirectly taking advantage of the contribution of cleistogamy to passive FHB resistance (e.g. Anapolis). Such genotypes could be most efficiently detected by using genomic estimated breeding values for FHB severity.

Supplementary Information The online version contains supplementary material available at https://doi.org/10.1007/s00122-022-04219-4.

Acknowledgements We dedicate this manuscript to Dr. Erhard Ebmeyer, former wheat breeder at KWS LOCHOW GMBH, Bergen, for his invaluable support of the scientific work in the German wheat community, his steady advises and great interest in our results.Many thanks to the technicians at the respective locations for their excellent work. The authors are highly indebted to Paul Gruner, University of Hohenheim, State Plant Breeding Institute, for his valuable comments on statistical issues.

Author's contribution statement TM and SK designed the experiment. SK performed and supervised the phenotypic evaluations for all traits in HOH and OLI during both years. JP produced the molecular data and helped with the interpretation. FA analysed and interpreted the whole data sets. FA wrote the draft manuscript. TM revised the draft manuscript. All authors read and approved the manuscript.

Funding Open Access funding enabled and organized by Projekt DEAL. This research was partly funded by the German Academic Exchange Service, Bonn, Germany, as a doctoral study grant to Félicien Akohoue (grant no. 91770158). The University of Hohenheim co-financed the field experiments and genotype sequencing.

Data availability All reference data that are not presented in this manuscript are available in the supplementary materials.

Declarations

Conflict of interest The authors declare no conflict of interest.

Ethical approval The authors declare that the experiments comply with the current laws of Germany.

Human and animal rights This research does not contain any studies on humans or animals.

References

Atashi-Rang G, Lucken KA (1978) Variability, combining ability, and interrelationships of anther length, anther extrusion, glume tenacity, and shattering in spring wheat. Crop Sci 18(2):267–272. https://doi.org/10.2135/cropsci1978.0011183X001800020018x

Baye A, Berihun B, Bantayehu M, Derebe B (2020) Genotypic and phenotypic correlation and path coefficient analysis for yield and yield-related traits in advanced bread wheat (Triticum aestivum

L) lines. Cogent Food Agric 6(1):1752603. https://doi.org/10.1080/23311932.2020.1752603
Bernal-Vasquez A-M, Utz HF, Piepho H-P (2016) Outlier detection methods for generalized lattices: a case study on the transition from ANOVA to REML. Theor Appl Genet 129(4):787–804. https://doi.org/10.1007/s00122-016-2666-6
Bonnett D, Li Y, Crossa J, Dreisigacker S, Basnet B, Pérez-Rodríguez P, Alvarado G, Jannink JL, Poland J, Sorrells M (2022) Response to early generation genomic selection for yield in wheat. Front Plant Sci. https://doi.org/10.3389/fpls.2021.718611
Brar GS, Brûlé-Babel AL, Ruan Y, Henriquez MA, Pozniak CJ, Kutcher HR, Hucl PJ (2019) Genetic factors affecting Fusarium head blight resistance improvement from introgression of exotic Sumai 3 alleles (including *Fhb1*, *Fhb2*, and *Fhb5*) in hard red spring wheat. BMC Plant Biol 19(1):179. https://doi.org/10.1186/s12870-019-1782-2
Buerstmayr M, Buerstmayr H (2015) Comparative mapping of quantitative trait loci for Fusarium head blight resistance and anther retention in the winter wheat population Capo × Arina. Theor Appl Genet 128(8):1519–1530. https://doi.org/10.1007/s00122-015-2527-8
Buerstmayr M, Buerstmayr H (2016) The semidwarfing alleles *Rht-D1b* and *Rht-B1b* show marked differences in their associations with anther-retention in wheat heads and with fusarium head blight susceptibility. Phytopathology 106(12):1544–1552. https://doi.org/10.1094/PHYTO-05-16-0200-R
Buerstmayr M, Buerstmayr H (2022) The effect of the Rht1 haplotype on Fusarium head blight resistance in relation to type and level of background resistance and in combination with Fhb1 and Qfhs ifa-5A. Theor Appl Genet. https://doi.org/10.1007/s00122-022-04088-x
Buerstmayr M, Steiner B, Buerstmayr H (2020) Breeding for Fusarium head blight resistance in wheat-Progress and challenges. Plant Breed 139(3):429–454. https://doi.org/10.1111/pbr.12797
Buerstmayr M, Wagner C, Nosenko T, Omony J, Steiner B, Nussbaumer T, Mayer KFX, Buerstmayr H (2021) Fusarium head blight resistance in European winter wheat: insights from genome-wide transcriptome analysis. BMC Genet 22(1):470. https://doi.org/10.1186/s12864-021-07800-1
Cuthbert PA, Somers DJ, Brulé-Babel A (2007) Mapping of Fhb2 on chromosome 6BS: a gene controlling Fusarium head blight field resistance in bread wheat (Triticum aestivum L). Theor Appl Genet 114(3):429–437. https://doi.org/10.1007/s00122-006-0439-3
De Mendiburu F (2016) Package'agricolae'. Statistical procedures for agricultural research. https://cran.r-project.org/package=agricolae
Dewey DR, Lu KH (1959) A correlation and path coefficient analysis of components of crested wheatgrass seed production. Agron J 51(9):515–518. https://doi.org/10.2134/agronj1959.00021962005100090002x
Endelman JB (2011) Ridge regression and other kernels for genomic selection with R package rrBLUP. Plant Genome. https://doi.org/10.3835/plantgenome2011.08.0024
Fernandes SB, Dias KOG, Ferreira DF, Brown PJ (2018) Efficiency of multi-trait, indirect, and trait-assisted genomic selection for improvement of biomass sorghum. Theor Appl Genet 131(3):747–755. https://doi.org/10.1007/s00122-017-3033-y
Gadaleta A, Colasuonno P, Giove SL, Blanco A, Giancaspro A (2019) Map-based cloning of QFhbmgb-2A identifies a WAK2 gene responsible for Fusarium head blight resistance in wheat. Sci Rep 9(1):6929. https://doi.org/10.1038/s41598-019-43334-z
Gaikpa DS, Koch S, Fromme FJ, Siekmann D, Würschum T, Miedaner T (2020) Genome-wide association mapping and genomic prediction of Fusarium head blight resistance, heading stage and plant height in winter rye (*Secale cereale*). Plant Breed 139(3):508–520. https://doi.org/10.1111/pbr.12810
Gaire R, de Arruda MP, Mohammadi M, Brown-Guedira G, Kolb FL, Rutkoski J (2022) Multi-trait genomic selection can increase selection accuracy for deoxynivalenol accumulation resulting from Fusarium head blight in wheat. Plant Genome 15(1):e20188. https://doi.org/10.1002/tpg2.20188
Ghimire B, Mergoum M, Martinez-Espinoza AD, Sapkota S, Pradhan S, Babar MA, Bai G, Dong Y, Buck JW (2022) Genetics of Fusarium head blight resistance in soft red winter wheat using a genome-wide association study. Plant Genome. https://doi.org/10.1002/tpg2.20222
Gilmour AR, Gogel BJ, Cullis BR, Welham SJ, Thompson R (2015) ASReml user guide release 4.1 functional specification. VSN International Ltd, Hemel Hempstead, HP1 1ES, UK www.vsni.co.uk
Granato ISC, Galli G, de Oliveira Couto EG, eSouza MB, Mendonça LF, Fritsche-Neto R (2018) snpReady: a tool to assist breeders in genomic analysis. Mol Breed 38(8):102. https://doi.org/10.1007/s11032-018-0844-8
Hackinger S, Zeggini E (2017) Statistical methods to detect pleiotropy in human complex traits. Open Biol 7(11):170125. https://doi.org/10.1098/rsob.170125
Hales B, Steed A, Giovannelli V, Burt C, Lemmens M, Molnár-Láng M, Nicholson P (2020) Type II Fusarium head blight susceptibility conferred by a region on wheat chromosome 4D. J Exp Bot 71(16):4703–4714. https://doi.org/10.1093/jxb/eraa226
Hay WT, Anderson JA, McCormick SP, Hojilla-Evangelista MP, Selling GW, Utt KD, Bowman MJ, Doll KM, Ascherl KL, Berhow MA, Vaughan MM (2022) Fusarium head blight resistance exacerbates nutritional loss of wheat grain at elevated CO_2. Sci Rep 12(1):15. https://doi.org/10.1038/s41598-021-03890-9
He X, Lillemo M, Shi J, Wu J, Bjørnstad Å, Belova T, Dreisigacker S, Duveiller E, Singh P (2016a) QTL characterization of Fusarium head blight resistance in CIMMYT bread wheat line Soru#1. PLoS ONE 11(6):e0158052. https://doi.org/10.1371/journal.pone.0158052
He X, Singh PK, Dreisigacker S, Singh S, Lillemo M, Duveiller E (2016b) Dwarfing genes *Rht-B1b* and *Rht-D1b* are associated with both type I FHB susceptibility and low anther extrusion in two bread wheat populations. PLoS ONE 11(9):e0162499. https://doi.org/10.1371/journal.pone.0162499
Hedden P (2003) The genes of the green revolution. Trends Genet 19(1):5–9. https://doi.org/10.1016/S0168-9525(02)00009-4
Herter CP, Ebmeyer E, Kollers S, Korzun V, Leiser WL, Würschum T, Miedaner T (2018) *Rht24* reduces height in the winter wheat population 'Solitär × Bussard' without adverse effects on Fusarium head blight infection. Theor Appl Genet 131(6):1263–1272. https://doi.org/10.1007/s00122-018-3076-8
Hinson PO, Adams CB, Dong X, Xue Q, Thapa S, Feng G, Kimura E, Pinchak B, Somenahally A, Ibrahim AMH (2022) Path analysis of phenotypic factors associated with grain protein in dryland winter wheat. J Crop Improv. https://doi.org/10.1080/15427528.2022.2042882
Huang M, Liu X, Zhou Y, Summers RM, Zhang Z (2019) BLINK a package for the next level of genome-wide association studies with both individuals and markers in the millions. GigaScience. 8(2):giy154. https://doi.org/10.1093/gigascience/giy154
Jiang Y, Zhao Y, Rodemann B, Plieske J, Kollers S, Korzun V, Ebmeyer E, Argillier O, Hinze M, Ling J, Röder MS, Ganal MW, Mette MF, Reif JC (2015) Potential and limits to unravel the genetic architecture and predict the variation of Fusarium head blight resistance in European winter wheat (*Triticum aestivum L*). Heredity 114(3):318–326. https://doi.org/10.1038/hdy.2014.104
Juliana P, Singh RP, Singh PK, Crossa J, Rutkoski JE, Poland JA, Bergstrom GC, Sorrells ME (2017) Comparison of models and

whole-genome profiling approaches for genomic-enabled prediction of *Septoria Tritici* Blotch, *Stagonospora Nodorum* Blotch, and tan spot resistance in wheat. Plant Genome 10(2):plantgenome2016.2008.0082. https://doi.org/10.3835/plantgenome2016.08.0082

Juliana P, He X, Marza F, Islam R, Anwar B, Poland J, Shrestha S, Singh GP, Chawade A, Joshi AK, Singh RP, Singh PK (2022) Genomic selection for wheat blast in a diversity panel, breeding panel and full-sibs panel. Front Plant Sci. https://doi.org/10.3389/fpls.2021.745379

Kaler AS, Gillman JD, Beissinger T, Purcell LC (2020) Comparing different statistical models and multiple testing corrections for association mapping in soybean and maize. Front Plant Sci. https://doi.org/10.3389/fpls.2019.01794

Kawada N, Kubo K (2008) Genotypic difference in resistance to Fusarium head blight and toxin accumulation in barley. In: Cereal Research Communications. 107–108

Khadka K, Kaviani M, Raizada MN, Navabi A (2021) Phenotyping and identification of reduced height (Rht) alleles (Rht-B1b and Rht-D1b) in a Nepali Spring wheat (*Triticum aestivum L*) diversity panel to enable seedling vigor selection. Agronomy. https://doi.org/10.3390/agronomy11122412

Khan MMH, Rafii MY, Ramlee SI, Jusoh M, Al Mamun M (2022) Path-coefficient and correlation analysis in bambara groundnut (Vigna subterranea [L] Verdc) accessions over environments. Sci Rep 12(1):245. https://doi.org/10.1038/s41598-021-03692-z

Korte A, Vilhjálmsson BJ, Segura V, Platt A, Long Q, Nordborg M (2012) A mixed-model approach for genome-wide association studies of correlated traits in structured populations. Nat Genet 44(9):1066–1071. https://doi.org/10.1038/ng.2376

Kubo K, Kawada N, Fujita M, Hatta K, Oda S, Nakajima T (2010) Effect of cleistogamy on Fusarium head blight resistance in wheat. Breed Sci 60(4):405–411. https://doi.org/10.1270/jsbbs.60.405

Liu Y, Salsman E, Fiedler JD, Hegstad JB, Green A, Mergoum M, Zhong S, Li X (2019) Genetic mapping and prediction analysis of FHB resistance in a hard red spring wheat breeding population. Front Plant Sci. https://doi.org/10.3389/fpls.2019.01007

Lu Q, Lillemo M, Skinnes H, He X, Shi J, Ji F, Dong Y, Bjørnstad Å (2013) Anther extrusion and plant height are associated with type I resistance to Fusarium head blight in bread wheat line 'Shanghai-3/Catbird.' Theor Appl Genet 126(2):317–334. https://doi.org/10.1007/s00122-012-1981-9

Mao S-L, Wei Y-M, Cao W, Lan X-J, Yu M, Chen Z-M, Chen G-Y, Zheng Y-L (2010) Confirmation of the relationship between plant height and Fusarium head blight resistance in wheat (Triticum aestivum L) by QTL meta-analysis. Euphytica 174(3):343–356. https://doi.org/10.1007/s10681-010-0128-9

Meier U (2001) BBCH Monograph: growth stages of mono-and dicotyledonous plants. 2 edn edn. Federal Biological Research Centre for Agriculture and Forestry, Bonn

Merrick LF, Burke AB, Zhang Z, Carter AH (2022) Comparison of single-trait and multi-trait genome-wide association models and inclusion of correlated traits in the dissection of the genetic architecture of a complex trait in a breeding program. Front Plant Sci. https://doi.org/10.3389/fpls.2021.772907

Mesterházy A (1995) Types and components of resistance to Fusarium head blight of wheat. Plant Breed 114(5):377–386. https://doi.org/10.1111/j.1439-0523.1995.tb00816.x

Miedaner T, Juroszek P (2021) Climate change will influence disease resistance breeding in wheat in Northwestern Europe. Theor Appl Genet 134(6):1771–1785. https://doi.org/10.1007/s00122-021-03807-0

Miedaner T, Ziegler D, Geiger H (1995) Variation and covariation for quantitative resistance to head blight (*Fusarium culmorum*) in two testcross series of S_2 lines in winter rye. Plant Breed 114(2):155–159. https://doi.org/10.1111/j.1439-0523.1995.tb00781.x

Miedaner T, Gang G, Geiger H (1996) Quantitative-genetic basis of aggressiveness of 42 isolates of *Fusarium culmorum* for winter rye head blight. Plant Dis 80(5):500–504

Miedaner T, Wilde F, Steiner B, Buerstmayr H, Korzun V, Ebmeyer E (2006) Stacking quantitative trait loci (QTL) for Fusarium head blight resistance from non-adapted sources in an European elite spring wheat background and assessing their effects on deoxynivalenol (DON) content and disease severity. Theor Appl Genet 112(3):562–569. https://doi.org/10.1007/s00122-005-0163-4

Miedaner T, Herter CP, Ebmeyer E, Kollers S, Korzun V (2019) Use of non-adapted quantitative trait loci for increasing Fusarium head blight resistance for breeding semi-dwarf wheat. Plant Breed 138(2):140–147. https://doi.org/10.1111/pbr.12683

Miedaner T, Lenhardt M, Grehl J, Gruner P, Koch S (2022) Dwarfing gene *Rht24* does not affect Fusarium head blight resistance in a large European winter wheat diversity panel. Euphytica 218(6):73. https://doi.org/10.1007/s10681-022-03028-6

Moreno-Amores J, Michel S, Miedaner T, Longin CFH, Buerstmayr H (2020) Genomic predictions for Fusarium head blight resistance in a diverse durum wheat panel: an effective incorporation of plant height and heading date as covariates. Euphytica 216(2):22. https://doi.org/10.1007/s10681-019-2551-x

Morrell CH (1998) Likelihood ratio testing of variance components in the linear mixed-effects model using restricted maximum likelihood. Biometrics. https://doi.org/10.2307/2533680

Muqaddasi QH, Reif JC, Röder MS, Basnet BR, Dreisigacker S (2019) Genetic mapping reveals large-effect QTL for anther extrusion in CIMMYT Spring wheat. Agronomy. https://doi.org/10.3390/agronomy9070407

Nannuru VKR, Windju SS, Belova T, Dieseth JA, Alsheikh M, Dong Y, McCartney CA, Henriques MA, Buerstmayr H, Michel S, Meuwissen THE, Lillemo M (2022) Genetic architecture of Fusarium head blight disease resistance and associated traits in Nordic spring wheat. Theor Appl Genet. https://doi.org/10.1007/s00122-022-04109-9

Olivoto T, de Souza VQ, Nardino M, Carvalho IR, Ferrari M, de Pelegrin AJ, Szareski VJ, Schmidt D (2017) Multicollinearity in path analysis: a simple method to reduce its effects. Agron J 109(1):131–142. https://doi.org/10.2134/agronj2016.04.0196

Ollier M, Talle V, Brisset A-L, Le Bihan Z, Duerr S, Lemmens M, Goudemand E, Robert O, Hilbert J-L, Buerstmayr H (2020) QTL mapping and successful introgression of the spring wheat-derived QTL *Fhb1* for Fusarium head blight resistance in three European triticale populations. Theor Appl Genet 133(2):457–477. https://doi.org/10.1007/s00122-019-03476-0

Ould Estaghvirou SB, Ogutu JO, Schulz-Streeck T, Knaak C, Ouzunova M, Gordillo A, Piepho H-P (2013) Evaluation of approaches for estimating the accuracy of genomic prediction in plant breeding. BMC Genet 14(1):860. https://doi.org/10.1186/1471-2164-14-860

Ozukum W, Avinashe H, Dubey N, Kalubarme S, Kumar M (2019) Correlation and path coefficient analyses in bread wheat (Triticum aestivum L). Plant Arch 19(2):3033–3038

Piepho H-P, Möhring J (2007) Computing heritability and selection response from unbalanced plant breeding trials. Genetics 177(3):1881–1888. https://doi.org/10.1534/genetics.107.074229

Piepho H, Williams E, Fleck M (2006) A note on the analysis of designed experiments with complex treatment structure. HortScience 41(2):446–452

Prat N, Guilbert C, Prah U, Wachter E, Steiner B, Langin T, Robert O, Buerstmayr H (2017) QTL mapping of Fusarium head blight

resistance in three related durum wheat populations. Theor Appl Genet 130(1):13–27. https://doi.org/10.1007/s00122-016-2785-0

R Core Team (2021) R: a language and environment for statistical computing. Version 4.1.3. R Foundation for Statistical Computing, https://www.R-project.org/, Vienna, Austria

Raherison E, Majidi MM, Goessen R, Hughes N, Cuthbert R, Knox R, Lukens L (2020) Evidence for the accumulation of nonsynonymous mutations and favorable pleiotropic alleles during wheat breeding. G3 Genes Genomes Genet 10(11):4001–4011. https://doi.org/10.1534/g3.120.401269

Righetti L, Bhandari DR, Rolli E, Tortorella S, Bruni R, Dall'Asta C, Spengler B (2021) Mycotoxin uptake in wheat-Eavesdropping Fusarium presence for priming plant defenses or a trojan horse to weaken them? Front Plant Sci. https://doi.org/10.3389/fpls.2021.711389

Ruan Y, Zhang W, Knox RE, Berraies S, Campbell HL, Ragupathy R, Boyle K, Polley B, Henriquez MA, Burt A, Kumar S, Cuthbert RD, Fobert PR, Buerstmayr H, DePauw RM (2020) Characterization of the genetic architecture for Fusarium head blight resistance in durum wheat: the complex association of resistance, flowering time, and height genes. Front Plant Sci. https://doi.org/10.3389/fpls.2020.592064

Sanchez-Garcia M, Bentley AR (2019) Chapter 9 Global journeys of adaptive wheat genes. In: Miedaner T, Korzun V (eds) Applications of genetic and genomic research in cereals. Woodhead Publishing. https://doi.org/10.1016/B978-0-08-102163-7.00009-0

Sandhu KS, Mihalyov PD, Lewien MJ, Pumphrey MO, Carter AH (2021) Genomic selection and genome-wide association studies for grain protein content stability in a nested association mapping population of wheat. Agronomy. https://doi.org/10.3390/agronomy11122528

Sari E, Berraies S, Knox RE, Singh AK, Ruan Y, Cuthbert RD, Pozniak CJ, Henriquez MA, Kumar S, Burt AJ, N'Diaye A, Konkin DJ, Cabral AL, Campbell HL, Wiebe K, Condie J, Lokuruge P, Meyer B, Fedak G, Clarke FR, Clarke JM, Somers DJ, Fobert PR (2018) High density genetic mapping of Fusarium head blight resistance QTL in tetraploid wheat. PLoS ONE 13(10):e0204362. https://doi.org/10.1371/journal.pone.0204362

Sari E, Knox RE, Ruan Y, Henriquez MA, Kumar S, Burt AJ, Cuthbert RD, Konkin DJ, Walkowiak S, Campbell HL, Singh AK, Ross J, Lokuruge P, Hsueh E, Boyle K, Sidebottom C, Condie J, Yates S, Pozniak CJ, Fobert PR (2020) Historic recombination in a durum wheat breeding panel enables high-resolution mapping of Fusarium head blight resistance quantitative trait loci. Sci Rep 10(1):7567. https://doi.org/10.1038/s41598-020-64399-1

Schulthess AW, Reif JC, Ling J, Plieske J, Kollers S, Ebmeyer E, Korzun V, Argillier O, Stiewe G, Ganal MW, Röder MS, Jiang Y (2017) The roles of pleiotropy and close linkage as revealed by association mapping of yield and correlated traits of wheat (Triticum aestivum L). J Exp Bot 68(15):4089–4101. https://doi.org/10.1093/jxb/erx214

Sidhu JS, Singh D, Gill HS, Brar NK, Qiu Y, Halder J, Al TR, Turnipseed B, Sehgal SK (2020) Genome-wide association study uncovers novel genomic regions associated with coleoptile length in hard winter wheat. Front Genet. https://doi.org/10.3389/fgene.2019.01345

Snijders C, Perkowski J (1990) Effects of head blight caused by *Fusarium culmorum* on toxin content and weight of wheat kernels. Phytopathology 80(6):566–570

Srinivasachary GN, Steed A, Hollins TW, Bayles R, Jennings P, Nicholson P (2008) Semi-dwarfing *Rht-B1* and *Rht-D1* loci of wheat differ significantly in their influence on resistance to Fusarium head blight. Theor Appl Genet 118(4):695. https://doi.org/10.1007/s00122-008-0930-0

Stage FK, Carter HC, Nora A (2010) Path analysis: an introduction and analysis of a decade of research. J Educ Res 98(1):5–13. https://doi.org/10.3200/JOER.98.1.5-13

Steiner B, Buerstmayr M, Wagner C, Danler A, Eshonkulov B, Ehn M, Buerstmayr H (2019a) Fine-mapping of the Fusarium head blight resistance QTL Qfhs.ifa-5A identifies two resistance QTL associated with anther extrusion. Theor Appl Genet 132(7):2039–2053. https://doi.org/10.1007/s00122-019-03336-x

Steiner B, Michel S, Maccaferri M, Lemmens M, Tuberosa R, Buerstmayr H (2019b) Exploring and exploiting the genetic variation of Fusarium head blight resistance for genomic-assisted breeding in the elite durum wheat gene pool. Theor Appl Genet 132(4):969–988. https://doi.org/10.1007/s00122-018-3253-9

Stram DO, Lee JW (1994) Variance components testing in the longitudinal mixed effects model. Biometrics 50(4):1171–1177. https://doi.org/10.2307/2533455

Su Z, Bernardo A, Tian B, Chen H, Wang S, Ma H, Cai S, Liu D, Zhang D, Li T, Trick H, Amand StP, Yu J, Zhang Z, Bai G (2019) A deletion mutation in *TaHRC* confers *Fhb1* resistance to Fusarium head blight in wheat. Nat Genet 51(7):1099–1105. https://doi.org/10.1038/s41588-019-0425-8

Tang C, Li M, Cao M, Lu R, Zhang H, Liu C, Huang S, Zhang P, Hu H, Zhao W, Wu L (2020) Transcriptome analysis suggests mechanisms for a novel flowering type: Cleistogamous wheat. Crop J 8(2):313–326. https://doi.org/10.1016/j.cj.2019.08.009

Tian X, Wen W, Xie L, Fu L, Xu D, Fu C, Wang D, Chen X, Xia X, Chen Q, He Z, Cao S (2017) Molecular mapping of reduced plant height gene *Rht24* in bread wheat. Front Plant Sci. https://doi.org/10.3389/fpls.2017.01379

Tian X, Zhu Z, Xie L, Xu D, Li J, Fu C, Chen X, Wang D, Xia X, He Z, Cao S (2019) Preliminary exploration of the source, spread, and distribution of *Rht24* reducing height in bread wheat. Crop Sci 59(1):19–24. https://doi.org/10.2135/cropsci2017.12.0711

Tian X, Xia X, Xu D, Liu Y, Xie L, Hassan MA, Song J, Li F, Wang D, Zhang Y, Hao Y, Li G, Chu C, He Z, Cao S (2022) *Rht24b*, an ancient variation of *TaGA2ox-A9*, reduces plant height without yield penalty in wheat. New Phytol 233(2):738–750. https://doi.org/10.1111/nph.17808

Timmusk S, Nevo E, Ayele F, Noe S, Niinemets Ü (2020) Fighting Fusarium pathogens in the era of climate change: a conceptual approach. Pathogens. https://doi.org/10.3390/pathogens9060419

Toebe M, Cargnelutti Filho A (2013) Multicollinearity in path analysis of maize (Zea mays L). J Cereal Sci 57(3):453–462. https://doi.org/10.1016/j.jcs.2013.01.014

Topi D, Babič J, Pavšič-Vrtač K, Tavčar-Kalcher G, Jakovac-Strajn B (2021) Incidence of Fusarium mycotoxins in wheat and maize from Albania. Molecules. https://doi.org/10.3390/molecules26010172

Usman MG, Rafii MY, Martini MY, Oladosu Y, Kashiani P (2017) Genotypic character relationship and phenotypic path coefficient analysis in chili pepper genotypes grown under tropical condition. J Sci Food Agric 97(4):1164–1171. https://doi.org/10.1002/jsfa.7843

Utz HF, Melchinger AE, Schön CC (2000) Bias and sampling error of the estimated proportion of genotypic variance explained by quantitative trait loci determined from experimental data in maize using cross validation and validation with independent samples. Genetics 154(4):1839–1849. https://doi.org/10.1093/genetics/154.4.1839

Valente BD, Rosa GJM, Gianola D, Wu X-L, Weigel K (2013) Is structural equation modeling advantageous for the genetic improvement of multiple traits? Genetics 194(3):561–572. https://doi.org/10.1534/genetics.113.151209

Van De Velde K, Thomas SG, Heyse F, Kaspar R, Van Der Straeten D, Rohde A (2021) N-terminal truncated *RHT-1* proteins generated by translational reinitiation cause semi-dwarfing of wheat Green

Revolution alleles. Mol Plant 14(4):679–687. https://doi.org/10.1016/j.molp.2021.01.002
VanRaden PM (2008) Efficient methods to compute genomic predictions. Int J Dairy Sci 91(11):4414–4423. https://doi.org/10.3168/jds.2007-0980
Venske E, dos Santos RS, Farias DDR, Rother V, da Maia LC, Pegoraro C, de Costa Oliveira A (2019) Meta-analysis of the QTLome of Fusarium head blight resistance in bread wheat: refining the rurrent puzzle. Front Plant Sci. https://doi.org/10.3389/fpls.2019.00727
Wang J, Zhang Z (2021) GAPIT version 3: boosting power and accuracy for genomic association and prediction. Genom Proteomics Bioinform. https://doi.org/10.1016/j.gpb.2021.08.005
Wickham H, Chang W, Henry L, Pedersen TL, Takahashi K, Wilke C, Woo K, Yutani H, Dunnington D (2021) Package 'ggplot2': create elegant data visualisations using the grammar of graphics. Version 3.3.5. https://github.com/tidyverse/ggplot2
Wilkinson PA, Allen AM, Tyrrell S, Wingen LU, Bian X, Winfield MO, Burridge A, Shaw DS, Zaucha J, Griffiths S, Davey RP, Edwards KJ, Barker GLA (2020) CerealsDB—new tools for the analysis of the wheat genome: update 2020. Database 2020:baaa060.https://doi.org/10.1093/database/baaa060
Wilson W, Dahl B, Nganje W (2018) Economic costs of Fusarium head blight, scab and deoxynivalenol. World Mycotoxin J 11(2):291–302. https://doi.org/10.3920/WMJ2017.2204
Windels CE (2000) Economic and social impacts of Fusarium head blight: Changing farms and rural communities in the northern great plains. Phytopathology 90(1):17–21. https://doi.org/10.1094/PHYTO.2000.90.1.17
Wright S (1918) On the nature of size factors. Genetics 3(4):367–374. https://doi.org/10.1093/genetics/3.4.367
Wright S (1922) Coefficients of inbreeding and relationship. Am Nat 56(645):330–338. https://doi.org/10.1086/279872
Wright S (1934) The method of path coefficients. Ann Math Stat 5(3):161–215. https://doi.org/10.1214/aoms/1177732676
Würschum T, Langer SM, Longin CFH (2015) Genetic control of plant height in European winter wheat cultivars. Theor Appl Genet 128(5):865–874. https://doi.org/10.1007/s00122-015-2476-2
Würschum T, Langer SM, Longin CFH, Tucker MR, Leiser WL (2017) A modern green revolution gene for reduced height in wheat. Plant J 92(5):892–903. https://doi.org/10.1111/tpj.13726
Xu K, He X, Dreisigacker S, He Z, Singh PK (2020) Anther extrusion and its association with Fusarium head blight in CIMMYT wheat germplasm. Agronomy. https://doi.org/10.3390/agronomy10010047
Yin L, Zhang H, Tang Z, Xu J, Yin D, Zhang Z, Yuan X, Zhu M, Zhao S, Li X, Liu X (2021) rMVP: a memory-efficient, visualization-enhanced, and parallel-accelerated tool for genome-wide association study. Genom Proteomics Bioinform 19(4):619–628. https://doi.org/10.1016/j.gpb.2020.10.007
Yoshiki A, Moriwaki K (2006) Mouse phenome research: implications of genetic background. ILAR J 47(2):94–102. https://doi.org/10.1093/ilar.47.2.94
Zajączkowska U, Denisow B, Łotocka B, Dołkin-Lewko A, Rakoczy-Trojanowska M (2021) Spikelet movements, anther extrusion and pollen production in wheat cultivars with contrasting tendencies to cleistogamy. BMC Plant Biol 21(1):136. https://doi.org/10.1186/s12870-021-02917-7
Zhang W, Boyle K, Brûlé-Babel AL, Fedak G, Gao P, Robleh DZ, Polley B, Cuthbert RD, Randhawa HS, Jiang F, Eudes F, Fobert PR (2020) Genetic characterization of multiple components contributing to Fusarium head blight resistance of FL62R1, a Canadian bread wheat developed using systemic breeding. Front Plant Sci. https://doi.org/10.3389/fpls.2020.580833
Zhang Y, Yang Z, Ma H, Huang L, Ding F, Du Y, Jia H, Li G, Kong Z, Ran C, Gu Z, Ma Z (2021) Pyramiding of Fusarium head blight resistance quantitative trait loci, Fhb1, Fhb4, and Fhb5, in modern Chinese wheat cultivars. Front Plant Sci. https://doi.org/10.3389/fpls.2021.694023
Zhao Z, Wang E, Kirkegaard JA, Rebetzke GJ (2022) Novel wheat varieties facilitate deep sowing to beat the heat of changing climates. Nat Clim Chang 12(3):291–296. https://doi.org/10.1038/s41558-022-01305-9
Zheng X (2015) Tutorials for the R/Bioconductor package SNPRelate. Department of Biostatistics, University of Washington, Seattle, USA, http://corearray.sourceforge.net/
Zhu T, Wang L, Rimbert H, Rodriguez JC, Deal KR, De Oliveira R, Choulet F, Keeble-Gagnère G, Tibbits J, Rogers J, Eversole K, Appels R, Gu YQ, Mascher M, Dvorak J, Luo M-C (2021) Optical maps refine the bread wheat *Triticum aestivum* cv. Chinese Spring Genome Assembly Plant J 107(1):303–314. https://doi.org/10.1111/tpj.15289
Zou KH, Tuncali K, Silverman SG (2003) Correlation and simple linear regression. Radiology 227(3):617–628. https://doi.org/10.1148/radiol.2273011499

Separation of the effects of two reduced height (*Rht*) genes and genomic background to select for less Fusarium head blight of short-strawed winter wheat (*Triticum aestivum* L.) varieties

Félicien Akohoue[1], Silvia Koch[1], Jörg Plieske[2], Thomas Miedaner[1*]

Supplementary information

Supplementary Tables

Table S1: Best linear unbiased estimations (BLUEs) of the eight traits across five environments. Available online at: https://static-content.springer.com/esm/art%3A10.1007%2Fs00122-022-04219-4/MediaObjects/122_2022_4219_MOESM1_ESM.xlsx

Table S2: SNP markers associated with plant height, FHB severity and anther retention from single trait genome-wide association study (ST-GWAS) models

Model[a]	Marker	Chr	Pos (Mbp)	UA/FA	FAF	-LOG10(p)	p_G (%)	Additive effect	FDR(p)
PH									
1	*rs20873*	4D	19.19	G/T	0.49	68.79	45.21	–7.02	3.3E-65
1	*rs10110*	6A	398.61	A/G	0.61	14.26	10.81	–3.93	2.2E-06
1 & 2	*rs13233*	2A	628.21	T/C	0.94	9.51	5.54	5.72	1.6E-06
1 & 2	*rs11421*	3B	850.79	A/G	0.13	10.11	3.11	0.03	5.2E-07
1 & 2	*rs23089*	3A	63.46	A/C	0.66	11.13	2.74	–2.02	7.5E-08
1 & 2	*rs8777*	5B	6.42	C/T	0.13	8.25	1.83	–1.99	8.6E-03
2	*rs19377*	5B	21.97	G/A	0.31	8.13	0.40	1.52	3.2E-05
1 & 2	*rs13973*	5B	21.76	T/C	0.70	7.33	0.05	1.60	1.6E-04
Total							69.69		
FHB severity									
1	*rs20873*	4D	19.19	T/G	0.51	15.42	26.36	5.97	7.6E-12
1 & 2	*rs3647*	5A	521.42	G/A	0.60	9.43	7.07	4.15	1.1E-03
1 & 2	*rs5192*	7B	661.18	A/G	0.66	6.83	7.03	5.27	2.2E-03
1 & 2	*rs13165*	2B	19.47	A/G	0.94	9.00	5.00	1.76	1.0E-05
1 & 2	*rs7788*	2A	419.17	A/G	0.36	8.62	3.83	–1.13	1.2E-05
1	*rs11875*	6A	2.73	T/C	0.84	8.15	3.41	2.67	2.8E-04
2	*rs4867*	6B	695.72	A/G	0.58	7.85	2.42	3.52	7.1E-05
1	*rs17561*	2B	54.19	T/C	0.93	10.44	1.84	2.01	1.1E-03
2	*rs14988*	2B	65.86	G/A	0.11	7.47	1.66	–3.89	1.4E-04
1	*rs8786*	4A	748.35	A/G	0.18	8.00	1.16	–1.41	2.2E-03
1	*rs1410*	4A	11.72	G/A	0.51	8.75	1.02	–1.99	1.2E-05
Total							60.74		
AR									
1	*rs20873*	4D	19.19	T/G	0.51	8.17	20.96	12.00	3.9E-03
1 & 2	*rs3629*	4A	712.25	G/A	0.16	8.76	8.47	–8.22	1.2E-05
2	*rs8776*	3A	521.92	A/G	0.83	8.04	5.07	6.12	3.6E-05
1 & 2	*rs7788*	2A	419.17	A/G	0.36	10.43	3.21	–2.72	7.4E-07
2	*rs7921*	3A	700.86	A/T	0.20	10.20	3.12	–7.86	3.1E-07

Model[a]	Marker	Chr	Pos (Mbp)	UA/FA	FAF	-LOG10(p)	p_G (%)	Additive effect	FDR(p)
1	*rs17724*	7A	694.67	A/G	0.16	9.48	2.21	–8.75	3.3E-06
1 & 2	*rs18356*	7A	207.68	G/A	0.54	8.40	0.71	1.02	2.0E-03
2	*rs10472*	5A	21.20	A/G	0.75	7.53	0.22	4.99	6.6E-04
2	*rs19553*	7A	654.74	C/T	0.42	7.32	0.20	0.71	1.6E-04
Total							44.17		

[a]: 1 = ST-GWAS$_1$ model where all markers were included, 2 = ST-GWAS$_2$ without markers linked to plant height on chromosomes 4D (*Rht-D1*) and 6A (*Rht24*); Chr = chromosome, Pos = physical position from the wheat reference genome RefSeq v.2.1, UA/FA = unfavourable allele /favourable allele, FAF = favourable allele frequency, -LOG10(p) = negative logarithm of p-value, p_G = proportion of genotypic variance explained, FDR (p) = false discovery rate p-value, PH = plant height, and AR = anther retention. Only -LOG10(p) and FDR (p) of ST-GWAS$_1$ were reported for significant markers which were common to both models

Table S3: Genomic prediction ability (rMG) and accuracy (rMG/H) for the five cross-validation sets including all markers

Sets	PH (cm)		FHB severity (%)		AR (%)	
	rMG	rMG/H	rMG	rMG/H	rMG	rMG/H
1	0.78	0.79	0.66	0.69	0.63	0.65
2	0.76	0.77	0.67	0.70	0.76	0.78
3	0.87	0.88	0.77	0.80	0.71	0.73
4	0.74	0.75	0.67	0.70	0.69	0.71
5	0.71	0.72	0.73	0.76	0.70	0.72
Mean	0.77	0.78	0.70	0.73	0.70	0.72
SE	0.06	0.06	0.05	0.05	0.05	0.05

PH = plant height, FHB = Fusarium head blight, AR = anther retention, SE = standard error; average prediction ability and accuracy are highlighted in red. Prediction ability and accuracy were significant at $p<0.001$

Table S4: Distribution of *Rht* genotypes within cross-validation sets

Sets	No*Rht*	*Rht-D1b*	*Rht24b*	*Rht-D1b+Rht24b*	Set size
1	30	11	21	18	80
2	20	11	20	29	80
3	16	17	16	31	80
4	11	10	30	29	80
5	18	11	24	28	81
Total	95	60	111	135	401

Table S4: Genomic prediction ability (rMG) and accuracy (rMG/H) for the five cross-validation sets based on genomic background only

Sets	PH		FHB severity		AR	
	rMG	rMG/H	rMG	rMG/H	rMG	rMG/H
1	0.48	0.48	0.51	0.53	0.52	0.54
2	0.45	0.45	0.54	0.56	0.68	0.70
3	0.42	0.42	0.61	0.64	0.64	0.66
4	0.52	0.53	0.43	0.45	0.55	0.57
5	0.58	0.59	0.56	0.58	0.57	0.59
Mean	0.49	0.49	0.53	0.55	0.59	0.61
SE	0.06	0.07	0.07	0.07	0.07	0.07

SE = standard error; average prediction ability and accuracy are highlighted in red. Prediction ability and accuracy were significant at $p<0.001$

Table S6: Significant markers sequences and physical positions of candidate genes. Available online at: https://static-content.springer.com/esm/art%3A10.1007%2Fs00122-022-04219-4/MediaObjects/122_2022_4219_MOESM1_ESM.xlsx

Supplementary Figures

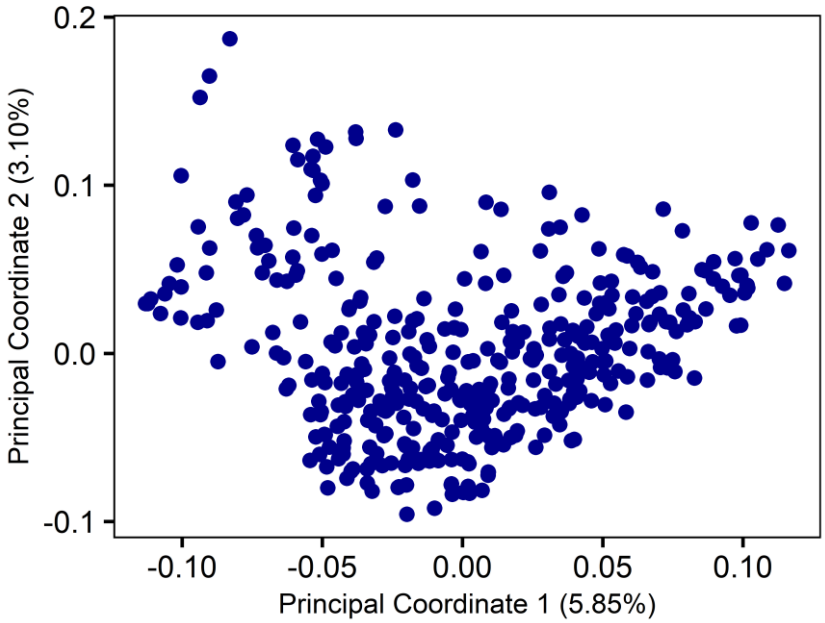

Fig. S1: Principal coordinate analysis of the 401 wheat genotypes included in the study

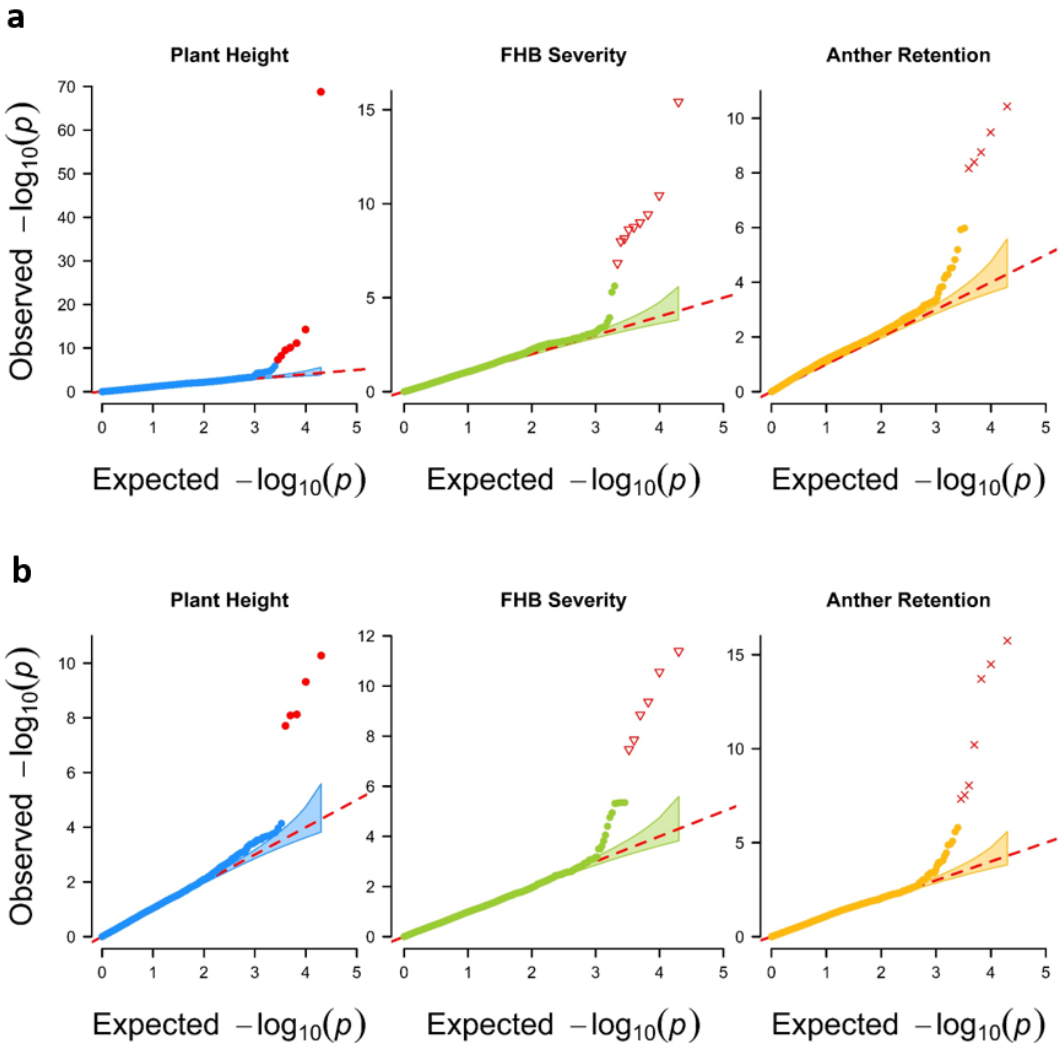

Fig. S2: Quantile-Quantile (Q-Q) plots showing the existence of true marker-trait associations (MTAs) from single trait genome-wide association studies (ST-GWAS): a = ST-GWAS$_1$ including all markers and b = ST-GWAS$_2$ without markers linked to plant height on chromosomes 4D (*Rht-D1*) and 6A (*Rht24*)

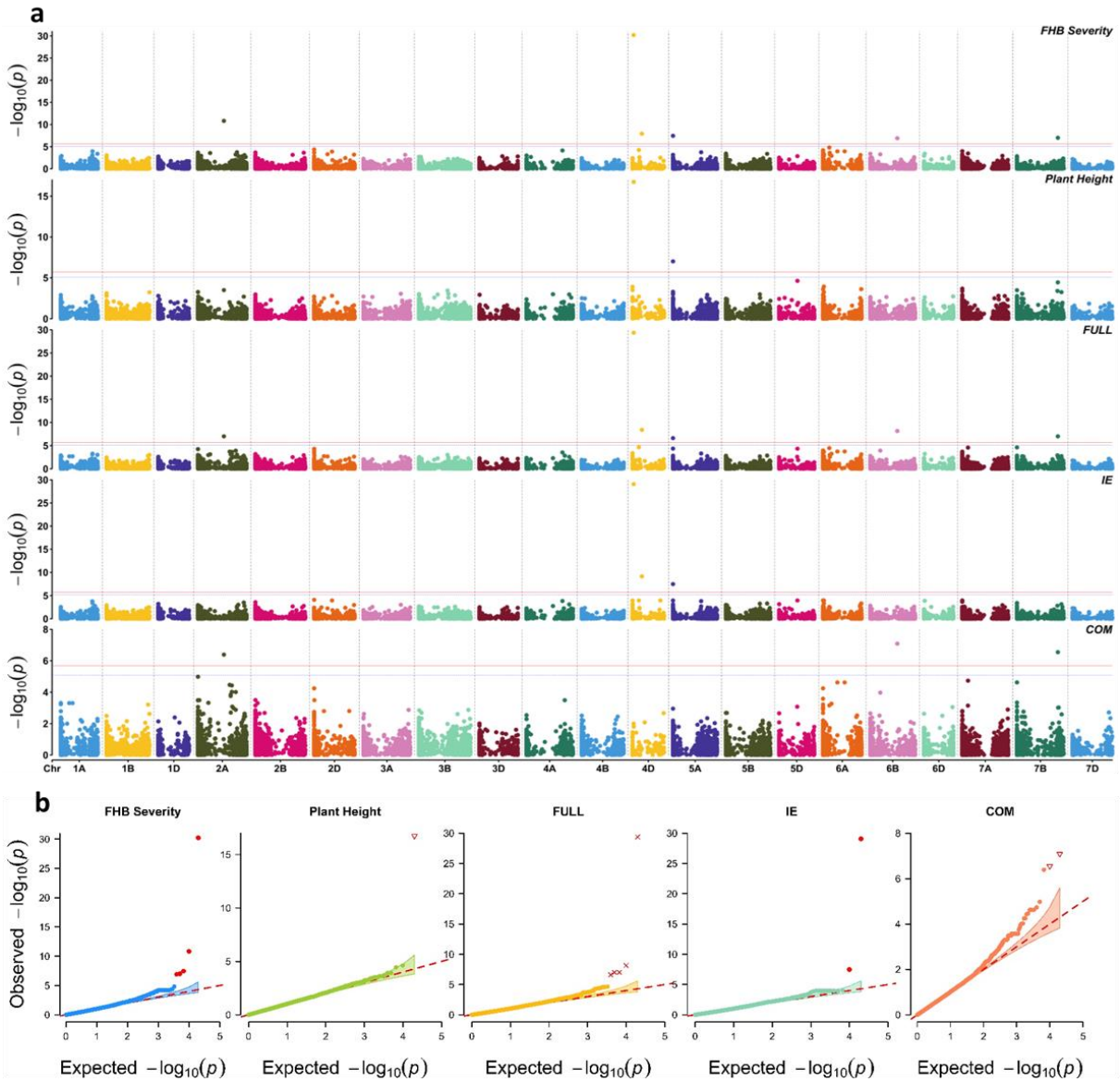

Fig. S3: Manhattan and Q-Q plots highlighting significant marker-trait associations (MTAs) for multi-trait genome-wide association studies (MT-GWAS): **a** = Manhattan plots of full model (FULL), common effects (COM), interaction effects (IE) between FHB severity and plant height; and **b** = Q-Q plots of full model (FULL), common effects (COM), interaction effects (IE) between FHB severity and plant height. The blue dotted line corresponds to an exploratory threshold of -LOG10(p) = 6 while the red plain line represents the Bonferroni corrected threshold cut-off of alpha = 0.01

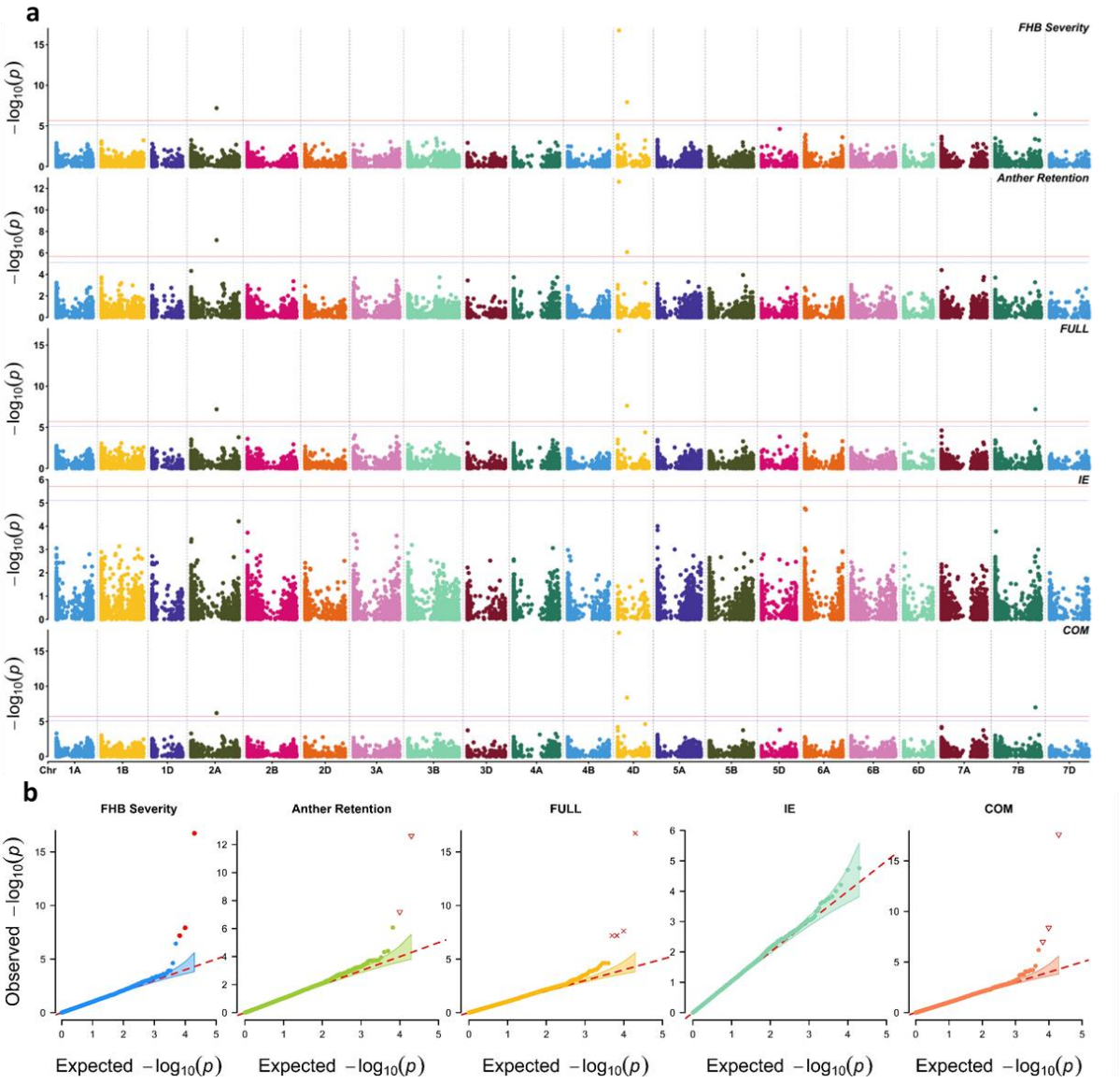

Fig. S4: Manhattan and Q-Q plots highlighting significant marker-trait associations (MTAs) for multi-trait genome-wide association studies (MT-GWAS). **a** = Manhattan plots of full model (FULL), common effects (COM), interaction effects (IE) between FHB severity and anther retention; and **b** = Q-Q plots of full model (FULL), common effects (COM), interaction effects (IE) between FHB severity and anther retention. The blue dotted line corresponds to an exploratory threshold of -LOG10(p) = 6 while the red plain line represents the Bonferroni-corrected threshold cut-off of alpha = 0.01

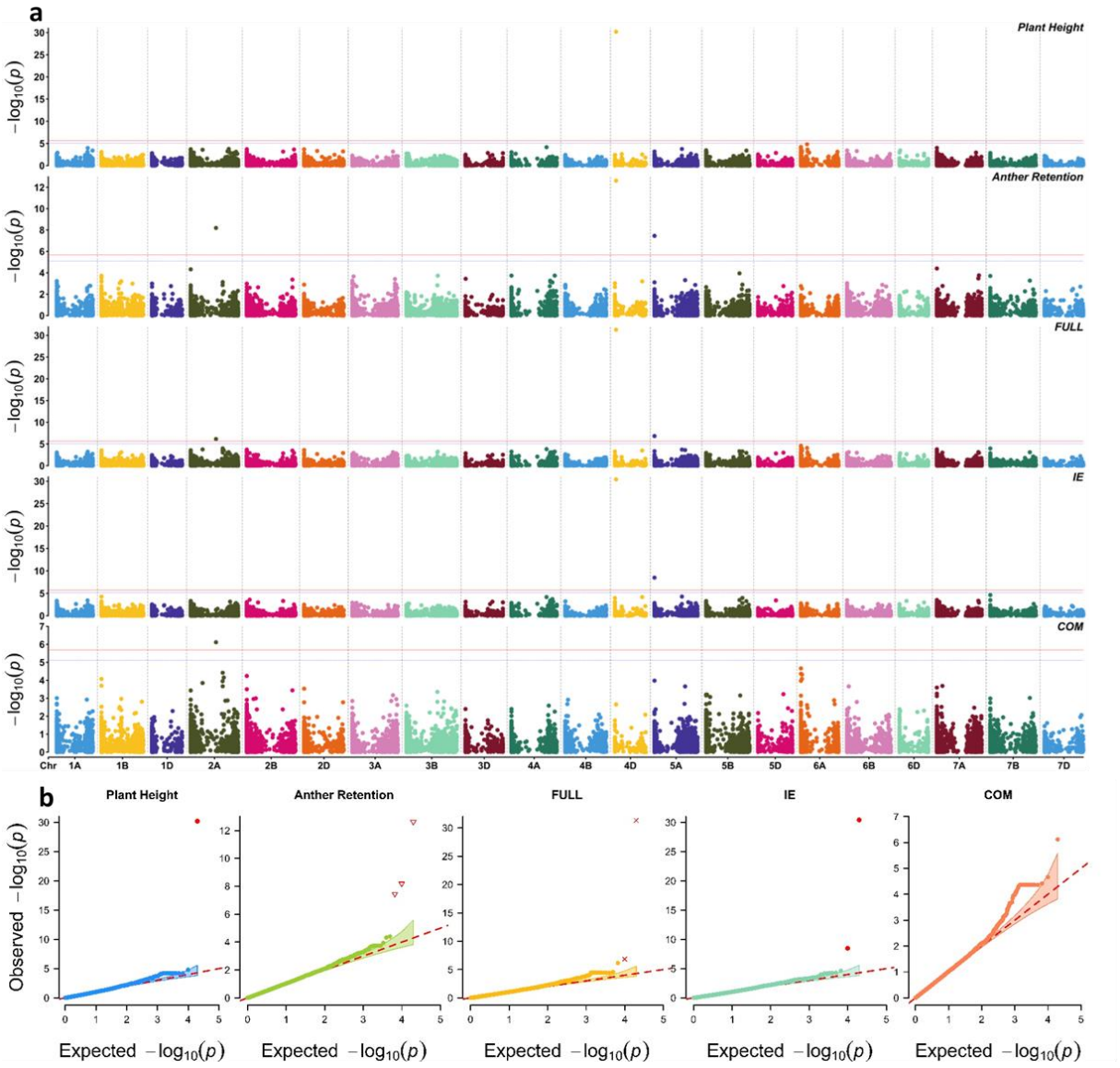

Fig. S5: Manhattan and Q-Q plots highlighting significant marker-trait associations (MTAs) for multi-trait genome-wide association studies (MT-GWAS). **a** = Manhattan plots of full model (FULL), common effects (COM), interaction effects (IE) between plant height and anther retention; and **b** = Q-Q plots of full model (FULL), common effects (COM), interaction effects (IE) between plant height and anther retention. The blue dotted line corresponds to an exploratory threshold of -LOG10(p) = 6 while the red plain line represents the Bonferroni-corrected threshold cut-off of alpha = 0.01

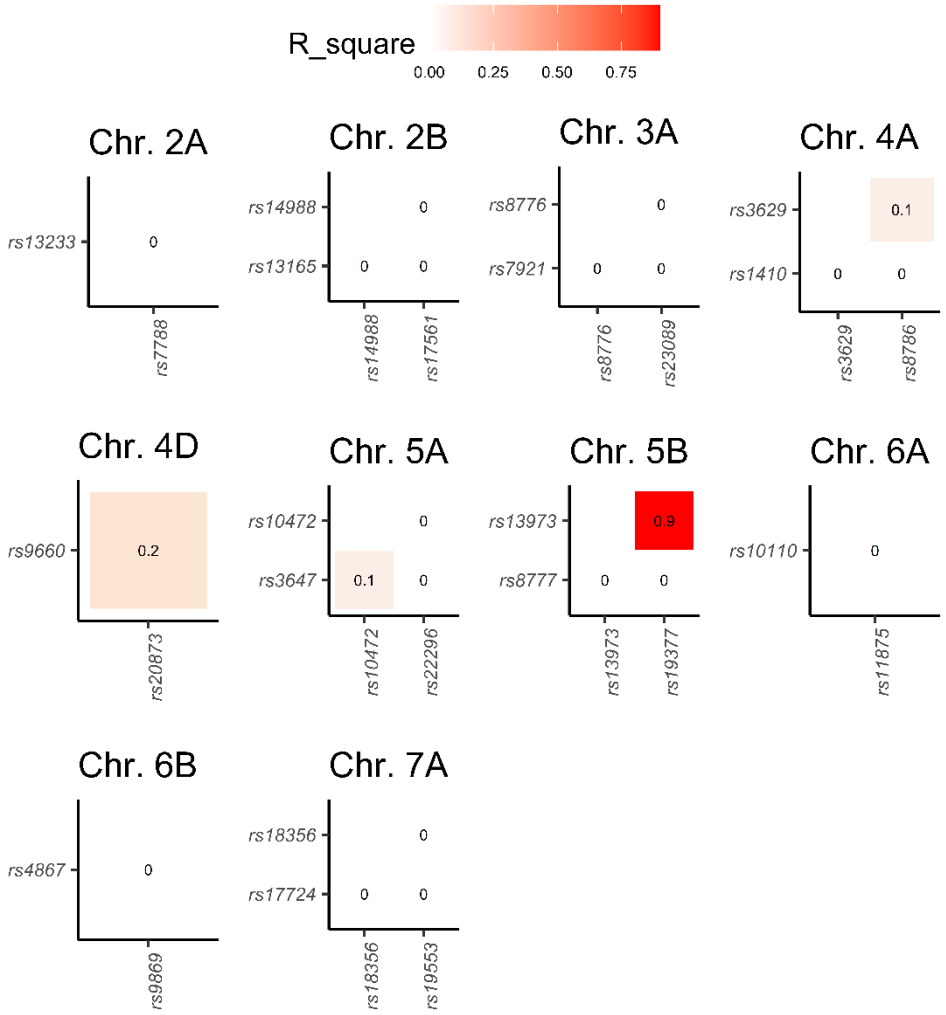

Fig. S6: Results of linkage disequilibrium among significant markers. Chr = chromosome

Chapter 3: Meta-analysis and co-expression analysis revealed stable QTL and candidate genes conferring resistances to Fusarium and Gibberella ear rots while reducing mycotoxin contamination in maize

Félicien Akohoue[1], Thomas Miedaner[1*]

[1]State Plant Breeding Institute, University of Hohenheim, Stuttgart, Germany;

*Correspondence: miedaner@uni-hohenheim.de (T.M.)

ORCID T.M.: https://orcid.org/0000-0002-9541-3726

Published in *Frontiers in Plant Science*. 2022; 13:1050891.

https://doi.org/10.3389/fpls.2022.1050891.

Submitted: 22 September 2022 / **Accepted**: 13 October 2022 / **Published**: 31 October 2022

frontiers | Frontiers in Plant Science

TYPE Systematic Review
PUBLISHED 31 October 2022
DOI 10.3389/fpls.2022.1050891

OPEN ACCESS

EDITED BY
Colin W. Hiebert,
Agriculture and Agri-Food Canada (AAFC), Canada

REVIEWED BY
German Sandoya,
University of Florida, United States
Malkhan Singh Gurjar,
Indian Agricultural Research Institute (ICAR), India

*CORRESPONDENCE
Thomas Miedaner
miedaner@uni-hohenheim.de

SPECIALTY SECTION
This article was submitted to Plant Breeding, a section of the journal Frontiers in Plant Science

RECEIVED 22 September 2022
ACCEPTED 13 October 2022
PUBLISHED 31 October 2022

CITATION
Akohoue F and Miedaner T (2022) Meta-analysis and co-expression analysis revealed stable QTL and candidate genes conferring resistances to Fusarium and Gibberella ear rots while reducing mycotoxin contamination in maize. *Front. Plant Sci.* 13:1050891. doi: 10.3389/fpls.2022.1050891

Meta-analysis and co-expression analysis revealed stable QTL and candidate genes conferring resistances to Fusarium and Gibberella ear rots while reducing mycotoxin contamination in maize

Félicien Akohoue and Thomas Miedaner*

State Plant Breeding Institute, University of Hohenheim, Stuttgart, Germany

Fusarium (FER) and Gibberella ear rots (GER) are the two most devastating diseases of maize (*Zea mays* L.) which reduce yield and affect grain quality worldwide, especially by contamination with mycotoxins. Genetic improvement of host resistance to effectively tackle FER and GER diseases requires the identification of stable quantitative trait loci (QTL) to facilitate the application of genomics-assisted breeding for improving selection efficiency in breeding programs. We applied improved meta-analysis algorithms to re-analyze 224 QTL identified in 15 studies based on dense genome-wide single nucleotide polymorphisms (SNP) in order to identify meta-QTL (MQTL) and colocalized genomic loci for fumonisin (FUM) and deoxynivalenol (DON) accumulation, silk (SR) and kernel (KR) resistances of both FER and GER, kernel dry-down rate (KDD) and husk coverage (HC). A high-resolution genetic consensus map with 36,243 loci was constructed and enabled the projection of 164 of the 224 collected QTL. Candidate genes (CG) mining was performed within the most refined MQTL, and identified CG were cross-validated using publicly available transcriptomic data of maize under *Fusarium graminearum* infection. The meta-analysis revealed 40 MQTL, of which 29 were associated each with 2-5 FER- and/or GER-related traits. Twenty-eight of the 40 MQTL were common to both FER and GER resistances and 19 MQTL were common to silk and kernel resistances. Fourteen most refined MQTL on chromosomes 1, 2, 3, 4, 7 and 9 harbored a total of 2,272 CG. Cross-validation identified 59 of these CG as responsive to FER and/or GER diseases. MQTL *ZmMQTL2.2*, *ZmMQTL9.2* and *ZmMQTL9.4* harbored promising resistance genes, of which *GRMZM2G011151* and *GRMZM2G093092* were specific to the resistant line for both diseases and encoded *"terpene synthase21 (tps21)"* and *"flavonoid O-methyltransferase2 (fomt2)"*, respectively. Our findings revealed stable refined MQTL harboring

promising candidate genes for use in breeding programs for improving FER and GER resistances with reduced mycotoxin accumulation. These candidate genes can be transferred into elite cultivars by integrating refined MQTL into genomics-assisted backcross breeding strategies.

KEYWORDS

Candidate genes, FUM and DON contaminations, Fusarium and Gibberella ear rots, genomic selection, QTL meta-analysis, type of resistance, *Zea mays* L.

Introduction

Maize (*Zea mays* L.) is the most important cereal crop in terms of grain production volume worldwide, and is set to become the first commercial crop in the coming decade (Shiferaw et al., 2011; Erenstein et al., 2022). The increase in production over the past quarter century was supported by more than 46 and 50% increase in area expansion and grain yield, respectively (Erenstein et al., 2022). Despite this remarkable progress and intensive research and development efforts deployed, maize production is still threatened by many biotic stress factors which are expected to worsen with the changing climate (Grote et al., 2021). About 38 pests and diseases were recently reported to cause 19–41% grain losses in maize on the global scale (Savary et al., 2019). Among these, Fusarium and Gibberella ear rots represent major yield- and quality-impacting maize diseases which occur across regions and countries (Eckard et al., 2011; Beukes et al., 2018; Ma et al., 2019; Perincherry et al., 2019; Machado et al., 2022).

Fusarium ear rot (FER) or "pink ear rot" is mainly caused by the *Fusarium fujikuroi* species complex with *F. verticillioides* (Sacc.) Nirenberg being the most harmful pathogen distributed across all continents with higher aggressiveness in warmer climatic regions (Boutigny et al., 2011; Tsehaye et al., 2017; Ncube et al., 2020). Meanwhile, Gibberella ear rot (GER), also known as "red ear rot" or "red fusariosis", is one of the most important maize ear rots in cooler climate zones, which is associated with the *F. graminearum* species complex with *F. graminearum sensu strictu* Schwabe (teleomorph *Gibberella zeae*) as the most dominant causal agent reported in North America, Australia, China and Europe (Gromadzka et al., 2016; Beukes et al., 2018; Castañares et al., 2019; Crippin et al., 2020; Pfordt et al., 2020; Dalla Lana et al., 2021; Machado et al., 2022). With the global changing climate and local weather variability and cultivation systems, both FER and GER are also frequently found on maize ears in the same locations with varying degrees of severity (Scauflaire et al., 2011; Schjøth and Sundheim, 2013; Shala-Mayrhofer et al., 2013; Pfordt et al., 2020; Czarnecka et al., 2022). Depending on the Fusarium species, different types of harmful mycotoxins are produced, of which fumonisins (FUM) and deoxynivalenol (DON) are the most predominant for FER and GER, respectively. FER and GER significantly reduce maize production and the accumulated mycotoxins can make the grains toxic for human consumption and animal feeding (Battilani and Logrieco, 2014; Logrieco et al., 2021).

Disease management practices such as tillage, crop rotation and fungicide application have minor effects on FER and GER severity and do not significantly increase the grain yield (Andriolli et al., 2016; Scarpino et al., 2018; Pfordt et al., 2020). In addition, available mycotoxin reduction technologies are labor- and cost-prohibitive, leading to a low adoption by farmers (Logrieco et al., 2021). Effective management strategies of FER and GER diseases and associated mycotoxins should consider integrating not only improved and environmentally friendly practices, but also improving plant resistance to the pathogens.

Several studies have reported germplasms with different levels of resistance to FER and GER worldwide (Reid et al., 2001a; Reid et al., 2001b; Reid et al., 2003; Gaikpa et al., 2021; Galiano-Carneiro et al., 2021). In Europe, Gaikpa et al. (2021) evaluated two European flint landrace populations ("*Kemater Landmais Gelb*" and "*Petkuser Ferdinand Rot*") and identified resistant lines which can be used for developing high-yielding hybrid cultivars with improved resistance to GER. In Canada, inbred lines with high resistance to FER and GER have been reported by Reid et al. (2001a; 2001b; 2003). Similarly, potential sources of resistance to FER were identified in China (Guo et al., 2020) and tropical regions including southern, western and central Africa (Tembo et al., 2022). The exploitation of existing resistance sources in breeding programs requires a clear understanding of the genetic architecture of FER- and GER-related traits, and underlying molecular mechanisms. FER and GER resistances are complex traits which were reported to be quantitatively inherited and are thus controlled by numerous quantitative trait loci (QTL) (Martin et al., 2012a; Butrón et al., 2015).

More than 300 QTL were reported for both FER and GER resistances and related traits in different mapping populations by applying both low-throughput technologies, namely single sequence repeats (SSR), restriction fragment

length polymorphisms (RFLP) and random amplified polymorphic DNA (RAPD) (Ali et al., 2005; Robertson-Hoyt et al., 2006; Li et al., 2011; Martin et al., 2011; Martin et al., 2012b), and dense genome-wide high-throughput technologies such as single nucleotide polymorphisms (SNP) (Giomi et al., 2016; Han et al., 2016; Kebede et al., 2016; Han et al., 2018; Wen et al., 2020; Yuan et al., 2020a; Gaikpa et al., 2021; Galiano-Carneiro et al., 2021; Zhou et al., 2021). This impressive amount of QTL reported through diverse studies offers a possibility for the application of genomics-assisted breeding strategies to efficiently and accurately improve ear rot resistances in maize. However, due to the complex nature of the traits, the application of these loci in breeding programs remains challenging and limited. Therefore, in order to make reported QTL more useful and facilitate their successful incorporation into breeding programs, a comprehensive and in-depth analysis of these loci needs to be carried out using appropriate statistical approaches like meta-analysis. QTL meta-analysis is an efficient approach which was developed by Goffinet and Gerber (2000) and has constantly improved during the past decade (Salvi and Tuberosa, 2015). The analysis allows the compilation of QTL observed in independent studies which are projected onto a consensus map in order to verify whether they represent a common genomic region on the genetic map or whether they correspond to different loci (Venske et al., 2019). This approach enables the identification of more refined and stable "real" QTL, also referred to as meta-QTL (MQTL), which are mostly involved in the variation of the traits. Moreover, in resistance breeding, the application of meta-analysis would help to identify refined (i.e. smaller in length) genomic regions which confer multi-disease resistances in crops. Furthermore, refined MQTL facilitate the identification and validation of candidate genes that are effectively involved into the variation of the traits. QTL meta-analysis has been successfully implemented to depict genetic architecture of different traits including Fusarium head blight (FHB) resistance and abiotic stress traits in wheat (*Triticum aestivum* L.) (Venske et al., 2019; Soriano et al., 2021), maize streak disease and low temperature tolerance in maize (Emeraghi et al., 2021; Yu et al., 2022) and nitrogen use efficiency in rice (*Oryza sativa* L.) (Sandhu et al., 2021).

To date, three QTL meta-analyses based on SSR and RFLP markers have been conducted on ear rot diseases in maize (Xiang et al., 2010; Xiang et al., 2012; Mideros et al., 2014). These authors included only one GER-related study by Ali et al. (2005), while the others were on FER- and *Aspergillus flavus*-caused ear rots. Moreover, SSR, RFLP and RAPD are low-throughput and complicated marker technologies which are unable to precisely identify the number and locations of genes controlling the traits, thereby leading to large QTL intervals (Yu et al., 2011; Venske et al., 2019). In addition, the identified MQTL lacked precision on flanking markers and genomic positions to enable identification of promising candidate genes to be targeted in breeding programs. With this, these studies can be considered as preliminary and more informational QTL meta-analyses on ear rot diseases.

In the subsequent years after these studies, there has been a revolution concerning genotyping technologies which led to the development of high throughput technologies for SNP including maizeSNP50 and Affymetrix microarray CGMB56K (Ganal et al., 2011), maizeSNP3072 (Tian et al., 2015) and GenoBaits maize10K (Guo et al., 2019) SNP arrays, as well as genotype-by-sequencing (GBS) technology (He et al., 2014) which can assess thousands of SNP at once. This has enabled the implementation of various QTL mapping studies, resulting in the accumulation of relevant information on QTL for FER and GER resistances and related traits, which should be jointly re-analyzed and updated to inform maize breeding strategies.

This study aims to (i) re-analyze and refine quantitative trait loci (QTL) reported by independent SNP-based QTL mapping studies for FER and GER silk resistance, kernel resistance, fumonisins and deoxynivalenol accumulation, kernel dry-down rate and husk coverage by applying a meta-analysis approach for identifying refined MQTL with precise genomic positions, thus revealing colocalization of genomic regions among the traits; (ii) identify candidate genes and (iii) describe the molecular mechanisms underlying resistance/susceptibility to FER and GER by analyzing the transcriptomic profiles of two contrasting maize lines (resistant *vs.* susceptible). To effectively identify most refined and stable MQTL, only SNP-based QTL mapping studies were included in the meta-analysis.

Materials and methods

Search strategy

To address our research questions, a paper-wise search was performed following the procedure described by Venske et al. (2019) and the updated guideline for systematic reviews and meta-analysis by Page et al. (2021). Searches were implemented in SCOPUS web-based, Web of Science (WoS) and Google Scholar (GoS) databases. To optimize search output, we used a combination of search terms and Boolean operators as follows: "ear rot" AND QTL AND (maize OR corn). Searches were done within the title, abstract and authors' keywords in SCOPUS and WoS, and within the title in GoS. Afterwards, the search results were firstly exported as Research Information System (RIS) and Comma-Separated Values (CSV) formats and merged to remove duplicates. Secondly, all unique publications were considered for a first screening based on the publication language, type, subject area, focus of the study, content, marker type and data availability (Table 1). Thirdly, publications that satisfied the inclusion criteria were further screened to collect relevant information about the reported QTL. For each QTL, key information was collected on: (i) traits; (ii) sources of resistance; (iii) type and size of the mapping populations; (iv)

logarithm of odds (LOD) score; (v) proportion of phenotypic variance explained by the QTL as measured by R^2; (vi) most closely flanking or single markers for interval mapping and single marker analysis, respectively; (vii) peak position and 95% confidence interval (CI) of the QTL (Supplementary File 1). LOD score was considered equal to 3 for single marker analysis where the exact LOD value was not reported. For studies which reported the genotypic variance explained (p_G) by QTL, we estimated the corresponding phenotypic variance (PVE) as follows:

$$PVE = p_G \; x \, H^2 \quad (1)$$

where H^2 is the heritability reported for the trait by the respective study. QTL with PVE<10%, 10%≤PVE<20% and PVE≥20% was considered as having minor, medium and major-effect on the trait, respectively. From the QTL mapping studies, six FER- and GER-related traits were collected and included in our meta-analysis: fumonisin accumulation (FUM), deoxynivalenol accumulation (DON), husk coverage (HC), kernel dry-down rate (KDD), kernel resistance (KR) and silk resistance (SR). FUM and DON were specific to FER and GER, respectively.

Consensus map construction

To project all the QTL collected from the diverse studies, a consensus map was constructed based on a linear programming algorithm in the LPmerge R package (Endelman and Plomion, 2014) which efficiently minimizes the error between markers' positions on the consensus map and the individual linkage maps. Based on the sequencing technology used in the original studies, a total of eight high-quality genetic maps which harbored a large number of SNP markers were selected and included in the analysis. For chip-based SNP markers, high-resolution consensus maps were obtained from Ganal et al. (2011); Liu et al. (2015) and Wen et al. (2020) for Illumina maizeSNP50, IBM Syn10 and GenoBaits maize10K SNP arrays, respectively. For GBS technology, we included the genetic map from Kebede et al. (2016). In addition, four linkage maps used by Giomi et al. (2016); Chen et al. (2016); Maschietto et al. (2017) and Zhou et al. (2021) were also included in the analysis. In the procedure, markers were assigned to bins based on their co-segregation, and the maximum interval between bins was set to k = 1–3. Thus, one consensus map was produced for each k value. The best k and corresponding consensus map were selected based on the root-mean-squared error (RMSE) between the consensus map and the linkage maps. The lower the RMSE, the higher the resolution of the respective consensus map. Spearman rank correlation analysis was performed to evaluate the degree of preservation of marker order between the consensus map and the individual genetic maps as well as the collinearity between the consensus map and the physical map B73 RefGen_v2. The proportion of markers which were arranged in the same order with those on the corresponding chromosomes on the physical map was also estimated. All analyses were conducted using R software v4.1.0 (R Core Team, 2021).

Meta-analysis of quantitative trait loci

QTL were projected onto the consensus map previously developed to identify MQTL on each linkage group. All projected QTL had their flanking markers information on at least one of the individual maps used to generate the consensus map. Prior to the projection, the confidence interval (CI) at 95% was estimated for each QTL using the following empirical formula described for each mapping population by Darvasi and Soller (1997) and Guo et al. (2006):

$$F_2 : CI = \frac{530}{N \, x \, R^2} \quad (2)$$

$$\text{Double haploid (DH)} : CI = \frac{287}{N \, x \, R^2} \quad (3)$$

$$\text{Recombinant inbred lines (RIL)} : CI = \frac{163}{N \, x \, R^2} \quad (4)$$

where N is the number of lines and R^2 is the phenotypic variance explained by the QTL.

TABLE 1 Inclusion and exclusion criteria.

Criteria	Inclusion
Publication language	English and/or French
Document type	Original research articles, books or book chapters
Subject	Agricultural and Biological Sciences
Focus	Fusarium ear rot (FER) in maize Gibberella ear rot (GER) in maize
Search string	"ear rot" AND QTL AND (maize OR corn)
Content	Mapping of quantitative trait loci (QTL) conferring resistance to Fusarium ear rot (FER) and Gibberella ear rot (GER) in maize.
Marker technology	Single nucleotide polymorphisms (SNP)
Data	Availability of sufficient information to enable proper meta-analysis of QTL associated with FER and/or GER

Afterwards, the calculated confidence intervals, original LOD score, R^2, QTL most likely position (middle point), as well as start and end positions (Supplementary File 1), were projected onto the consensus map using the *Veyrieras* two-step clustering procedure based on a Gaussian mixture model which parameter estimates were obtained by applying the expectation-maximization (EM) algorithm in BioMercator V4.2.3 software (Arcade et al., 2004; Veyrieras et al., 2007; Sosnowski et al., 2012). Considering the known correlations among the traits, the QTL were analyzed together as one trait referred to as DT (Chungu et al., 1996; Löffler et al., 2010a; Kebebe et al., 2015; Kebede et al., 2016). In the first step (1/2), the projected QTL were clustered on each chromosome or linkage group assuming varying numbers of MQTL or "real QTL" (k). The maximum number of MQTL (kmax) was the total number of QTL on the linkage group minus one QTL. For example, on a linkage group with 20 QTL, kmax was set to 19. The number of random starting points and convergence threshold for the EM algorithm were set to 50 and $1.e^{-8}$, respectively. MQTL model with the best k was the one showing the lowest value and the highest weight for at least three of the following parameters: Akaike Information Criterion (AIC), corrected Akaike Information Criterion (AICc and AIC_3), Bayesian Information Criterion (BIC) and Average Weight of Evidence (AWE). In the second step (2/2), the k MQTL were displayed according to the chosen model (Veyrieras et al., 2007). Each MQTL was represented by at least two original QTL with overlapping confidence intervals, and shared no QTL with other MQTL on the same chromosome (Yu et al., 2022). With this, original QTL which overlapped with two or more MQTL were discarded from the analysis. The position of the MQTL was determined based on the mean of the original QTL distribution maximizing the likelihood. The phenotypic variance explained by each MQTL was calculated as the mean R^2 of the original respective QTL (Yu et al., 2022). Furthermore, the meta-analysis was compared with marker-trait associations (MTA) studies by identifying the number of MTA reported for each trait, which were located within identified MQTL.

Candidate genes mining and expression analysis

From the meta-analysis, we selected the most refined MQTL which were considered for candidate genes (CG) mining and transcriptomic analysis. MQTL were selected using the criteria described by Venske et al. (2019) and Soriano et al. (2021) as follows: (1) the selected MQTL was constituted by at least two overlapping original QTL; (2) CI (95%) of the MQTL was lower than the average CI of the respective QTL; (3) MQTL was shorter than 20 Mbp in physical distance; (4) and phenotypic variance explained by the MQTL was equal or greater than 10%. Candidate genes within each of the selected MQTL were mined based on the physical positions of flanking markers by surveying the maize annotation browser of the reference genome (B73 RefGen_v3) which is available from the MaizeGDB database (Lawrence, 2007) (https://www.maizegdb.org/gbrowse/maize_v3). Physical positions of flanking markers were obtained from Unterseer et al. (2016); Kebede et al. (2016) and Liu et al. (2015). Low confidence genes and transposable elements were excluded.

To identify which of these CG were differentially expressed when challenged with *F. graminearum*, we conducted a transcriptional expression analysis based on RNA-Seq data for Gibberella ear rot published by Kebede et al. (2018) available from the NCBI Gene Expression Omnibus (GSE92448) (https://www.ncbi.nlm.nih.gov/geo/query/acc.cgi?acc=GSE92448). The authors evaluated over two years (2004 and 2006) the transcriptomic profiles of two maize lines; CO441 (FER and GER resistant) and B37 (FER and GER susceptible) under control conditions (mock) and after inoculation with *F. graminearum*. Inoculation was done 11 days after controlled pollination using the kernel inoculation method (Reid et al., 2002; Kebede et al., 2018). Maize ears were collected one and two days after inoculation (DAI) and RNA was extracted in bulk per testing year from developing kernels (Kebede et al., 2018). Gene expression levels were determined based on mock vs. Fusarium comparisons by calculating transcripts per million (TPM) as follows:

$$TPM = \frac{RPKM_i \times 10^6}{\sum_i^n RPKM} \quad (5)$$

where $RPKM_i$ is the reads per kilobase million of the i^{th} gene/transcript, and n is the total number of genes/transcripts. RPKM was estimated for each gene based on the total exon reads (ER), mapped reads (MR, in millions) and exon length (EL, in kb) as:

$$RPKM = \frac{ER}{MR \times EL} \quad (6)$$

According to Kebede et al. (2018), genes were considered as differentially expressed if the respective corrected False discovery rate (FDR) p-value was equal or lower than 0.05, fold change≥2 and TPM≥5. The differentially expressed genes identified through the transcriptomic analysis where further searched for protein evidence against the MaizeGDB (Lawrence, 2007) and the Nation Center for Biotechnology Information (NCBI, https://www.ncbi.nlm.nih.gov/) to identify corresponding annotations and ontology terms.

Results

Identification and screening of relevant publications for FER- and GER-related traits

Based on the search terms indicated previously, a total of 153 papers were identified from SCOPUS (64), WoS (55) and GoS (34) as described by the preferred reporting items for systematic review and meta-analyses (PRISMA) flow diagram available in

Supplementary File 2. From this, 43 unique publications were obtained with publication year ranging from 1993 to 2022 after removing duplicates (89), review articles and meta-analyses (11) and publications related to trait inheritance (1), gene expression (8) and FER resistance on seedlings (1). One paper published in Chinese was removed (Wen et al., 2021a). Five (9.3%) publications were solely focused on Aspergillus ear rot (Busboom and White, 2004; Willcox et al., 2013; Smith et al., 2019) and one publication on Diplodia ear rot (Baer et al., 2021), and were therefore excluded. This resulted into 37 papers which focused on deciphering the genetic architecture of FER- and GER-related traits in maize. Fifteen of these papers concentrated on QTL identification based on low-throughput technologies such as SSR, RFLP, and RADP markers (Pè et al., 1993; Ali et al., 2005; Martin et al., 2011; Martin et al., 2012b), and validation of QTL reported in previous studies (Martin et al., 2012c; Brauner et al., 2017). In addition, one SNP-based QTL mapping publication was excluded due to missing information on QTL genetic position, flanking markers as well as LOD score and PVE (Morales et al., 2019). Finally, 22 publications satisfied our inclusion criteria and were therefore considered for full text screening. Fifteen publications were SNP-based QTL mapping studies which were used to collect relevant information required for the QTL meta-analysis (Supplementary File 2) (Chen et al., 2016; Giomi et al., 2016; Han et al., 2016; Kebede et al., 2016; Maschietto et al., 2017; Han et al., 2018; Galić et al., 2019; Wen et al., 2020; Yuan et al., 2020a; Galiano-Carneiro et al., 2021; Giomi et al., 2021; Wen et al., 2021b; Zhou et al., 2021; Feng et al., 2022; Guo et al., 2022). Seven papers were related to genome-wide association study and used to cross-validate the meta-analysis (Butrón et al., 2019; Samayoa et al., 2019; Wu et al., 2020; Gaikpa et al., 2021; Gesteiro et al., 2021; Liu et al., 2021; da Silva et al., 2022).

Characterization of QTL reported based on high-throughput SNP technologies for FER- and GER-related traits

From the 15 SNP-based QTL mapping studies, a total of 224 QTL were reported for FER- and GER- related traits (Table 2, Supplementary File 1). QTL were identified using three types of populations such as recombinant inbred lines (RIL), double-haploid (DH) and F_2 populations. Resistant parental lines used in the different studies were sourced from a wide distribution range including Argentina, Brazil, Canada, China, Europe, United States of America (USA), and the International Maize and Wheat Improvement Center (CIMMYT).

Considering the three FER-related traits, 121 QTL were reported and distributed across all chromosomes (Figure 1A). Thirteen QTL were reported for FUM on all chromosomes except for chromosomes 2, 8 and 10, while 97 QTL were identified for KR on all chromosomes. Eleven QTL were identified for SR across chromosomes 2, 3, 5, and 6 (Figure 1A). Twelve and one QTL for FUM exhibited minor (PVE<10%) and medium (10%≤PVE<20%) effects, respectively (Figure 1B). 32 and six QTL for KR had medium and major effects (PVE≥20%), respectively. In addition, nine and one QTL for SR exerted minor and medium effects on the trait, respectively (Figure 1B).

For the five GER-related traits, 103 QTL were identified across all chromosomes (Figure 1C). A total of 17 QTL were reported for DON on all chromosomes except for chromosomes 6 and 8, while 21 QTL were identified for KR on all chromosomes except chromosome 6. 53 QTL were reported for SR across all chromosomes. Six QTL were identified for HC across chromosomes 1, 4, 6, 7 and 9, while six QTL were reported for KDD on chromosomes 1, 3, 6 and 8 (Figure 1C). Seven and one QTL for DON had medium and major effects, respectively, while most QTL for KR (20 QTL) exhibited minor effects (Figure 1D). Similarly, 18 and four of the 53 QTL for SR had medium and major effects, respectively. Most QTL for HC (5 QTL) and all QTL for KDD had minor and medium effects on the traits (Figure 1D).

High-resolution consensus map generated for QTL projection

The consensus map was composed of SNP markers and generated based on eight genetic linkage maps. The map was of high resolution and presented a total of 36,243 loci with a total length of 3,132.48 cM (Table 3). The Spearman rank correlation analysis revealed strong correlations (average ρ = 0.86–0.99) between marker order on the consensus and individual genetic maps (Table 3). Each chromosome was, on average, 313.25 cM long and composed of 3,624 SNP markers. The average genetic distance between adjacent markers ranged from 0.15 to 0.28 cM depending on the chromosome (Table 3). Attempts to increase the number of loci and length of the map through the inclusion of additional genetic maps resulted in several conflict orders. A comparison of the consensus map with physical map obtained from the reference map B73 RefGen_v2, showed high collinearity with strong correlations (ρ = 0.73–0.91). On average, 72% of markers were arranged in the same order with those on the corresponding chromosomes of the physical map, indicating a high consistency between the consensus map and the physical map B73 RefGen_v2. This shows that the current consensus map generated in this study was the best harmonious combination, and was therefore used as the base for the QTL projection and meta-analysis. The consensus map is made available through Supplementary File 3.

QTL colocalization and meta-QTL for the FER- and GER-related traits based on QTL mapping studies

From the total of 224 QTL, 164 QTL were projected on the consensus map (Figures 2, 3). The remaining 60 QTL could not

TABLE 2 Characteristics of SNP-based QTL mapping studies on resistance to Fusarium (FER) and Gibberella ear rot (GER) analysed in this study.

Donor	Origin	Type	Size	Disease	Traits	Number of QTL	References
LP4637	Argentina	RIL	298	GER	SR	8	Giomi et al., 2016
CO441	Canada	RIL	410	GER	SR, KR, KDD, HC	32	Kebede et al., 2016
European flint	Europe	DH	114	GER	DON	6	Han et al., 2018
European dent	Europe	DH	130	GER	DON	2	Han et al., 2018
Cheng351	China	F2	118	GER	SR	3	Wen et al., 2020
Dan598	China	F2	200	GER	SR	8	Wen et al., 2020
JiV203	China	F2	175	GER	SR	11	Wen et al., 2020
IBMSyn10	USA	DH	298	GER	SR	1	Yuan et al., 2020a
DH4866	China	RIL	204	GER	KR	11	Zhou et al., 2021
T3	Brazil	DH	266	GER	SR	3	Galiano-Carneiro et al., 2021
UH006 and UH007	Europe	DH	639	GER	SR, DON	22	Han et al., 2016
CML495	CIMMYT	DH	201	FER	KR	4	Chen et al., 2016
CML449	CIMMYT	F2	272	FER	KR	6	Chen et al., 2016
CML492	CIMMYT	F2	277	FER	KR	11	Chen et al., 2016
CO441	Canada	F2	188	FER	FUM, KR	24	Maschietto et al., 2017
IBMSyn4	USA	RIL	191	FER	KR	3	Galić et al., 2019
LP4637	Argentina	RIL	120	FER	SR	7	Giomi et al., 2021
Cheng351	China	F2	117	FER	KR	5	Wen et al., 2021b
Dan598	China	F2	200	FER	KR	10	Wen et al., 2021b
JiV203	China	F2	174	FER	KR	15	Wen et al., 2021b
DTMA165	CIMMYT	F2	152	FER	KR	9	Guo et al., 2022
8107	China	F2	220	FER	KR	8	Guo et al., 2022
B73xdiploperennis	China	RIL	215	FER	KR	7	Feng et al., 2022
B73xparviglumis	China	RIL	113	FER	KR	3	Feng et al., 2022
Zheng58xparviglumis	China	RIL	122	FER	KR	5	Feng et al., 2022

CIMMYT, International Maize and Wheat Improvement Center; RIL, recombinant inbred lines; DH, double haploid; DON, deoxynivalenol accumulation; FUM, fumonisin accumulation; HC, husk coverage; KDD, kernel dry-down rate; KR, kernel resistance; SR, silk resistance.

be projected due to lack of information (markers' names and positions) on the flanking markers in the original studies (25 QTL) or the absence of the markers on the consensus map (35 QTL) generated in this study. For both FER and GER, the projection showed that confidence intervals of QTL for different traits overlapped on several chromosomes, indicating colocalization of resistance QTL for the two diseases with two or more traits. To refine MQTL, QTL with large confidence intervals (CI 95%≥80 cM) on chromosomes 1, 6 and 10 were excluded from the meta-analysis. Likewise, QTL which overlapped two or more independent MQTL on chromosomes 2, 4, 5, 7 and 9 were also excluded from the analysis. A total of 40 MQTL were identified across all chromosomes and constituted each by 2–10 overlapping original QTL (Supplementary File 4). On average, 70–100% of CI of individual QTL contributed to the definition of each MQTL. CI of identified MQTL were 1.4–36.4-fold lower than the average CI of respective original QTL. 32 of the 40 MQTL were constituted of original QTL from 2–7 different studies and populations (Supplementary File 4). The highest number of MQTL was observed on chromosomes 1 and 3 (Figure 2), and the lowest on chromosomes 6 and 10 (Figure 3). From the 40 MQTL, seven and five MQTL were specific to FER and GER, respectively, while 28 MQTL were common to both diseases.

Four and six MQTL were found for DON and FUM, respectively, while KR and SR of FER were controlled by 30 and 6 MQTL, respectively (Supplementary File 4). Sixteen and 24 MQTL were found for KR and SR of GER, respectively, while HC and KDD were controlled by six MQTL each (Supplementary File 4). Contrary to KR and SR, no specific MQTL where identified for FUM, DON, HC and KDD. However, the analysis identified individual QTL *qFER12* on chromosome 5 and *qGER12* on chromosome 9 as independent specific QTL for FUM and DON, respectively. Considering both diseases, several MQTL were shared among the traits, with the exception of DON versus HC (Table 4). Four MQTL were shared between KR and SR of FER, while 15 MQTL were common to KR of FER and SR of GER (Table 4).

Comparison of meta-analysis with association mapping studies

Based on the seven association mapping studies on FER and GER resistances, about 178 MTA were reported for FUM, KR of

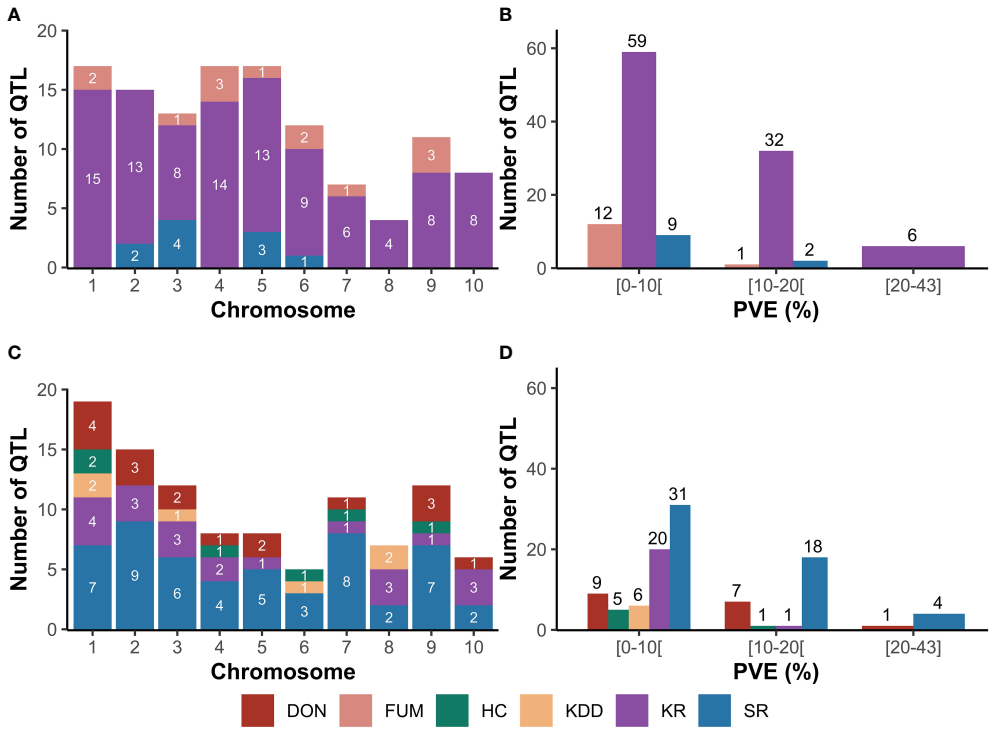

FIGURE 1
Original QTL reported from SNP-based mapping studies for Fusarium ear rot (FER) and Gibberella ear rot (GER). **(A)**, distribution of QTL for FER across chromosomes; **(B)**, phenotypic variance explained (PVE) by QTL for FER; **(C)**, distribution of QTL for GER across chromosomes; **(D)**, phenotypic variance explained by QTL for GER. DON, deoxynivalenol accumulation; FUM , fumonisin accumulation; HC, husk coverage; KDD, kernel dry-down rate; KR, kernel resistance; SR, silk resistance.

TABLE 3 Characteristics of consensus map generated from eight high quality genetic maps composed of SNP markers.

Chr	Length (cM)	Number of markers	Average DM (cM)	Average ρ with IGM	Range of ρ with IGM	ρ with physical map	Consistent proportion (%)
1	450.72	5,839	0.20	0.88	0.82–0.95	0.80	0.68
2	316.00	4,001	0.28	0.97	0.91–1.00	0.86	0.71
3	463.30	4,074	0.28	0.98	0.96–0.99	0.85	0.70
4	319.29	3,876	0.24	0.99	0.99–0.99	0.87	0.73
5	318.31	3,885	0.27	0.95	0.84–1.00	0.75	0.73
6	120.26	3,093	0.15	0.86	0.77–0.99	0.73	0.69
7	371.10	3,175	0.24	0.80	0.61–0.95	0.74	0.71
8	287.80	3,059	0.20	0.95	0.88–1.00	0.80	0.72
9	254.90	2,696	0.25	0.98	0.96–1.00	0.91	0.71
10	230.80	2,545	0.26	0.98	0.97–1.00	0.83	0.72
Genome	3,132.48	36,243	0.24	0.93		0.81	0.72

Chr, chromosome; DM, distance between markers; ρ, Spearman rank correlation coefficient; IGM, individual genetic maps used for the consensus map construction. Physical map was obtained from the reference map B73 RefGen_v2. Consistent proportion is the proportion of markers arranged in the same order with those on the corresponding chromosomes of the physical map.

FER and SR of GER using diverse germplasm collections and breeding populations worldwide (Table 5). 170 MTA were reported for FER-related traits such as FUM (81 MTA) and KR (89 MTA). Depending on the traits, FER-related MTA were distributed across all chromosomes (Supplementary File 5). The remaining eight MTA were exclusively reported by one GER-related study (Gaikpa et al., 2021) for SR across chromosomes 2, 4, 5, 6, and 9 (Supplementary File 5). Unlike QTL, a single MTA

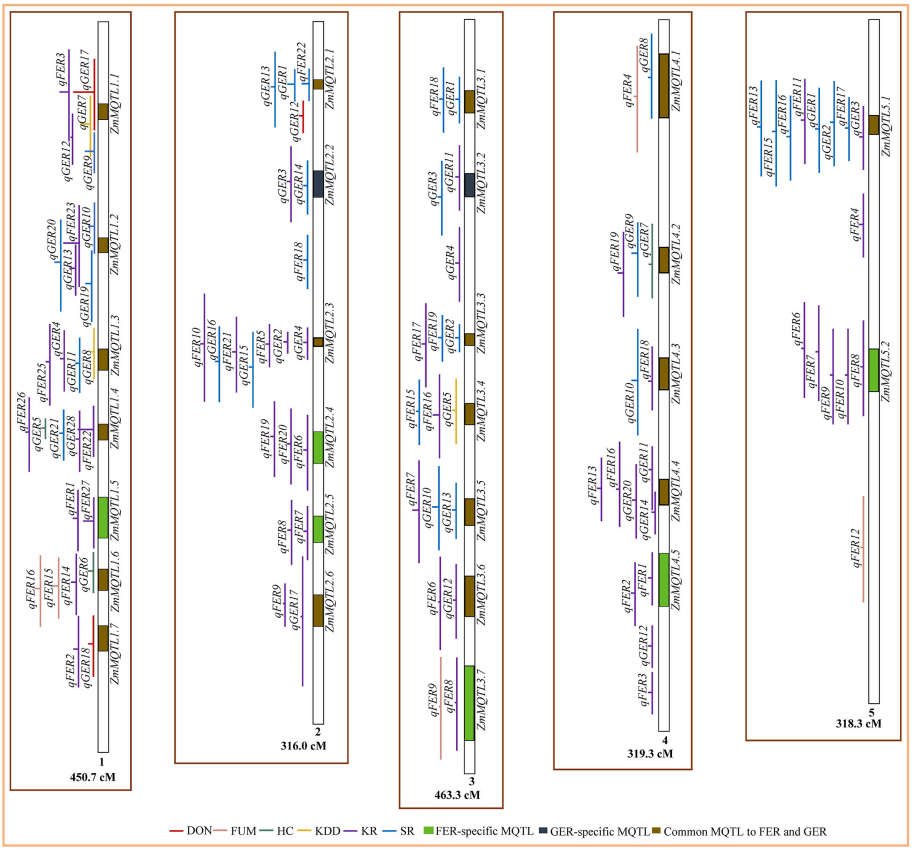

FIGURE 2
Colocalization of QTL for Fusarium ear rot (FER) and Gibberella ear rot (GER) and identification of meta-QTL (MQTL) on chromosomes 1–5. The line in the middle of each QTL represents its LOD score in the original work. The longer this line, the higher the LOD score of the respective QTL. DON, deoxynivalenol accumulation; FUM, fumonisin accumulation; HC, husk coverage; KDD, kernel dry-down rate; KR, kernel resistance; SR, silk resistance.

does not have confidence interval, and was therefore considered as a specific QTL location, but not as a whole QTL. A cross-validation with the meta-analysis showed that physical positions of 33 of the reported MTA were located within 16 MQTL (Table 6). The proportion of MTA located within MQTL ranged from 7.14% on chromosome 2 to 50% on chromosome 8. No MTA reported on chromosomes 5, 6 and 10 fell within our MQTL (Table 6).

Differentially expressed candidate genes within the most refined MQTL

From the 40 MQTL identified in this study, 14 MQTL satisfied the four criteria defined earlier, and were therefore selected as the most refined MQTL (Table 7). Selected MQTL were distributed across chromosomes 1, 2, 3, 4, 7 and 9, with 2–7 overlapping original QTL. The CI was 2.65–14.80 cM, with an average PVE of 10–29.67%. The distance between flanking markers of the respective MQTL was 0.63–15.55 Mbp. Based on the physical positions of the flanking markers, a total of 2,272 candidate genes, excluding transposable elements, were mined within the confidence intervals of the selected MQTL (Table 7, Supplementary File 6). For each MQTL, an average of 162 CG were identified with the only exception of *ZmMQTL1.2*, where only 10 CG were projected. The highest number of CG was observed with *ZmMQTL4.3* (342 CG, Table 7).

Gene expression analysis using RNA-Seq data from Kebede et al. (2018), revealed that 59 of the CG were differentially expressed based on mock vs. Fusarium comparisons at 1–2 DAI (Supplementary File 7). Seven CG were specific to the resistant line (CO441), 36 to the susceptible line (B37) and 16 common to both lines. At 1 DAI, only genes *GRMZM2G093092* and *GRMZM2G423331* were differentially expressed in CO441, while 15 genes were differentially expressed in B37 (Supplementary File 7). Comparing to the respective controls (mock), all CG were upregulated in both lines, with the exception of *GRMZM2G135617*, *GRMZM2G164340* and

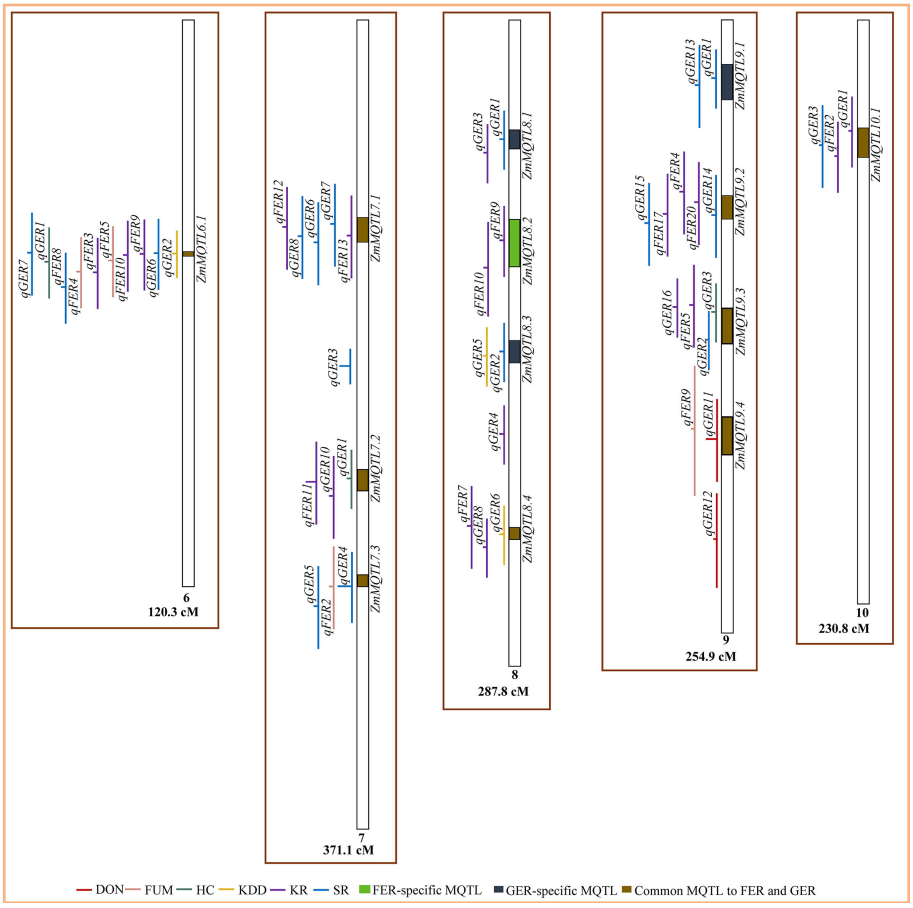

FIGURE 3
Colocalization of QTL for Fusarium ear rot (FER) and Gibberella ear rot (GER) and identification of meta-QTL (MQTL) on chromosomes 6–10. The line in the middle of each QTL represents its LOD score in the original work. The longer this line, the higher the LOD score of the respective QTL. DON, deoxynivalenol accumulation; FUM, fumonisin accumulation; HC, husk coverage; KDD, kernel dry-down rate; KR, kernel resistance; SR, silk resistance.

GRMZM2G126732, which were specifically downregulated (Fold change = −3.3 to −5.7) in B37 at 2 DAI. Expression levels of line-specific genes were 19.6–387.6 TPM in CO441 and 4.6–481.9 TPM in B37 (Supplementary File 7). For the common CG, the expression levels were 6.2–128.5 TPM in CO441 and 6.0–168.4 TPM in B37 (Figure 4). At 2 DAI, the expression of common CG *GRMZM2G342033*, *GRMZM2G323943*, *GRMZM2G423331* were 1.5–2-fold higher in CO441 than B37.

Functional categories of 46 of the 59 differentially expressed CG were summarized in Figure 5. The remaining 13 CG, of which seven B37-specific CG, two CO441-specific CG (*GRMZM2G337191* and *GRMZM2G703858*) and four common CG, were annotated as "*uncharacterized protein*" (Supplementary File 8). Annotated CO441-specific CG were *GRMZM2G011151*, *GRMZM2G093092*, *GRMZM2G156785*, *GRMZM2G340656* and *GRMZM2G472643*, which were mainly involved in binding, kinase and transferase activities, signal transduction, secondary metabolism, cell wall metabolism and defense response (Figure 5, Supplementary File 8). Regarding the most important common CG (mostly expressed in CO441), *GRMZM2G342033* encoded "*S-norcoclaurine synthase2*" which was involved in lyase activity and defense response (Supplementary File 8). In addition, *GRMZM2G423331* encoded "*flavonoid O-methyltransferase4 (fomt4)*" which catalyzed sakuranetin (phytoalexin) biosynthesis and cell wall metabolism. Contrary to CO441-specific CG, no B37-specific CG was involved in defense response, signal transduction and secondary metabolites biosynthesis (Figure 5). Ethylene biosynthesis were catalyzed by "*1-aminocyclopropane-1-carboxylate synthase2 (acs2)*" encoded by *GRMZM2G164405*. Similarly, *GRMZM2G146108* encoded "*small auxin up RNA11 (saur11)*" which was involved in auxin biosynthesis. However, this gene was only highly expressed at 1 DAI. In addition, *GRMZM2G067402* encoded "*hemoglobin1 (hb1)*" which was

TABLE 4 Number of meta-QTL shared among the evaluated traits.

Trait	Fusarium ear rot			Gibberella ear rot				
	FUM	KR	SR	DON	HC	KDD	KR	SR
Fusarium ear rot:								
KR	3	-						
SR	1	4	-					
Gibberella ear rot:								
DON	1	2	1	-				
HC	2	6	1	0	-			
KDD	1	5	2	1	1	-		
KR	0	13	1	1	3	3	-	
SR	3	15	5	2	4	4	11	-

DON, Deoxynivalenol accumulation; FUM, fumonisin accumulation; HC, husk coverage; KDD, kernel dry-down rate; KR, kernel resistance; SR, silk resistance. Each meta-QTL was common to different pairs of traits.

TABLE 5 Characteristics of association mapping studies on resistance to Fusarium (FER) and Gibberella ear rot (GER) used in this study for validation.

Donor	Type	Size	Disease	Trait	Number of MTA	References
Worldwide panel	IL	270	FER	FUM	38	Samayoa et al., 2019
EPS21 MAGIC population	RIL	352	FER	KR	13	Butrón et al., 2019
BT-1	RIL	250	FER	KR	18	Wu et al., 2020
Kemater Landmais Gelb landrace	DH	250	GER	SR	8	Gaikpa et al., 2021
CMLs, DTMA AM panel and SYN_DH	IL	874	FER	KR	58	Liu et al., 2021
EPS21 MAGIC population	RIL	339	FER	FUM	24	Gesteiro et al., 2021
Embrapa's panel	IL	205	FER	FUM	19	da Silva et al., 2022

RIL, recombinant inbred lines; IL, inbred lines; DH, double haploid; FUM, fumonisin accumulation; KR, kernel resistance; SR, silk resistance.

involved in cell death under infection. Other B37-specific CG encoded many proteins which were involved in unspecific activities like ATP, ion and pyridoxal binding, oxidation-reduction process, transport and kinase activity (Figure 5, Supplementary File 8).

Discussion

Based on dense genome-wide SNP technology, 224 QTL, of which 121 and 103 QTL for FER- and GER-related traits, respectively, have been reported during the last two decades in maize. These loci were jointly re-analyzed and clustered into a total of 40 more refined MQTL controlling one or more traits like DON, FUM, HC, KDD, KR and SR. Contrary to meta-analyses by Xiang et al. (2010); Xiang et al. (2012) and Mideros et al. (2014) based on low-throughput markers (RFLP, SSR and RAPD), and which included only one GER-related study, the MQTL identified in this study were more refined with precision on the locations and flanking markers to facilitate their integration into breeding programs. Since the available algorithms did not allow a direct integration of association studies in the meta-analysis, we further superimposed physical positions of 178 GWAS-detected MTA with the MQTL intervals. Depending on the chromosome, about 7–50% of MTA from six independent studies fell within different MQTL (Table 6). This firstly shows the high quality of our MQTL analysis, and secondly suggests the need for new bioinformatic tools that can integrate association mapping studies in meta-analysis to better elucidate genetic basis of FER- and GER-related traits, and find interesting loci that might be included in trait introgression strategies. Furthermore, FER and GER resistance- and susceptibility-promoting genes, and underlying molecular mechanisms were also discussed within 14 most refined MQTL through a transcriptomic analysis using recently published RNA-Seq data by Kebede et al. (2018). We will include in the discussion also results from relevant papers that could not be included in the meta-analysis because they did not fulfil the basic requirements.

Co-inheritance of Fusarium and Gibberella ear rot resistances in maize

Our results revealed that the most refined MQTL *ZmMQTL1.5* (243.46–259.01 Mbp) and *ZmMQTL2.2*

TABLE 6 Number of marker-trait associations (MTA) located within identified meta-QTL (MQTL).

MQTL[a]	Physical position (Start–End, Mbp)	Trait and number of MTA[b]		MTA proportion (%)[c]	Source of resistant alleles	References
		FER	GER			
ZmMQTL1.1	7.09–9.68	KR (2)		22.72	Tropical maize germplasm, heterotic Tangsipingtou and Reid	Wu et al., 2020; Liu et al., 2021
ZmMQTL1.5	243.46–259.01	KR (1)			Tropical maize germplasm	Samayoa et al., 2019; Liu et al., 2021
ZmMQTL1.6	280.22–287.9	KR (2)			Tropical maize germplasm	Liu et al., 2021
ZmMQTL2.2	13.30–20.58		SR (1)	7.14	Kemater Landmais Gelb	Gaikpa et al., 2021
ZmMQTL3.3	164.70–168.68	KR (1)		20.00	Tropical maize germplasm	Liu et al., 2021
ZmMQTL3.6	211.85–215.42	KR (1)			EPS21 MAGIC population	Butrón et al., 2019
ZmMQTL3.7	219.19–229.39	KR (4)			Tropical maize germplasm	Liu et al., 2021
ZmMQTL4.1	2.10–5.24	FUM (2)		17.24	Worldwide panel	Samayoa et al., 2019
ZmMQTL4.4	173.55–180.3	KR (2)			EPS21 MAGIC population, CMLs, DTMA AM panel and SYN_DH	Butrón et al., 2019; Liu et al., 2021
ZmMQTL7.1	17.98–27.83	KR (1)		20.00	EPS21 MAGIC population	Butrón et al., 2019
ZmMQTL7.2	137.54–143.29	KR (1)			Tropical maize germplasm	Liu et al., 2021
ZmMQTL7.3	159.73–160.48	FUM (3)			EPS21 MAGIC population	Gesteiro et al., 2021
ZmMQTL8.1	4.11–12.94	KR (1)		50.00	EPS21 MAGIC population	Butrón et al., 2019
ZmMQTL8.2	20.80–81.7	KR (2)			Tropical maize germplasm	Liu et al., 2021
ZmMQTL9.2	113.95–129.03	KR (4)		44.44	Tropical maize germplasm	Liu et al., 2021
ZmMQTL9.3	137.29–141.47	KR (4)	SR (1)		Kemater Landmais Gelb, Tropical maize germplasm	Gaikpa et al., 2021; Liu et al., 2021

CI, confidence interval; FER, Fusarium ear rot; GER, Gibberella ear rot; FUM, fumonisin accumulation; KR, kernel resistance; SR, silk resistance.
[a]Meta-QTL name referred to Zea mays abbreviated as Zm, followed by MQTL, the corresponding chromosome, and identification number on the chromosome.
[b]Values in parentheses are the number of MTA for each trait, which are located within corresponding MQTL.
[c]Proportion of reported MTA per chromosome, which were located within MQTL.

(13.3–20.58 Mbp) with PVE>10% were specific to FER and GER, respectively (Figure 2, Table 7). This confirms that Fusarium and Gibberella ear rots are two different types of maize ear rots, and breeding for resistance to these diseases can be implemented separately. In contrast, 28 of the 40 MQTL identified in this study were common to both FER and GER resistances and were distributed across all chromosomes. This impressive number of common genomic loci offers a great opportunity to breed for multiple resistance to ear rots, particularly in maize production areas prone to both FER and GER. Previous meta-analysis by Xiang et al. (2010) also revealed 15 MQTL conferring resistance to both FER and GER. In addition, Giomi et al. (2016), also reported four QTL for both FER and GER using a multi-trait multiple interval mapping in an Argentinian mapping population. Furthermore, the relationship between FER and GER has been phenotypically investigated by Löffler et al. (2010a) who found flint and dent genotypes which were resistant to both diseases. Depending on the testing years, Schaafsma et al. (2006) found moderate to strong correlations (r = 0.40–0.75) between FER and GER resistances in different sets of Canadian commercial hybrid cultivars. Butrón et al. (2015) also reported a highly significant correlation (r = 0.71) between FER and GER resistances. These authors concluded that breeding for resistance to FER would more likely affect resistance to GER and vice versa. These findings emphasize that improving multiple resistance to FER and GER is feasible and can be efficiently achieved through the integration of identified common MQTL into breeding programs.

Meta-QTL and types of ear rot resistance

For both FER and GER, the existence of specific MQTL for SR (e.g. *ZmMQTL3.1* and *ZmMQTL9.1*) and KR (e.g. *ZmMQTL1.5*, *ZmMQTL2.4*) (Figures 2, 3, Supplementary File 4) demonstrates that silk and kernel resistances represent two major types of active resistance reactions to ear rot diseases in maize as previously reported by Reid et al. (1996a); Chungu et al. (1996); Plienegger and Lemmens (2002); Mesterházy et al. (2012) and Kebebe et al. (2015). Reinprecht et al. (2008) also demonstrated that silk and kernel resistances were two different traits to be considered when breeding for GER resistance in maize. The main difference between the two types resides in the inoculation techniques used, mimicking different pathogen entry

TABLE 7 Selected meta-QTL (MQTL) and corresponding candidate genes (CG).

MQTL[a]	Number of QTL	Disease and trait		Number of Populations	PVE (%)	CI 95% (cM)	Physical distance (Mbp)	Number of CG
		FER	GER					
ZmMQTL1.2	5	KR	KR, SR	4	10.60	4.72	3.04	10
ZmMQTL1.4	5	KR	HC, KR, SR	5	14.00	5.85	7.00	146
ZmMQTL1.5	2	KR		2	11.50	14.80	15.55	331
ZmMQTL1.7	2	KR	DON	2	11.00	8.00	7.28	226
ZmMQTL2.1	4	SR	DON, SR	3	11.75	3.02	0.63	30
ZmMQTL2.2	2		KR, SR	2	13.00	9.74	7.28	201
ZmMQTL2.3	7	KR	KR, SR	5	10.00	2.65	6.18	68
ZmMQTL3.3	3	KR, SR	SR	2	10.00	3.75	3.98	77
ZmMQTL4.3	2	KR	SR	2	17.00	11.51	14.50	342
ZmMQTL4.4	5	KR	KR	2	13.40	8.89	6.75	155
ZmMQTL7.1	5	KR	SR	2	15.20	7.75	9.85	143
ZmMQTL7.3	3	FUM	SR	2	29.67	3.89	0.75	37
ZmMQTL9.2	5	KR	SR	3	10.40	8.00	15.08	304
ZmMQTL9.4	2	FUM	DON	2	13.50	11.71	5.94	202

CI, confidence interval; FER, Fusarium ear rot; GER, Gibberella ear rot; SR, silk resistance; KR, kernel resistance; DON, deoxynivalenol accumulation; FUM, fumonisin accumulation; KDD, kernel dry-down rate; HC, husk coverage; PVE, phenotypic variance explained.
[a]Meta-QTL name referred to Zea mays abbreviated as Zm, followed by MQTL, the corresponding chromosome, and identification number on the chromosome.

modes (Chungu et al., 1996). Silk resistance occurs after inoculation of the silk channel, while kernel resistance occurs after inoculation in the middle of the ear. Under natural conditions, the fungus can enter the ear *via* the silk channel (silk resistance), and directly through wounds created by hail, insects or agricultural tools and machines (kernel resistance) (Nerbass et al., 2016; Blandino et al., 2017).

Our study identified four MQTL for both silk and kernel resistances of FER, and 15 MQTL for kernel resistance of FER and silk resistance of GER. Eleven MQTL were also found to control both silk and kernel resistances of GER (Table 4). This finding indicates the existence of genomic regions with multiple resistance which could be exploited in breeding programs aiming to improve ear rot resistance in maize. Based on SSR, RFLP and RADP markers, Ali et al. (2005) also reported one genomic region located on chromosome 1 (*BC373_650-S116_1*) and one on chromosome 7 (*BC324_1400-umc1407*) which controlled both silk and kernel GER resistances. In addition, the relationship between the two types of resistances was investigated by Chungu et al. (1996) who found positive strong phenotypic correlations (r = 0.77–0.89). Moderate correlation (r = 0.66) was reported between the two traits by Löffler et al. (2010b). Similarly, Kebebe et al. (2015) reported moderate to very strong genotypic correlations (r_g = 0.60–0.99) between the two traits and demonstrated that both silk channel and kernel inoculation techniques ranked genotypes in a similar way. From the 19 MQTL, eight were identified as the most refined MQTL explaining considerable phenotypic variance (average PVE = 10–17%) with 2–7 overlapping QTL which were identified from 2–5 populations evaluated across different environments (Table 7). This firstly exhibits these MQTL as important genomic loci controlling both types of resistance, and secondly implies that the integration of these MQTL into breeding programs is likely to improve stable multiple resistances to FER and GER due to both silk channel and kernel infections. Both resistance types are important for environments where the European corn borer (*Ostrinia nubilalis*) regularly occurs, because the insect-driven wounding of the cob in the 2nd generation of the insect might result in strong kernel infection additionally to silk infection that mainly occurs when it rains during silking. With this, the use of insect resistant genotypes under natural conditions (and without any other wounding factors), would reduce fungal infection of the kernels even if the genotypes are not resistant to the fungi. This could lead to co-occurrence of resistance QTL for both diseases although they have genetically nothing in common. So far, co-localization of genomic regions for insect and fungal resistances has not been established for maize ear rots.

Colocalization of genomic regions controlling KR, SR and mycotoxin accumulation

DON shared two MQTL with KR of FER and/or GER (*ZmMQTL1.1* and *ZmMQTL1.7*) and two MQTL with SR of FER and/or GER (*ZmMQTL1.1* and *ZmMQTL2.1*) (Table 4, Supplementary File 4). Similarly, FUM shared three MQTL with

MQTL	GeneID	mock_CO441, 1DAI	Fg_CO441, 1DAI	mock_CO441, 2DAI	Fg_CO441, 2DAI	mock_B37, 1DAI	Fg_B37, 1DAI	mock_B37, 2DAI	Fg_B37, 2DAI
ZmMQTL1.5	*GRMZM2G031938*			53.0	111.1			50.7	112.9
	GRMZM2G323943				16.4				9.3
ZmMQTL1.7	*GRMZM2G338809*			6.6	33.4			14.5	41.6
	GRMZM2G347043			40.1	118.3	33.0	91.1	25.5	141.9
	GRMZM2G361210				15.3				75.2
ZmMQTL2.2	*GRMZM2G050234*				9.5				61.2
	GRMZM2G120016			6.2	46.2		55.7		168.4
	GRMZM2G342033				18.3		10.2		13.0
ZmMQTL3.3	*GRMZM2G086845*			31.1	89.7	43.7	142.7	39.0	123.9
ZmMQTL4.4	*GRMZM2G015912*				20.0				30.4
	GRMZM2G035704				26.3				41.6
	GRMZM2G139293			16.8	67.5			22.7	104.1
ZmMQTL9.2	*GRMZM2G065696*			12.1	53.1	6.0	33.6	5.8	52.4
	GRMZM2G113860				8.0		12.1		35.1
ZmMQTL9.4	*GRMZM2G036351*				16.8		15.0		30.0
	GRMZM2G423331	7.8	84.7	6.9	128.5		17.2		67.4

FIGURE 4
Expression levels in transcripts per million (TPM) of the common candidate genes in resistant (CO441) and susceptible (B37) lines under control conditions (mock) vs. *F. graminearum* (Fg) comparisons. Bar charts show the relative importance of the expression levels of each gene. MQTL, meta-QTL; DAI, days after inoculation.

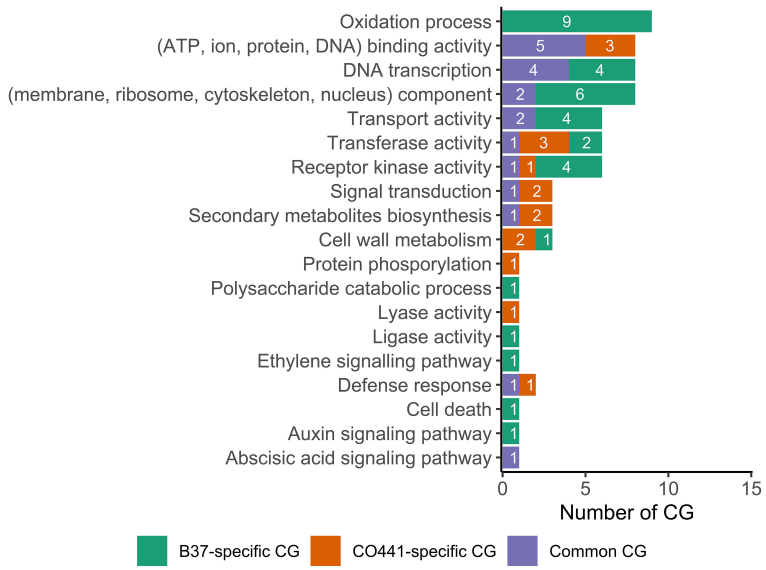

FIGURE 5
Gene ontology terms of the differentially expressed candidate genes (CG) between resistant (CO441) and susceptible (B37) lines under *Fusarium graminearum* infection.

KR of FER (*ZmMQTL1.6*, *ZmMQTL3.7* and *ZmMQTL6.1*) and three with SR of FER and/or GER (*ZmMQTL4.1*, *ZmMQTL6.1* and *ZmMQTL7.3*). This indicates the existence of common genomic regions between mycotoxin accumulation and the two types of active resistance in maize. For GER, Martin et al. (2011) using SSR markers to analyze 150 DH lines derived from UH007×UH006, also found one QTL on chromosome 2 which was common to DON accumulation and silk resistance. This was supported by the existence of a strong positive genotypic correlation (r = 0.95) between the two traits (Martin et al., 2011). In addition, Szabo et al. (2018) detected strong positive correlations between GER severity and DON contamination with correlations of r = 0.95 and r = 0.82 for *F. graminearum* and *F. culmorum*, respectively. They concluded that GER resistance is an important indicator of lower toxin contamination. Genotypes with higher GER resistance would

have lower DON accumulation as indicated by Bolduan et al. (2009). Similar observations were made by Miedaner et al. (2015) who found moderate to strong correlations (r = 0.60–0.90) between DON measured by immunotests and GER severity, indicating that DON could be predicated by GER severity. For FER, Butrón et al. (2015) observed strong correlations (r = 0.97) between disease severity and FUM. Similarly, Cao et al. (2022) found strong genotypic correlation (r_g = 0.85) between FUM and FER severity after kernel inoculation. Based on this, selection for FER-resistant lines would indirectly reduce fumonisins accumulation (Maschietto et al., 2017; Galić et al., 2019).

However, our analysis also revealed the existence of one specific QTL for FUM (*qFER12*, PVE = 8%) on chromosome 5 (Figure 2) and one for DON (*qGER12*, PVE = 15%) on chromosome 9 (Figure 3), which were identified as independent MQTL for these traits. This implies that it would be more relevant to consider evaluating DON and FUM as separate traits from FER and GER severity, particularly if the breeder targets those specific genomic regions. Although resistant genotypes had generally low toxin contamination, Reid et al. (1996b) and Dalla Lana et al. (2022) demonstrated that the relationship between DON and GER severity was more complex and non-linear. Genotypes with different disease severity might exhibit similar mycotoxin concentrations. In wheat, Wang et al. (2021) investigating the complex relationship between FHB and DON, found individual genotypes with low disease severity that exhibited high DON accumulation. In the USA, Dalla Lana et al. (2021) analyzed DON in maize ears over four years and showed that its accumulation was affected by multiple weather conditions. They indicated that from a total of 483 asymptomatic ears, 196 (about 41%) exhibited detectable level of 0.05 mg/kg for DON accumulation, and 46 (approximately 10%) showed 1–5 mg/kg of DON. Moreover, Mesterhazy et al. (2022) evaluated 18 commercial maize hybrids from Hungary for different ear rots including FER and GER, and observed a lack of phenotypic correlations between ear rot resistance and toxins, indicating that toxins analysis is necessary. Therefore, indirect selection for DON or FUM using disease severity would be feasible and more effective through the exploitation of identified common MQTL, however, advanced lines should be further analyzed for DON and/or FUM accumulation in a later stage of the selection cycle. Furthermore, MQTL *ZmMQTL9.4* (145.46–151.40 Mbp) on chromosome 9 was common to FUM and DON. This firstly demonstrates the existence of genomic regions with resistance to multiple mycotoxin accumulation, and secondly indicates that selection for resistance to one mycotoxin using this MQTL would reduce accumulation of the other mycotoxin. The same has been reported on the basis of phenotypic data by Miedaner et al. (2015) for the co-occurrence of resistances to DON and zearalenone, another mycotoxin produced by *F. graminearum*.

Morphological traits and their association with FER and GER infections in maize

Several MQTL for SR and KR of both FER and GER were also detected in association with KDD (e.g. *ZmMQTL1.1* and *ZmMQTL6.1*), and HC (*ZmMQTL1.4*, and *ZmMQTL6.1*) (Table 4, Supplementary File 4). This indicates that morphological traits such as kernel dry-down rate and husk coverage may have a passive contribution to both silk and kernel resistances in maize. Kernel dry-down rate and husk coverage represent natural barriers which reduce infection by blocking the pathogen entry into the ear or the kernel. Passive resistance due to morphological traits was also reported for FHB disease in wheat by several studies (Mesterházy, 1995; Buerstmayr and Buerstmayr, 2015; Buerstmayr et al., 2020; Ruan et al., 2020; Xu et al., 2020). Husk characteristics were reported as important traits in protecting the ears from pathogen infection (Warfield and Davis, 1996; Jiang et al., 2020). Butoto et al. (2022) found a low negative correlation (r = −0.30) between husk coverage and FER severity. In addition, moderate genotypic correlations (r = 0.39–0.61) were detected between husk coverage and Diplodia ear rot severity due to *Stenocarpella maydis* infection across three locations (Rossouw et al., 2002). The positivity of the correlations found by Rossouw et al. (2002) is explained by the fact that the authors evaluated the husk coverage based on a scale opposite to the previous paper. Therefore, the tighter the husk over the ear, the lower the ear rot severity.

Common genomic regions were also reported by Xiang et al. (2012) when investigating the relationships between grain moisture content and ear rot resistance in maize. Depending on the maturity stage of the kernels, Kebebe et al. (2015) found in Canada moderate to strong negative genotypic correlations between kernel dry-down rate and silk resistance (r = −0.58 to −0.90) and kernel resistance (r = −0.67 to −0.79) for GER. Thus, genotypes with fast drying kernels would have relatively lower GER severity. Substantially high selection efficiencies (0.52–0.84) were observed by Kebebe et al. (2015) when selecting for less kernel infection using kernel dry-down rate, whereas lower selection efficiencies (0.29–0.32) were found for silk channel infection. Since silk inoculation is usually earlier (5-6 days post silking) than kernel inoculation (15-21 days post silking), the infection through silk channel would have significantly progressed before the onset of kernel dry-down. This indicates that despite the existence of common genomic loci between kernel dry-down rate and FER and GER resistances, the use of kernel dry-down rate as an indirect trait to improve ear rot resistance might not be as effective as the direct selection for disease severity, especially for SR. Moreover, additional investigations are required to elucidate the interactions between kernel dry-down rate and grain yield and related traits in maize.

Resistance and susceptibility genes controlling FER and GER in maize

Based on transcriptomic data reported by Kebede et al. (2018) for GER, 59 candidate genes harbored by 14 of the MQTL identified in this study were differentially expressed in one resistant line (CO441) and one susceptible line (B37) after inoculation with *F. graminearum* (Supplementary File 7). This emphasizes the importance of these MQTL as targets for improving multiple resistance to ear rot diseases in maize. Thirteen of these candidate genes were annotated as "*uncharacterized protein*" (Supplementary File 8), and therefore require further investigations to characterize corresponding proteins to better elucidate their roles in the resistance or susceptibility to ear rot in maize. GER-specific MQTL *ZmMQTL2.2* and the common MQTL *ZmMQTL9.4* harbored two different defense response genes such as *GRMZM2G342033* and *GRMZM2G423331*, respectively. Similarly, the common MQTL *ZmMQTL9.2* (113.95–129.03 Mbp) harbored two defense response genes, namely *GRMZM2G011151* and *GRMZM2G093092* which were specific to CO441. In comparison to the susceptible line, the expression levels of *GRMZM2G342033* and *GRMZM2G423331* at 2 DAI in CO441 were constitutively stronger with TPM two-fold higher than that in B37.

GRMZM2G342033 encoded "*S-norcoclaurine synthase2*" which had about 71.3% of identity with "*S-norcoclaurine synthase*" previously reported as a member of the pathogenesis-related protein 10 (PR10) family (Lee and Facchini, 2010; Nida et al., 2021). The PR10 family proteins have been extensively reported for their antifungal activity (Xie et al., 2010; Wu et al., 2016), and their crucial role in resistance against GER pathogens (Mohammadi et al., 2011). Xie et al. (2010) identified another PR10 gene (*ZmPR10.1*) on chromosome 10 which conferred resistance to Aspergillus ear rot caused by *Aspergillus flavus* in maize. Similarly, in a previous transcriptional analysis, Lanubile et al. (2014) also identified *GRMZM2G342033* as "*S-norcoclaurine synthase-like*" which was involved in resistance to FER in maize.

GRMZM2G011151 was annotated as "*terpene synthase21* (*tps21*)" which has been previously reported by Ding et al. (2017) as a α/β-costic acid pathway candidate gene in maize. *tps21* enables the biosynthesis of α/β-selinene volatiles which are in turn converted into α/β-costic acids, promoting resistance to fungal pathogen infections (Block et al., 2019). α/β-costic acids are non-volatile diterpenoids which were demonstrated to inhibit growth of several fungal species including *F. graminearum*, *F. verticillioides*, *Rhizopus microsporus*, *Aspergillus parasiticus*, and *Cochliobolus heterostrophus* (Ding et al., 2017). Moreover, near-isogenic lines (NILs) lacking functional copies of *tps21* exhibited a high susceptibility to Fusarium species compared to functional NILs (Ding et al., 2017). Lanubile et al. (2014) also identified *GRMZM2G011151* as a defense response gene to FER which was specifically differentially expressed in CO441 compared to another susceptible line (CO354).

Similar to *GRMZM2G011151*, *GRMZM2G093092* and *GRMZM2G423331* were reported as candidate defense response genes to GER (Kebede et al., 2018), which encoded the "*flavonoid O-methyltransferase2 (fomt2)*" and "*flavonoid O-methyltransferase4 (fomt4)*" proteins, respectively. *FOMT2* and *FOMT4* proteins catalyze the biosynthesis of sakuranetin, a well-characterized flavonoid which negatively affected the germination of fungal spores in rice (Kodama et al., 1992; Hasegawa et al., 2014). *GRMZM2G423331* was also identified in a recent transcriptomic analysis by Förster et al. (2022) as a *FOMT4* gene which is involved in the flavonoid pathway related to a general response to *F. graminearum* and *F. verticillioides* in maize. Recently, Maschietto et al. (2017) found that *GRMZM2G093092* was uniquely expressed in CO441 compared to CO354 after infection with *F. verticillioides*. In addition, *FOMT2* and *FOMT4* enable cell-wall reinforcement and higher lignification which both inhibit fungus growth and the development of the disease. These results suggest the biosynthesis of different secondary metabolites or phytoalexins (e.g. terpenoid and flavonoid) which occurs after initial infection with FER- and GER-causing species. Moreover, Balcerzak et al. (2012) indicated that during the infection, fungus-specific genes like *feruloyl esterase (FAE)* are activated to enable the biosynthesis of pathogen-associated molecule patterns (PAMPs), like oligogalacturonides. These molecules firstly degrade the cell wall to facilitate the infection, and secondly are perceived as elicitors by pathogen recognition receptor kinases. This results in successive oxidation-reduction reactions leading to reaction oxygen species (ROS) production (Kebede et al., 2018; Yuan et al., 2020b) and the activation of defense response and phytoalexin-coding genes (Förster et al., 2022). Given the specificity of genes *GRMZM2G011151* and *GRMZM2G093092* to the resistant genotype, and the fact that they were harbored by a common MQTL (*ZmMQTL9.2*) to FER and GER, their incorporation into breeding programs would efficiently improve a broad-based resistance to both Fusarium and Gibberella ear rots in maize.

Furthermore, we also identified 36 candidate genes which were uniquely differentially expressed in the susceptible line, suggesting the existence of ear rot susceptibility genes in maize. The gene *GRMZM2G164405* harbored by *ZmMQTL2.2* encoded the "*1-aminocyclopropane-1-carboxylate synthase2 (acs2)*" protein which was involved in the biosynthesis of ethylene and pyridoxal phosphate binding activity. Since *ZmMQTL2.2* is a GER-specific MQTL, this finding demonstrates that ethylene-signaling pathway is associated with susceptibility to GER in maize as previously indicated by Kebede et al. (2018). Similar results were reported by Chen et al. (2009) who found that ethylene-signaling increased susceptibility and premature cell death after inoculation with *F. graminearum* and DON in wheat and barley (*Hordeum vulgare* L.).

However, under infection with *F. verticillioides*, Maschietto et al. (2017) found that the expression level of gene *GRMZM2G053503* located on chromosome 8 at position 35.56 Mbp, was 1.23-fold higher in CO441 than in CO354. This gene encodes "*ethylene-responsive factor-like protein 1*" which is involved in resistance to FER in maize. Interestingly, *GRMZM2G053503* is located within the FER-specific MQTL *ZmMQTL8.2* (20.8–81.7 Mbp) which was not considered in our transcriptomic analysis. This demonstrates that the ethylene-signaling pathway plays differential roles in maize ear rot depending on the Fusarium species. In addition to *GRMZM2G164405*, another interesting susceptibility gene was *GRMZM2G146108* located within the MQTL *ZmMQTL9.4*. This gene was annotated as "*hemoglobin1 (hb1)*" which enabled programmed cell death in the susceptible line. So far, to the best of our knowledge, *GRMZM2G146108* has not been attributed to FER and/or GER susceptibility in maize, and thus merits further examination. The attenuation of the ethylene-signaling pathway could improve GER resistance in moderately to highly susceptible genotypes. This could be done through the application of RNA interference (RNA_i) technology (Das and Sherif, 2020) on *GRMZM2G164405* as described for "*Ethylene Insensitive 2 (EIN2)*" gene with FHB and DON accumulation caused by *F. graminearum* in wheat and barley (Chen et al., 2009). Alternatively, the susceptibility genes could be knocked out by the clustered regularly interspaced short palindromic repeats (CRISPR) technology (Campenhout et al., 2019; Wada et al., 2020). Both attempts would also biologically validate the contribution of these genes in the maize/ear rot pathosystems.

Strategies for the successful introgression of resistance genes to FER and GER into elite materials

Genetic resources from diverse geographical origins contributed to the 40 MQTL identified in this study (Table 2, Tables 5, 6). In Europe, flint and dent germplasms including the "Kemater Landmais Gelb" (KE) landrace population harbored several resistance alleles which could be introgressed into elite cultivars for enhanced ear rot resistance (Han et al., 2016; Han et al., 2018; Gaikpa et al., 2021). However, FER and GER resistances are complex polygenic traits, and our results demonstrated that more than 65% of the MQTL had minor (PVE<10%) effects on the respective traits. This indicates that the exploitation of these MQTL using marker-assisted selection (MAS) would require intensive breeding and marker efforts and might not yield a significant selection gain. Although MAS has been successfully implemented to improve traits controlled by one or a few large-effect genes in several crops (Kuchel et al., 2007; Hasan et al., 2021), its potential in improving complex traits remains limited as previously discussed in wheat and barley by Miedaner and Korzun (2012). As implication, the successful introgression of the resistance genes for stronger and durable multi-disease resistances, calls for more advanced and sophisticated genomic approaches, like genomic selection (Bhat et al., 2016; Gaikpa and Miedaner, 2019; Budhlakoti et al., 2022). For FER and GER resistances, this could be achieved through the application of the integrated genomics-assisted breeding scheme suggested by Miedaner et al. (2020). This approach is implemented in two steps, including: (i) introgression of the resistant donor (e.g. KE lines) by backcrossing to the susceptible line used as recurrent parent without marker selection, and (ii) application of genomic selection following a recurrent selection scheme for an accelerated selection for FER and/or GER resistances as well as adaptation traits (Miedaner et al., 2020). Identified MQTL can be efficiently incorporated in the genomic selection model built in the second step.

Conclusions

Understanding the genetic basis and molecular mechanisms controlling Fusarium and Gibberella ear rots is a key requirement for the development of maize varieties with improved multi-disease resistances and related traits. Based on 164 projected QTL from 15 studies, we demonstrated the existence of 40 MQTL which revealed colocalization of genomic regions governing FER and GER silk and kernel resistances, FUM and DON accumulation, kernel dry-down rate and husk coverage. Three of the most refined MQTL (*ZmMQTL2.2*, *ZmMQTL9.2* and *ZmMQTL9.4*) for FER- and/or GER-related traits harbored promising resistance genes which were constitutively and strongly expressed in the resistant line (CO441) analyzed in the published transcriptomic study by Kebede et al. (2018). The effectiveness of the introgression of these candidate genes from identified sources of resistance into susceptible varieties through genomics-assisted backcross breeding strategies need to be explored to systematically improve ear rot resistances while reducing mycotoxins contamination in maize.

Data availability statement

The original contributions presented in the study are included in the article/Supplementary Material. Further inquiries can be directed to the corresponding author.

Author contributions

FA designed the study, conducted literature search, conducted data analysis and wrote the manuscript. TM

conducted an in-depth review of the manuscript. All authors contributed to the article and approved the submitted version.

Funding

This research was partly funded by the German Academic Exchange Service, Bonn, Germany as a doctoral study grant to Félicien Akohoue (grant no. 91770158) and partly by the University of Hohenheim.

Acknowledgments

We wish to express our sincere gratitude to Mr. Serge Alindekon, University of Rostock, Germany, for his valuable help with literature search using Web of Science. Many thanks to Prof. Linda J. Harris from Eastern Cereal and Oilseed Research Centre, Agriculture and Agri-Food Canada, Ottawa, Canada, and Prof. Guangfei Zhou from State Key Laboratory for Crop Genetics and Germplasm Enhancement, Nanjing Agricultural University, China, for sharing with us genetic maps used in their respective studies.

Conflict of interest

The authors declare that the research was conducted in the absence of any commercial or financial relationships that could be construed as a potential conflict of interest.

Publisher's note

All claims expressed in this article are solely those of the authors and do not necessarily represent those of their affiliated organizations, or those of the publisher, the editors and the reviewers. Any product that may be evaluated in this article, or claim that may be made by its manufacturer, is not guaranteed or endorsed by the publisher.

Supplementary material

The Supplementary Material for this article can be found online at: https://www.frontiersin.org/articles/10.3389/fpls.2022.1050891/full#supplementary-material

References

Ali, M. L., Taylor, J. H., Jie, L., Sun, G., William, M., Kasha, K. J., et al. (2005). Molecular mapping of QTLs for resistance to gibberella ear rot, in corn, caused by *Fusarium graminearum*. *Genome* 48 (3), 521–533. doi: 10.1139/G05-014

Andriolli, C. F., Casa, R. T., Kuhnem, P. R., Bogo, A., Zancan, R. L., and Reis, E. M. (2016). Timing of fungicide application for the control of gibberella ear rot of maize. *Trop. Plant Pathol.* 41 (4), 264–269. doi: 10.1007/s40858-016-0095-3

Arcade, A., Labourdette, A., Falque, M., Mangin, B., Chardon, F., Charcosset, A., et al. (2004). BioMercator: integrating genetic maps and QTL towards discovery of candidate genes. *Bioinformatics* 20 (14), 2324–2326. doi: 10.1093/bioinformatics/bth230

Baer, O. T., Laude, T. P., Reano, C. E., Gregorio, G. B., Diaz, M. G. Q., Pabro, L. J. A., et al. (2021). Diplodia ear rot resistance QTL identified in maize (*Zea mays* l.) using multi-parent double-haploid population mapping. *Sabrao J. Breed Genet.* 53 (1), 112–125.

Balcerzak, M., Harris, L. J., Subramaniam, R., and Ouellet, T. (2012). The feruloyl esterase gene family of *Fusarium graminearum* is differentially regulated by aromatic compounds and hosts. *Fungal Biol.* 116 (4), 478–488. doi: 10.1016/j.funbio.2012.01.007

Battilani, P., and Logrieco, A. F. (2014). "Global risk maps for mycotoxins in wheat and maize," in *Mycotoxin reduction in grain chains*, eds. J. F. Austin and A. F. Logrieco. (USA: John Wiley & Sons), 309–326. doi: 10.1002/9781118832790.ch22

Beukes, I., Rose, L. J., van Coller, G. J., and Viljoen, A. (2018). Disease development and mycotoxin production by the *Fusarium graminearum* species complex associated with south African maize and wheat. *Eur. J. Plant Pathol.* 150 (4), 893–910. doi: 10.1007/s10658-017-1331-5

Bhat, J. A., Ali, S., Salgotra, R. K., Mir, Z. A., Dutta, S., Jadon, V., et al. (2016). Genomic selection in the era of next generation sequencing for complex traits in plant breeding. *Front. Genet.* 7. doi: 10.3389/fgene.2016.00221

Blandino, M., Scarpino, V., Giordano, D., Sulyok, M., Krska, R., Vanara, F., et al. (2017). Impact of sowing time, hybrid and environmental conditions on the contamination of maize by emerging mycotoxins and fungal metabolites. *Ital J. Agron.* 12 (3), 215–224. doi: 10.4081/ija.2017.928

Block, A. K., Vaughan, M. M., Schmelz, E. A., and Christensen, S. A. (2019). Biosynthesis and function of terpenoid defense compounds in maize (*Zea mays*). *Planta* 249 (1), 21–30. doi: 10.1007/s00425-018-2999-2

Bolduan, C., Miedaner, T., Schipprack, W., Dhillon, B. S., and Melchinger, A. E. (2009). Genetic variation for resistance to ear rots and mycotoxins contamination in early European maize inbred lines. *Crop Sci.* 49 (6), 2019–2028. doi: 10.2135/cropsci2008.12.0701

Boutigny, A., Beukes, I., Small, I., Zuhlke, S., Spiteller, M., van Rensburg, B. J., et al. (2011). Fusarium ear rot pathogens and their mycotoxins associated with south African maize. *Phytopathology* 101 (6), S18–S18. Abstract from APS-IPPC 2011 Joint Meeting; 2011 6–1 August; Honolulu, Hawaii.

Brauner, P. C., Melchinger, A. E., Schrag, T. A., Utz, H. F., Schipprack, W., Kessel, B., et al. (2017). Low validation rate of quantitative trait loci for gibberella ear rot resistance in European maize. *Theor. Appl. Genet.* 130 (1), 175–186. doi: 10.1007/s00122-016-2802-3

Budhlakoti, N., Kushwaha, A. K., Rai, A., Chaturvedi, K. K., Kumar, A., Pradhan, A. K., et al. (2022). Genomic selection: A tool for accelerating the efficiency of molecular breeding for development of climate-resilient crops. *Front. Genet.* 13. doi: 10.3389/fgene.2022.832153

Buerstmayr, M., and Buerstmayr, H. (2015). Comparative mapping of quantitative trait loci for fusarium head blight resistance and anther retention in the winter wheat population capo × arina. *Theor. Appl. Genet.* 128 (8), 1519–1530. doi: 10.1007/s00122-015-2527-8

Buerstmayr, M., Steiner, B., and Buerstmayr, H. (2020). Breeding for fusarium head blight resistance in wheat-progress and challenges. *Plant Breed* 139 (3), 429–454. doi: 10.1111/pbr.12797

Busboom, K. N., and White, D. G. (2004). Inheritance of resistance to aflatoxin production and aspergillus ear rot of corn from the cross of inbreds B73 and Oh516. *Phytopathology* 94 (10), 1107–1115. doi: 10.1094/PHYTO.2004.94.10.1107

Butoto, E. N., Brewer, J. C., and Holland, J. B. (2022). Empirical comparison of genomic and phenotypic selection for resistance to fusarium ear rot and fumonisin contamination in maize. *Theor. Appl. Genet.* 135 (8), 2799–2816. doi: 10.1007/s00122-022-04150-8

Butrón, A., Reid, L. M., Santiago, R., Cao, A., and Malvar, R. A. (2015). Inheritance of maize resistance to gibberella and fusarium ear rots and kernel contamination with deoxynivalenol and fumonisins. *Plant Pathol.* 64 (5), 1053–1060. doi: 10.1111/ppa.12351

Butrón, A., Santiago, R., Cao, A., Samayoa, L. F., and Malvar, R. A. (2019). QTLs for resistance to fusarium ear rot in a multiparent advanced generation intercross (MAGIC) maize population. *Plant Dis.* 103 (5), 897–904. doi: 10.1094/PDIS-09-18-1669-RE

Campenhout, C. V., Cabochette, P., Veillard, A.-C., Laczik, M., Zelisko-Schmidt, A., Sabatel, C., et al. (2019). Guidelines for optimized gene knockout using CRISPR/Cas9. *BioTechniques* 66 (6), 295–302. doi: 10.2144/btn-2018-0187

Cao, A., de la Fuente, M., Gesteiro, N., Santiago, R., Malvar, R. A., and Butrón, A. (2022). Genomics and pathways involved in maize resistance to fusarium ear rot and kernel contamination with fumonisins. *Front. Plant Sci.* 13. doi: 10.3389/fpls.2022.866478

Castañares, E., Martínez, M., Cristos, D., Rojas, D., Lara, B., Stenglein, S., et al. (2019). Fusarium species and mycotoxin contamination in maize in Buenos Aires province, Argentina. *Eur. J. Plant Pathol.* 155 (4), 1265–1275. doi: 10.1007/s10658-019-01853-5

Chen, J., Shrestha, R., Ding, J., Zheng, H., Mu, C., Wu, J., et al. (2016). Genome-wide association study and QTL mapping reveal genomic loci associated with fusarium ear rot resistance in tropical maize germplasm. *G3: Genes Genomes Genet.* 6 (12), 3803–3815. doi: 10.1534/g3.116.034561

Chen, X., Steed, A., Travella, S., Keller, B., and Nicholson, P. (2009). *Fusarium graminearum* exploits ethylene signalling to colonize dicotyledonous and monocotyledonous plants. *New Phytol.* 182 (4), 975–983. doi: 10.1111/j.1469-8137.2009.02821.x

Chungu, C., Mather, D. E., Reid, L. M., and Hamilton, R. I. (1996). Comparison of techniques for inoculating maize silk, kernel, and cob tissues with *Fusarium graminearum*. *Plant Dis.* 80 (1), 81–84. doi: 10.1094/PD-80-0081

Crippin, T., Limay-Rio, V., Renaud, J. B., Schaafsma, A. W., Sumarah, M. W., and Miller, J. D. (2020). *Fusarium graminearum* populations from maize and wheat in Ontario, Canada. *World Mycotoxin J.* 13 (3), 355–366. doi: 10.3920/WMJ2019.2532

Czarnecka, D., Czubacka, A., Agacka-Mołdoch, M., Trojak-Goluch, A., and Księżak, J. (2022). The occurrence of fungal diseases in maize in organic farming versus an integrated management system. *Agronomy* 12, (3). doi: 10.3390/agronomy12030558

Dalla Lana, F., Madden, L. V., Carvalho, C. P., and Paul, P. A. (2022). Impact of gibberella ear rot on grain quality and yield components in maize as influenced by hybrid reaction. *Plant Dis.* doi: 10.1094/PDIS-01-22-0148-RE

Dalla Lana, F., Madden, L. V., and Paul, P. A. (2021). Natural occurrence of maize gibberella ear rot and contamination of grain with mycotoxins in association with weather variables. *Plant Dis.* 105 (1), 114–126. doi: 10.1094/PDIS-05-20-0952-RE

Darvasi, A., and Soller, M. (1997). A simple method to calculate resolving power and confidence interval of QTL map location. *Behav. Genet.* 27 (2), 125–132. doi: 10.1023/A:1025685324830

da Silva, K. J., Guimarães, C. T., Tinoco, S., Bernardino, K., Trindade, R., Queiroz, V. A. V., et al. (2022). A genome-wide association study investigating fumonisin contamination in a panel of tropical maize elite lines. *Euphytica* 218 (9), 130. doi: 10.1007/s10681-022-03082-0

Das, P. R., and Sherif, S. M. (2020). Application of exogenous dsRNAs-induced RNAi in agriculture: Challenges and triumphs. *Front. Plant Sci.* 11. doi: 10.3389/fpls.2020.00946

Ding, Y., Huffaker, A., Köllner, T. G., Weckwerth, P., Robert, C. A. M., Spencer, J. L., et al. (2017). Selinene volatiles are essential precursors for maize defense promoting fungal pathogen resistance. *Plant Physiol.* 175 (3), 1455–1468. doi: 10.1104/pp.17.00879

Eckard, S., Wettstein, F. E., Forrer, H.-R., and Vogelgsang, S. (2011). Incidence of fusarium species and mycotoxins in silage maize. *Toxins* 3 (8), 949–967. doi: 10.3390/toxins3080949

Emeraghi, M., Achigan-Dako, E. G., Nwaoguala, C. N. C., and Oselebe, H. (2021). Maize streak virus research in Africa: an end or a crossroad. *Theor. Appl. Genet.* 134 (12), 3785–3803. doi: 10.1007/s00122-021-03914-y

Endelman, J. B., and Plomion, C. (2014). LPmerge: an r package for merging genetic maps by linear programming. *Bioinformatics* 30 (11), 1623–1624. doi: 10.1093/bioinformatics/btu091

Erenstein, O., Jaleta, M., Sonder, K., Mottaleb, K., and Prasanna, B. M. (2022). Global maize production, consumption and trade: trends and R&D implications. *Food Security.* 14 , 1295–1319. doi: 10.1007/s12571-022-01288-7

Feng, X., Xiong, H., Zheng, D., Xin, X., Zhang, X., Wang, Q., et al. (2022). Identification of *Fusarium verticillioides* resistance alleles in three maize populations with teosinte gene introgression. *Front. Plant Sci.* 13. doi: 10.3389/fpls.2022.942397

Förster, C., Handrick, V., Ding, Y., Nakamura, Y., Paetz, C., Schneider, B., et al. (2022). Biosynthesis and antifungal activity of fungus-induced O-methylated flavonoids in maize. *Plant Physiol.* 188 (1), 167–190. doi: 10.1093/plphys/kiab496

Gaikpa, D. S., Kessel, B., Presterl, T., Ouzunova, M., Galiano-Carneiro, A. L., Mayer, M., et al. (2021). Exploiting genetic diversity in two European maize landraces for improving gibberella ear rot resistance using genomic tools. *Theor. Appl. Genet.* 134 (3), 793–805. doi: 10.1007/s00122-020-03731-9

Gaikpa, D. S., and Miedaner, T. (2019). Genomics-assisted breeding for ear rot resistances and reduced mycotoxin contamination in maize: methods, advances and prospects. *Theor. Appl. Genet.* 132 (10), 2721–2739. doi: 10.1007/s00122-019-03412-2

Galić, V., Šimić, D., Franić, M., Brkić, A., Jambrović, A., Brkić, J., et al. (2019). Analysis of fusarium ear rot and fumonisin contamination in testcrosses of a maize biparental population. *Crop Breed Appl. Biotechnol.* 19 (1), 40–46. doi: 10.1590/1984-70332019v19n1a06

Galiano-Carneiro, A. L., Kessel, B., Presterl, T., Gaikpa, D. S., Kistner, M. B., and Miedaner, T. (2021). Multi-parent QTL mapping reveals stable QTL conferring resistance to gibberella ear rot in maize. *Euphytica* 217, (1). doi: 10.1007/s10681-020-02748-x

Ganal, M. W., Durstewitz, G., Polley, A., Bérard, A., Buckler, E. S., Charcosset, A., et al. (2011). A large maize (*Zea mays* l.) SNP genotyping array: Development and germplasm genotyping, and genetic mapping to compare with the B73 reference genome. *PloS One* 6 (12), e28334. doi: 10.1371/journal.pone.0028334

Gesteiro, N., Cao, A., Santiago, R., Malvar, R. A., and Butrón, A. (2021). Genomics of maize resistance to kernel contamination with fumonisins using a multiparental advanced generation InterCross maize population (MAGIC). *BMC Plant Biol.* 21, (1). doi: 10.1186/s12870-021-03380-0

Giomi, G. M., Kreff, E. D., Iglesias, J., Fauguel, C. M., Fernandez, M., Oviedo, M. S., et al. (2016). Quantitative trait loci for fusarium and gibberella ear rot resistance in Argentinian maize germplasm. *Euphytica* 211 (3), 287–294. doi: 10.1007/s10681-016-1725-z

Giomi, G. M., Sampietro, D. A., Velazco, J. G., Iglesias, J., Fernández, M., Oviedo, M. S., et al. (2021). Map overlapping of QTL for resistance to fusarium ear rot and associated traits in maize. *Euphytica* 217, (5). doi: 10.1007/s10681-021-02814-y

Goffinet, B., and Gerber, S. (2000). Quantitative trait loci: A meta-analysis. *Genetics* 155 (1), 463–473. doi: 10.1093/genetics/155.1.463

Gromadzka, K., Górna, K., Chełkowski, J., and Waśkiewicz, A. (2016). Mycotoxins and related fusarium species in preharvest maize ear rot in Poland. *Plant Soil Environ.* 62 (8), 348–354. doi: 10.17221/119/2016-PSE

Grote, U., Fasse, A., Nguyen, T. T., and Erenstein, O. (2021). Food security and the dynamics of wheat and maize value chains in Africa and Asia. *Front. Sustain Food Syst.* 4. doi: 10.3389/fsufs.2020.617009

Guo, B., Sleper, D. A., Lu, P., Shannon, J. G., Nguyen, H. T., and Arelli, P. R. (2006). QTLs associated with resistance to soybean cyst nematode in soybean: meta-analysis of QTL locations. *Crop Sci.* 46 (2), 595–602. doi: 10.2135/cropsci2005.04-0036-2

Guo, Z., Wang, S., Li, W.-X., Liu, J., Guo, W., Xu, M., et al. (2022). QTL mapping and genomic selection for fusarium ear rot resistance using two $F_{2:3}$ populations in maize. *Euphytica* 218 (9), 131. doi: 10.1007/s10681-022-03083-z

Guo, Z., Wang, H., Tao, J., Ren, Y., Xu, C., Wu, K., et al. (2019). Development of multiple SNP marker panels affordable to breeders through genotyping by target sequencing (GBTS) in maize. *Mol. Breed* 39 (3), 37. doi: 10.1007/s11032-019-0940-4

Guo, Z., Zou, C., Liu, X., Wang, S., Li, W. X., Jeffers, D., et al. (2020). Complex genetic system involved in fusarium ear rot resistance in maize as revealed by GWAS, bulked sample analysis, and genomic prediction. *Plant Dis.* 104 (6), 1725–1735. doi: 10.1094/PDIS-07-19-1552-RE

Han, S., Miedaner, T., Utz, H. F., Schipprack, W., Schrag, T. A., and Melchinger, A. E. (2018). Genomic prediction and GWAS of gibberella ear rot resistance traits in dent and flint lines of a public maize breeding program. *Euphytica* 214, (1). doi: 10.1007/s10681-017-2090-2

Han, S., Utz, H. F., Liu, W., Schrag, T. A., Stange, M., Würschum, T., et al. (2016). Choice of models for QTL mapping with multiple families and design of the training set for prediction of fusarium resistance traits in maize. *Theor. Appl. Genet.* 129 (2), 431–444. doi: 10.1007/s00122-015-2637-3

Hasan, N., Choudhary, S., Naaz, N., Sharma, N., and Laskar, R. A. (2021). Recent advancements in molecular marker-assisted selection and applications in plant breeding programmes. *J. Genet. Eng. Biotechnol.* 19 (1), 128. doi: 10.1186/s43141-021-00231-1

Hasegawa, M., Mitsuhara, I., Seo, S., Okada, K., Yamane, H., Iwai, T., et al. (2014). Analysis on blast fungus-responsive characters of a flavonoid phytoalexin sakuranetin; accumulation in infected rice leaves, antifungal activity and detoxification by fungus. *Molecules* 19 (8), 11404–11418. doi: 10.3390/molecules190811404

He, J., Zhao, X., Laroche, A., Lu, Z.-X., Liu, H., and Li, Z. (2014). Genotyping-by-sequencing (GBS), an ultimate marker-assisted selection (MAS) tool to accelerate plant breeding. *Front. Plant Sci.* 5. doi: 10.3389/fpls.2014.00484

Jiang, S., Zhang, H., Ni, P., Yu, S., Dong, H., Zhang, A., et al. (2020). Genome-wide association study dissects the genetic architecture of maize husk tightness. *Front. Plant Sci.* 11. doi: 10.3389/fpls.2020.00861

Kebebe, A. Z., Reid, L. M., Zhu, X., Wu, J., Woldemariam, T., Voloaca, C., et al. (2015). Relationship between kernel drydown rate and resistance to gibberella ear rot in maize. *Euphytica* 201 (1), 79–88. doi: 10.1007/s10681-014-1185-2

Kebede, A. Z., Johnston, A., Schneiderman, D., Bosnich, W., and Harris, L. J. (2018). Transcriptome profiling of two maize inbreds with distinct responses to gibberella ear rot disease to identify candidate resistance genes. *BMC Genet.* 19, (1). doi: 10.1186/s12864-018-4513-4

Kebede, A. Z., Woldemariam, T., Reid, L. M., and Harris, L. J. (2016). Quantitative trait loci mapping for gibberella ear rot resistance and associated agronomic traits using genotyping-by-sequencing in maize. *Theor. Appl. Genet.* 129 (1), 17–29. doi: 10.1007/s00122-015-2600-3

Kodama, O., Miyakawa, J., Akatsuka, T., and Kiyosawa, S. (1992). Sakuranetin, a flavanone phytoalexin from ultraviolet-irradiated rice leaves. *Phytochemistry* 31 (11), 3807–3809. doi: 10.1016/S0031-9422(00)97532-0

Kuchel, H., Fox, R., Reinheimer, J., Mosionek, L., Willey, N., Bariana, H., et al. (2007). The successful application of a marker-assisted wheat breeding strategy. *Mol. Breed* 20 (4), 295–308. doi: 10.1007/s11032-007-9092-z

Lanubile, A., Ferrarini, A., Maschietto, V., Delledonne, M., Marocco, A., and Bellin, D. (2014). Functional genomic analysis of constitutive and inducible defense responses to *Fusarium verticillioides* infection in maize genotypes with contrasting ear rot resistance. *BMC Genet.* 15, (1). doi: 10.1186/1471-2164-15-710

Lawrence, C. J. (2007). "MaizeGDB," in *Plant bioinformatics: Methods and protocols*. Ed. D. Edwards (Totowa, NJ: Humana Press), pp 331–pp 345. doi: 10.1007/978-1-59745-535-0_16

Lee, E.-J., and Facchini, P. (2010). Norcoclaurine synthase is a member of the pathogenesis-related 10/Bet v1 protein family. *Plant Cell* 22 (10), 3489–3503. doi: 10.1105/tpc.110.077958

Li, Z. M., Ding, J. Q., Wang, R. X., Chen, J. F., Sun, X. D., Chen, W., et al. (2011). A new QTL for resistance to fusarium ear rot in maize. *J. Appl. Genet.* 52 (4), 403–406. doi: 10.1007/s13353-011-0054-0

Liu, Y., Hu, G., Zhang, A., Loladze, A., Hu, Y., Wang, H., et al. (2021). Genome-wide association study and genomic prediction of fusarium ear rot resistance in tropical maize germplasm. *Crop J.* 9 (2), 325–341. doi: 10.1016/j.cj.2020.08.008

Liu, H., Niu, Y., Gonzalez-Portilla, P. J., Zhou, H., Wang, L., Zuo, T., et al. (2015). An ultra-high-density map as a community resource for discerning the genetic basis of quantitative traits in maize. *BMC Genet.* 16 (1), 1078. doi: 10.1186/s12864-015-2242-5

Löffler, M., Kessel, B., Ouzunova, M., and Miedaner, T. (2010a). Population parameters for resistance to *Fusarium graminearum* and *Fusarium verticillioides* ear rot among large sets of early, mid-late and late maturing European maize (*Zea mays* l.) inbred lines. *Theor. Appl. Genet.* 120 (5), 1053–1062. doi: 10.1007/s00122-009-1233-9

Löffler, M., Miedaner, T., Kessel, B., and Ouzunova, M. (2010b). Mycotoxin accumulation and corresponding ear rot rating in three maturity groups of European maize inoculated by two fusarium species. *Euphytica* 174 (2), 153–164. doi: 10.1007/s10681-009-0080-8

Logrieco, A., Battilani, P., Leggieri, M. C., Jiang, Y., Haesaert, G., Lanubile, A., et al. (2021). Perspectives on global mycotoxin issues and management from the mycokey maize working group. *Plant Dis.* 105 (3), 525–537. doi: 10.1094/PDIS-06-20-1322-FE

Ma, N., Abdul Haseeb, H., Xing, F., Su, Z., Shan, L., and Guo, W. (2019). *Fusarium avenaceum*: A toxigenic pathogen causing ear rot on maize in yunnan province, China. *Plant Dis.* 103 (6), 1424. doi: 10.1094/PDIS-11-18-2034-PDN

Machado, F. J., de Barros, A. V., McMaster, N., Schmale, D. G., Vaillancourt, L. J., and Del Ponte, E. M. (2022). Aggressiveness and mycotoxin production by *Fusarium meridionale* compared with f. *graminearum maize ears stalks field. Phytopathol.* 112 (2), 271–277. doi: 10.1094/PHYTO-04-21-0149-R

Martin, M., Dhillon, B. S., Miedaner, T., and Melchinger, A. E. (2012a). Inheritance of resistance to gibberella ear rot and deoxynivalenol contamination in five flint maize crosses. *Plant Breed* 131 (1), 28–32. doi: 10.1111/j.1439-0523.2011.01908.x

Martin, M., Miedaner, T., Dhillon, B. S., Ufermann, U., Kessel, B., Ouzunova, M., et al. (2011). Colocalization of QTL for gibberella ear rot resistance and low mycotoxin contamination in early European maize. *Crop Sci.* 51 (5), 1935–1945. doi: 10.2135/cropsci2010.11.0664

Martin, M., Miedaner, T., Schwegler, D. D., Kessel, B., Ouzunova, M., Dhillon, B. S., et al. (2012b). Comparative quantitative trait loci mapping for gibberella ear rot resistance and reduced deoxynivalenol contamination across connected maize populations. *Crop Sci.* 52 (1), 32–43. doi: 10.2135/cropsci2011.04.0214

Martin, M., Schipprack, W., Miedaner, T., Dhillon, B. S., Kessel, B., Ouzunova, M., et al. (2012c). Variation and covariation for gibberella ear rot resistance and agronomic traits in testcrosses of doubled haploid maize lines. *Euphytica* 185 (3), 441–451. doi: 10.1007/s10681-012-0623-2

Maschietto, V., Colombi, C., Pirona, R., Pea, G., Strozzi, F., Marocco, A., et al. (2017). QTL mapping and candidate genes for resistance to fusarium ear rot and fumonisin contamination in maize. *BMC Plant Biol.* 17, (1). doi: 10.1186/s12870-017-0970-1

Mesterházy, A. (1995). Types and components of resistance to fusarium head blight of wheat. *Plant Breed* 114 (5), 377–386. doi: 10.1111/j.1439-0523.1995.tb00816.x

Mesterházy, A., Lemmens, M., and Reid, L. M. (2012). Breeding for resistance to ear rots caused by fusarium spp. *maize - A review. Plant Breed* 131 (1), 1–19. doi: 10.1111/j.1439-0523.2011.01936.x

Mesterhazy, A., Szieberth, D., Toldine, E. T., Nagy, Z., Szabó, B., Herczig, B., et al. (2022). Updating the methodology of identifying maize hybrids resistant to ear rot pathogens and their toxins–artificial inoculation tests for kernel resistance to *Fusarium graminearum*, f. verticillioides and *Aspergillus flavus*. *J. Fungi* 8, (3). doi: 10.3390/jof8030293

Mideros, S. X., Warburton, M. L., Jamann, T. M., Windham, G. L., Paul Williams, W., and Nelson, R. J. (2014). Quantitative trait loci influencing mycotoxin contamination of maize: Analysis by linkage mapping, characterization of near-isogenic lines, and meta-analysis. *Crop Sci.* 54 (1), 127–142. doi: 10.2135/cropsci2013.04.0249

Miedaner, T., Boeven, A. L. G., Gaikpa, D. S., Kistner, M. B., and Grote, C. P. (2020). Genomics-assisted breeding for quantitative disease resistances in small-grain cereals and maize. *Int. J. Mol. Sci.* 21, (24). doi: 10.3390/ijms21249717

Miedaner, T., Han, S., Kessel, B., Ouzunova, M., Schrag, T., Utz, F. H., et al. (2015). Prediction of deoxynivalenol and zearalenone concentrations in *Fusarium graminearum* inoculated backcross populations of maize by symptom rating and near-infrared spectroscopy. *Plant Breed* 134 (5), 529–534. doi: 10.1111/pbr.12297

Miedaner, T., and Korzun, V. (2012). Marker-assisted selection for disease resistance in wheat and barley breeding. *Phytopathology* 102 (6), 560–566. doi: 10.1094/PHYTO-05-11-0157

Mohammadi, M., Anoop, V., Gleddie, S., and Harris, L. J. (2011). Proteomic profiling of two maize inbreds during early gibberella ear rot infection. *Proteomics* 11 (18), 3675–3684. doi: 10.1002/pmic.201100177

Morales, L., Zila, C. T., Mejía, D. E. M., Arbelaez, M. M., Balint-Kurti, P. J., Holland, J. B., et al. (2019). Diverse components of resistance to fusarium verticillioides infection and fumonisin contamination in four maize recombinant inbred families. *Toxins* 11, (2). doi: 10.3390/toxins11020086

Ncube, E., Truter, M., Flett, B. C., Van Den Berg, J., Erasmus, A., and Viljoen, A. (2020). Fungal mycoflora associated with *Busseola fusca* frass in maize plants. *Afr Entomol* 28 (2), 394–405. doi: 10.4001/003.028.0394

Nerbass, F. R., Casa, R. T., Kuhnem, P. R., Bogo, A., Sangoi, L., Fingstag, M. D., et al. (2016). Evaluation of *Fusarium graminearum* inoculation methods in maize ears and hybrid reaction to gibberella ear rot under southern Brazilian environmental conditions. *Eur. J. Plant Pathol.* 144 (1), 45–53. doi: 10.1007/s10658-015-0746-0

Nida, H., Lee, S., Li, Y., and Mengiste, T. (2021). Transcriptome analysis of early stages of sorghum grain mold disease reveals defense regulators and metabolic pathways associated with resistance. *BMC Genet.* 22 (1), 295. doi: 10.1186/s12864-021-07609-y

Page, M. J., McKenzie, J. E., Bossuyt, P. M., Boutron, I., Hoffmann, T. C., Mulrow, C. D., et al. (2021). The PRISMA 2020 statement: an updated guideline for reporting systematic reviews. *BMJ* 372, n71. doi: 10.1136/bmj.n71

Pè, E. M., Gianfranceschi, L., Taramino, G., Tarchini, R., Angelini, P., Dani, M., et al. (1993). Mapping quantitative trait loci (QTLs) for resistance to *Gibberella zeae* infection in maize. *Mol. Gen. Genet.* 241 (1-2), 11–16. doi: 10.1007/BF00280195

Perincherry, L., Lalak-Kańczugowska, J., and Stępień, Ł. (2019). Fusarium-produced mycotoxins in plant-pathogen interactions. *Toxins* 11, (11). doi: 10.3390/toxins11110664

Pfordt, A., Schiwek, S., Rathgeb, A., Rodemann, C., Bollmann, N., Buchholz, M., et al. (2020). Occurrence, pathogenicity, and mycotoxin production of *Fusarium temperatum* in relation to other fusarium species on maize in Germany. *Pathogens* 9 (11), 1–21. doi: 10.3390/pathogens9110864

Plienegger, J., and Lemmens, M. (2002). Kolbenfaule–gibt es sortenunterschiede? *Mais* 30 (3), 95–97. Abstract from Deutsches Maiskomitee e.V. (DMK), Bonn, Germany.

R Core Team (2021). *R: A language and environment for statistical computing. version 4.1.3* (Vienna, Austria: R Foundation for Statistical Computing). Available at: https://www.R-project.org/.

Reid, L. M., Hamilton, R. I., and Mather, D. E. (1996a). *Screening maize for resistance to gibberella ear rot* (Canada: Agriculture & Agri-Food Canada, Research Branch, Eastern Cereal & Oilseed Research Centre).

Reid, L. M., McDiarmid, G., Parker, A. J., and Woldemariam, T. (2003). CO441 corn inbred line. *Can. J. Plant Sci.* 83 (1), 79–80. doi: 10.4141/P02-058

Reid, L. M., McDiarmid, G., Parker, A. J., Woldemariam, T., and Hamilton, R. I. (2001a). CO388 and CO389 corn inbred lines. *Can. J. Plant Sci.* 81 (3), 457–459. doi: 10.4141/P00-053

Reid, L. M., McDiarmid, G., Parker, A. J., Woldemariam, T., and Hamilton, R. I. (2001b). CO430, CO431 and CO432 corn inbred lines. *Can. J. Plant Sci.* 81 (2), 283–284. doi: 10.4141/P00-118

Reid, L. M., Stewart, D. W., and Hamilton, R. I. (1996b). A 4-year study of the association between gibberella ear rot severity and deoxynivalenol concentration. *J. Phytopathol.* 144 (9-10), 431–436. doi: 10.1111/j.1439-0434.1996.tb00319.x

Reid, L. M., Woldemariam, T., Zhu, X., Stewart, D. W., and Schaafsma, A. W. (2002). Effect of inoculation time and point of entry on disease severity in fusarium graminearum, fusarium verticillioides, or *Fusarium subglutinans* inoculated maize ears. *Can. J. Plant Pathol.* 24 (2), 162–167. doi: 10.1080/07060660309506991

Reinprecht, Y., Wu, X., Yan, S., Labey, L., Dasilva, E., Martin, J. C., et al. (2008). A microarray-based approach for identifying genes for resistance to *Fusarium graminearum* in maize (*Zea mays* l.). *Cereal Res. Commun. 36 (SUPPL.* 6), 253–259. doi: 10.1556/CRC.36.2008.Suppl.B.23

Robertson-Hoyt, L. A., Jines, M. P., Balint-Kurti, P. J., Kleinschmidt, C. E., White, D. G., Payne, G. A., et al. (2006). QTL mapping for fusarium ear rot and fumonisin contamination resistance in two maize populations. *Crop Sci.* 46 (4), 1734–1743. doi: 10.2135/cropsci2005.12-0450

Rossouw, J. D., van Rensburg, J. B. J., and van Deventer, C. S. (2002). Breeding for resistance to ear rot of maize, caused by stenocarpella maydis (Berk) sutton. 1. evaluation of selection criteria. *S Afr J. Plant Soil* 19 (4), 182–187. doi: 10.1080/02571862.2002.10634462

Ruan, Y., Zhang, W., Knox, R. E., Berraies, S., Campbell, H. L., Ragupathy, R., et al. (2020). Characterization of the genetic architecture for fusarium head blight resistance in durum wheat: The complex association of resistance, flowering time, and height genes. *Front. Plant Sci.* 11 doi: 10.3389/fpls.2020.592064

Salvi, S., and Tuberosa, R. (2015). The crop QTLome comes of age. *Curr. Opin. Biotechnol.* 32, 179–185. doi: 10.1016/j.copbio.2015.01.001

Samayoa, L. F., Cao, A., Santiago, R., Malvar, R. A., and Butron, A. (2019). Genome-wide association analysis for fumonisin content in maize kernels. *BMC Plant Biol.* 19, 1–11. doi: 10.1186/s12870-019-1759-1

Sandhu, N., Pruthi, G., Prakash Raigar, O., Singh, M. P., Phagna, K., Kumar, A., et al. (2021). Meta-QTL analysis in rice and cross-genome talk of the genomic regions controlling nitrogen use efficiency in cereal crops revealing phylogenetic relationship. *Front. Genet.* 12. doi: 10.3389/fgene.2021.80721

Savary, S., Willocquet, L., Pethybridge, S. J., Esker, P., McRoberts, N., and Nelson, A. (2019). The global burden of pathogens and pests on major food crops. *Nat. Ecol. Evol.* 3 (3), 430–439. doi: 10.1038/s41559-018-0793-y

Scarpino, V., Reyneri, A., Sulyok, M., Krska, R., and Blandino, M. (2018). Impact of the insecticide application to maize cultivated in different environmental conditions on emerging mycotoxins. *Field Crops Res.* 217, 188–198. doi: 10.1016/j.fcr.2017.12.018

Scauflaire, J., Mahieu, O., Louvieaux, J., Foucart, G., Renard, F., and Munaut, F. (2011). Biodiversity of fusarium species in ears and stalks of maize plants in Belgium. *Eur. J. Plant Pathol.* 131 (1), 59–66. doi: 10.1007/s10658-011-9787-1

Schaafsma, A. W., Tamburic-Ilincic, L., and Reid, L. M. (2006). Fumonisin B1 accumulation and severity of fusarium ear rot and gibberella ear rot in food-grade corn hybrids in Ontario after inoculation according to two methods. *Can. J. Plant Pathol.* 28 (4), 548–557. doi: 10.1080/07060660609507333

Schjøth, J. E., and Sundheim, L. (2013). Epidemic significance of planting time and hybrid on fusarium infection of maize in two agroecological zones of Zambia. *Acta Agric. Scand. - B Soil Plant Sci.* 63 (2), 153–161. doi: 10.1080/09064710.2012.733727

Shala-Mayrhofer, V., Varga, E., Marjakaj, R., Berthiller, F., Musolli, A., Berisha, D., et al. (2013). Investigations on fusarium spp. and their mycotoxins causing fusarium ear rot of maize in Kosovo. *Food Addit Contam Part B Surveill* 6 (4), 237–243. doi: 10.1080/19393210.2013.804885

Shiferaw, B., Prasanna, B. M., Hellin, J., and Bänziger, M. (2011). Crops that feed the world 6. past successes and future challenges to the role played by maize in global food security. *Food Secur.* 3 (3), 307. doi: 10.1007/s12571-011-0140-5

Smith, J. S., Williams, W. P., Windham, G. L., Xu, W. W., Warburton, M. L., and Bhattramakki, D. (2019). Identification of quantitative trait loci contributing resistance to aflatoxin accumulation in maize inbred Mp715. *Mol. Breed* 39, (6). doi: 10.1007/s11032-019-0997-0

Soriano, J. M., Colasuonno, P., Marcotuli, I., and Gadaleta, A. (2021). Meta-QTL analysis and identification of candidate genes for quality, abiotic and biotic stress in durum wheat. *Sci. Rep.* 11 (1), 11877. doi: 10.1038/s41598-021-91446-2

Sosnowski, O., Charcosset, A., and Joets, J. (2012). BioMercator V3: an upgrade of genetic map compilation and quantitative trait loci meta-analysis algorithms. *Bioinformatics* 28 (15), 2082–2083. doi: 10.1093/bioinformatics/bts313

Szabo, B., Toth, B., Toth Toldine, E., Varga, M., Kovacs, N., Varga, J., et al. (2018). A new concept to secure food safety standards against fusarium species and *Aspergillus flavus* and their toxins in maize. *Toxins* 10, (9). doi: 10.3390/toxins10090372

Tembo, E., Minnaar-Ontong, A., Menkir, A., Marais, G., Magorokosho, C., and Labuschagne, M. T. (2022). Inheritance of resistance to *Fusarium verticillioides* ear rot in maize inbred lines of southern, West and central Africa origin. *Crop Sci.*, 62 (5), 1813–1833. doi: 10.1002/csc2.20776

Tian, H.-L., Wang, F.-G., Zhao, J.-R., Yi, H.-M., Wang, L., Wang, R., et al. (2015). Development of maizeSNP3072, a high-throughput compatible SNP array, for DNA fingerprinting identification of Chinese maize varieties. *Mol. Breed* 35 (6), 136. doi: 10.1007/s11032-015-0335-0

Tsehaye, H., Brurberg, M. B., Sundheim, L., Assefa, D., Tronsmo, A., and Tronsmo, A. M. (2017). Natural occurrence of fusarium species and fumonisin on maize grains in Ethiopia. *Eur. J. Plant Pathol.* 147 (1), 141–155. doi: 10.1007/s10658-016-0987-6

Unterseer, S., Pophaly, S. D., Peis, R., Westermeier, P., Mayer, M., Seidel, M. A., et al. (2016). A comprehensive study of the genomic differentiation between temperate dent and flint maize. *Genome Biol.* 17 (1), 137. doi: 10.1186/s13059-016-1009-x

Venske, E., dos Santos, R. S., D.d.R., F., Rother, V., da Maia, L. C., Pegoraro, C., et al. (2019). Meta-analysis of the QTLome of fusarium head blight resistance in bread wheat: Refining the rurrent puzzle. *Front. Plant Sci.* 10. doi: 10.3389/fpls.2019.00727

Veyrieras, J.-B., Goffinet, B., and Charcosset, A. (2007). MetaQTL: a package of new computational methods for the meta-analysis of QTL mapping experiments. *BMC Bioinf.* 8 (1), 49. doi: 10.1186/1471-2105-8-49

Wada, N., Ueta, R., Osakabe, Y., and Osakabe, K. (2020). Precision genome editing in plants: state-of-the-art in CRISPR/Cas9-based genome engineering. *BMC Plant Biol.* 20 (1), 234. doi: 10.1186/s12870-020-02385-5

Wang, R., Hua, C., Hu, Y., Li, L., Sun, Z., and Li, T. (2021). Two different inoculation methods unveiled the relative independence of DON accumulation in wheat kernels from disease severity on spike after infection by fusarium head blight. *Toxins* 13, (5). doi: 10.3390/toxins13050353

Warfield, C. Y., and Davis, R. M. (1996). Importance of the husk covering on the susceptibility of corn hybrids to fusarium ear rot. *Plant Dis.* 80 (2), 208–210. doi: 10.1094/PD-80-0208

Wen, J., Shen, Y. Q., Wang, Z. Y., Li, S. J., Mo, L. Y., Lei, Y. H., et al. (2021a). QTL mapping of resistance to fusarium ear rot in maize based on image analysis. *Sci. Agric. Sin.* 54 (13), 2724–2736. doi: 10.3864/j.issn.0578-1752.2021.13.003

Wen, J., Shen, Y. Q., Xing, Y. X., Wang, Z. Y., Han, S. P., Li, S. J., et al. (2020). QTL mapping of resistance to gibberella ear rot in maize. *Mol. Breed* 40, (10). doi: 10.1007/s11032-020-01173-1

Wen, J., Shen, Y. Q., Xing, Y. X., Wang, Z. Y., Han, S. P., Li, S. J., et al. (2021b). QTL mapping of fusarium ear rot resistance in maize. *Plant Dis.* 105 (3), 558–565. doi: 10.1094/PDIS-02-20-0411-RE

Willcox, M. C., Davis, G. L., Warburton, M. L., Windham, G. L., Abbas, H. K., Betrán, J., et al. (2013). Confirming quantitative trait loci for aflatoxin resistance from Mp313E in different genetic backgrounds. *Mol. Breed* 32 (1), 15–26. doi: 10.1007/s11032-012-9821-9

Wu, J., Kim, S. G., Kang, K. Y., Kim, J.-G., Park, S.-R., Gupta, R., et al. (2016). Overexpression of a pathogenesis-related protein 10 enhances biotic and abiotic stress tolerance in rice. *Plant Pathol. J.* 32 (6), 552–562. doi: 10.5423/PPJ.OA.06.2016.0141

Wu, Y., Zhou, Z., Dong, C., Chen, J., Ding, J., Zhang, X., et al. (2020). Linkage mapping and genome-wide association study reveals conservative QTL and candidate genes for fusarium rot resistance in maize. *BMC Genet.* 21, (1). doi: 10.1186/s12864-020-6733-7

Xiang, K., Reid, L. M., Zhang, Z. M., Zhu, X. Y., and Pan, G. T. (2012). Characterization of correlation between grain moisture and ear rot resistance in maize by QTL meta-analysis. *Euphytica* 183 (2), 185–195. doi: 10.1007/s10681-011-0440-z

Xiang, K., Zhang, Z. M., Reid, L. M., Zhu, X. Y., Yuan, G. S., and Pan, G. T. (2010). A meta-analysis of QTL associated with ear rot resistance in maize. *Maydica* 55 (3-4), 281–290.

Xie, Y.-R., Chen, Z.-Y., Brown, R. L., and Bhatnagar, D. (2010). Expression and functional characterization of two pathogenesis-related protein 10 genes from *Zea mays*. *J. Plant Physiol.* 167 (2), 121–130. doi: 10.1016/j.jplph.2009.07.004

Xu, K., He, X., Dreisigacker, S., He, Z., and Singh, P. K. (2020). Anther extrusion and its association with fusarium head blight in CIMMYT wheat germplasm. *Agronomy* 10, (1). doi: 10.3390/agronomy10010047

Yuan, G., Chen, B., Peng, H., Zheng, Q., Li, Y., Xiang, K., et al. (2020a). QTL mapping for resistance to ear rot caused by *Fusarium graminearum* using an IBM Syn10 DH population in maize. *Mol. Breed* 40, (9). doi: 10.1007/s11032-020-01158-0

Yuan, G., He, X., Li, H., Xiang, K., Liu, L., Zou, C., et al. (2020b). Transcriptomic responses in resistant and susceptible maize infected with *Fusarium graminearum*. *Crop J.* 8 (1), 153–163. doi: 10.1016/j.cj.2019.05.008

Yu, H., Xie, W., Wang, J., Xing, Y., Xu, C., Li, X., et al. (2011). Correction: Gains in QTL detection using an ultra-high density SNP map based on population sequencing relative to traditional RFLP/SSR markers. *PloS One* 6 (3), e17595. doi: 10.1371/journal.pone.0017595

Yu, T., Zhang, J., Cao, J., Cao, S., Li, W., and Yang, G. (2022). A meta-analysis of low temperature tolerance QTL in maize. *Electron J. Biotechnol.* 58, 82–91. doi: 10.1016/j.ejbt.2022.05.002

Zhou, G., Li, S., Ma, L., Wang, F., Jiang, F., Sun, Y., et al. (2021). Mapping and validation of a stable quantitative trait locus conferring maize resistance to gibberella ear rot. *Plant Dis.* 105, (7). doi: 10.1094/PDIS-11-20-2487-RE

Meta-analysis and co-expression analysis revealed stable QTL and candidate genes conferring resistances to Fusarium and Gibberella ear rots while reducing mycotoxin contamination in maize

Félicien Akohoue[1], Thomas Miedaner[1*]

Supplementary information

Supplementary File 1: Information recorded on quantitative trait loci (QTL) reported by 15 SNP-based studies on resistance to Fusarium and Gibberella ear rots related traits in maize. QTL highlighted in grey were not included in the meta-analysis. Available online at: https://www.frontiersin.org/articles/10.3389/fpls.2022.1050891/full#supplementary-material

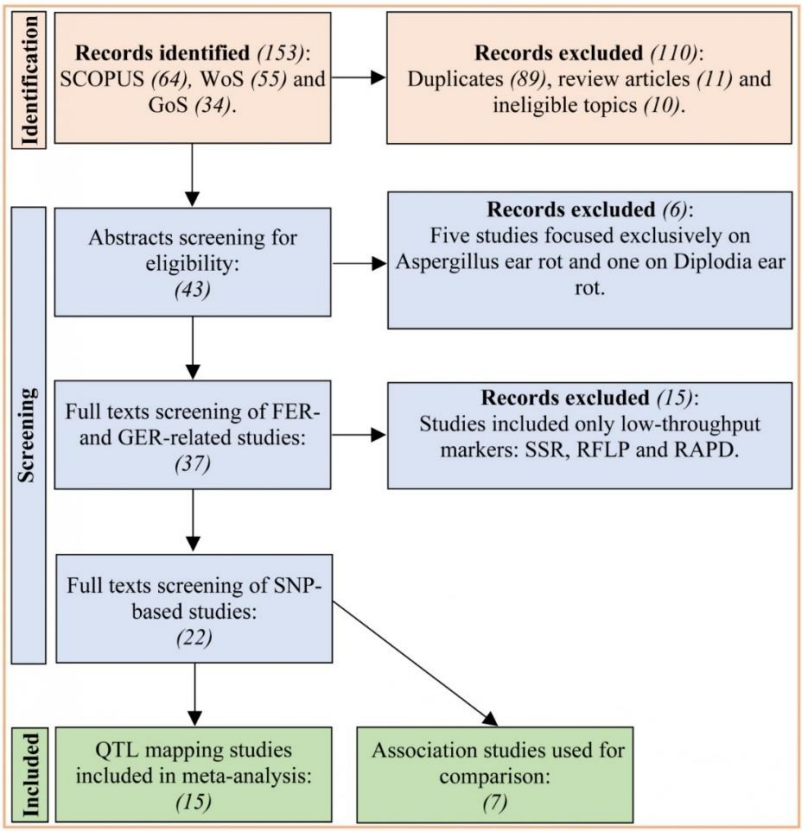

Supplementary File 2: Preferred reporting items for systematic review and meta-analyses (PRISMA) flow diagram. WoS = Web of Science, GoS = Google Scholar, RAPD = random amplified polymorphic DNA, RFLP = restriction fragment length polymorphisms, SNP = single nucleotide polymorphism, SSR = single sequence repeats. Numbers of publications are indicated in parenthesis for each category

Supplementary File 3: Consensus map. Available online at: https://www.frontiersin.org/articles/10.3389/fpls.2022.1050891/full#supplementary-material

Supplementary File 4: Characterization of meta-QTL (MQTL) identified based on the 15 QTL mapping studies. CI = confidence interval, PVE = phenotypic variance explained, FER = Fusarium ear rot, GER = Gibberella ear rot, SR = silk resistance, KR = kernel resistance, DON = Deoxynivalenol accumulation, FUM = fuminosin accumulation, KDD = kernel dry-down rate, HC = husk coverage. Meta-QTL name referred to *Zea mays* abbreviated as *Zm*, followed by MQTL, the corresponding chromosome, and identification number on the chromosome. Available online at: https://www.frontiersin.org/articles/10.3389/fpls.2022.1050891/full#supplementary-material

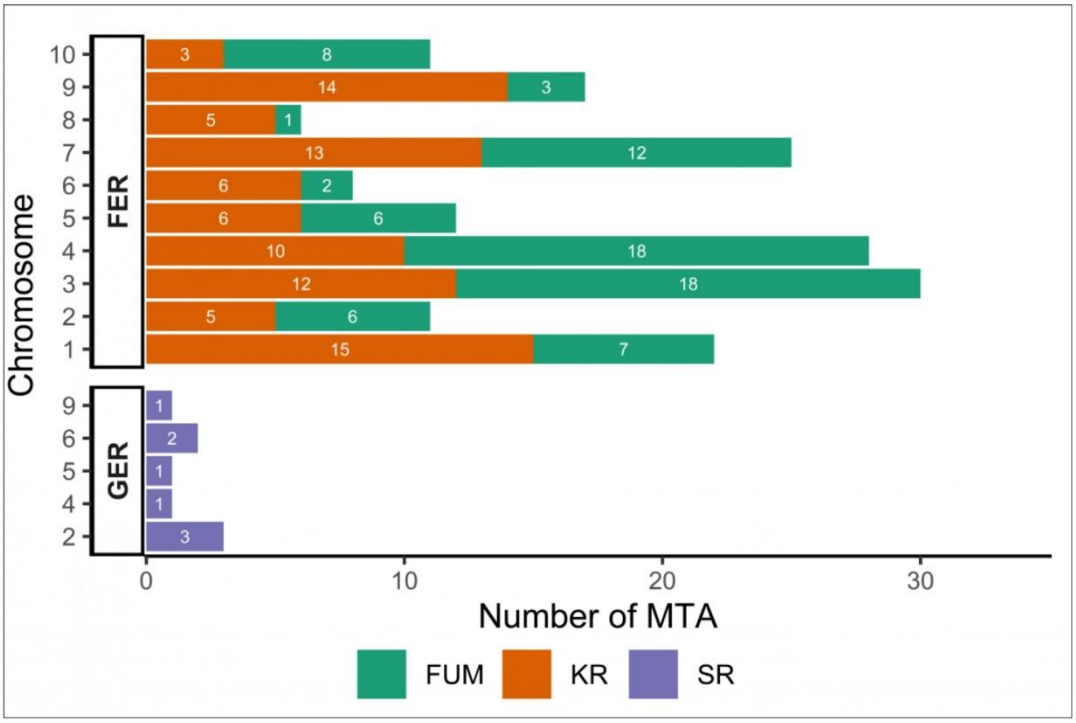

Supplementary File 5: Marker-trait associations (MTA) from genome-wide association study (GWAS) reported for Fusarium ear rot (FER) and Gibberella ear rot (GER). FUM = fumonisin accumulation, KR = kernel resistance, SR = silk resistance

Supplementary File 6: Candidate genes mined within major and most refined meta-QTL (MQTL). Available online at: https://www.frontiersin.org/articles/10.3389/fpls.2022.1050891/full#supplementary-material

Supplementary File 7: Expression level in transcripts per million (TPM) of differentially expressed candidate genes (CG) in two maize lines under control conditions and after infection with *Fusarium graminearum*. DAI = days after inoculation, FC = fold change. Available online at: https://www.frontiersin.org/articles/10.3389/fpls.2022.1050891/full#supplementary-material

Supplementary File 8: Annotation and ontology terms and functional category of differentially expressed candidate genes (CG) in both resistant (CO441) and susceptible (B37) lines within meta-QTL (MQTL). Available online at: https://www.frontiersin.org/articles/10.3389/fpls.2022.1050891/full#supplementary-material

Chapter 4: Effectiveness of introgression of resistance loci for Gibberella ear rot from two European flint landraces into adapted elite maize (*Zea mays* L.)

Félicien Akohoue[1], Silvia Koch[1], Bärbel Lieberherr[1], Bettina Kessel[2], Thomas Presterl[2], Thomas Miedaner[1*]

[1]State Plant Breeding Institute, University of Hohenheim, Stuttgart, Germany;

[2]Kleinwanzlebener Saatzucht (KWS) KWS SAAT SE & Co. KGaA, Einbeck, Germany;

*Correspondence: thomas.miedaner@uni-hohenheim.de (T.M.)

ORCID T.M.: https://orcid.org/0000-0002-9541-3726

Published in *PLoS ONE*. 2023; 18(9): e0292095.

https://doi.org/10.1371/journal.pone.0292095.

Submitted: 16 March 2023 / **Accepted**: 12 September 2023 / **Published**: 27 September 2023.

PLOS ONE

RESEARCH ARTICLE

Effectiveness of introgression of resistance loci for Gibberella ear rot from two European flint landraces into adapted elite maize (*Zea mays* L.)

Félicien Akohoue[1], Silvia Koch[1], Bärbel Lieberherr[1], Bettina Kessel[2], Thomas Presterl[2], Thomas Miedaner[1]*

1 State Plant Breeding Institute, University of Hohenheim, Stuttgart, Germany, **2** Kleinwanzlebener Saatzucht (KWS) KWS SAAT SE & Co. KGaA, Einbeck, Germany

* miedaner@uni-hohenheim.de

Citation: Akohoue F, Koch S, Lieberherr B, Kessel B, Presterl T, Miedaner T (2023) Effectiveness of introgression of resistance loci for Gibberella ear rot from two European flint landraces into adapted elite maize (*Zea mays* L.). PLoS ONE 18(9): e0292095. https://doi.org/10.1371/journal.pone.0292095

Editor: Lewis Lukens, University of Guelph, CANADA

Received: March 16, 2023

Accepted: September 12, 2023

Published: September 27, 2023

Data Availability Statement: All relevant data are within the manuscript and its Supporting Information files.

Funding: This study was funded by the German Academic Exchange Service (DAAD), Bonn, Germany (grant no. 91770158), KWS SAAT SE & Co. KGaA, Einbeck, Germany and the University of Hohenheim. The funders had no role in study design, data collection and analysis, decision to publish, or preparation of the manuscript.

Abstract

European flint landraces are a major class of maize possessing favorable alleles for improving host resistance to Gibberella ear rot (GER) disease which reduces yield and contaminates the grains with mycotoxins. However, the incorporation of these landraces into breeding programs requires a clear understanding of the effectiveness of their introgression into elite materials. We evaluated 15 pre-selected doubled haploid (DH) lines from two European flint landraces, "Kemater Landmais Gelb" (KE) and "Petkuser Ferdinand Rot" (PE), together with two adapted elite flint lines and seven standard lines for GER severity as the main trait, and several adaptation traits (plant height, days to silking, seed-set, plant vigor) across four environments. From this evaluation, three KE DH lines and one PE DH line, with the lowest GER severity, were selected and used as donor parents that were crossed with the two adapted and GER susceptible flint lines (Flint1 and Flint2) to develop six bi-parental DH populations with 34−145 DH lines each. Each DH population was evaluated across two locations. Correlations between GER severity, which was the target trait, and adaptation traits were weak (−0.02 to 0.19). GER severity of lines from PE landrace was on average 2-fold higher than lines from KE landrace, indicating a clear superiority of the KE landrace lines. Mean GER severity of the DH populations was 39.4−61.0% lower than the adapted elite flint lines. All KE-derived DH populations were on average more resistant (27.0−36.7%) than the PE-derived population (51.0%). Highly resistant lines (1.3−5.2%) were found in all of the populations, suggesting that the DH populations can be successfully integrated into elite breeding programs. The findings demonstrate that selected KE landrace lines used as donors were effective in improving GER resistance of the adapted elite inbreds.

Introduction

Maize (*Zea mays* L.) is the most important cereal crop before wheat (*Triticum aestivum* L.) and rice (*Oryza* sp.) for worldwide production. In Northwestern (NW) Europe, maize

Competing interests: The authors have declared that no competing interests exist.

cultivation started on a large scale with the upcoming of hybrid cultivars in the 1960s. However, in the 500 years since Columbus' voyages, a great array of landraces were cultivated in NW Europe which descended mainly from Northern flints introduced from Northeastern United States of America (USA) or Canada in the 16th and 17th century [1]. These landraces evolved upon a long time and adapted in the allogamous crop by selection for specific agro-climatic conditions. They are highly heterozygous and show a high within landrace genetic variance as indicated, for example, for ergot resistance in rye populations [2] and for agronomic traits in maize [3]. This was a motivation to produce doubled haploid (DH) line libraries of selected landraces [4] and to test them for adaptation and target traits.

Unfortunately, all these landraces disappeared with the advent of hybrid cultivars [5], however, they may contain favorable alleles not present in elite gene pools. The flint gene pool is still indispensable for maize cultivation in NW Europe because of its earliness and cold tolerance [6], but relies on only a few first-cycle founder lines extracted from a handful landraces [3]. Molecular studies show that only a tiny fraction of the landraces have been incorporated into modern flint elite lines [7]. Lines derived from landraces, however, have a yield gap to the elite material and are often lacking important adaptation traits like earliness, lodging tolerance, resistance to corn smut (*Ustilago maydis*) and viruses like sugar cane mosaic virus (SCMV) or maize dwarf mosaic virus (MDMV). Frequent tillering and disorders of male and female flowering may also inhibit their use. However, the extreme level of uniformity introduced by artificial selection renders modern elite materials vulnerable to adverse environmental factors and new and emerging pest and diseases [8].

Biotic stress is a major production constraint for maize. Over 38 pests and pathogens, of which Fusarium and Gibberella ear and stalk rots and northern corn leaf blight are the major diseases reported in NW Europe [9]. These diseases gained more importance in NW Europe in the last decade, a development that will continue with increasing temperatures due to climate change [10, 11]. All pathogens and pests together reduce at present grain yield by 22.5% on a global scale in maize [9]. From this, ear and stalk rots together contribute at least 7% to yield gaps. New resistance sources are therefore an important factor to reduce yield gap in hybrid maize production.

Ear rot diseases significantly affect grain production and contaminate grains with mycotoxins [12–14]. In cooler regions such as Europe, northern United States, Canada and some higher altitudes in Africa, Gibberella ear rot (GER) is one of the major types that infect greater proportions of maize [15–20]. GER is caused by the *Fusarium graminearum* species complex, with *F. graminearum sensu strictu* Schwabe (teleomorph *Gibberella zeae*) as the most dominant causal agent. This fungus reduces grain weight per ear, hence the yield [12], and contaminates kernels with several mycotoxins of which deoxynivalenol (DON) and zearalenone (ZON) are the most abundant [21]. Up to 48% of yield reduction was reported by Vigier et al. [13] after GER infection in susceptible inbred lines in Canada. Existing management options are mainly related to best agronomic practices, the adoption of mycotoxin reduction technologies, the utilization of fungicides to control pathogens infections [22–24] and resistance breeding [25, 26].

Previous pre-breeding studies revealed a high genetic diversity and the existence of new sources of resistance against GER in European maize landraces [27, 28]. Brauner et al. [29] investigated the performance of testcrosses of DH lines from European flint maize landraces and demonstrated their high potential for the improvement of elite germplasm. Gaikpa et al. [27] reported eight QTL significantly associated with GER resistance in "Kemater Landmais Gelb" (KE, from Austria) landrace. Recently, Akohoue and Miedaner [30] conducted a quantitative trait loci (QTL) meta-analysis which revealed that diverse sources of resistance, including the KE landrace, contributed to the identification of 40 meta-QTL harbouring several putative resistance genes. This demonstrates that the European flint landraces represent

important sources of resistance which could be explored for their introgression into elite cultivars. Here we want to test the possibility for using selected lines from landraces for improvement of elite maize for Gibberella ear rot (GER) resistance.

This study aims to (i) select GER-resistant lines from KE and PE landraces to be used as donor parents in crosses with two adapted and highly susceptible flint lines to generate six DH populations, (ii) evaluate the effectiveness of the introgression of GER resistance genes into the adapted lines using donor lines from KE and PE landraces, and (iii) select most GER-resistant lines from each DH population and compare their performance with the two susceptible flint lines. GER severity was our target trait evaluated in the study. Plant height, days to silking, seed-set and plant vigor were recorded only as adaptation traits to evaluate their interaction with GER severity and describe the selected GER-resistant lines from each DH population in comparison with the two adapted susceptible flint lines.

Materials and methods

Plant materials and field experiments

Two experiments were followed in this study: (1) Testing of 15 landrace DH lines for their GER resistance in 2021 and 2022, and (2) testing of DH populations derived from crosses of two adapted susceptible flint lines with four donor landrace DH lines.

Testing of 15 DH lines in 2021 and 2022 (experiment 1)

Eight DH lines from "*Kemater Landmais Gelb*" (KE, from Austria) landrace and seven DH lines from "*Petkuser Ferdinand Rot*" (PE, from Germany) landrace were selected from a previous study by Gaikpa et al. [27] out of 250 lines per landrace. These 15 DH lines were evaluated in Hohenheim (HOH, near Stuttgart) and Gondelsheim (GON, near Karlsruhe) in Germany in 2021 and 2022. Two adapted GER-susceptible flint lines (Flint1 and Flint2) and seven standard checks (Table 1) were also included, making a total of 24 lines which were evaluated at each location using a randomized complete block design (RCBD) with three replicates in 2021 and an alpha lattice design with two replicates in 2022 (see below). Parental and standard lines were therefore included in both experiments, so we had four environments for these materials

Table 1. Recipient and standard lines included in experiments 1 and 2 and their corresponding Gibberella ear rot (GER) status.

Line	Code	GER status
Recipient parents:		
Flint1	Flint1	susceptible
Flint2	Flint2	susceptible
Standard checks:		
Check_Dent_res	Dent_res	resistant
Check_Dent_sus	Dent_sus	susceptible
Check_Flint_res	Flint_res	resistant
Check_Flint_sus	Flint_sus	susceptible
CO354	CO354	susceptible
F353	F353	resistant
CO441	CO441	resistant

GER severity was the percentage of a maize ear visually affected by mycelium. All lines were evaluated for GER severity at two locations in 2021 and 2022

https://doi.org/10.1371/journal.pone.0292095.t001

(2 locations, 2 years). Standard checks CO441 and CO354 were provided by Prof. Lana M. Reid from Eastern Cereal and Oilseed Research Centre, Central Experimental Farm, Agriculture and Agri-Food Canada, Ottawa, Canada [31], while the French dent line F353 was provided by INRAE, Paris, France. Other standard checks such as Check-Dent-res, Check-Dent-sus, Check-Flint-res and Check-Flint-sus, as well as the adapted flint lines (Flint1 and Flint2) were provided by KWS SAAT SE & Co. KGaA. In each experiment, each plot consisted of 20 plants in a single row of 3 m length with an inter-row spacing of 0.75 m and within-row spacing of 0.15 m. From this experiment 1 in 2021, KE3, KE7 and KE8 were selected as GER-resistant DH lines, and PE2 as a moderately GER-resistant DH line by artificial infection.

Testing of landrace-derived DH populations in 2022 (Experiment 2)

Six doubled haploid (DH) populations were generated from the following F1 crosses: Flint1×KE3, Flint2×KE3, Flint1×KE7, Flint2×KE7, Flint2×KE8 and Flint1×PE2 with 81, 82, 34, 65, 127 and 145 DH lines, respectively, as outcome of the established method for maize DH production by vivo induction of maternal haploids by a male haploid inducer genotype. These landrace-derived DH populations can also be considered as the first generation of GER resistance introgression into elite lines. KE3, KE7, KE8 and PE2 selected from experiment 1 (2021) were used as GER resistance donor parents, while Flint1 and Flint2 were included as susceptible recipient parents. All materials were multiplied in an off-season program in Chile by KWS SAAT SE & Co. KGaA, Germany.

Afterwards, all the 534 DH lines developed from the six DH populations were evaluated in 2022, together with the 24 parental lines and standard checks from experiment 1 at the same two locations, using an alpha lattice design with two replicates. Plot size was as explained above for experiment 1.

Artificial inoculations and data collection

Inoculation and data collection were performed similarly for both experiments. The highly aggressive *F. graminearum* isolate IFA66 kindly provided by Prof. Dr. Marc Lemmens (University of Natural Resources and Life Sciences, Vienna, Austria) was used to prepare our inoculum suspension following the protocol of Reid et al. [32]. IFA66 was originally isolated by the Department für Agrarbiotechnologie, IFA-Tulln (Tulln an der Donau, Austria) from maize [33]. An aggressiveness test of this isolate (coded as Fg1) was done by Miedaner et al. [34] who revealed that IFA66 was not significantly different from the most aggressive isolates. Exactly 2 mL of the inoculum suspension containing 1.5×10^4 spores.mL^{-1} [27, 35, 36] were applied with a one-needle vaccinator with automatic refill on the silk channel of each cob at 10 plants per row. Artificial inoculations were done five to six days after silk emergence.

All phenotypic traits were recorded for ten maize plants per plot individually. GER severity, which was our target trait, was rated as the percentage of a maize ear visually affected by mycelium, with a score of 0% representing no visible infection and 100% means that all kernels per cob were infected. Additionally, important adaptation traits such as days to silking (DS), plant height (PH, cm), seed-set (SS, %) and plant vigor (PV) were also recorded. DS was recorded when at least 50% of plants per row showed female flowers. SS was collected during disease rating as the percentage of a maize ear covered by kernels. PV was rated 30 to 35 days after sowing at each location on a scale of 1–9 using the height of the plants and color and size of the leaves as criteria, where 1 = very short plants, very small yellowish leaf blades, very poor vigor, and 9 = very tall plants, very large and green leaf blades, excellent vigor [37].

Data analysis

Basically, we used plot data for each trait. The raw data of the ten plants per plot was first explored to remove outliers per row using the Bonferroni-Holm approach based on re-scaled median absolute deviation (MAD) for standardizing residuals (BH-MADR) described by Bernal-Vasquez et al. [38]. Afterwards, plants with seed-set of 0% were also removed. This resulted in the removal of about 10% of the entire data set. To reduce heterogeneity and ensure the normality of the data, GER severity was transformed using the arcsine square root method [39]. Pearson correlation analysis was conducted between the original GER severity and the transformed values to assess the validity of the transformation.

Furthermore, a two-stage analysis was performed for each trait, following the fully efficient procedure described in detail by Piepho et al. [40] and Buntaran et al. [41]. The procedure is said "fully efficient" because the full variance-covariance matrix of adjusted means in the first stage is forwarded to the second stage of the analysis. According to Buntaran et al. [41], estimates from the fully efficient two-stage analysis are highly correlated (0.97) with the standard single-stage analysis, showing the similar performance of the two types of analysis. Here, the application of the two-stage analysis was relevant for estimating adjusted means of parental and standard lines which were included in the two experimental designs (RCBD and alpha lattice) applied in the study. The data was hierarchized by trial within environment and block.

In the first stage, the data was aggregated at trial level and best linear unbiased estimators (BLUEs) were calculated for the lines following the mixed linear model:

$$\text{RCBD}: \quad Y_{ik} = \mu + G_i + B_k + \varepsilon_{ik} \tag{1}$$

$$\text{Alpha lattice design}: \quad Y_{ikp} = \mu + G_i + Rp + B_{pk} + \varepsilon_{ikp} \tag{2}$$

where Y_{ik} = response of genotype i in block k; Y'_{ikp} = response of genotype i in replicate p and block k; μ = general mean effect, G_i = genotype, R_p = replicate, B_{pk} = block nested within replicate, and ε_{ik} and ε_{ikp} = residual error. In these models, genotype was fixed while replicate and block were used as random effects. The RCBD equation applied to the experiment evaluating the parents and standard lines in 2021 (experiment 1), while the alpha lattice equation analyzed the experiment evaluating the parents, standard lines in 2022 (experiment 1) and the six DH populations in 2022 (experiment 2).

In the second stage, a mixed linear model was fitted across environments using the BLUEs and the full variance-covariance matrix from the first stage to estimate variance components and broad sense heritability for each trait as follows:

$$Y_{il} = \mu + G_i + E_l + GE_{il} + \varepsilon_{il} \tag{3}$$

where Y_{il} = BLUE of genotype i within environment l; μ = general mean effect, G_i = genotype i within environment l, E_l = environment, GE_{il} = genotype by environment interaction and ε_{il} = residual error associated with BLUE of genotype i within environment l. Variance-covariance matrix was used to separate genotype-environment interaction and the residual variances.

Dummy variables (0, 1) were used to separate populations, donor and recipient parents [42]. For each population, in defining the dummy variable, 1 was applied for all lines belonging to the population and 0 for others lines. The interaction between genotype and each dummy variable (*Dummy*:*genotype*) generated estimates for all lines coded as 1. Therefore, this interaction term was applied to subset the data and estimate variance components for each population separately. Genotype, environment and genotype-environment effects were used as random in the second stage model to estimate variance components. The likelihood ratio test (LRT) was implemented to analyze significance of variance components [43].

Broad sense heritability (H^2) was estimated as follows [44, 45]:

$$H^2 = \left(1 - \frac{\bar{v}_{\Delta...}^{BLUP}}{2\sigma_g^2}\right) \quad (4)$$

where σ_g^2 is the genotypic variance, $\bar{v}_{\Delta}^{BLUP}$ is the average standard error of difference of two genotypic best linear unbiased predictions (BLUP). Outlier removal, the two-stage analysis and heritability estimates were performed using ASReml v.4.1 [46].

The genotypic coefficient of variation (CV_G, %) was calculated for each trait as:

$$CV_G = \left(\frac{\sqrt{\sigma_g^2}}{Mean}\right) x\ 100 \quad (5)$$

where σ_g^2 is the genotypic variance. In addition, coefficient of variation due to error (CV_{ε}, %) was estimated by replacing the genotypic variance (σ_g^2) by the residual variance (σ_ε^2) in Eq 5.

Based on the BLUEs for GER severity (S1 Table), five best DH lines were selected within each DH population, and their GER severity and BLUEs for adaptation traits were compared to those of the recipient parents and the standard checks. All analyses were conducted in the R software v4.1.0 [47].

Results

Frequency distributions and correlations among GER severity and adaptation traits (experiment 1 + 2)

For illustrating the genotypic variation across both experiments, we firstly present the analysis of the histograms based on best linear unbiased estimations across environments (Fig 1). GER severity and the adaptation traits were quantitatively distributed; with the exception of SS (Fig 1). Most lines exhibited relatively high seed-set across landraces and DH populations. Lines from both landraces have been previously selected for seed-set by Gaikpa et al. [27], and the adapted flint lines had high seed-set (>95%).

Low phenotypic correlations (−0.04 to 0.19) were observed between GER severity and the adaptation traits (Fig 1). Significant negative correlation (−0.46) was detected between DS and SS, which might be due to the increased average temperature recorded in 2022 in all environments; that might lead to seed abortion in late lines. A highly significant correlation was found between original and transformed GER severity, confirming the reliability of the inferences based on the arcsine square root transformation applied in our study. It is of particular interest that the correlation between GER and PV is of low importance, an indication that the low plant vigour of part of the lines does not have a strong effect on *F. graminearum* infection.

Genetic variation of GER severity and adaptation traits within 15 DH lines from landraces (experiment 1)

Within lines drawn from both KE and PE landraces, considerable genetic variation was observed for all traits (Table 2). Genotype by environment interaction variances for GER severity were significant and represented about 1% and 54% of the genotypic variance for KE and PE lines, respectively. Broad sense heritability ranged from 0.62 to 0.98, with the lowest value observed for seed-set (SS) (Table 2). Heritability estimate and genetic coefficient of variation (CV_G) of GER severity were considerably higher in lines from KE landrace than that of

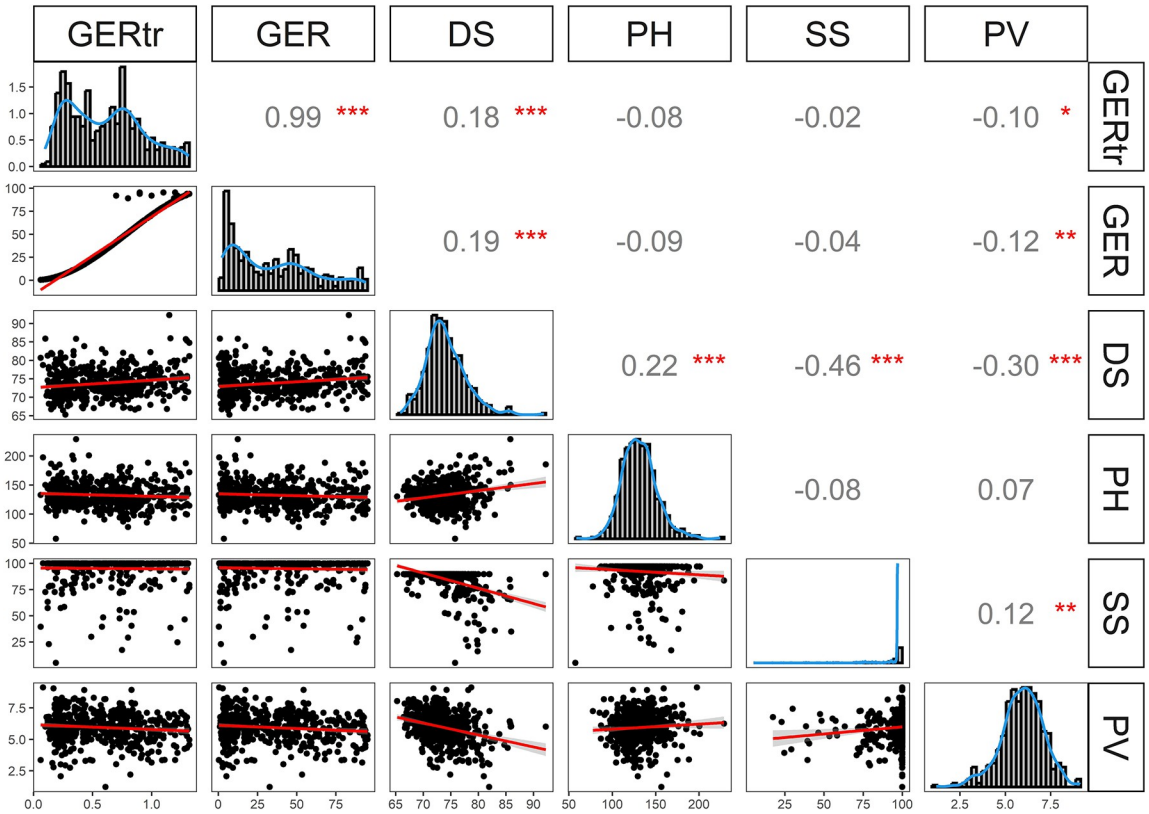

Fig 1. Frequency distributions and correlations among Gibberella ear rot (GER) severity (original values, %), transformed GER severity (GER_{tr}), plant height (PH, cm), days to silking (DS), seed-set (SS, %) and plant vigor (PV) based on best linear unbiased estimations of the 15 landraces lines, two recipient parents, nine standard checks and 534 doubled haploid lines from the six populations. *, ** significant at $p<0.05$, 0.01, respectively.

https://doi.org/10.1371/journal.pone.0292095.g001

PE landrace lines. The coefficient of variation due to error (CV_ε) was low (0.78–24.10) for all traits and lower than the CV_G, except for GER severity of PE landrace (Table 2).

PH = plant height, DS = days to silking, SS = seed-set, PV = plant vigor, CV_G = genotypic coefficient of variation (%), CV_ε = coefficient of variation of error (%), σ^2_G = genotypic

Table 2. Descriptive statistics, variance components and heritability estimates of adaptation traits and Gibberella ear rot (GER) severity of 15 lines drawn from Kemater and Petkuser landraces.

Trait	Unit	CV_G	CV_ε	σ^2_G	σ^2_{GE}	σ^2_ε	H^2
Kemater landrace:							
GER	%	65.37	24.10	20.60	0.20	2.80	0.98
PH	cm	13.38	2.76	490.90	164.30	20.86	0.93
DS	days	3.09	0.78	6.23	3.92	0.40	0.89
SS	%	6.27	4.42	27.37	8.13	20.41	0.62
PV	-	11.26	6.14	0.47	0.33	0.14	0.63
Petkuser landrace:							
GER	%	8.88	17.42	1.10	0.60	4.30	0.76
PH	cm	10.41	3.44	234.90	192.50	25.67	0.86
DS	days	4.15	0.84	11.57	1.97	0.48	0.95
SS	%	11.12	7.51	67.49	15.22	30.78	0.67
PV	-	15.37	7.79	0.78	0.31	0.20	0.67

https://doi.org/10.1371/journal.pone.0292095.t002

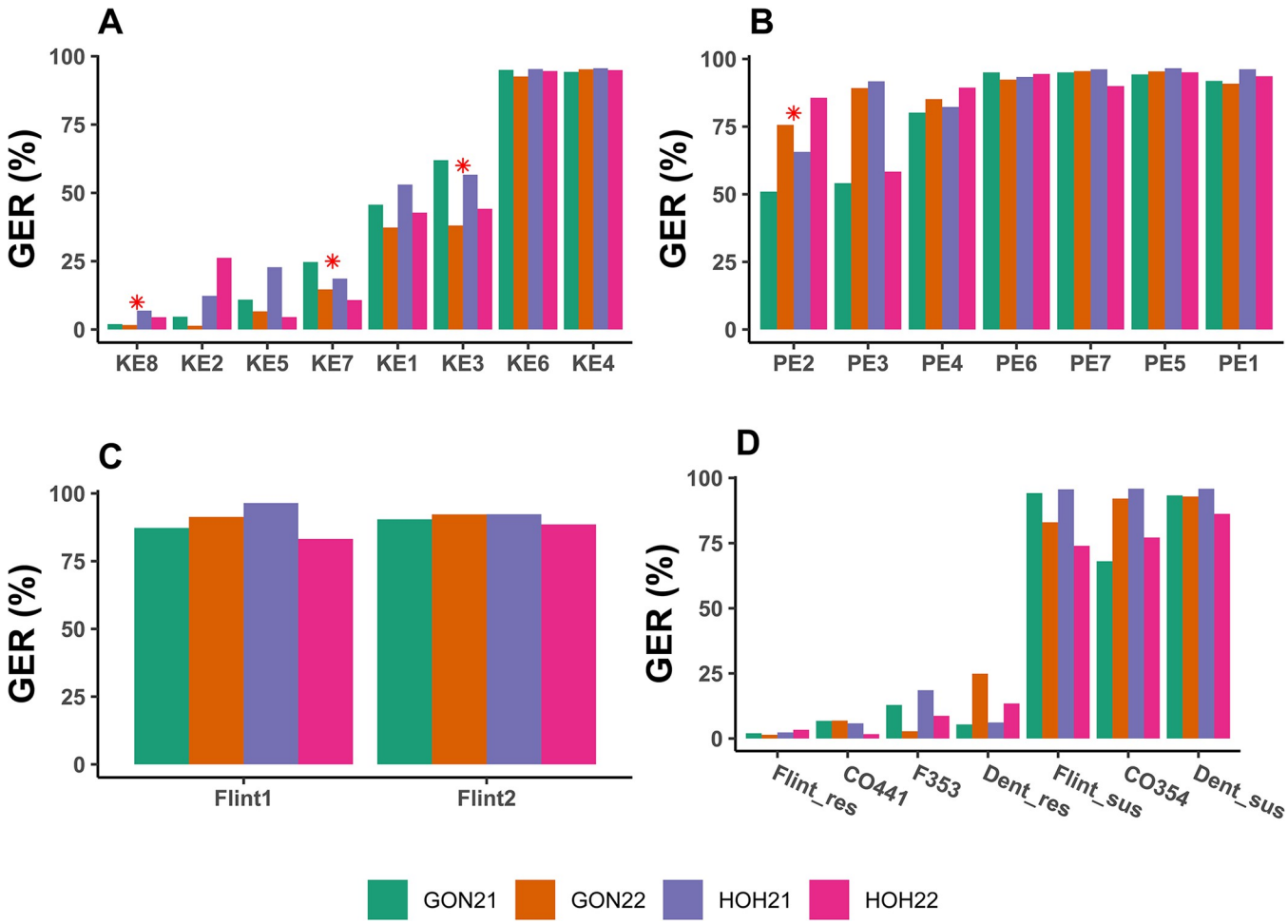

Fig 2. Barplots showing Gibberella ear rot (GER) severity (back-transformed values, %) of parental and standard lines evaluated at each of two locations (GON and HOH) in 2021 and 2022. GON21, GON22, HOH21, HOH22 are the four environments based on location × year combinations. (**A**) doubled haploid lines of Kemater (KE) landrace used as donor parents, (**B**) doubled haploid lines of Petkuser (PE) landrace used as donor parents, (**C**) recipient parents and (**D**) standard lines (res = resistant, sus = susceptible). The asterisk (*) indicates lines selected as donor parents for development of doubled haploid populations.

https://doi.org/10.1371/journal.pone.0292095.g002

variance, σ^2_{GE} = genotype x environment interaction, σ^2_{ε} = residual variance, H^2 = broad sense heritability. The lines were evaluated at two locations in 2021 and 2022. All CV, variance, and heritability estimates were computed with arcsine transformed GER values, variance components of GER severity were multiplied by 100 and minimum, maximum and mean were estimated from back-transformed best linear unbiased estimations (BLUEs) of GER

In 2021, GER severity was low to moderate (2.0–62.0%) at both locations in six KE DH lines such as KE8, KE2, KE5, KE7, KE1 and KE3 (Fig 2A, S2 Table). In contrary to lines from KE landrace, GER severity was higher (>50%) in all lines drawn from PE landrace (Fig 2B, S2 Table). The lowest GER severity was observed with line PE2 within this landrace. GER severity was high (87.3–96.5%) for the adapted parents Flint1 and Flint2 (Fig 2C, S2 Table). Resistant standard lines included in the experiments showed very low to low GER severity (1.4–18.5%), while susceptible standards were highly infected (68.0–95.9%) (Fig 2D, S2 Table).

In 2022, similar ranges were observed for GER severity in both KE and PE DH lines, the adapted parents Flint1 and Flint2, and standard checks. Based on this result, KE8, KE7, KE3

Table 3. Variance components, heritability estimates of arcsine transformed Gibberella ear rot (GER) severity of doubled haploid lines within six landrace-derived populations evaluated at two locations in 2022.

Population	Descriptive statistics					Variances and heritability			
	Min	Mean	Max	CV_G	CV_ε	σ^2_G	σ^2_{GE}	σ^2_ε	H^2
DH(Flint1×KE3)	1.55	36.71	96.60	34.35	6.87	5.00	5.30	0.20	0.64
DH(Flint1×KE7)	1.56	26.97	68.04	8.19	14.19	0.20	8.40	0.60	0.55
DH(Flint2×KE3)	1.61	36.58	98.99	30.72	6.85	4.00	5.50	0.20	0.62
DH(Flint2×KE7)	1.50	29.42	96.77	43.78	9.55	6.30	3.60	0.30	0.68
DH(Flint2×KE8)	1.30	33.06	96.02	42.25	5.16	6.70	4.20	0.10	0.83
DH(Flint2×PE2)	1.85	50.95	97.44	35.80	5.63	8.10	5.60	0.20	0.70

Min = minimum, Max = maximum, CV_G = genotypic coefficient of variation, CV_ε = coefficient of variation of error, σ^2_G = genotypic variance, σ^2_{GE} = genotype x environment interaction, σ^2_ε = residual variance, H^2 = broad sense heritability. All CV, variance, and heritability estimates were computed with arcsine transformed GER values, variance components of GER severity were multiplied by 100 and minimum, maximum and mean were estimated from back-transformed best linear unbiased estimations (BLUEs) of GER

https://doi.org/10.1371/journal.pone.0292095.t003

and PE2 which were highly to moderately resistant to GER disease across locations and years, and were selected and crossed with the susceptible adapted parents Flint1 and Flint2 to generate the six DH populations.

Genetic variation of GER severity within six doubled haploid populations from crosses with elite maize (experiment 2)

Based on the transformed GER severity, significant genotypic and genotype by environment interaction variances were observed within the six DH populations (Table 3). The genotypic variance was 1.4–1.8-fold higher than the genotype by environment interaction in Flint2×PE2, Flint2×KE8 and Flint2×KE7. Depending on the population, the genotypic coefficient of variation was relatively high in all populations, with the exception of Flint1×KE7. Coefficient of variation due to error was low (<20%) for all populations and lower than CV_G, except for Flint1×KE7 (Table 3). The broad sense heritability estimates were moderate (0.55) to high (0.83), with the lowest value observed in Flint1×KE7 and the highest in Flint2×KE8 (Table 3).

Comparison of GER severity of landrace-derived DH populations with recipient parents and performance of the five best lines within each population (experiment 2)

Based on mean GER severity, significant difference was observed between KE-derived populations and PE-derived population (Fig 3). No significant differences were observed among the five KE-derived populations. Flint2×PE2, a PE-derived population exhibited the highest average GER severity (51.0%), while lower GER severity (27.0–36.7%) was observed in KE-derived DH populations, although both recipient flint lines were similarly susceptible (Fig 3). In addition, on average, the six DH populations were more resistant than the recipient parents (Fig 3). In comparison to the mean performance of Flint1 (87.2%) and Flint2 (90.4%) across the two locations in 2022, average GER severity was reduced by 39.4–61.0% in the DH populations. GER severity reduction was higher in all KE-derived populations (53.6–61.0% reduction) than the PE-derived population (39.4% reduction).

From the six DH populations, the five best lines were very resistant, with mean GER severity of 17–168-fold lower than mean GER severity of Flint2 and Flint1 (Table 4). Furthermore,

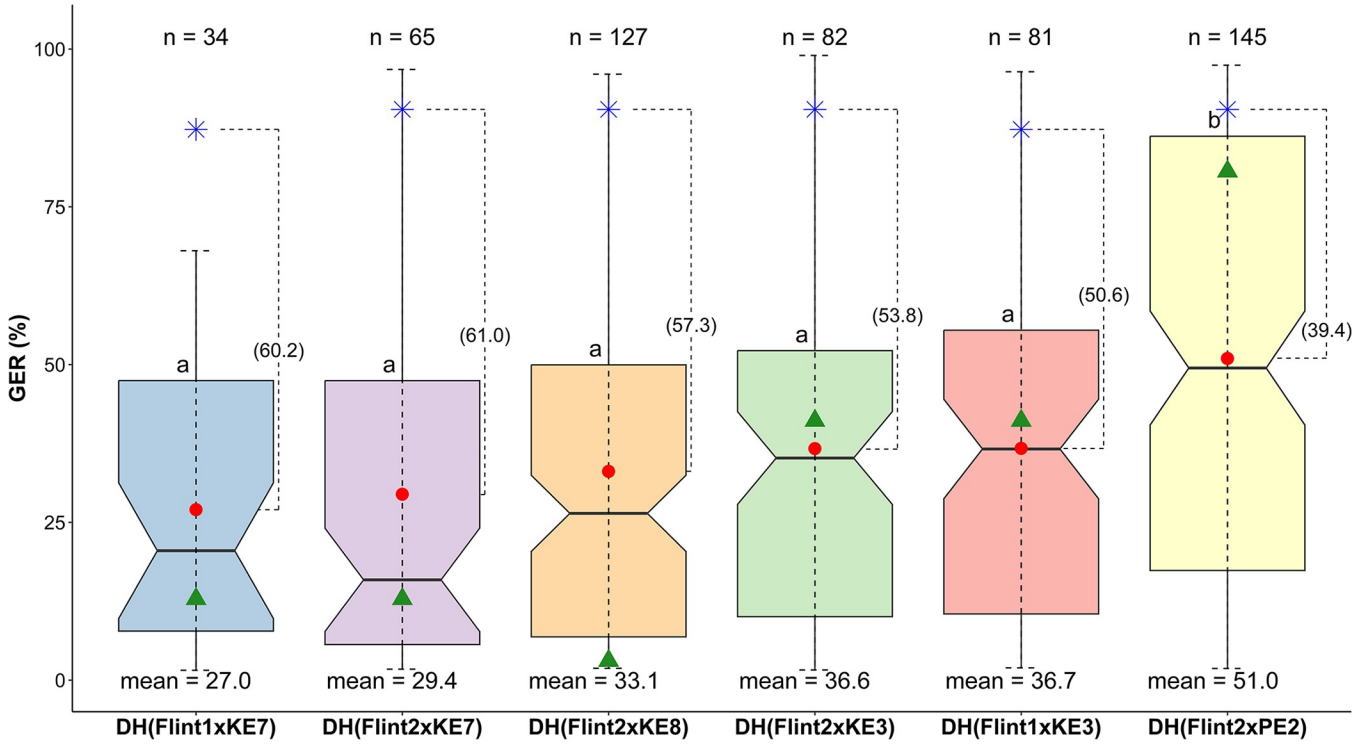

Fig 3. Boxplots showing Gibberella ear rot (GER) severity (back-transformed values, %) of DH populations evaluated at two locations in 2022. n indicates the number of doubled haploid lines analyzed per population. Horizontal lines within boxes indicate the median. For each box, the notch represents 95% confidence interval for the median. Red point, green triangle in each box and blue asterisk (*) indicate mean GER severity of each DH population, donor parent and recipient parent, respectively. Values in parenthesis are the differences between population mean and mean GER severity of the corresponding recipient parent. Boxes with the same letter are statistically identical at $p<0.05$.

https://doi.org/10.1371/journal.pone.0292095.g003

GER severity of selected lines were similar to that of Flint_res which was the most resistant standard check included in the study. Regardless of the populations, the selected lines exhibited similar performances for all adaptation traits, except for average SS which was relatively low for lines 101 (39.5%) and 283 (23.0%) from Flint1×KE7 and Flint2×KE7, respectively (Table 4). Average PV was also relatively low for lines 101 (3.3) and 501 (3.1) from Flint1×KE7 and Flint2×PE2. In comparison with the recipient parents, average DS and PV of selected lines were similar in the six populations. However, most selected lines were relatively shorter in all populations than the recipient parents.

Discussion

The exploitation of European landrace germplasm could be of paramount importance for developing elite materials with improved Gibberella ear rot resistance. We selected three DH lines from Kemater landrace and one DH line from Petkuser landrace, which had varying degrees of GER resistance and used them as donors to develop six DH populations to improve GER resistance of two adapted flint lines (Flint1 and Flint2) included as recipient parents. The six DH populations with a total of 534 DH lines were on average 39.4–61.0% less infected than the mean performance of the adapted flint lines. Within each DH population, the performance of five most resistant DH lines from each population was discussed for consideration in elite maize breeding programs. We will also include results from Gaikpa et al. [27] to discuss the relative stability of GER resistance of the 15 KE and PE lines evaluated in this study.

Table 4. Performances of the five best doubled haploid (DH) lines within each population in comparison with recipient parents and standard checks evaluated at two locations in 2022.

Population	Line	GER (%)	DS (days)	PH (cm)	SS (%)	PV (1–9)
DH(Flint1×KE3)	70	1.55	70.29	133.80	94.96	6.54
DH(Flint1×KE3)	45	1.60	76.27	139.95	93.74	5.31
DH(Flint1×KE3)	87	1.65	71.20	131.33	97.74	6.77
DH(Flint1×KE3)	67	1.95	70.65	122.55	96.99	6.28
DH(Flint1×KE3)	19	2.86	71.88	159.27	90.99	9.04
DH(Flint1×KE7)	101	1.56	80.64	132.93	39.54	3.34
DH(Flint1×KE7)	107	2.40	75.79	155.80	57.43	5.05
DH(Flint1×KE7)	110	3.57	69.32	152.80	92.96	6.48
DH(Flint1×KE7)	114	4.35	70.50	156.13	90.91	6.32
DH(Flint1×KE7)	93	5.20	67.62	145.86	89.99	7.85
DH(Flint2×KE3)	145	1.61	70.44	110.00	96.83	6.76
DH(Flint2×KE3)	142	2.23	66.69	147.76	97.74	5.91
DH(Flint2×KE3)	150	2.49	74.25	123.46	99.50	6.37
DH(Flint2×KE3)	175	2.86	67.35	114.08	93.91	5.44
DH(Flint2×KE3)	132	3.21	70.23	128.97	98.00	6.93
DH(Flint2×KE7)	250	1.50	74.55	144.39	57.43	6.47
DH(Flint2×KE7)	219	1.70	78.72	197.65	99.00	9.12
DH(Flint2×KE7)	283	1.88	78.16	147.75	22.98	6.38
DH(Flint2×KE7)	284	1.88	73.37	118.95	97.00	6.15
DH(Flint2×KE7)	254	1.95	76.22	145.20	78.61	5.02
DH(Flint2×KE8)	363	1.30	71.39	145.60	94.99	5.73
DH(Flint2×KE8)	364	1.68	71.50	125.08	96.02	6.23
DH(Flint2×KE8)	315	1.88	68.22	131.33	95.74	6.27
DH(Flint2×KE8)	317	1.88	70.67	105.61	96.99	5.54
DH(Flint2×KE8)	327	1.88	77.62	169.92	77.78	6.79
DH(Flint2×PE2)	566	1.85	85.88	150.00	72.61	6.00
DH(Flint2×PE2)	460	2.21	72.05	105.95	94.83	7.77
DH(Flint2×PE2)	561	2.21	73.40	113.68	96.99	6.26
DH(Flint2×PE2)	501	2.54	81.67	125.55	78.61	3.11
DH(Flint2×PE2)	568	3.21	71.34	129.58	95.01	7.46
Recipient	Flint1	87.26	74.64	165.40	95.33	7.16
Recipient	Flint2	90.42	76.50	169.90	96.99	6.26
Standard checks	Flint_res	2.39	186.90	81.97	97.93	6.38
Standard checks	Dent_sus	89.55	187.50	85.71	97.83	6.43
-	Gross mean	9.95	80.10	135.70	87.47	6.32
-	LSD 5%	7.30	5.57	14.08	22.15	5.01

GER = Gibberella ear rot severity (back-transformed values), PH = plant height, DS = days to silking, SS = seed-set, PV = plant vigor (1 = no vigour, 9 = highest vigour), LSD 5% = Fisher's least significant difference at 5% significance level

https://doi.org/10.1371/journal.pone.0292095.t004

Genetic variation and heritability estimates of GER severity within lines from landraces and landrace-derived DH populations

Genotypic variances (σ^2_G) within DH lines from KE landrace were generally much higher than within DH lines drawn from PE landrace and were further reduced in derived DH populations. Similarly, heritability was higher in KE landrace lines (0.98) than PE landrace lines (0.76), and in both KE- and PE-derived DH populations (0.55–0.83). The remarkably high

entry-mean heritability (0.98) detected in the study indicates that GER is a highly heritable trait, but also highlights an appropriate field phenotyping as indicated by Piepho and Möhring [45]. Gaikpa et al. [27] who evaluated 500 DH lines from both KE and PE landraces reported similar high heritability estimates (0.80 for KE and 0.77 for PE) for GER severity. Furthermore, heritability observed within the six DH populations included in our study confirms the results of Galiano-Carneiro et al. [35] who reported similar values (0.24–0.72) when evaluating six Brazilian donor-derived DH populations across environments in Brazil and Europe. The existence of significant genetic variation observed in our study indicates that the DH populations can be used in QTL mapping studies to identify and validate resistance loci for accelerating breeding for GER resistance in elite maize materials.

The genotype by environment interaction (σ^2_{GE}) was also significant within lines from both KE and PE landraces and derived DH populations, even though it was lower than the genotypic variance. Significant genotype by environment interactions in this pathosystem were also reported by Akohoue et al. [36], Gaikpa et al. [27] and Bolduan et al. [48]. The relative magnitude of σ^2_G compared to σ^2_{GE} was higher within landrace lines than the derived DH populations, revealing that the contribution of genotype by environment interaction to GER resistance was more important in the DH populations.

Differential GER resistance of European flint landraces

Our study demonstrated that mean GER severity of the seven PE DH lines was on average about 2.1-fold higher than GER severity of the eight KE DH lines across the four environments. This demonstrates a clear superiority of lines from "*Kemater Landmais Gelb*" landrace over "*Petkuser Ferdinand Rot*" landrace lines with regards to resistance to Gibberella ear rot in maize. Gaikpa et al. [27] evaluated 250 DH lines from each landrace and found that average GER severity within PE landrace was 1.3-fold higher than that within KE landrace. Similarly, Akohoue et al. [36] reported that GER severity of PE DH lines evaluated in four environments in Germany was 1.3-fold higher that KE DH lines. Furthermore, based on genome-wide association study (GWAS) of 250 KE DH lines, Gaikpa et al. [27] reported eight GER resistance loci with individual additive effect size of −3.27 to −5% and a total of 33.69% of genotypic variance explained. In contrary to the KE landrace, no significant marker-trait associations were identified for GER severity within PE landrace using the GWAS approach. This firstly demonstrates that GER resistance is quantitatively inherited with both additive and dominance effects as reported by Butrón et al. [49], Martin et al. [50] and Mesterházy et al. [51]. Although additive gene action is predominant, Martin et al. [50] also found significant dominance effects in a cross (D152×UH007) for GER resistance and in four crosses for DON contamination (D152×UH006, D152×UH007, UH007×UH006, UH009×UH006). Secondly, the absence of significant marker-trait associations reported within the PE landrace confirms that QTL effects of GER resistance within this landrace might be too low to be exploited through marker-assisted selection.

Moreover, the average GER severity of KE DH lines (40.94%) observed in the present study was similar to GER severity of 44.12% and 42.13% reported for DH lines from the same landrace population by Gaikpa et al. [27] and Akohoue et al. [36], respectively. Lines KE1, KE2, KE3, KE5, KE7 and KE8 which were moderately to highly resistant in this study were also identified by Gaikpa et al. [27] as resistant genotypes across four different environments (Fig 4). A compilation of our results with those of Gaikpa et al. [27] for the same landrace lines revealed that resistant lines KE2, KE5, KE7 and KE8 maintained a relatively low mean GER severity (<30%) across all environments, while KE1 and KE3 were more unstable with GER severity of 3.6–62% (Fig 4A). This demonstrates a relative stability of GER resistant KE

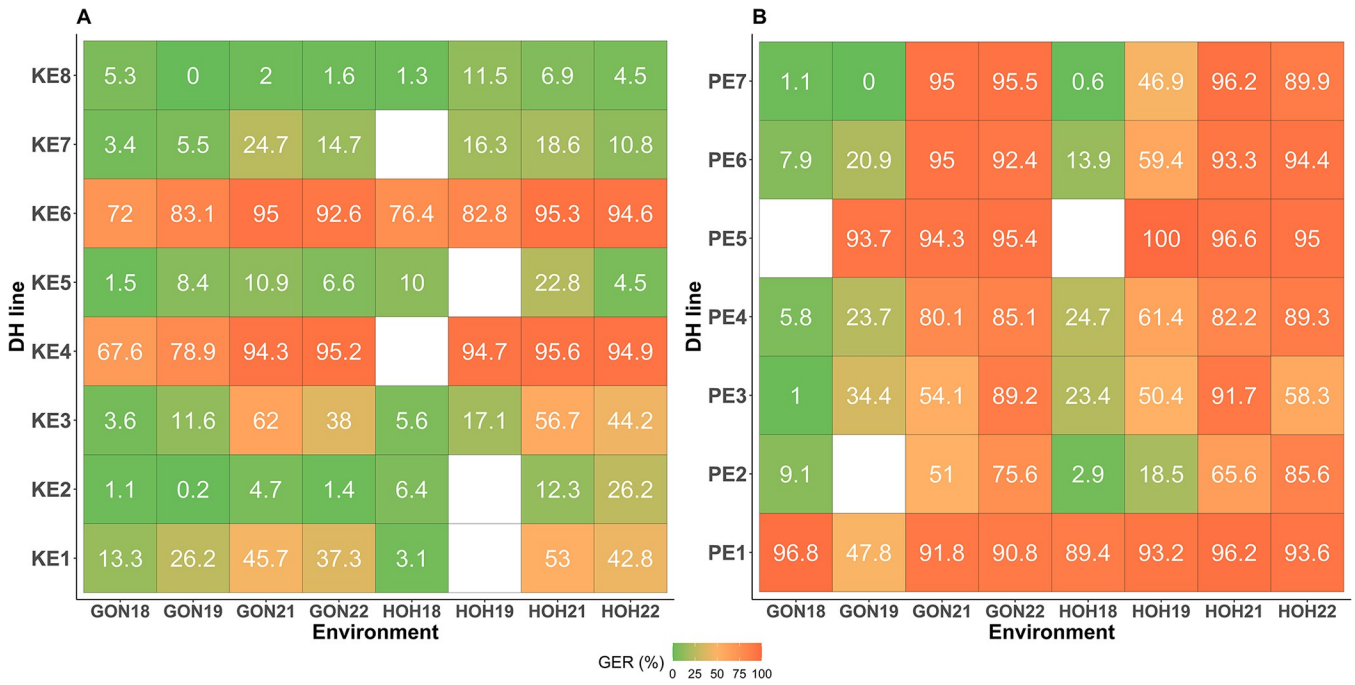

Fig 4. Heatmaps showing relative stability of mean Gibberella ear rot (GER) severity (back-transformed values, %) of lines drawn from landraces evaluated in eight environments (= two locations × four years). (**A**) GER severity of eight doubled haploid (DH) lines from Kemater landrace and (**B**) GER severity of seven DH lines from Petkuser landrace. Color gradient shows the relative severity and stability of GER infections in each environment. Mean GER severity in 2018 and 2019 were reported by Gaikpa et al. [27].

https://doi.org/10.1371/journal.pone.0292095.g004

landrace lines across environments. In contrary to KE landrace, mean GER severity of PE landrace lines in our study (86.19%) was 1.5–1.6-fold higher than that reported by Gaikpa et al. [27] (58.57%) and Akohoue et al. [36] (55.04%). In addition, mean GER severity of PE lines were highly variable (0–85.6%) across environments (Fig 4B). This reveals that the reaction of the PE landrace lines to GER infection across environments was less stable than that of the KE landrace lines. In contrary to moderately resistant lines, susceptible lines (KE4, KE6, PE1 and PE5) were stable with very high GER severity in all environments. Stability of GER resistance was also investigated by Dalla Lana et al. [52] who evaluated 15 maize hybrids to Gibberella ear rot across 30 environments (= 3 years × 10 locations) in the USA, and found also differences in the stability according to the resistance level. Butrón et al. [49] also reported a low stability of GER resistance when evaluating two maize crosses (CO359 × CO441 and EP42 × EP77) across four environments in Canada and Spain. This emphasizes the need for evaluating landrace lines across multiple environments in order to select most resistant and stable lines which could be used as donor parents in breeding programs. Environment-specific GER resistance breeding targets should also be defined for a better and more efficient exploitation of the large existing genetic diversity within landraces. In addition, with recent advances and availability of molecular genomic information on the trait [27, 30, 53, 54], genomics-assisted selection could be applied for accelerated evaluation for GER resistance in maize.

Effectiveness of GER resistance introgression into elite inbreds

On average, GER severity of the DH populations was 39–61% lower than that of the two adapted elite lines (Fig 3). This is an indication that the selected donor landrace lines were effective in improving GER resistance of the adapted elite inbreds. In addition, the finding

confirms the usefulness of selected donor landrace lines for improving the resistance of European adapted flint lines as demonstrated by Galiano-Carneiro et al. [35] using Brazilian tropical DH lines as donor parents.

Moreover, the PE-derived DH population was significantly more susceptible than the KE-derived populations. This, once again confirms the superiority of KE landrace donors for transferring GER resistance into elite materials.

The five best DH lines selected within each populations were 17–168-fold more resistant than the elite lines. The lines exhibited similar average performances with the elite lines for days to flowering, seed-set and plant vigor, with the exception of lines 101 and 283 from Flint1×KE7 and Flint2×KE7, respectively, which had a lower seed-set (Table 4). This shows that they are already adapted according to DS, PH, SS, and PV; however, this should be validated through further evaluations especially for grain and stover yield. This is not astonishing because the landraces were innately adapted to the eco-climatic conditions of NW Europe. In addition, the selected lines showed similar GER resistance compared to the most resistant standard check included in the study. This may be explained by the high genetic diversity observed within the DH populations where the best lines exhibit very low GER severity (<10%), while the most susceptible lines show very high GER severity across environments. This exhibits the high potential of the six DH populations evaluated in this study of which the best lines could be integrated into elite breeding programs for improving GER resistance. However, best lines from these populations should be further evaluated through multi-location and multi-year trials to select the most stable lines to be recommended for improved and sustainable hybrid maize production. In addition, it is also important to evaluate the combining ability of the selected lines for grain yield and GER resistance, their resistance to other ear rot pathogens (i.e. *F. verticillioides*) as well as their response to mycotoxin contaminations.

Conclusions

Understanding the effectiveness of introgression of GER resistance from landraces into elite materials is required to better exploit the potential of European flint landraces. The use of KE landrace as donor lines was more effective for reducing GER severity of susceptible elite lines than PE landrace. Our results showed that the derived DH populations are genetically diverse and of high interest for use in maize breeding programs. The introgression of GER resistance genes into elite materials could be accelerated through the application of genomics-assisted selection within populations. Considering the complexity and quantitative nature of GER resistance, backcross selection could be combined with genomic selection and prediction which seem to be the most relevant molecular approaches that could be implemented within each population to rapidly improve GER resistance of elite materials as indicated by Akohoue and Miedaner [30]. Given the existence of significant genotype by environment interaction within the DH populations, the integration of genomics-assisted breeding for increased selection efficiency could be implemented within environment to better exploit QTL by environment interaction and define area-specific breeding targets. The selected lines from each DH population had similar GER resistance than the highly resistant standard line included in the study. These best lines could be incorporated into breeding programs across multiple locations and years to select the most stable lines.

Supporting information

S1 Table. Best linear unbiased estimations (BLUEs) of Gibberella ear rot (GER) severity (back-transformed values, %), days to silking (DS, days), plant height (PH, cm), seed-set (SS, %), and plant vigor (PV) across environments. Doubled haploid (DH) populations were

evaluated across two locations, while others lines were evaluated across four environments.
(XLSX)

S2 Table. Back-transformed best linear unbiased estimations (BLUEs) of Gibberella ear rot (GER) severity of parental and standard lines evaluated at two locations (GON and HOH) in 2021 and 2022. 4_ENV = mean of GER severity (back-transformed values, %) across the four environments, LSD 5% = Fisher's least significant difference at 5% significance level. GER severity was the percentage of a maize ear visually affected by mycelium.
(XLSX)

Acknowledgments

We are grateful to INRAE, Paris, France, for supporting this research by providing the French dent line "F353". Prof. Lana M. Reid (retired) from Eastern Cereal and Oilseed Research Centre, Central Experimental Farm, Agriculture and Agri-Food Canada, Ottawa, Canada, is also thanked for providing the lines CO441 and CO354 for comparison. Lines from KWS SAAT SE & Co. KGaA are proprietary to the company and are available on request for scientists without any commercial interest. A respective MTA must be signed in advance.

Author Contributions

Conceptualization: Félicien Akohoue, Bettina Kessel, Thomas Presterl, Thomas Miedaner.

Data curation: Félicien Akohoue.

Formal analysis: Félicien Akohoue.

Funding acquisition: Félicien Akohoue, Bettina Kessel, Thomas Presterl, Thomas Miedaner.

Investigation: Félicien Akohoue, Silvia Koch, Bärbel Lieberherr.

Methodology: Félicien Akohoue, Silvia Koch, Bärbel Lieberherr, Bettina Kessel, Thomas Miedaner.

Project administration: Bettina Kessel, Thomas Presterl, Thomas Miedaner.

Supervision: Thomas Miedaner.

Validation: Thomas Miedaner.

Visualization: Félicien Akohoue.

Writing – original draft: Félicien Akohoue.

Writing – review & editing: Bettina Kessel, Thomas Presterl, Thomas Miedaner.

References

1. Rebourg C, Chastanet M, Gouesnard B, Welcker C, Dubreuil P, Charcosset A. Maize introduction into Europe: The history reviewed in the light of molecular data. Theor Appl Genet. 2003; 106(5):895–903. https://doi.org/10.1007/s00122-002-1140-9 PMID: 12647065
2. Mirdita V, Dhillon BS, Geiger HH, Miedaner T. Genetic variation for resistance to ergot (*Claviceps purpurea* [Fr.] Tul.) among full-sib families of five populations of winter rye (*Secale cereale* L.). Theor Appl Genet. 2008; 118(1):85–90. https://doi.org/10.1007/s00122-008-0878-0 PMID: 18797841
3. Böhm J, Schipprack W, Utz HF, Melchinger AE. Tapping the genetic diversity of landraces in allogamous crops with doubled haploid lines: a case study from European flint maize. Theor Appl Genet. 2017; 130(5):861–73. https://doi.org/10.1007/s00122-017-2856-x PMID: 28194473

4. Strigens A, Schipprack W, Reif JC, Melchinger AE. Unlocking the genetic diversity of maize landraces with doubled haploids opens new avenues for breeding. PLoS One. 2013; 8(2):e57234. https://doi.org/10.1371/journal.pone.0057234 PMID: 23451190

5. Barrière Y, Alber D, Dolstra O, Lapierre C, Motto M, Ordás Pérez A, et al. Past and prospects of forage maize breeding in Europe. II. History, germplasm evolution and correlative agronomic changes. Maydica. 2006:435–49.

6. Tenaillon MI, Charcosset A. A European perspective on maize history. C R Biol. 2011; 334(3):221–8. https://doi.org/10.1016/j.crvi.2010.12.015 PMID: 21377617

7. Messmer MM, Melchinger AE, Boppenmaier J, Brunklaus-Jung E, Herrmann RG. Relationships among early European maize inbreds: I. Genetic diversity among flint and dent lines revealed by RFLPs. Crop Sci. 1992; 32(6):cropsci1992.0011183X003200060001x. https://doi.org/10.2135/cropsci1992.0011183X003200060001x.

8. Wulff BBH, Moscou MJ. Strategies for transferring resistance into wheat: from wide crosses to GM cassettes. Front Plant Sci. 2014; 5. https://doi.org/10.3389/fpls.2014.00692 PMID: 25538723

9. Savary S, Willocquet L, Pethybridge SJ, Esker P, McRoberts N, Nelson A. The global burden of pathogens and pests on major food crops. Nat Ecol Evol. 2019; 3(3):430–9. Epub 2019/02/06. https://doi.org/10.1038/s41559-018-0793-y PMID: 30718852.

10. Miedaner T, Juroszek P. Global warming and increasing maize cultivation demand comprehensive efforts in disease and insect resistance breeding in north-western Europe. Plant Pathol. 2021; 70 (5):1032–46. https://doi.org/10.1111/ppa.13365

11. Juroszek P, von Tiedemann A. Climatic changes and the potential future importance of maize diseases: A short review. J Plant Dis Prot. 2013; 120(2):49–56. https://doi.org/10.1007/BF03356454

12. Dalla Lana F, Madden LV, Carvalho CP, Paul PA. Impact of Gibberella ear rot on grain quality and yield components in maize as influenced by hybrid reaction. Plant Dis. 2022; 106(12):3061–75. https://doi.org/10.1094/PDIS-01-22-0148-RE PMID: 35536201

13. Vigier B, Reid LM, Dwyer LM, Stewart DW, Sinha RC, Arnason JT, Butler G. Maize resistance to Gibberella ear rot: symptoms, deoxynivalenol, and yield. Can J Plant Pathol. 2001; 23(1):99–105. https://doi.org/10.1080/07060660109506915

14. Reid LM, Stewart DW, Hamilton RI. A 4-Year study of the association between Gibberella ear rot severity and deoxynivalenol concentration. J Phytopathol. 1996; 144(9–10):431–6. https://doi.org/10.1111/j.1439-0434.1996.tb00319.x.

15. Chilaka CA, De Boevre M, Atanda OO, De Saeger S. Occurrence of Fusarium mycotoxins in cereal crops and processed products (Ogi) from Nigeria. Toxins. 2016; 8(11). https://doi.org/10.3390/toxins8110342 PMID: 27869703

16. Miller SS, Reid LM, Harris LJ. Colonization of maize silks by *Fusarium graminearum*, the causative organism of gibberella ear rot. Can J Bot. 2007; 85(4):369–76. https://doi.org/10.1139/B07-027

17. Görtz A, Oerke E-C, Steiner U, Waalwijk C, de Vries I, Dehne H-W. Biodiversity of Fusarium species causing ear rot of maize in Germany. Cereal Res Commun. 2008; 36(6):617–22. https://doi.org/10.1556/CRC.36.2008.Suppl.B.51

18. Pfordt A, Schiwek S, Rathgeb A, Rodemann C, Bollmann N, Buchholz M, Karlovsky P, von Tiedemann A. Occurrence, pathogenicity, and mycotoxin production of *Fusarium temperatum* in relation to other Fusarium species on maize in Germany. Pathogens. 2020; 9(11):1–21. https://doi.org/10.3390/pathogens9110864 PMID: 33105838

19. Ferrigo D, Raiola A, Causin R. Fusarium toxins in cereals: Occurrence, legislation, factors promoting the appearance and their management. Molecules. 2016; 21(5). https://doi.org/10.3390/molecules21050627 PMID: 27187340

20. Logrieco A, Mulè G, Moretti A, Bottalico A. Toxigenic Fusarium species and mycotoxins associated with maize ear rot in Europe. Eur J Plant Pathol. 2002; 108(7):597–609. https://doi.org/10.1023/A:1020679029993

21. Abdallah M F., De Boevre M, Landschoot S, De Saeger S, Haesaert G, Audenaert K. Fungal endophytes control *Fusarium graminearum* and reduce trichothecenes and zearalenone in maize. Toxins [Internet]. 2018; 10(12).

22. Khokhar MK, Sharma SS, Gupta R. Integrated management of post flowering stalk rot of maize caused by *Fusarium verticillioides*. Indian Phytopathol. 2014; 67(3):228–33.

23. Shin J-H, Han J-H, Lee JK, Kim KS. Characterization of the maize stalk rot pathogens *Fusarium subglutinans* and *F. temperatum* and the effect of fungicides on their mycelial growth and colony formation. Plant Pathol J. 2014; 30(4):397–406. https://doi.org/10.5423/PPJ.OA.08.2014.0078 PMID: 25506304

24. Logrieco A, Battilani P, Leggieri MC, Jiang Y, Haesaert G, Lanubile A, et al. Perspectives on global mycotoxin issues and management from the Mycokey maize working group. Plant Dis. 2021; 105 (3):525–37. https://doi.org/10.1094/PDIS-06-20-1322-FE WOS:000663983700001. PMID: 32915118

25. Kebede AZ, Reid LM, Voloaca C, De Schiffart R, Wu J, Woldemariam T, et al. CO476 corn inbred line. Can J Plant Sci. 2021; 101(2):287–91. https://doi.org/10.1139/cjps-2020-0065 WOS:000634691300015.

26. Kebede AZ, Reid LM, Voloaca C, De Schiffart R, Wu J, Woldemariam T, et al. CO475 corn inbred line. Can J Plant Sci. 2021; 101(2):292–7. https://doi.org/10.1139/cjps-2020-0057 WOS:000634691300016.

27. Gaikpa DS, Kessel B, Presterl T, Ouzunova M, Galiano-Carneiro AL, Mayer M, et al. Exploiting genetic diversity in two European maize landraces for improving Gibberella ear rot resistance using genomic tools. Theor Appl Genet. 2021; 134(3):793–805. https://doi.org/10.1007/s00122-020-03731-9 PMID: 33274402

28. Hölker AC, Mayer M, Presterl T, Bolduan T, Bauer E, Ordas B, et al. European maize landraces made accessible for plant breeding and genome-based studies. Theor Appl Genet. 2019; 132(12):3333–45. https://doi.org/10.1007/s00122-019-03428-8 PMID: 31559526

29. Brauner PC, Schipprack W, Utz HF, Bauer E, Mayer M, Schön C-C, et al. Testcross performance of doubled haploid lines from European flint maize landraces is promising for broadening the genetic base of elite germplasm. Theor Appl Genet. 2019; 132(6):1897–908. https://doi.org/10.1007/s00122-019-03325-0 PMID: 30877313

30. Akohoue F, Miedaner T. Meta-analysis and co-expression analysis revealed stable QTL and candidate genes conferring resistances to Fusarium and Gibberella ear rots while reducing mycotoxin contamination in maize. Front Plant Sci. 2022; 13:1050891. https://doi.org/10.3389/fpls.2022.1050891 PMID: 36388551

31. Reid LM, McDiarmid G, Parker AJ, Woldemariam T. CO441 corn inbred line. Can J Plant Sci. 2003; 83 (1):79–80. https://doi.org/10.4141/P02-058

32. Reid LM, Hamilton RI, Mather DE. Screening maize for resistance to Gibberella ear rot. Canada: Agriculture & Agri-Food Canada, Research Branch, Eastern Cereal & Oilseed Research Centre; 1996. 40 p.

33. Pastircak M, Lemmens M, Srobarova A. Reaction of maize hybrids to ear rot caused by *Fusarium graminearum* Schwabe. Plant Prot Sci. 2002; 38(11):569–71.

34. Miedaner T, Bolduan C, Melchinger AE. Aggressiveness and mycotoxin production of eight isolates each of *Fusarium graminearum* and *Fusarium verticillioides* for ear rot on susceptible and resistant early maize inbred lines. Eur J Plant Pathol. 2010; 127(1):113–23. https://doi.org/10.1007/s10658-009-9576-2

35. Galiano-Carneiro AL, Kessel B, Presterl T, Gaikpa DS, Kistner MB, Miedaner T. Multi-parent QTL mapping reveals stable QTL conferring resistance to Gibberella ear rot in maize. Euphytica. 2021; 217(1). https://doi.org/10.1007/s10681-020-02748-x

36. Akohoue F, Gaikpa DS, Kessel B, Presterl T, Miedaner T. Variance components and correlations between doubled haploid lines from two European flint landraces and their corresponding testcrosses for Gibberella ear rot resistance, silking time, and plant height in maize. Agronomy. 2021; 11(6). https://doi.org/10.3390/agronomy11061039

37. Adetimirin VO, Kim S-K, Szczech M. Factors associated with emergence of Shrunken-2 maize in Korea. J Agric Sci. 2006; 144(1):63–8. Epub 2006/01/16. https://doi.org/10.1017/S002185960500571X

38. Bernal-Vasquez A-M, Utz HF, Piepho H-P. Outlier detection methods for generalized lattices: a case study on the transition from ANOVA to REML. Theor Appl Genet. 2016; 129(4):787–804. https://doi.org/10.1007/s00122-016-2666-6 PMID: 26883044

39. Ahrens WH, Cox DJ, Budhwar G. Use of the arcsine and square root transformations for subjectively determined percentage data. Weed Sci. 1990; 38(4–5):452–8. Epub 2017/06/12. https://doi.org/10.1017/S0043174500056824

40. Piepho H-P, Möhring J, Schulz-Streeck T, Ogutu JO. A stage-wise approach for the analysis of multi-environment trials. Biom J. 2012; 54(6):844–60. https://doi.org/10.1002/bimj.201100219 PMID: 23007738

41. Buntaran H, Piepho H-P, Schmidt P, Rydén J, Halling M, Forkman J. Cross-validation of stagewise mixed-model analysis of Swedish variety trials with winter wheat and spring barley. Crop Sci. 2020; 60 (5):2221–40. https://doi.org/10.1002/csc2.20177.

42. Piepho H, Williams E, Fleck M. A note on the analysis of designed experiments with complex treatment structure. HortScience. 2006; 41(2):446–52.

43. Morrell CH. Likelihood ratio testing of variance components in the linear mixed-effects model using restricted maximum likelihood. Biometrics. 1998:1560–8. https://doi.org/10.2307/2533680. PMID: 9883552

44. Cullis BR, Smith AB, Coombes NE. On the design of early generation variety trials with correlated data. J Agric Biol Environ Stat. 2006; 11(4):381–93.

45. Piepho H-P, Möhring J. Computing heritability and selection response from unbalanced plant breeding trials. Genetics. 2007; 177(3):1881–8. https://doi.org/10.1534/genetics.107.074229 PMID: 18039886

46. Butler D, Cullis B, Gilmour A, Gogel B. Asreml: An R package to fit the linear mixed model. Journal of Statistical Software. 2015.

47. R Core Team. R: A language and environment for statistical computing. Version 4.1.3. Vienna, Austria: R Foundation for Statistical Computing, https://www.R-project.org/, 2021.

48. Bolduan C, Miedaner T, Utz HF, Dhillon BS, Melchinger AE. Genetic variation in testcrosses and relationship between line per se and testcross performance for resistance to Gibberella ear rot in maize. Crop Sci. 2010; 50(5):1691–6. https://doi.org/10.2135/cropsci2009.10.0623

49. Butrón A, Reid LM, Santiago R, Cao A, Malvar RA. Inheritance of maize resistance to gibberella and fusarium ear rots and kernel contamination with deoxynivalenol and fumonisins. Plant Pathol. 2015; 64 (5):1053–60. https://doi.org/10.1111/ppa.12351.

50. Martin M, Dhillon BS, Miedaner T, Melchinger AE. Inheritance of resistance to Gibberella ear rot and deoxynivalenol contamination in five flint maize crosses. Plant Breed. 2012; 131(1):28–32. https://doi.org/10.1111/j.1439-0523.2011.01908.x

51. Mesterházy A, Lemmens M, Reid LM. Breeding for resistance to ear rots caused by *Fusarium* spp. in maize—A review. Plant Breed. 2012; 131(1):1–19. https://doi.org/10.1111/j.1439-0523.2011.01936.x

52. Dalla Lana F, Paul PA, Minyo R, Thomison P, Madden LV. Stability of hybrid maize reaction to Gibberella ear rot and Deoxynivalenol contamination of grain. Phytopathology. 2020; 110(12):1908–22. https://doi.org/10.1094/PHYTO-05-20-0194-R PMID: 32689899

53. Kebede AZ, Woldemariam T, Reid LM, Harris LJ. Quantitative trait loci mapping for Gibberella ear rot resistance and associated agronomic traits using genotyping-by-sequencing in maize. Theor Appl Genet. 2016; 129(1):17–29. https://doi.org/10.1007/s00122-015-2600-3 PMID: 26643764

54. Kebede AZ, Johnston A, Schneiderman D, Bosnich W, Harris LJ. Transcriptome profiling of two maize inbreds with distinct responses to Gibberella ear rot disease to identify candidate resistance genes. BMC Genomics. 2018; 19(1). https://doi.org/10.1186/s12864-018-4513-4 PMID: 29426290

Effectiveness of introgression of resistance loci for Gibberella ear rot from two European flint landraces into adapted elite maize (*Zea mays* L.)

Félicien Akohoue[1], Silvia Koch[1], Bärbel Lieberherr[1], Bettina Kessel[2], Thomas Presterl[2], Thomas Miedaner[1*]

Supplementary information

S1 Table: Best linear unbiased estimations (BLUEs) of Gibberella ear rot (GER) severity (back-transformed values, %), days to silking (DS, days), plant height (PH, cm), seed-set (SS, %), and plant vigor (PV) across environments. Doubled haploid (DH) populations were evaluated across two locations, while others lines were evaluated across four environments. Available online at: https://doi.org/10.1371/journal.pone.0292095.s001

S2 Table: Back-transformed best linear unbiased estimations (BLUEs) of Gibberella ear rot (GER) severity of parental and standard lines evaluated at two locations (GON and HOH) in 2021 and 2022. 4_ENV = mean of GER severity (back-transformed values, %) across the four environments, LSD 5% = Fisher's least significant difference at 5% significance level. GER severity was the percentage of a maize ear visually affected by mycelium

Line	GON21 (%)	HOH21 (%)	GON22 (%)	HOH22 (%)	4_ENV
Kemater Landmais Gelb landrace:					
KE1	45.67	53.02	37.28	42.75	44.68
KE2	4.68	12.29	1.36	26.23	11.14
KE3	61.95	56.66	38.04	44.15	50.20
KE4	94.25	95.61	95.19	94.92	94.99
KE5	10.89	22.79	6.64	4.53	11.21
KE6	95.00	95.30	92.58	94.56	94.36
KE7	24.69	18.61	14.65	10.76	17.18
KE8	1.97	6.90	1.63	4.48	3.75
Petkuser Ferdinand Rot landrace:					
PE1	91.83	96.18	90.83	93.57	93.10
PE2	50.95	65.60	75.60	85.60	69.44
PE3	54.08	91.70	89.20	58.33	73.33
PE4	80.12	82.24	85.12	89.34	84.21
PE5	94.25	96.56	95.36	95.02	95.30
PE6	95.00	93.33	92.43	94.43	93.80
PE7	95.00	96.15	95.49	89.94	94.15
Recipient parents:					
Flint1	87.27	96.45	91.32	83.20	89.56
Flint2	90.44	92.32	92.27	88.58	90.90
Standard checks:					
CO354	68.01	95.87	92.06	77.12	83.27
CO441	6.80	5.85	6.86	1.67	5.30
Dent_res	5.41	6.15	24.87	13.46	12.47
Dent_sus	93.30	95.85	92.88	86.21	92.06
F353	12.88	18.54	2.80	8.71	10.73
Flint_res	2.02	2.34	1.44	3.34	2.29
Flint_sus	94.19	95.62	83.00	73.94	86.67
LSD (5%)	-	-	-	-	11.20

Chapter 5: Variance components and correlations between doubled haploid lines from two European flint landraces and their corresponding testcrosses for Gibberella ear rot resistance, silking time, and plant height in maize

Félicien Akohoue[1], David Sewordor Gaikpa[1], Bettina Kessel[2], Thomas Presterl[2] and Thomas Miedaner[1,*]

[1]State Plant Breeding Institute, University of Hohenheim, Stuttgart, Germany;

[2]Kleinwanzlebener Saatzucht (KWS) KWS SAAT SE & Co. KGaA, Einbeck, Germany;

*Correspondence: thomas.miedaner@uni-hohenheim.de (T.M.)

ORCID T.M.: https://orcid.org/0000-0002-9541-3726

Published in *Agronomy*. 2021; 11(6):1039.

https://doi.org/10.3390/agronomy11061039.

Submitted: 20 April 2021 / **Accepted**: 20 May 2021 / **Published**: 22 May 2021

agronomy

MDPI

Article

Variance Components and Correlations between Doubled Haploid Lines from Two European Flint Landraces and Their Corresponding Testcrosses for Gibberella Ear Rot Resistance, Silking Time, and Plant Height in Maize

Félicien Akohoue [1], David Sewordor Gaikpa [1,2], Bettina Kessel [3], Thomas Presterl [3] and Thomas Miedaner [1,*]

[1] State Plant Breeding Institute, University of Hohenheim, 70599 Stuttgart, Germany; akohoue.f@gmail.com (F.A.); davidsewordor@gmail.com (D.S.G.)
[2] Rijk Zwaan B.V., 2678 ZG De Lier, The Netherlands
[3] Kleinwanzlebener Saatzucht (KWS) KWS SAAT SE & Co. KGaA, 37574 Einbeck, Germany; bettina.kessel@kws.com (B.K.); thomas.presterl@kws.com (T.P.)
* Correspondence: miedaner@uni-hohenheim.de

Abstract: Predicting the resistance of hybrids from lines is a relevant approach for accelerating the improvement of disease resistance in hybrid breeding. In this study, genetic variation and covariation among 76 DH lines from two flint landraces, Kemater (KE) and Petkuser (PE), and their corresponding testcrosses (TC) were estimated for the first time for this material for Gibberella ear rot (GER), days to silking (DS), and plant height (PHT). Lines and TC were evaluated in four and two environments, respectively, under artificial infection with GER. TC were, on average, 42% less GER infected than their lines. TC matured 3–4 days earlier and were about 110 cm taller than the lines. GER resistance was 10% higher in KE lines and TC than PE lines and TC. Significant ($p < 0.001$) genotypic and genotype-by-environment interaction variances were found for all traits. Genotypic variances were generally smaller among TC than lines. Broad-sense heritability estimates were moderate to high for GER severity (0.56–0.82) and high for DS (0.78–0.88) and PHT (0.86–0.94) with higher values always observed in lines. Significant, moderate correlations between TC and line per se performance were found for GER resistance in both KE and PE (r = 0.37 and 0.55, respectively). For the two agronomic traits, correlations were higher (r = 0.59–0.76) than for GER resistance. Genomic prediction accuracies were moderate to high for GER resistance (r = 0.49–0.63) and generally higher for DS and PHT. In conclusion, a pre-selection of DH lines for GER resistance should be feasible; however, TC should be additionally tested on a later selection stage to aim for GER-resistant hybrid cultivars.

Keywords: Gibberella ear rot resistance; *Fusarium graminearum*; correlations; genomic prediction accuracy; testcrosses; line per se

Citation: Akohoue, F.; Gaikpa, D.S.; Kessel, B.; Presterl, T.; Miedaner, T. Variance Components and Correlations between Doubled Haploid Lines from Two European Flint Landraces and Their Corresponding Testcrosses for Gibberella Ear Rot Resistance, Silking Time, and Plant Height in Maize. *Agronomy* **2021**, *11*, 1039. https://doi.org/10.3390/agronomy11061039

Academic Editor: David Van Sanford

Received: 20 April 2021
Accepted: 20 May 2021
Published: 22 May 2021

1. Introduction

Maize (*Zea mays* L.) is the most important cereal crop after wheat (*Triticum aestivum* L.) and rice (*Oryza sativa* L.) and is grown for food and feed across the world [1–3]. It is considered a major food source with a high contribution to food and nutrition security in diverse regions such as Africa, where the consumption ranges from 52 to 328 g/person/day [1,4]. In industrial countries, maize is often used for feeding livestock in Europe and ethanol production in the United States [2].

Unfortunately, persisting yield gaps were found in maize production across regions [5,6]. Projections in maize production demonstrated the necessity for intensive improvement efforts to close the existing yield gaps in order to satisfy food and feed demands by the growing human populations by 2050 [5,6]. Producers are experiencing several constraints, including high disease infections that cause huge grain losses from field to storage, resulting in up to 30% of yield loss [7]. Toxigenic ear rots are major components

thereof [8], causing a serious threat to food and feed safety because of their ability to produce a wide range of mycotoxins [9–12]. Different types of toxigenic ear rots caused by Fusarium spp. occur depending on the geographical location and prevailing climate or weather [13]. In cooler regions, such as Europe, northern United States, Canada and some higher altitudes in Africa, Gibberella ear rot (GER) and Fusarium ear rots (FER) are the major types that infect greater proportions of maize. Gibberella ear rot is caused by *Fusarium graminearum* or its sexual stage known as *Gibberella zeae*, which reduces yield, affects grain quality, and contaminates the grains with mycotoxins, such as deoxynivalenol (DON) and zearalenone (ZON) [14,15]. Fusarium ear rot is caused by *F. verticillioides* (teleomorph *G. fujikoroi*) and some other fungi. In Germany, Gibberella and Fusarium ear rot infections were recently reported as the most dominant disease in maize with their relative occurrence depending on temperature and humidity in the respective year [16].

Mycotoxin contamination is a strong impetus for breeding Fusarium resistance. Their quantification, however, is costly and not achievable in large breeding populations with thousands of entries. Inoculation with an aggressive *F. graminearum* isolate led to strong phenotypic correlations between GER symptoms and DON concentrations amounting to r = 0.95 for inbred lines and r = 0.88–0.91 for testcrosses (TC) as reported by Bolduan et al. [17]. Accordingly, the phenotypic correlation between GER and DON was r = 0.93 and between GER and ZON r = 0.91 in another set of elite TC [18]. Correlations between GER severity and DON or ZON concentrations were also very strong in a larger line population (n = 182, r = 0.97 and 0.92, respectively) [19]. Thus, it is not necessary to invest in the costly and time-consuming mycotoxin analyses as long as artificial infections with an aggressive isolate are performed.

Fungicides are currently not released for this purpose in Germany as they are not fully efficient in the control of *Fusarium* species. They are also harmful to health and the environment [20]. Moreover, the development of high-yielding varieties with improved disease resistance was reported as the most appropriate approach to effectively reduce ear rot damages in maize [14,21–23]. The identification of resistance sources and use of appropriate breeding methods are major steps forward in developing highly ear-rot-resistant maize varieties. European maize landraces encompass several QTLs controlling GER severity that can be introgressed in high-yielding maize varieties [24].

The importance and accuracy of using the performance of parental lines as predictors of hybrid performance were analysed previously for ear rot resistance in maize [18] and Fusarium head blight in wheat [25] but only in European materials. For agronomic traits in maize, these correlations have been established already [26,27]. Predicting hybrid resistance from line per se is relevant for reducing selection cycle length, facilitating early breeding stage selection, and maximising gains from selection [28]. Generally, lines display a greater genetic variation and are selected as a first step before using TC for selecting general combining ability (GCA). Thus, a pre-selection of inbred lines on GER resistance would allow one to integrate only the more resistant fraction into the resource-demanding GCA tests. The availability of DH lines should allow for a more accurate prediction because the DH lines are fully inbred and masking effects are avoided. The effective and accurate prediction of hybrid performance requires significant associations between performances of the hybrids and lines for the traits of interest. Because this parameter is highly dependent on the maize materials used, we estimated for the first time the variances and covariances for GER severity from two European flint landraces. In particular, we aimed to analyse: (i) the genetic variation of Gibberella ear rot resistance, silking time, and plant height among the double haploid (DH) lines from two European flint landraces and their corresponding TC, and (ii) the accuracy of using line performance as a predictor of hybrid performance for Gibberella ear rot resistance. We hypothesise that: (i) genotypic variances are higher in DH lines than the TC and that (ii) DH line performance is a good predictor of TC for GER resistance.

2. Materials and Methods

2.1. Plant Materials

In this study, we used 40 and 36 double haploid (DH) lines from two European flint maize landraces, "Kemater Landmais Gelb" (KE, from Austria) and "Petkuser Ferdinand Rot" (PE, from Germany), respectively, and their corresponding 76 testcrosses (TC), using the French dent line "F353" provided by INRAE as tester [29]. The lines were chosen for testcrossing based on their agronomic appearance in 2018 out of a total set of 500 DH lines described in detail by Gaikpa et al. [24]. The respective crosses were made in an off-season program in Chile.

2.2. Field Experiments

Field experiments were conducted in Hohenheim (near Stuttgart) and Gondelsheim (near Karlsruhe) in Germany. The 76 DH lines were inoculated in 2018 and 2019 in each of the two locations, while the 76 corresponding TC were evaluated in 2019 at the same two locations. The experiments were conducted using two alpha-lattice designs with two replicates each grown adjacent to each other. The line experiment was reported very recently in detail [24]. Therefore, we give here for brevity the most important points only. Each plot consisted of 20 plants in a single row of 3 m length with a distance between rows of 0.75 m and within rows of 0.15 m. Both DH lines and TC were inoculated using the aggressive *Fusarium graminearum* isolate IFA66 described by Bolduan et al. [17] and generously shared by Prof. Dr. M. Lemmens, IFA Tulln, Austria. The ears of 8–10 plants per plot were inoculated at 4–6 days after 50% silk emergence, leaving out the border plants. Approximately 2 mL and 3 mL of the inoculum (concentration 1.5×10^4 spores mL^{-1}) for lines and TC, respectively, were injected into each ear through the silk channel [30]. Data were recorded on Gibberella ear rot (GER) severity (%), days to silking (DS), and plant height (PHT, cm). GER severity was visually recorded at physiological maturity of 8–10 plants per plot as the percentage of symptomatic kernels per ear on a quantitative scale from 0–100%, where 0% = no Fusarium mould visible and 100% = entire ear covered with Fusarium mould [31].

2.3. Statistical Analysis

Separately for lines and TC, trait values were used to calculate the best linear unbiased estimates (BLUEs) and variance components using the ASReml-R 3.0 package [32] following the mixed linear model described by Gaikpa et al. [24]. The broad-sense (H^2) heritability was estimated following the standard procedure described by Hallauer et al. [33].

Pearson's product–moment correlation test was performed for GER severity, days to silking (DS), and plant height (PHT) to investigate association patterns between TC and line per se performance of the two DH populations (KE and PE) using the function "cor.test" in R software version 4.0.3 [34]. Moreover, correlations between GER severity and the two agronomic traits were determined. Cross-validation genomic prediction (GP) accuracies were determined using DH lines as the training set and the corresponding testcrosses as the validation set for the two populations separately using the R package "rrBLUP" [35,36]. We used the high-density Affymetrix® Axiom® Maize Genotyping Array optimised for temperate maize [37] with 388,999 SNP markers, as described previously in detail by Gaikpa et al. [24].

3. Results

3.1. Testcrosses and DH Line Performances across Environments

DH lines showed a large variation for GER severity and the two agronomic traits (Table 1). The differences from the line performance in four vs. two environments were rather small, and the reactions of KE and PE lines were similar. GER severity was, on average, 10% higher in DH lines and TC of the PE population than DH lines and TC of the KE population in all environments (Table 1). TC were much less infected with GER than

the lines and their range was smaller. TC were, on average, 4.04 days and 3.15 days earlier and 109.86 cm and 117.25 cm taller than the DH lines for KE and PE, resp. (Table 1).

Table 1. Means and ranges of Gibberella ear rot (GER) severity, days to silking (DS), and plant height (PHT) for DH lines and testcrosses (TC) from "Kemater Landmais Gelb" (KE) and "Petkuser Ferdinand Rot" (PE) across four and two environments (Env.), respectively.

Parameter	DH Lines–4 Env		DH Lines–2 Env		TC–2 Env	
	KE	PE	KE	PE	KE	PE
GER (%)						
Minimum	16.49	11.44	25.11	33.09	0.74	3.48
Maximum	86.82	91.90	93.60	94.54	50.76	54.20
Mean	42.13	55.04	54.98	63.92	11.82	22.33
DS (days)						
Minimum	73.71	70.27	75.76	74.27	75.77	75.00
Maximum	86.37	84.73	92.21	86.99	82.19	80.99
Mean	79.54	78.98	82.57	81.07	78.53	77.92
PHT (cm)						
Minimum	96.32	70.51	96.53	72.66	217.56	201.23
Maximum	189.79	145.55	203.80	149.69	297.52	268.95
Mean	129.30	110.98	133.84	114.24	243.70	231.49

Large differences were observed between DH lines and TC in GER severity for both landraces with Petkuser always being more susceptible (Figure 1).

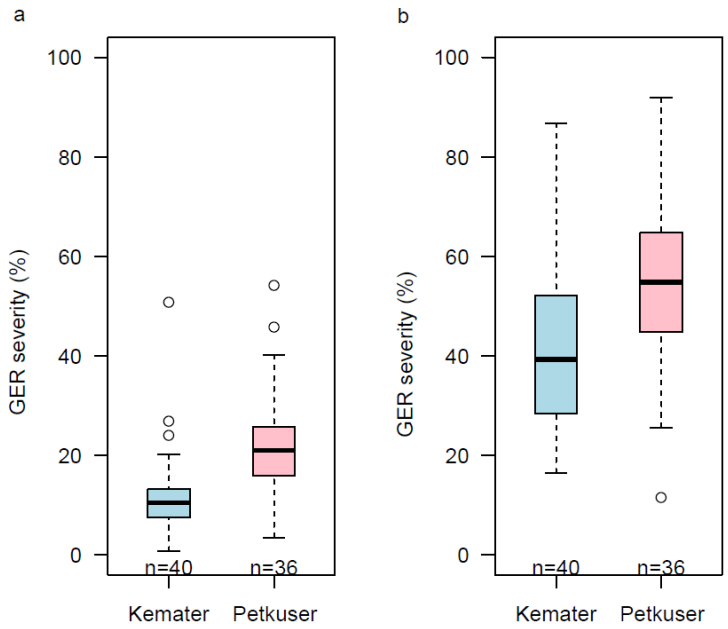

Figure 1. Box plots showing Gibberella ear rot (GER) severity for (**a**) testcrosses (TC), and (**b**) DH lines of "Kemater Landmais Gelb" and "Petkuser Ferdinand Rot" (2 environments). The thick horizontal lines in the boxes represent the median values; n = number of entries.

3.2. Variance Components and Heritability Estimates in Testcrosses and DH Lines

Significant ($p < 0.01$) genotypic and genotype-by-environment (G × E) interaction variances were found for all traits among both TC and DH lines (Table 2). Genotypic variances were higher for DH lines than for testcrosses in all traits, as expected. Broad-sense heritability (H^2) was moderate to high, depending on the trait and population. Genotypic variances (σ_g^2) for GER severity and PHT of the DH lines were higher in KE than PE landraces, while the opposite was found for DS. On the other hand, in TC, the

genotypic variances (σ_g^2) of GER and DS were higher for PE than KE, resulting in higher H^2 in PE than KE for both traits.

Table 2. Variance components and broad-sense heritabilities (H^2) for Gibberella ear rot severity (GER), days to silking (DS), and plant height (PHT) for DH lines and TC performance from "Kemater Landmais Gelb" (KE) and "Petkuser Ferdinand Rot" (PE).

Population	Parameter	GER (%)	DS (days)	PHT (cm)
DH lines				
KE	σ_g^2	259.81	8.87	416.66
	σ_{ge}^2	78.82	3.28	60.04
	σ_ε^2	308.70	3.58	86.26
	H^2	0.82	0.88	0.94
PE	σ_g^2	211.48	11.16	207.73
	σ_{ge}^2	114.31	2.40	55.56
	σ_ε^2	308.70	3.58	86.26
	H^2	0.76	0.91	0.89
TC				
KE	σ_g^2	39.48	1.36	207.33
	σ_{gl}^2	31.49	0.26	28.65
	σ_ε^2	63.13	1.02	68.72
	H^2	0.56	0.78	0.87
PE	σ_g^2	67.26	2.35	191.90
	σ_{gl}^2	28.14	0.16	26.79
	σ_ε^2	63.13	1.02	68.72
	H^2	0.69	0.88	0.86

Furthermore, G × E interaction variances represented 6.81–79.76% of the genotypic variances (σ_g^2) for all traits in the two populations (Table 2). In the KE population, the relative importance of G×E interaction variance (σ_{ge}^2) was higher among TC (79.76% of σ_g^2) than among DH lines (30.33% of σ_g^2) for GER severity. On the contrary, the relative proportion of G×E interaction variance was relatively higher in DH lines than TC lines for DS and similar in both lines for PHT. In the PE population, GxE interaction variances were smaller in TC lines than DH lines in comparison to the corresponding genotypic variances for all traits.

3.3. Correlations and Genomic Prediction Accuracies between Testcrosses and DH Line Performances under Gibberella Ear Rot Infection

Positive significant correlations were detected between DH lines and testcrosses for both KE and PE populations (Figure 2a). The correlation for GER severity was moderate between KE lines and TC (r = 0.37) and also for PE lines and TC (r = 0.55). However, the correlation observed for GER severity was lower compared to that of days to silking and plant height, which revealed high positive correlations between line per se and testcrosses for both KE and PE populations (Figure 2). In addition, correlation coefficients were lower in the KE population for GER severity and days to silking but not for plant height. In addition, pairwise correlations between GER severity, days to silking, and plant height were weak and non-significant for both DH and TC lines in the two populations (Figure S1).

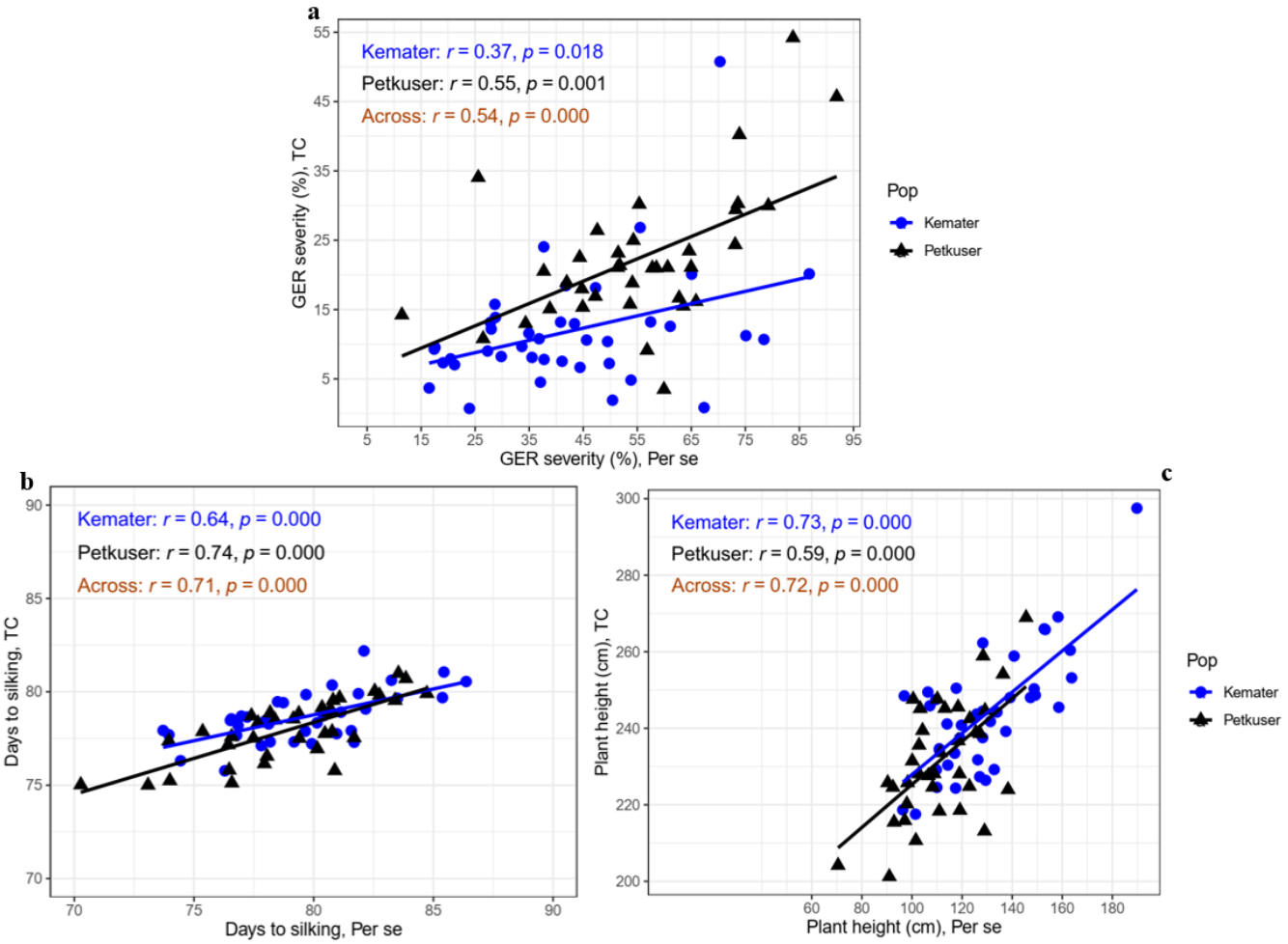

Figure 2. Scatter plots showing correlations (r) between testcross (TC) and line per se performance of two landrace populations (Pop) for (**a**) Gibberella ear rot (GER) severity, (**b**) days to silking, and (**c**) plant height.

The genomic prediction analysis using the line per se data as the training set and the TC as the validation set revealed a relatively high cross-validation prediction accuracy (0.49 for KE and 0.63 for PE) for GER severity (Figure 3) compared to what was reported previously within KE and PE DH lines [24]. Genomic prediction accuracies were relatively higher (0.49 to 0.85) compared to the phenotypic correlations for all traits. However, the prediction accuracy for GER severity remained lower compared to that of days to silking and plant height in both the KE and PE populations. Likewise, the prediction accuracies in the KE population were lower compared to those of the PE population for all traits.

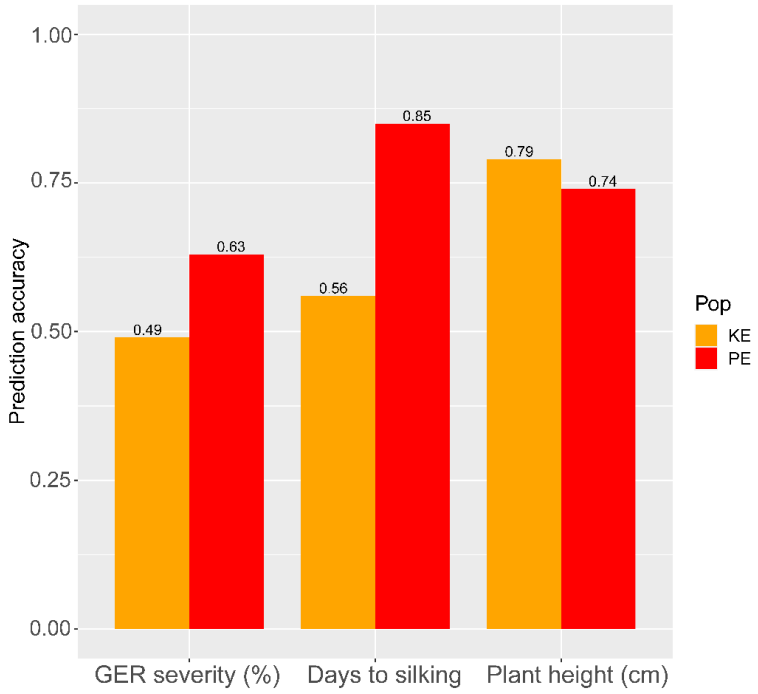

Figure 3. Cross-validated prediction accuracies for Gibberella ear rot (GER) severity, days to silking, and plant height using the line per se data as the training set and the corresponding testcrosses as the validation set for "Kemater Landmais Gelb" (KE) and "Petkuser Ferdinand Rot" (PE).

4. Discussion

Understanding association patterns between DH lines and TC with regard to key traits of interest is of paramount importance for the accurate selection of parents in hybrid breeding schemes. This study was conducted to investigate for the first time the GER resistance among TC and DH lines from two old European landraces, Kemater (KE) and Petkuser (PE), and to compare the correlations with the agronomic traits days to silking and plant height.

4.1. DH Lines Are Considerably More Susceptible Than Their Testcrosses

The DH lines revealed a much higher GER severity than that of their corresponding TC for both landraces. This difference is governed by (1) the resistance of the tester, (2) the inheritance of GER resistance, and (3) the effect of inbreeding depression. The choice of the tester is an important feature in hybrid breeding. A good tester should discriminate the lines and rank them correctly for their general combining ability for the trait [38]. In our case, the tester may have been very resistant, and/or the resistance could have been due, at least partly, to dominant alleles. GER resistance was reported to be quantitatively inherited with both additive and dominance effects according to Butrón et al. [39] and Martin et al. [15]. For the KE population, the presence of additive gene effects was recently shown by Gaikpa et al. [24] using GWAS and genomic prediction approaches. Plant height did perfectly follow the expectations of a two times higher line per se variance than testcross variance under the assumption of an additive gene action. The real cause of the difference between line and TC performance can, however, not be determined, because the tester line was unfortunately not included in the experiment. However, in the following year, the tester line F353 proved to be moderately susceptible to GER (25–57%, Bettina Kessel, pers. commun.). The large effect of the tester on GER resistance was shown previously by Löffler et al. [18], who used two highly susceptible flint testers with 74% and 89% GER severity, respectively, with the outcome that the inbred lines were more resistant than the TC. In contrast, Bolduan et al. [17] used a resistant and a highly susceptible tester (26% vs. 97% GER resistance), and the TC were similarly susceptible or resistant (30% vs. 73%).

Another cause for the high mean susceptibility of the lines could be inbreeding depression by uncovering recessive deleterious variants [40]. These DH lines were directly drawn from the landraces by female pathogenesis and are unselected samples being fully inbred in one step; i.e., they have never been selected for inbreeding tolerance before. Thus, inbreeding depression is expected to be high, and, indeed, many signs of inbreeding defects were visible among the line populations, such as low emergence rate, poor growth rate, lodging, poor seed set, and high tillering. Additionally, unwanted traits—such as high leaf chlorosis; tillering; and extreme susceptibility to common smut (*Ustilago maydis*), common rust (*Puccinia sorghi*), and several viruses—were reported [24,41,42]. This is the reason why about 70% of DH lines from such landraces could not be used in practical breeding [41]. Because *F. graminearum* is a fungus that could exploit the physiological weakness of hosts to accelerate the infection process, inbreeding depression might have favoured GER severity [19]. Although all DH lines have the same maximal inbreeding coefficient, they can still suffer differently from inbreeding depression according to their genomic makeup, and it has recently been shown that considerable parts of the genome are randomly lost during inbreeding [40]. Therefore, there could be an interaction between the suffering from inbreeding depression and GER severity that varies among the lines but, on average, leads to a much higher susceptibility of lines vs. TC. On the other hand, inbreeding depression also indicates heterosis for GER resistance in TC. Accordingly, Bolduan et al. [17] found a low-to-moderate mid-parent heterosis for GER resistance within elite flint lines of 9 percentage points for the susceptible tester and 34 percentage points for the more resistant one. In our study, the TC were, on average, three to four days earlier and about 110 cm taller than the DH lines, reflecting the known high heterosis of these agronomic traits.

Our results revealed that DH lines of the KE population were, on average, more resistant to Gibberella ear rot (GER) than DH lines of the PE population. This is in accordance with the results of a larger study on the same landraces with 250 DH lines per landrace. Similarly, TC developed from the KE population were more resistant than those from the PE population.

Good hybrid performance for GER resistance is also stressed by Mesterhazy et al. [22] with different *Fusarium* spp. ear rots, indicating that hybrid breeding could considerably help to better manage ear rot diseases and achieve higher food safety when both parents of the hybrid are under selection.

4.2. Variance Components Show Large Differences between Lines and Testcrosses

Genotypic variances for DH lines were very high for GER severity. Accordingly, broad-sense heritability (H^2) estimates of GER resistance in KE and PE populations were, respectively, 0.82 and 0.76 in lines, and 0.56 and 0.69 in derived TC. These estimates were higher than values reported by Wen et al. [21]. However, the two agronomic traits showed even higher heritability estimates throughout, especially for the TC.

For all traits and populations analysed, the genotypic variances and heritability estimates for DH lines were higher than for TC following quantitative–genetic expectations [17,43]. However, although we used a single line as tester, the variances among lines were much higher than expected. Again, this may be due to random inbreeding effects among lines that also inflate the variances. Additionally, the presence of non-additive gene effects, particularly with GER severity and days to silking, could be a cause. Of course, the differences in genotypic variances also reflect the high differences in means between DH lines and TC.

4.3. Moderate Associations and Genomic Prediction Accuracies between Line and Testcross Performance

Positive moderate associations between TC and DH lines were found for GER severity (r~0.5) averaged over both landraces. This is consistent with previous studies that found similar association patterns between TC and line per se for GER rating [17] and reduced mycotoxins concentrations [18] in European elite maize. The existence of significant associations could facilitate the prediction of hybrid performance from line per se as

reported by Ertiro et al. [26] for fodder quality traits in maize. However, associations for days to silking and plant height were considerably higher when calculated across populations (r ~ 0.7), indicating a preponderance of additive inheritance for these traits and reflecting the higher H^2. Accordingly, the prediction of days to silking and plant height of maize hybrids by their line per se performance is already routine in large-scale breeding programs [27,44]. For GER resistance, however, the moderate estimates of the correlation between DH lines and TC, which are confirmed by the literature, will result in only a moderately correlated indirect selection response for TC [17]. Therefore, there should only be a mild selection for line performance followed by selection among TC in a subsequent step. In any event, TC are produced for selecting the combining ability for yield. When selecting the 10% best KE lines, these were also among the 10% best TC; however, for PE this was not the case. Furthermore, relatively high prediction accuracies were found for GER resistance over both landraces (r ~ 0.6), indicating the relevance of genomic selection in predicting GER resistance of hybrids using line per se performance [13]. Our genomic prediction should be considered as preliminary due to the restricted number of entries and environments; however, it is a first promising approach that should definitely be pursued further.

The pre-selection on the basis of line performance has the enormous advantage that the full variance of the lines is under selection, although the total variation might be triggered by inbreeding defects. However, the most susceptible lines should nonetheless be discarded, as they could lead to seed quality issues in line multiplication and commercial hybrid production. Lines should at least have a basic resistance to GER to avoid bad seed quality and low emergence rates.

5. Conclusions

The development of high-yielding varieties with improved disease resistance is an appropriate approach to effectively reduce Gibberella ear rot (GER) damage in maize. Significant genetic variation is available in DH lines from the Kemater (KE) and Petkuser (PE) landraces to effectively develop high GER-resistant maize hybrids. Large genetic variation was found among lines for GER severity, days to silking, and plant height. TC were considerably more resistant to GER than DH lines. Moderate correlations were found between TC and DH lines for GER resistance, indicating the possibility of a pre-selection of large DH populations by discarding the most susceptible lines in a first selection stage before a second more rigid selection on a TC basis to develop GER-resistant maize hybrids. Considering the presence of large genotype-by-environment interaction variances and the complexity of quantitative traits, genomic approaches, such as genome-wide association (GWAS) and genomic selection (GS), could be used as a complement of phenotyping for more effective prediction of GER resistance of hybrids from line performance.

Supplementary Materials: The following are available online at https://www.mdpi.com/article/10.3390/agronomy11061039/s1, Figure S1: Scatter plots showing correlations (R) between GER severity and the two agronomic traits. (a) GER severity vs. days to silking for line per se, (b) GER severity vs. plant height for line per se, (c) GER severity vs. days to silking for TC, and (d) GER severity vs. plant height for TC.

Author Contributions: Conceptualisation, T.M. and D.S.G.; methodology, T.M.; software, F.A. and D.S.G.; validation, F.A. and D.S.G.; formal analysis, F.A. and D.S.G.; investigation, D.S.G.; resources, B.K., T.P.; data curation, F.A. and B.K.; writing—original draft preparation, F.A.; writing—review and editing, T.M., D.S.G.; visualisation, F.A.; supervision, T.M.; project administration, T.M. and T.P.; funding acquisition, F.A. and D.S.G. All authors have read and agreed to the published version of the manuscript.

Funding: This research was partially funded by the German Academic Exchange Service, Bonn, Germany as a doctoral study grant to David S. Gaikpa (grant no. 91650671) and to Félicien Akohoue (grant no. 91770158).

Institutional Review Board Statement: Not applicable.

Informed Consent Statement: Not applicable.

Data Availability Statement: Data is contained within the article or supplementary material.

Acknowledgments: We are thankful to KWS SAAT SE & Co. KGaA, Einbeck, Germany, for supporting this research by producing the genetic materials and conducting the maize experiments in Gondelsheim. INRAE, Paris, France, is also thanked for supporting this research by providing the French dent line "F353".

Conflicts of Interest: The authors declare no conflict of interest.

References

1. Ranum, P.; Peña-Rosas, J.P.; Garcia-Casal, M.N. Global maize production, utilization, and consumption. *Ann. N. Y. Acad. Sci.* **2014**, *1312*, 105–112. [CrossRef] [PubMed]
2. Dowswell, C.R.; Paliwal, R.L.; Cantrell, R.P. *Maize in the Third World*; Routledge: New York, NY, USA, 2019.
3. Verheye, W. Growth and production of maize: Traditional low-input cultivation. In *Land Use, Land Cover and Soil Sciences*; UNESCO-EOLSS Publishers: Oxford, UK, 2010; pp. 1–23.
4. Chaudhary, H.K.; Kaila, V.; Rather, S.A. Maize. In *Alien Gene Transfer in Crop Plants*; Springer Science and Business Media LLC: Berlin/Heidelberg, Germany, 2013; Volume 2, pp. 27–50.
5. Ray, D.K.; Mueller, N.D.; West, P.C.; Foley, J.A. Yield trends are insufficient to double global crop production by 2050. *PLoS ONE* **2013**, *8*, e66428. [CrossRef] [PubMed]
6. Suh, S.; Johnson, J.A.; Tambjerg, L.; Sim, S.; Broeckx-Smith, S.; Reyes, W.; Chaplin-Kramer, R. Closing yield gap is crucial to avoid potential surge in global carbon emissions. *Glob. Environ. Chang.* **2020**, *63*, 102100. [CrossRef]
7. Lanubile, A.; Maschietto, V.; Borrelli, V.M.; Stagnati, L.; Logrieco, A.F.; Marocco, A. Molecular basis of resistance to fusarium ear rot in maize. *Front. Plant Sci.* **2017**, *8*, 1774. [CrossRef]
8. Qin, P.; Xu, J.; Jiang, Y.; Hu, L.; Van Der Lee, T.; Waalwijk, C.; Zhang, W.; Xu, X. Survey for toxigenic Fusarium species on maize kernels in China. *World Mycotoxin J.* **2020**, *13*, 213–224. [CrossRef]
9. Szabo, B.; Toth, B.; Toldine, E.T.; Varga, M.; Kovacs, N.; Varga, J.; Kocsube, S.; Palagyi, A.; Bagi, F.; Budakov, D.; et al. A new concept to secure food safety standards against fusarium species and aspergillus flavus and their toxins in maize. *Toxins* **2018**, *10*, 372. [CrossRef]
10. Atanasova-Penichon, V.; Barreau, C.; Richard-Forget, F. Antioxidant secondary metabolites in cereals: Potential involvement in resistance to fusarium and mycotoxin accumulation. *Front. Microbiol.* **2016**, *7*, 566. [CrossRef] [PubMed]
11. Chilaka, C.A.; De Boevre, M.; Atanda, O.O.; De Saeger, S. Occurrence of fusarium mycotoxins in cereal crops and processed products (Ogi) from Nigeria. *Toxins* **2016**, *8*, 342. [CrossRef]
12. James, A.; Zikankuba, V.L. Mycotoxins contamination in maize alarms food safety in sub-Sahara Africa. *Food Control.* **2018**, *90*, 372–381. [CrossRef]
13. Gaikpa, D.S.; Miedaner, T. Genomics-assisted breeding for ear rot resistances and reduced mycotoxin contamination in maize: Methods, advances and prospects. *Theor. Appl. Genet.* **2019**, *132*, 2721–2739. [CrossRef]
14. Mesterházy, Á.; Lemmens, M.; Reid, L.M. Breeding for resistance to ear rots caused by Fusarium spp. in maize—A review. *Plant Breed.* **2012**, *131*, 1–19. [CrossRef]
15. Martin, M.; Dhillon, B.S.; Miedaner, T.; Melchinger, A.E. Inheritance of resistance to Gibberella ear rot and deoxynivalenol contamination in five flint maize crosses. *Plant Breed.* **2011**, *131*, 28–32. [CrossRef]
16. Pfordt, A.; Romero, L.R.; Schiwek, S.; Karlovsky, P.; Von Tiedemann, A. Impact of environmental conditions and agronomic practices on the prevalence of fusarium species associated with ear- and stalk rot in maize. *Pathogens* **2020**, *9*, 236. [CrossRef]
17. Bolduan, C.; Miedaner, T.; Utz, H.F.; Dhillon, B.S.; Melchinger, A.E. Genetic variation in testcrosses and relationship between line per se and testcross performance for resistance to gibberella ear rot in maize. *Crop. Sci.* **2010**, *50*, 1691–1696. [CrossRef]
18. Löffler, M.; Kessel, B.; Ouzunova, M.; Miedaner, T. Covariation between line and testcross performance for reduced mycotoxin concentrations in European maize after silk channel inoculation of two Fusarium species. *Theor. Appl. Genet.* **2010**, *122*, 925–934. [CrossRef]
19. Miedaner, T.; Han, S.; Kessel, B.; Ouzunova, M.; Schrag, T.; Utz, F.H.; Melchinger, A.E. Prediction of deoxynivalenol and zearalenone concentrations inFusarium graminearuminoculated backcross populations of maize by symptom rating and near-infrared spectroscopy. *Plant Breed.* **2015**, *134*, 529–534. [CrossRef]
20. Baweja, P.; Kumar, S.; Kumar, G. Fertilizers and pesticides: Their impact on soil health and environment. In *Soil Health*, 1st ed.; Giri, B., Varma, A., Eds.; Springer Nature Switzerland AG: Cham, Switzerland, 2020; Volume 59, pp. 265–285.
21. Wen, J.; Shen, Y.; Xing, Y.; Wang, Z.; Han, S.; Li, S.; Yang, C.; Hao, D.; Zhang, Y. QTL mapping of resistance to Gibberella ear rot in maize. *Mol. Breed.* **2020**, *40*, 94. [CrossRef]
22. Mesterhazy, A.; Toth, E.T.; Szel, S.; Varga, M.; Toth, B. Resistance of maize hybrids to *Fusarium graminearum*, *F. culmorum*, and *F. verticillioides* ear rots with toothpick and silk channel inoculation, as well as their toxin production. *Agronomy* **2020**, *10*, 1283. [CrossRef]

23. Wang, Y.; Zhou, Z.; Gao, J.; Wu, Y.; Xia, Z.; Zhang, H.; Wu, J. The mechanisms of maize resistance to fusarium verticillioides by comprehensive analysis of RNA-seq data. *Front. Plant Sci.* **2016**, *7*, 1654. [CrossRef] [PubMed]
24. Gaikpa, D.S.; Kessel, B.; Presterl, T.; Ouzunova, M.; Galiano-Carneiro, A.L.; Mayer, M.; Melchinger, A.E.; Schön, C.-C.; Miedaner, T. Exploiting genetic diversity in two European maize landraces for improving Gibberella ear rot resistance using genomic tools. *Theor. Appl. Genet.* **2021**, *134*, 793–805. [CrossRef]
25. Miedaner, T.; Schulthess, A.W.; Gowda, M.; Reif, J.C.; Longin, C.F.H. High accuracy of predicting hybrid performance of Fusarium head blight resistance by mid-parent values in wheat. *Theor. Appl. Genet.* **2016**, *130*, 461–470. [CrossRef]
26. Ertiro, B.T.; Zeleke, H.; Friesen, D.; Blümmel, M.; Twumasi-Afriyie, S. Relationship between the performance of parental inbred lines and hybrids for food-feed traits in maize (*Zea mays* L.) in Ethiopia. *Field Crop. Res.* **2013**, *153*, 86–93. [CrossRef]
27. Edlich-Muth, C.; Muraya, M.M.; Altmann, T.; Selbig, J. Phenomic prediction of maize hybrids. *Biosystems* **2016**, *146*, 102–109. [CrossRef]
28. Cobb, J.N.; Juma, R.U.; Biswas, P.S.; Arbelaez, J.D.; Rutkoski, J.; Atlin, G.; Hagen, T.; Quinn, M.; Ng, E.H. Enhancing the rate of genetic gain in public-sector plant breeding programs: Lessons from the breeder's equation. *Theor. Appl. Genet.* **2019**, *132*, 627–645. [CrossRef]
29. Bauer, E.; Falque, M.; Walter, H.; Bauland, C.; Camisan, C.; Campo, L.; Meyer, N.; Ranc, N.; Rincent, R.; Schipprack, W.; et al. Intraspecific variation of recombination rate in maize. *Genome Biol.* **2013**, *14*, R103. [CrossRef] [PubMed]
30. Reid, L.M.; Mather, D.E.; Hamilton, R.I. Distribution of deoxynivalenol in Fusarium graminearum-infected maize ears. *Phytopathology* **1996**, *86*, 110–114. [CrossRef]
31. Reid, L.; Hamilton, R. Effects of inoculation position, timing, macroconidial concentration, and irrigation on resistance of maize toFusarium graminearuminfection through kernels. *Can. J. Plant Pathol.* **1996**, *18*, 279–285. [CrossRef]
32. Butler, D.; Cullis, B.; Gilmour, A.; Gogel, B. *Analysis of Mixed Models for S–Language Environments: ASReml–R Reference Manual*; Queensland DPI: Brisbane, Australia, 2007; Available online: http://www.vsni.co.uk/resources/doc/asreml-R.pdf (accessed on 25 March 2021).
33. Hallauer, A.; Russell, W.A.; Lamkey, K. Corn breeding. In *Corn and Corn Improvement*, 3rd ed.; Sprague, G.F., Dudley, J.W., Eds.; American Society of Agronomy, Inc.: Madison, WI, USA, 1988; Volume 18, pp. 463–564.
34. R Core Team. *R: A Language and Environment for Statistical Computing*; Foundation for Statistical Computing: Vienna, Austria, 2020.
35. Endelman, J.B. Ridge regression and other kernels for genomic selection with R package rrBLUP. *Plant Genome* **2011**, *4*, 250–255. [CrossRef]
36. Endelman, J.B.; Jannink, J.-L. Shrinkage estimation of the realized relationship matrix. *G3 Genes Genomes Genet.* **2012**, *2*, 1405–1413. [CrossRef]
37. Unterseer, S.; Bauer, E.; Haberer, G.; Seidel, M.; Knaak, C.; Ouzunova, M.; Meitinger, T.; Strom, T.M.; Fries, R.; Pausch, H.; et al. A powerful tool for genome analysis in maize: Development and evaluation of the high density 600 k SNP genotyping array. *BMC Genom.* **2014**, *15*, 823. [CrossRef]
38. Matzinger, D.F. Comparison of three types of testers for the evaluation of inbred lines of corn1. *Agron. J.* **1953**, *45*, 493–495. [CrossRef]
39. Butrón, A.; Reid, L.M.; Santiago, R.; Cao, A.; Malvar, R.A. Inheritance of maize resistance to gibberella and fusarium ear rots and kernel contamination with deoxynivalenol and fumonisins. *Plant Pathol.* **2015**, *64*, 1053–1060. [CrossRef]
40. Roessler, K.; Muyle, A.; Diez, C.M.; Gaut, G.R.J.; Bousios, A.; Stitzer, M.C.; Seymour, D.K.; Doebley, J.F.; Liu, Q.; Gaut, B.S. The genome-wide dynamics of purging during selfing in maize. *Nat. Plants* **2019**, *5*, 980–990. [CrossRef] [PubMed]
41. Böhm, J.; Schipprack, W.; Utz, H.F.; Melchinger, A.E. Tapping the genetic diversity of landraces in allogamous crops with doubled haploid lines: A case study from European flint maize. *Theor. Appl. Genet.* **2017**, *130*, 861–873. [CrossRef]
42. Strigens, A.; Schipprack, W.; Reif, J.C.; Melchinger, A.E. Unlocking the genetic diversity of maize landraces with doubled haploids opens new avenues for breeding. *PLoS ONE* **2013**, *8*, e57234. [CrossRef] [PubMed]
43. Wricke, G.; Weber, E. *Quantitative Genetics and Selection in Plant Breeding*; Walter de Gruyter: Berlin, Germany, 2010.
44. Wang, N.; Wang, H.; Zhang, A.; Liu, Y.; Yu, D.; Hao, Z.; Ilut, D.; Glaubitz, J.C.; Gao, Y.; Jones, E.; et al. Genomic prediction across years in a maize doubled haploid breeding program to accelerate early-stage testcross testing. *Theor. Appl. Genet.* **2020**, *133*, 2869–2879. [CrossRef]

Variance components and correlations between doubled haploid lines from two European flint landraces and their corresponding testcrosses for Gibberella ear rot resistance, silking time, and plant height in maize

Félicien Akohoue[1], David Sewordor Gaikpa[1], Bettina Kessel[2], Thomas Presterl[2] and Thomas Miedaner[1,*]

Supplementary information

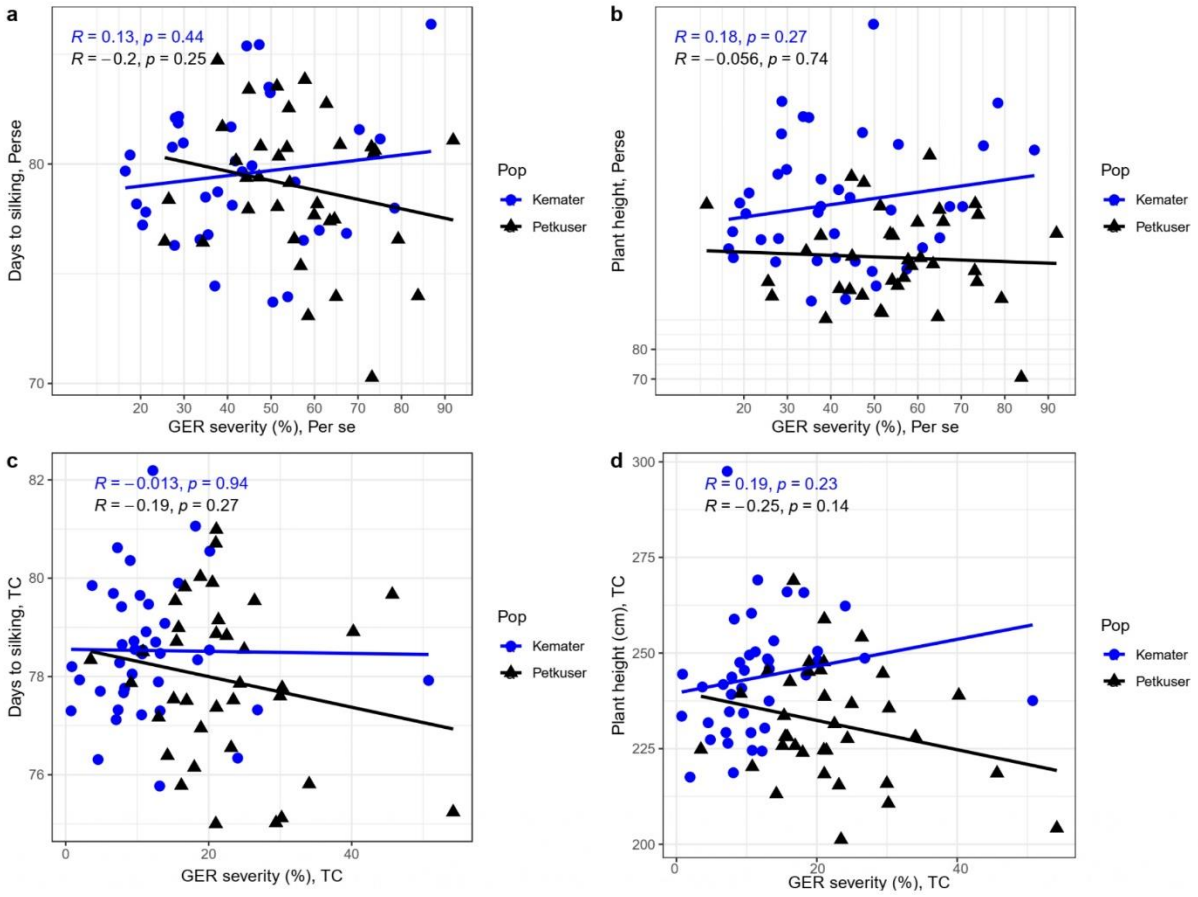

Figure S1. Scatter plots showing correlations (R) between GER severity and the two agronomic traits. (a) GER severity vs. Days to silking for line per se (b) GER severity vs. plant height for line per se, (c) GER severity vs. Days to silking for TC, and (d) GER severity vs. plant height for TC

Chapter 6: General discussion

Harnessing genetic resources to tackle Fusarium head blight (FHB) in wheat and Gibberella ear rot (GER) in maize

The European winter wheat diversity panel and flint maize landraces represent rich sources of allelic diversity that can be exploited via appropriate breeding strategies to improve resistance to quality- and yield-impacting Fusarium diseases such as FHB and GER in wheat and maize, respectively. Based on 401 cultivars from the European winter wheat diversity panel (Figure 7A), our work revealed the existence of highly significant genetic variances for FHB severity (Chapter 2). Based on the presence/absence of semi-dwarfing "*b*" and tall "*a*" alleles of *Rht-D1* and *Rht-24*, we clustered the diversity panel into four genotypic groups, namely *Rht24a+Rht-D1a* (also referred to as *NoRht* in Chapter 2), *Rht24b+Rht-D1a*, *Rht24a+Rht-D1b*, and *Rht24b+Rht-D1b*. Recently, Miedaner et al. (2022) analysed 420 winter wheat cultivars from the same diversity panel, and observed highly significant genetic variation for FHB resistance within these genotypic groups. Similarly, in maize, we detected high genetic variances within KE and PE landraces for GER resistance. Gaikpa et al. (2021) also evaluated these landraces for GER resistance and revealed a clear population structure and high genetic variances (Figure 7B).

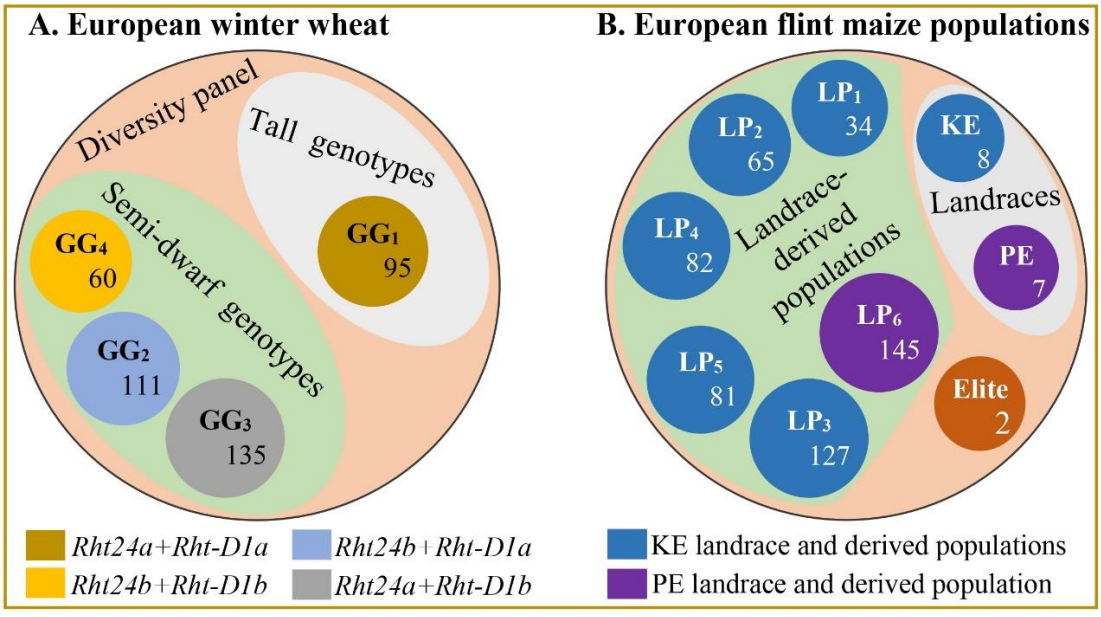

Figure 7: European winter wheat genotypic groups (GG) with/without *Rht* genes and flint maize landraces and derived populations included in our study. Numbers indicate groups or populations sizes. KE = Kemater landrace, PE = Petkuser landrace, LP = landrace-derived populations

Our results showed that entry-mean heritability estimates were high for FHB resistance as well as GER resistance. High heritability estimate is an indication of appropriate field phenotyping (Piepho and Möhring, 2007), and highlights the high potential for the application of genomics-assisted breeding for increased genetic gains (Xu et al., 2017; Zhang et al., 2017). In wheat, sixty-five meta-QTL were recently reported for FHB resistance by Venske et al. (2019) based on QTL identified in 76 diverse studies. To fully exploit existing genetic diversity and efficiently address FHB disease, we applied a combination of path coefficients analysis and genomics-assisted breeding approaches which was relevant for elucidating the complex interactions between FHB resistance and morphological traits as well as underlying molecular basis. The effect of *Rht24b* on anther retention was evaluated and we demonstrated the potential of genomic background resistance to reduce FHB severity within semi-dwarf winter wheat genotypes.

Furthermore, in maize, an impressive number of genomic loci that are responsible for the genetic variation of ear rot resistance was reported by several isolated studies within diverse populations, including the European flint landraces (Wen et al., 2020; Gaikpa et al., 2021; Galiano-Carneiro et al., 2021). These individual loci were clustered into 40 meta-QTL (MQTL), of which 14 refined and stable MQTL to suggest appropriate genomics-assisted breeding strategies for the exploitation of these loci (Chapter 3). We assessed the introgression of the flint landraces into elite materials using six bi-parental populations with a total of 534 DH lines (Figure 7B), which also showed significant genetic variation (Chapter 4). The possibility to accelerate the development of hybrid varieties with improved GER resistance was explored for each landrace population using both phenotypic and genomic prediction approaches (Chapter 5). The findings have implications with concrete suggestions to enhance resistance to FHB and GER diseases in winter wheat and maize, respectively.

Complex interactions between Fusarium head blight resistance and morphological traits and effect of *Rht24b* on anther retention in wheat

Morphological traits were reported to have a passive contribution to resistance or susceptibility to Fusarium head blight disease in wheat (Tessmann and van Sanford, 2019; Buerstmayr et al., 2020). Based on the diversity panel of 401 winter wheat cultivars evaluated across five environments, our study confirmed the existence of low to high genotypic correlations between FHB severity and number of spikelets, ear length, anther retention and plant height. From these,

anther retention had a strong positive correlation (r_g = 0.74) with FHB severity, while plant height showed a high negative correlation (r_g = −0.64) with FHB severity (Figure 8).

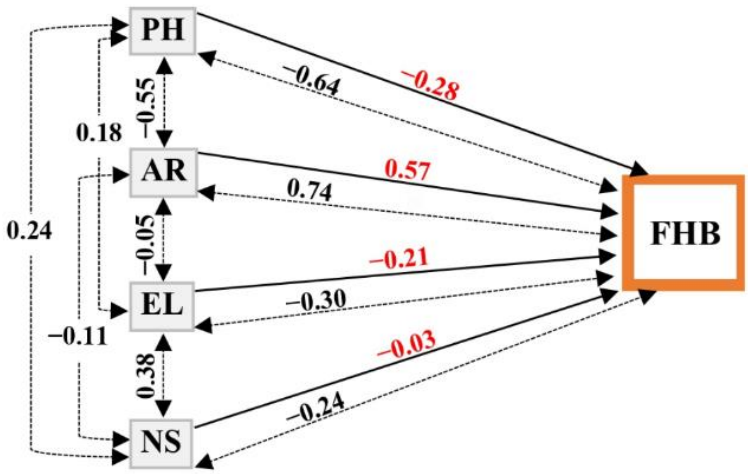

Figure 8: Path diagram showing genotypic correlations (indicated by double-dashed-arrowed lines) and direct path effects (in red indicated by single-arrowed lines) of plant height (PH), anther retention (AR), ear length (EL) and number of spikelets (NS) on FHB severity (FHB)

Strong positive phenotypic correlations were also reported between FHB severity and anther retention by Steiner et al. (2019) (r_p = 0.88) and Buerstmayr and Buerstmayr (2015) (r_p = 0.63). Numerous studies also reported moderate to high negative correlations between FHB severity and anther extrusion, the opposite of anther retention (Lu et al., 2013; Xu et al., 2020; Nannuru et al., 2022). Moreover, using 144 DH lines derived from a three-way cross among Chinese cultivars Sumai 3/Saikai 165/U24, Kubo et al. (2013) demonstrated that small differences in anther extrusion had significant effect on FHB resistance. Similarly, negative phenotypic correlations were reported between FHB severity and plant height, with varying strength (r_p = −0.23 to r_p = −0.62) across environments and studies (Ruan et al., 2020; Nannuru et al., 2022).

Furthermore, the decomposition of the genotypic correlations revealed that the causal system formed by the morphological traits explained about 67% of the variation of FHB severity (Table 3 in Chapter 2). Anther retention had the highest direct path effect (0.57) on FHB severity (Figure 8), showing that an increase of 1% in the standard deviation of anther retention implies a direct increase of 0.57% in the standard deviation of FHB severity. Likewise, plant height exhibited a direct path effect of −0.28 on FHB severity. This indicates that a decrease of 1 cm in the standard deviation of plant height implies a direct increase of 0.28% in the standard deviation of FHB severity. In addition, the findings revealed the existence of a slightly higher indirect path effect (−0.31) of plant height on FHB severity via anther retention (Table 3 in Chapter 2). This demonstrates that plant height affects FHB severity through anther retention, and an indirect selection strategy for FHB resistance using morphological traits

should consider a simultaneous integration of these two traits. However, the phenotypic evaluation for anther retention in large breeding populations can be labor-intensive and time-consuming. Therefore, the effective incorporation of this trait into multiple trait selection strategies can be facilitated by the exploitation of quantitative trait loci which have pleiotropic effects on FHB resistance and anther retention.

The high genotypic correlations and path effects observed between FHB resistance, plant height and anther retention indicates the existence of common genomic loci among these traits. Based on our findings, FHB resistance shared six pleiotropic loci on chromosomes 4D, 6B, 5A, 7B and 2A with plant height, four pleiotropic loci on chromosomes 4D, 2A, and 7B with anther retention (Table 4 in Chapter 2). All together, these loci explained 56.2% and 24.3% of the genotypic correlations of FHB severity with plant height and anther retention, respectively. *Rht-D1* linked to marker *TG0011a* on chromosome 4D was a major locus with a negative pleiotropic effect, explaining about 27% of the negative genotypic correlation between FHB severity and plant height. This is an evidence that wheat genotypes with *Rht-D1b* has higher FHB susceptibility. Miedaner et al. (2022) demonstrated that *Rht-D1b* increased FHB susceptibility by 37% based on 420 winter wheat cultivars. Liu et al. (2013) also found a negative pleiotropic effect for *Rht-D1b* on FHB resistance by analyzing a total of 383 recombinant inbred lines (RILs) from two mapping populations (B/M and E/MO) derived from two US soft red winter wheat cultivars. However, other loci on chromosomes 6B, 7B and 2A exhibited a positive pleiotropic effect, thereby reducing the negative effect of *Rht-D1* on FHB resistance. The potential of these positive pleiotropic loci in reducing FHB severity, plant height and anther retention can be further evaluated to facilitate their effective integration in multiple trait selection strategies. Moreover, high anther extrusion is necessary for a successful hybrid wheat breeding (Boeven et al., 2016). To this end, the exploitation of the pleiotropic loci to select for high anther extrusion (or low anther retention) would help to develop hybrid wheat cultivars with higher FHB resistance.

Unlike *Rht-D1*, our results revealed that *Rht24* linked to marker *BS00022120_51* had no pleiotropic effect on FHB resistance and anther retention (Figure 4b, 4c in Chapter 2). In addition, the two-way analysis of variance on the effects of semi-dwarfing genes shows that the main effect of *Rht24* was not significant on FHB severity and anther retention (Table 1). This firstly confirms findings of Miedaner et al. (2022) and Herter et al. (2018) that *Rht24* does not affect FHB resistance, and secondly demonstrates for the first time that *Rht24* no significant effect on anther retention which is highly correlated with FHB resistance. The findings exhibit

Rht24 as a major FHB- and anther retention-neutral semi-dwarf gene which can be efficiently exploited in breeding programs. Moreover, the interaction between *Rht-D1* and *Rht24* was not significant for all traits (Table 2), indicating an absence of a significant epistatic interaction between the two *Rht* genes.

Table 2: Mean squares of analysis of variance including 401 cultivars for the effects of *Rht-D1* and *Rht24*, and their interaction on FHB severity, plant height (PH) and anther retention (AR)

Trait	***Rht-D1* (df = 1)**	***Rht24* (df = 1)**	***Rht-D1*x*Rht24* (df = 1)**	**Residuals**
PH	19736***	2855***	14^{ns}	44
FHB severity	14242***	28^{ns}	0^{ns}	97
AR	57704***	292^{ns}	7^{ns}	370

*** significant at p-value < 0.001, ns = non-significant at p < 0.05, Df = degree of freedom

In comparison with tall cultivars (with *Rht24a* and *Rht-D1a*), average plant height of cultivars with *Rht24b*, *Rht-D1b* and their combination (*Rht24b+Rht-D1b*) was reduced by 5.9, 13.7 and 18.8 cm, respectively (Figure 9).

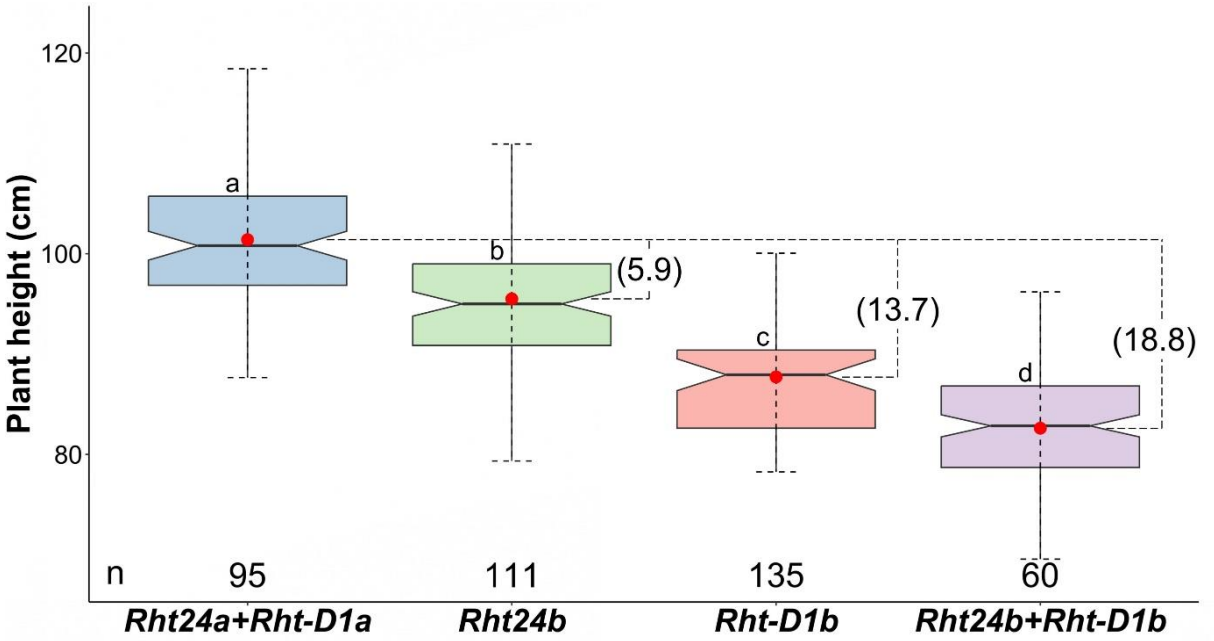

Figure 9: Plant height reduction by semi-dwarfing alleles *Rht24b*, *Rh-D1b* and their combination. Red point within each box and n represent the average plant height and size of each group of genotypes, respectively. Values in parenthesis refers to the difference between the average plant height of tall genotypes (*Rht24a+Rht-D1a*) and other groups. Boxes with the same letters are statistically identical

Similar plant height reduction patterns were recently found for *Rht-D1b* (13.6 cm) and *Rht24b* (6.8 cm) by Miedaner et al. (2022) within the same winter wheat diversity panel. A height reduction of 6−7.9 cm was also indicated for *Rht24b* by Tian et al. (2017) based on 256 recombinant inbred lines developed from the cross of two Chinese lines. Moreover, Herter et al. (2018) also reported reduction effects of 8.96 and 11.53 cm for *Rht24b* and *Rht-D1b*, respectively. This demonstrates that breeders can combine *Rht24b* with *Rht-D1b* to significantly reduce plant height and satisfy the high interest for semi-dwarf wheat genotypes.

Reduction effect of genomic background on Fusarium head blight severity within wheat cultivars possessing *Rht-D1b*

Along with the potential of FHB-neutral *Rht* loci (i.e. *Rht24*) as discussed earlier, our results revealed a considerably higher genetic variation regarding FHB severity and anther retention within cultivars with *Rht-D1b* or the combination *Rht24b+Rht-D1b* compared to cultivars without *Rht-D1b* (Table 5 in Chapter 2). FHB severity ranges were 20.3−68.3% and 23.1−70.7% within *Rht-D1b* and *Rht24b+Rht-D1b* groups, respectively, revealing the existence of resistant cultivars despite the negative effect of *Rht-D1b* on FHB resistance. This indicates a FHB-reduction effect exerted by the genomic background, which has the ability to counterbalance the negative effect of *Rht-D1b* on FHB resistance as reported for spring wheat by Buerstmayr and Buerstmayr (2022). In their study, the authors evaluated four different sets of near-isogenic lines (NILs) with contrasting levels and types of background resistance (Types I and II resistances) and demonstrated that high background resistance reduces the negative effect of *Rht1*-genes on FHB resistance.

In our work, the genomic background within each cultivar comprises all locally adapted genomic loci with the exception of *Rht* genes. Based on genome-wide association study (GWAS) incorporating the whole diversity panel, the proportion of genotypic variation explained by significant genomic background markers was about 12 and 6% higher for FHB severity and anther retention, respectively, than that pertaining to *Rht-D1b* (Figure 6 in Chapter 2). This, once again, highlights the potential of genomic background in adjusting FHB resistance and anther retention.

The evaluation of the effect of genomic background showed that the estimation of genomic estimated breeding values (GEBV) using genomic prediction approach was more effective than GWAS-detected markers, even though both methods were moderately correlated (Figure 8 in Chapter 2). Since most genomic background loci only exert small effects on the traits, they

cannot be efficiently detected using the standard GWAS which is a threshold-based approach (Korte and Farlow, 2013; Tibbs-Cortes et al., 2021). Depending on the FHB status of the cultivar or the degree of anther retention, GEBV was either negative or positive (Figure 10). For FHB severity, a negative GBEV refers to genomic background resistance, leading to varying degrees of FHB resistance. Similarly, for anther retention, a negative GBEV corresponds to low anther retention or high anther extrusion. On contrary, a positive GBEV represents high anther retention and genomic background susceptibility, thus, higher FHB severity. The findings demonstrate that best cultivars (FHB severity ≤ 30%) with or without *Rht-D1b* have higher background resistance on contrary to worst cultivars with *Rht-D1b* (Figure 10).

In addition, the genomic background for anther retention was highly negative for most cultivars with low FHB severity, except Anapolis which exhibited positive GBEV (>30) corresponding to anther retention of 99.63%. Anapolis is a cleistogamous genotype whose anthers remain retained at flowering and therefore preventing fungal spores from entering the spikelets. The passive contribution of cleistogamy to pathogen resistance has been previously discussed for FHB resistance in wheat by Gilsinger et al. (2005) and Kubo et al. (2010).

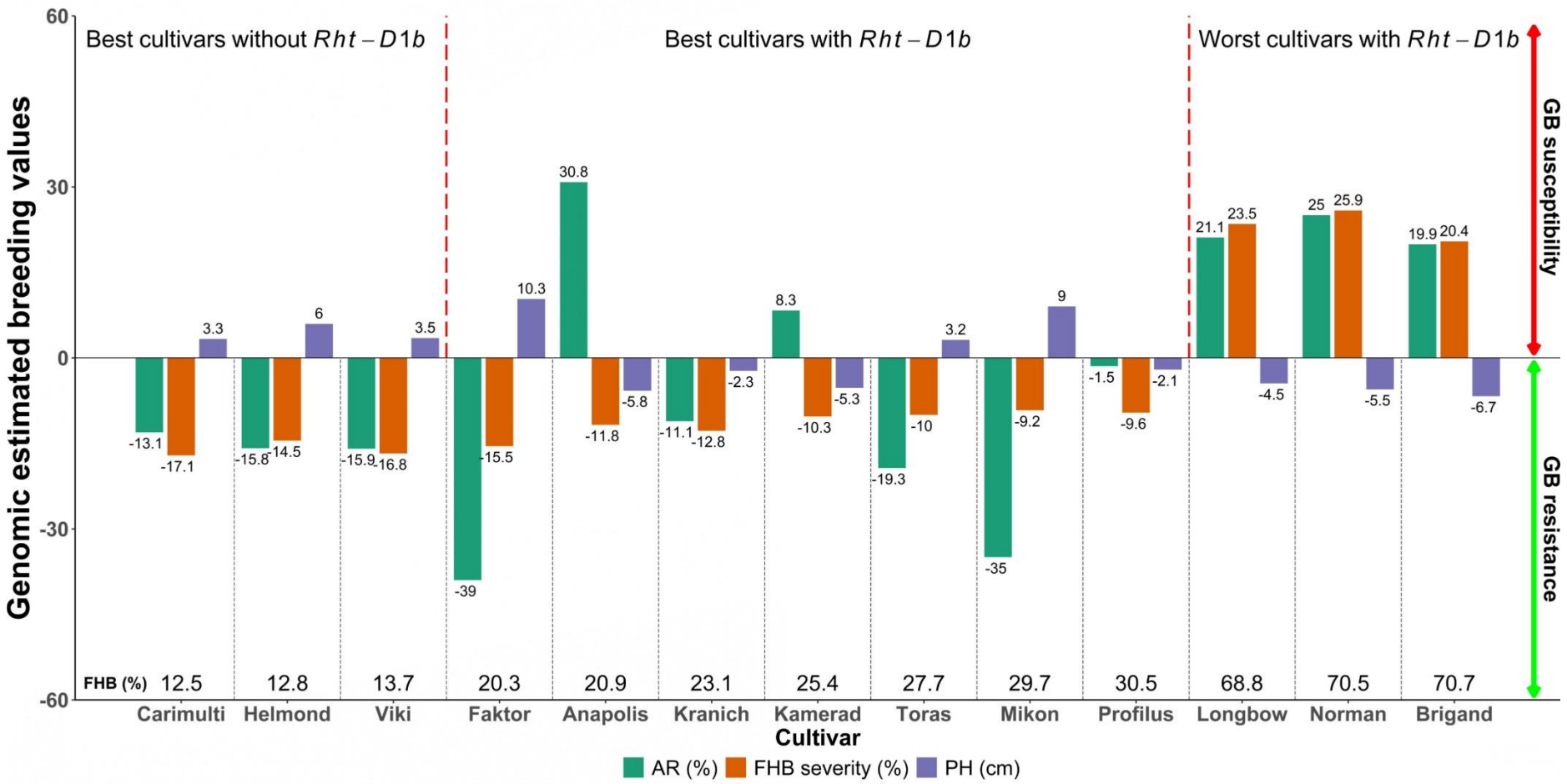

Figure 10: Genomic estimated breeding values representing the genomic background (GB) estimated for Fusarium head blight (FHB) severity, plant height (PH) and anther retention (AR) within cultivars with and without *Rht-D1b*. GB susceptibility/GB resistance = from breeder's point of view

Stable quantitative trait loci for ear rot diseases and resistance genes for introgression into elite maize materials

Maize ear rot resistance is controlled by several loci with small effects which confirm the quantitative and complex nature of the trait. QTL from individual studies were clustered into 40 meta-QTL of which 27 had a phenotypic variance explained (PVE) ≤ 10%. Most of these loci (28 MQTL) were common to Fusarium and Gibberella ear rots, indicating the high co-inheritance of different types of maize ear rot. Moderate to high phenotypic correlations were also found between FER and GER by Schaafsma et al. (2006) and Butrón et al. (2015). Depending on the breeding objective and environment, breeders can focus on one type of ear rot (i.e. GER) with the expectation that selected resistant lines are also resistant to the other type (i.e. FER).

Within each type of ear rot, several loci were common to silk (channel) resistance (SR) and kernel resistance (KR) (Figure 11). Although SR and KR are two different types of active resistance to ear rot diseases in maize, moderate to high correlations have also been detected between them (Löffler et al., 2010b; Kebebe et al., 2015). Harnessing the common loci identified in our study for SR and KR will help to increase maize resistance to the two major pathogen entry modes into the cob. To initiate the infection, fungal spores usually penetrate maize cobs via silk channel or directly the kernels through openings and wounds created by insects' injury, hail and agricultural tools or machines.

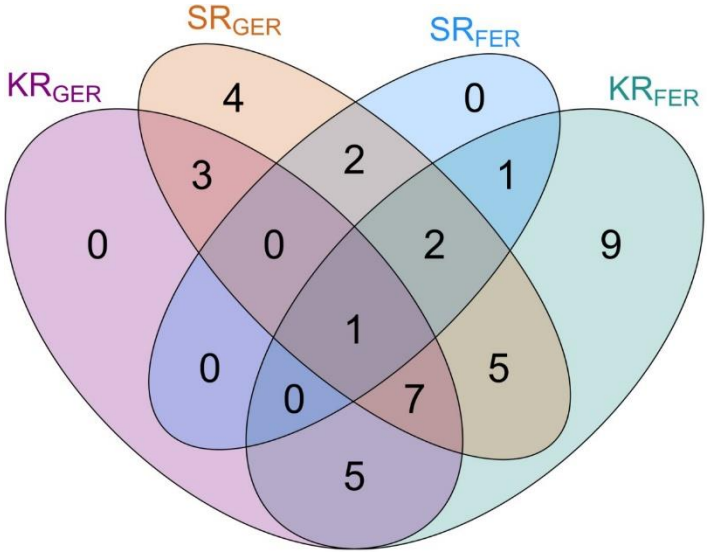

Figure 11: Number of meta-quantitative trait loci shared by silk (channel) resistance (SR) and kernel resistance (KR) of Gibberella ear rot (GER) and Fusarium ear rot (FER)

Furthermore, ear rot resistance candidate genes were detected within identified meta-QTL in our study. From these resistance-promoting genes, *GRMZM2G011151* and *GRMZM2G093092* harbored by MQTL *ZmMQTL9.2* (113.95−129.03 Mbp) on chromosome 9 were uniquely

identified in the resistant line (CO441) (Figure 5 in Chapter 3). These genes are mainly involved in defense response to pathogens, cell wall metabolism, secondary metabolites biosynthesis and signal transduction, demonstrating that their introgression into elite materials would help to develop high yielding maize cultivars with improved ear rot resistance. In addition to resistance genes, several ear rot susceptibility-promoting genes were exclusively identified within the susceptible line (B37). The contribution of these susceptibility genes can be biologically validated using the clustered regularly interspaced short palindromic repeats (CRISPR) technology which can also reduce disease severity within susceptible cultivars (Campenhout et al., 2019; Wada et al., 2020). This will have major implications for the validation of the contribution of these genes and molecular breeding for ear rots resistance in maize.

The European flint landraces contributed to different MQTL (i.e. *ZmMQTL2.2*, *ZmMQTL9.3*) harboring promising resistance-promoting genes (Table 6 in Chapter 3). Our results revealed that GER severity of six doubled haploid populations derived from crosses between moderate to highly resistant KE and PE landraces lines and two susceptible elite lines, was 39−61% lower than the elite lines (Figure 3 in Chapter 4). This demonstrates that the European flint landraces can be effectively harnessed in breeding programs to increase resistance to GER within elite materials. The successful introgression of favorable alleles from landraces into elite lines has been demonstrated for drought tolerance within subtropical maize landraces by Barbosa et al. (2021). Moreover, Galiano-Carneiro et al. (2021) have also successfully transferred GER resistance from Brazilian tropical donors into elites materials. KE landrace-derived populations were about 1.4−2-fold more resistant than the PE landrace-derived population which exhibited the highest GER severity (51%). This shows the GER resistance superiority of KE landrace over PE landrace as previously reported by Gaikpa et al. (2021). Moreover, our results revealed that KE landrace lines were on average 2-fold more resistant than PE landrace lines (Table 1 in Chapter 4). In addition, GER resistant PE landrace lines were less stable across environments than resistant KE landrace lines (Figure 5 in Chapter 4). This indicates that to ensure significant breeding progress, breeders can use the best KE landrace lines as donors to improve GER resistance of elite materials.

Furthermore, for the same KE landrace donor, GER severity of derived populations was similar for the two elite lines. This highlights that introgression of GER resistance from KE landrace can be equally effective across different elite materials. Based on the breeder's equation and

5% selection intensity, moderate to very high genetic advance was observed within the six landrace-derived populations evaluated in our study.

Prediction accuracy of Gibberella ear rot resistance of hybrid cultivars based on corresponding parental lines performance

In addition to introgressing resistances into elite materials, KE and PE landraces can also be exploited to develop hybrid maize varieties with higher resistance to GER disease. The existence of low to moderate mid-parent heterosis has been previously demonstrated by Bolduan et al. (2010) for GER resistance. Based on our results, KE and PE landrace lines were on average 8.2-fold and 5.3-fold, respectively, less resistant than their corresponding testcrosses (Table 1 in Chapter 5). This shows an effect of the tester line, but also the high potential for hybrid development with improved GER resistance. Moreover, moderate phenotypic correlations were detected between testcrosses and their parental lines for GER resistance. Similarly, moderate genomic prediction accuracy was observed between testcrosses and parents for GER resistance within both KE and PE landraces. Similar association patterns between line per se and testcrosses have also been reported by Bolduan et al. (2010) for GER resistance and Löffler et al. (2011) for mycotoxin concentrations in European maize. To accelerate hybrid development, breeders can pre-select parental lines at the early stage of the breeding programs; however, the best crosses should be further evaluated at a later stage of the program across different environments.

Strategies for FHB and GER resistances breeding in wheat and maize, respectively

Fusarium diseases such as FHB in wheat and GER in maize can be effectively and accurately tackled through the application of advanced genomics-assisted breeding approaches, like genomic selection and prediction. Both FHB and GER resistances are quantitatively inherited (with similar heritability ranges), and thus controlled by several minor loci. With genomic selection and prediction, breeders can simultaneously and efficiently exploit all loci to aim for higher disease resistance with significant breeding progress. Thus, the use of marker-assisted selection (MAS) to improve these traits will not produce significant breeding progress. In implementing MAS, only a few significant loci are incorporated, thus limiting its potential when applied to quantitative traits (Jeon et al., 2023).

In winter wheat, our work demonstrated that:

- Simultaneous breeding for FHB resistance, plant height and anther retention can be achieved by integrating pleiotropic loci identified among these traits into breeding programs. Selection for high anther extrusion (or low anther retention) could be easily achieved, what will make hybrid wheat cultivars generally more resistant to FHB;
- *Rht24b* can be integrated into breeding programs to reduce plant height without a negative effect on FHB resistance, though it exerts a lower height reduction effect than *Rht-D1*. *Rht24b* is a FHB-neutral semi-dwarfing allele which does not also affect anther retention that is highly correlated with FHB resistance;
- Genomic background resistance can be harnessed using genomic estimated breeding values to improve resistance to FHB within genotypes with *Rht-D1b*. High genomic background resistance can counterbalance the negative effect of *Rht-D1b* on FHB resistance;
- Breeders can combine *Rht24b* and *Rht-D1b* to significantly reduce plant height, thus satisfying the high interest for short-strawed genotypes, and apply genomic background resistance to improve resistance to FHB within the genotypes. This, however, calls for the use of larger populations which is not a challenge since breeding populations are usually of large sizes.

Likewise, in maize, the findings imply that:

- Breeders can effectively improve resistance to GER in elite materials by harnessing KE and PE landraces as sources of resistance. It is worth emphasizing that the use of KE landrace as donor is more effective for reducing GER susceptibility of elite lines than PE landrace;
- GER resistance introgression can be much faster and more accurate using DH lines and exploiting refined genomic loci harboring promising resistance genes identified in our study. Among other advantages, DH technology allows the production of completely homozygous maize lines within a single year in contrary to the conventional breeding method which requires several years of inbreeding to reach homozygosity (still with some residual heterogeneity) within breeding programs (Chaikam et al., 2019). Genomic selection incorporating identified genomic loci can be implemented within DH populations to select GER resistant lines with good adaptation traits;

- Within KE and PE landraces, breeders can select GER resistant parents with the expectation that derived crosses are more resistant. Best crosses should be further tested at an advanced stage of the breeding program to achieve GER resistant hybrid varieties development.

Summary

Fusarium head blight (FHB) in wheat and Fusarium (FER) and Gibberella ear rot (GER) in maize are major cereal diseases which reduce yield and contaminate kernels with several mycotoxins. In Europe, these diseases contribute to significant yield gaps and high mycotoxin risks across countries. However, existing management strategies related to agronomic practices are not fully effective, with some of them being cost-prohibitive. Enhancing host plant resistance is additionally required for managing the diseases more effectively and sustainably. Unfortunately, breeding for FHB resistance is challenged by complex interactions with morphological traits and the quantitative nature of the trait. In maize, available genetic resources have not been fully exploited to improve GER resistance in elite materials.

In this work, we elucidated the complex interactions between FHB resistance and morphological traits, like plant height (PH) and anther retention (AR) in wheat. The effect of reduced height (*Rht*) gene *Rht24* on AR and the contribution of genomic background (GB) to FHB resistance in semi-dwarf genotypes were also assessed. GB refers to all genomic loci, except major *Rht* genes, that affect the traits. To achieve this, 401 winter wheat cultivars were evaluated across five environments (location × year combination). All cultivars were genotyped using Illumina 25 K Infinium single-nucleotide polymorphism array. We performed correlation and path coefficient analysis, and combined single and multi-trait genome-wide association studies (GWAS). Our findings revealed significant genotypic correlations and path effects between FHB severity with PH and AR, which were controlled by several pleiotropic loci. FHB severity and PH shared both negatively and positively acting pleiotropic loci, while only positively acting pleiotropic loci were detected between FHB severity and AR. *Rht-D1* is a major pleiotropic gene which exerted a negative effect on FHB resistance. These pleiotropic loci contribute to our understanding of the complex genetic basis of FHB resistance, and their exploitation can help to simultaneously select for FHB resistance with PH and AR. Contrary to *Rht-D1b*, *Rht24b* had no negative effect on FHB resistance and AR. This exhibits *Rht24* as an important FHB-neutral *Rht* gene which can be integrated into breeding programs. Genomic estimated breeding values (GEBV) were calculated for each cultivar to assess GB. We observed highly negative GEBV for FHB severity within resistant wheat cultivars. Susceptible cultivars exhibited positive GEBV. Genomic prediction has a great potential and can be exploited by selecting for semi-dwarf winter wheat genotypes with higher FHB resistance due to their genomic background resistance.

To tackle maize ear rot diseases, refined and stable quantitative trait loci (QTL) harboring candidate genes conferring resistances to FER and GER were identified. The effectiveness of introgression of two European flint landraces, namely “Kemater Gelb Landmais” (KE) and “Petkuser Ferdinand Rot” (PE) was evaluated. The prediction accuracy of using line performance as a predictor of hybrid performance for GER resistance was also evaluated within the two landraces. We applied a meta-QTL (MQTL) analysis based on 15 diverse SNP-based QTL mapping studies and performed gene expression analysis using published RNA-seq data on GER resistance. In total, 40 MQTL were identified, of which 14 most refined MQTL harbored promising candidate genes for use in breeding programs for improving FER and GER resistances. 28 MQTL were common to both FER and GER, with most of them being shared between silk (channel) and kernel resistances. This highlights the co-inheritance of FER and GER resistances as well as types of active resistance. Resistance genes can be transferred into elite cultivars by integrating refined MQTL into genomics-assisted breeding strategies. Afterwards, four GER resistant doubled haploid (DH) lines from both KE and PE landraces were crossed with two susceptible elite lines to generate six bi-parental populations with a total of 534 DH lines which were evaluated for GER resistance. GER severity within the six landrace-derived populations were reduced by 39−61% compared to the susceptible elite lines. Moderate to high genetic advance was observed within each population, and the use of KE landrace as a donor was generally more effective than PE landrace. This shows promise in enhancing resistance to GER in elite materials using the European flint landraces as donors. Furthermore, per se performance of 76 DH lines from both landraces was used to predict GER resistance of their corresponding testcrosses (TC). Moderate phenotypic and genomic prediction accuracy between TC and line per se performance was found for GER resistance. This implies that pre-selecting lines for GER resistance is feasible; however, TC should be additionally tested on a later selection stage to aim for GER-resistant hybrid cultivars.

Zusammenfassung

Ährenfusariosen (FHB) bei Weizen und Fusarium- (FER) und Gibberella-Kolbenfäule (GER) bei Mais sind wichtige Getreidekrankheiten. In Europa tragen diese Krankheiten zu erheblichen Ertragseinbußen und hohen Mykotoxinrisiken in den einzelnen Ländern bei. Die bestehenden Kontrollstrategien im Zusammenhang mit pflanzenbaulichen Praktiken sind jedoch nicht voll wirksam, und einige von ihnen sind zu kostspielig. Um die Krankheiten wirksamer und nachhaltiger zu bekämpfen, muss deshalb die Resistenz der Wirtspflanzen gestärkt werden. Leider wird die Züchtung auf FHB-Resistenz durch komplexe Wechselwirkungen mit morphologischen Merkmalen und der quantitativen Natur des Merkmals erschwert. Bei Mais wurden die verfügbaren genetischen Ressourcen bisher nicht vollständig genutzt, um die GER-Resistenz von Elitematerial zu verbessern.

In dieser Arbeit haben wir die komplexen Wechselwirkungen zwischen FHB-Resistenz und morphologischen Merkmalen wie Wuchshöhe (PH) und Antherenretention (AR) bei Weizen aufgeklärt. Außerdem wurden die Auswirkungen des Gens *Rht24* für reduzierte Wuchshöhe (*reduced height*, *Rht*) auf AR und der Beitrag des genomischen Hintergrunds (GB) zur FHB-Resistenz bei kurzstrohigen Genotypen untersucht. GB bezieht sich auf alle Genloci, mit Ausnahme der bekannten *Rht*-Gene, die die jeweiligen Merkmale beeinflussen. Zu diesem Zweck wurden 401 Winterweizensorten in fünf Umwelten (Ort × Jahr-Kombinationen) bewertet. Alle Sorten wurden mit dem Illumina 25k Infinium Single-Nukleotid-Polymorphismus-Array genotypisiert. Wir führten Korrelations- und Pfadkoeffizientenanalysen durch und kombinierten genomweite Assoziationsstudien (GWAS) mit einzelnen bzw. mehreren Merkmalen. Unsere Ergebnisse zeigten signifikante genotypische Korrelationen und Pfadeffekte zwischen FHB-Befallsstärke und PH und AR, die von mehreren pleiotropen Loci kontrolliert wurden. FHB-Befallsstärke und PH hatten sowohl negativ als auch positiv wirkende pleiotrope Loci gemeinsam, während zwischen FHB-Befallsstärke und AR nur positiv wirkende pleiotrope Loci gefunden wurden. *Rht-D1* ist ein wichtiges pleiotropes Gen, dessen kurzstrohiges Allel einen negativen Einfluss auf die FHB-Resistenz ausübt. Diese pleiotropen Loci tragen zu unserem Verständnis der komplexen genetischen Grundlage der FHB-Resistenz bei, und ihre Nutzung kann dazu beitragen, gleichzeitig mit verringerter PH und AR auf FHB-Resistenz zu selektieren. Im Gegensatz zu *Rht-D1b* hatte *Rht24b* keine Auswirkungen auf FHB-Resistenz und AR. Dies zeigt, dass *Rht24* ein wichtiges FHB-neutrales *Rht*-Gen ist, das in Zuchtprogramme integriert werden kann. Zur Bewertung des GB wurden für jede Sorte genomisch geschätzte Zuchtwerte (GEBV) berechnet. Bei

resistenten Weizensorten beobachteten wir einen stark negativen GEBV für FHB-Befallsstärke. Anfällige Sorten wiesen einen positiven GEBV auf. Die genomische Vorhersage hat ein großes Potenzial und kann durch die Selektion von kurzstrohigen Winterweizengenotypen mit höherer FHB-Resistenz aufgrund ihrer genomischen Hintergrundresistenz genutzt werden.

Zur Bekämpfung von Mais-Kolbenfäule wurden stabile quantitative Merkmalsloci (QTL) identifiziert, die Kandidatengene für Resistenzen gegen FER und GER beherbergen. Die Wirksamkeit der Introgression von Resistenzen aus zwei europäischen Flint-Landrassen, nämlich "Kemater Gelber Landmais" (KE) und "Petkuser Ferdinand Rot" (PE), wurde bewertet. Die Vorhersagegenauigkeit der Verwendung der Linienleistung als Vorhersage für die Hybridleistung bei der GER-Resistenz wurde ebenfalls innerhalb der beiden Landrassen bewertet. Wir haben eine Meta-QTL-Analyse (MQTL) auf der Grundlage von 15 SNP-basierten QTL-Kartierungsstudien durchgeführt und eine Genexpressionsanalyse anhand veröffentlichter RNAseq-Daten zur GER-Resistenz vorgenommen. Insgesamt wurden 40 MQTL identifiziert, von denen die 14 stabilsten MQTL vielversprechende Kandidatengene für den Einsatz in Zuchtprogrammen zur Verbesserung von FER- und GER-Resistenzen enthielten. 28 MQTL waren sowohl für FER- als auch GER-Resistenz verantwortlich, wobei die meisten sowohl für Narbenfaden- als auch Körnerresistenz verantwortlich waren. Die Resistenz kann in Elitesorten übertragen werden, indem präzisierte MQTL in genomgestützte Züchtungsstrategien integriert werden. Anschließend wurden vier GER-resistente doppelhaploide (DH) Linien aus KE- und PE-Landrassen mit zwei anfälligen Elitelinien gekreuzt, um sechs bi-parentale Populationen mit insgesamt 534 DH-Linien zu erzeugen, die mehrortig auf GER-Resistenz untersucht wurden. Der GER-Befallsstärke war bei den sechs von Landrassen abgeleiteten Populationen im Vergleich zu den anfälligen Elitelinien im Mittel um 39-61% reduziert. Durch Einkreuzung der jeweiligen Population kann ein mäßiger bis hoher genetischer Fortschritt erzielt werden, die Verwendung der KE-Landrasse als Spender war effektiver als die der PE-Landrasse. Dies ist ein vielversprechender Ansatz, um die Resistenz von Elitematerialien gegen GER zu verbessern. Darüber hinaus wurde die Leistung von 76 DH-Linien aus beiden Landrassen zur Vorhersage der GER-Resistenz der entsprechenden Testkreuzungen (TC) verwendet. Für die GER-Resistenz wurde eine mäßige phänotypische und genomische Vorhersagegenauigkeit zwischen TC und der Leistung der Linie festgestellt. Eine Vorselektion von Linien auf GER-Resistenz ist deshalb möglich; die

Leistung der TC sollte jedoch in einer späteren Selektionsphase zusätzlich getestet werden, um GER-resistente Hybridsorten zu erhalten.

General references

Ali, M.L., Taylor, J.H., Jie, L., Sun, G., William, M., Kasha, K.J., et al. (2005). Molecular mapping of QTLs for resistance to Gibberella ear rot, in corn, caused by *Fusarium graminearum*. *Genome* 48(3)**,** 521-533. doi: 10.1139/G05-014.

Anderson, J.A., Chao, S., and Liu, S. (2007). Molecular breeding using a major QTL for Fusarium head blight resistance in wheat. *Crop Sci* 47(S3)**,** S-112-S-119. doi: https://doi.org/10.2135/cropsci2007.04.0006IPBS.

Anderson, J.A., Stack, R.W., Liu, S., Waldron, B.L., Fjeld, A.D., Coyne, C., et al. (2001). DNA markers for Fusarium head blight resistance QTLs in two wheat populations. *Theor Appl Genet* 102(8)**,** 1164-1168. doi: 10.1007/s001220000509.

Arie, T. (2019). Fusarium diseases of cultivated plants, control, diagnosis, and molecular and genetic studies. *J Pestic Sci* 44(4)**,** 275-281. doi: 10.1584/jpestics.J19-03.

Bai, G., and Shaner, G. (2004). Management and resistance in wheat and barley to Fusarium head blight. *Annu Rev Phytopathol* 42(1)**,** 135-161. doi: 10.1146/annurev.phyto.42.040803.140340.

Barbosa, P.A.M., Fritsche-Neto, R., Andrade, M.C., Petroli, C.D., Burgueño, J., Galli, G., et al. (2021). Introgression of maize diversity for drought tolerance: Subtropical maize landraces as source of new positive variants. *Front Plant Sci* 12(2023). doi: 10.3389/fpls.2021.691211.

Beukes, I., Rose, L.J., van Coller, G.J., and Viljoen, A. (2018). Disease development and mycotoxin production by the *Fusarium graminearum* species complex associated with South African maize and wheat. *Eur J Plant Pathol* 150(4)**,** 893-910. doi: 10.1007/s10658-017-1331-5.

Boeven, P.H.G., Longin, C.F.H., Leiser, W.L., Kollers, S., Ebmeyer, E., and Würschum, T. (2016). Genetic architecture of male floral traits required for hybrid wheat breeding. *Theor Appl Genet* 129(12)**,** 2343-2357. doi: 10.1007/s00122-016-2771-6.

Bolduan, C., Miedaner, T., Utz, H.F., Dhillon, B.S., and Melchinger, A.E. (2010). Genetic variation in testcrosses and relationship between line per se and testcross performance

for resistance to Gibberella ear rot in maize. *Crop Sci* 50(5)**,** 1691-1696. doi: 10.2135/cropsci2009.10.0623.

Brar, G.S., Brûlé-Babel, A.L., Ruan, Y., Henriquez, M.A., Pozniak, C.J., Kutcher, H.R., et al. (2019). Genetic factors affecting Fusarium head blight resistance improvement from introgression of exotic Sumai 3 alleles (including *Fhb1*, *Fhb2*, and *Fhb5*) in hard red spring wheat. *BMC Plant Biol* 19(1)**,** 179. doi: 10.1186/s12870-019-1782-2.

Buerstmayr, M., and Buerstmayr, H. (2015). Comparative mapping of quantitative trait loci for Fusarium head blight resistance and anther retention in the winter wheat population Capo × Arina. *Theor Appl Genet* 128(8)**,** 1519-1530. doi: 10.1007/s00122-015-2527-8.

Buerstmayr, M., and Buerstmayr, H. (2016). The semidwarfing alleles *Rht-D1b* and *Rht-B1b* show marked differences in their associations with anther-retention in wheat heads and with Fusarium Head Blight susceptibility. *Phytopathology* 106(12)**,** 1544-1552. doi: 10.1094/PHYTO-05-16-0200-R.

Buerstmayr, M., and Buerstmayr, H. (2022). The effect of the *Rht1* haplotype on Fusarium head blight resistance in relation to type and level of background resistance and in combination with *Fhb1* and *Qfhs.ifa-5A*. *Theor Appl Genet*. doi: 10.1007/s00122-022-04088-x.

Buerstmayr, M., Steiner, B., and Buerstmayr, H. (2020). Breeding for Fusarium head blight resistance in wheat-Progress and challenges. *Plant Breed* 139(3)**,** 429-454. doi: 10.1111/pbr.12797.

Butrón, A., Reid, L.M., Santiago, R., Cao, A., and Malvar, R.A. (2015). Inheritance of maize resistance to Gibberella and Fusarium ear rots and kernel contamination with deoxynivalenol and fumonisins. *Plant Pathol* 64(5)**,** 1053-1060. doi: 10.1111/ppa.12351.

Campenhout, C.V., Cabochette, P., Veillard, A.-C., Laczik, M., Zelisko-Schmidt, A., Sabatel, C., et al. (2019). Guidelines for optimized gene knockout using CRISPR/Cas9. *BioTechniques* 66(6)**,** 295-302. doi: 10.2144/btn-2018-0187.

Castañares, E., Martínez, M., Cristos, D., Rojas, D., Lara, B., Stenglein, S., et al. (2019). Fusarium species and mycotoxin contamination in maize in Buenos Aires province, Argentina. *Eur J Plant Pathol* 155(4)**,** 1265-1275. doi: 10.1007/s10658-019-01853-5.

Chaikam, V., Molenaar, W., Melchinger, A.E., and Boddupalli, P.M. (2019). Doubled haploid technology for line development in maize: technical advances and prospects. *Theor Appl Genet* 132(12)**,** 3227-3243. doi: 10.1007/s00122-019-03433-x.

Chungu, C., Mather, D.E., Reid, L.M., and Hamilton, R.I. (1996). Comparison of techniques for inoculating maize silk, kernel, and cob tissues with *Fusarium graminearum*. *Plant Dis* 80(1)**,** 81-84. doi: 10.1094/PD-80-0081.

Dalla Lana, F., Madden, L.V., Carvalho, C.P., and Paul, P.A. (2022). Impact of Gibberella ear rot on grain quality and yield components in maize as influenced by hybrid reaction. *Plant Dis* 106(12)**,** 3061-3075. doi: 10.1094/PDIS-01-22-0148-RE.

Dalla Lana, F., Madden, L.V., and Paul, P.A. (2021). Natural occurrence of maize Gibberella ear rot and contamination of grain with mycotoxins in association with weather variables. *Plant Dis* 105(1)**,** 114-126. doi: 10.1094/PDIS-05-20-0952-RE.

Del Ponte, E.M., Moreira, G.M., Ward, T.J., O'Donnell, K., Nicolli, C.P., Machado, F.J., et al. (2021). *Fusarium graminearum* Species Complex: A bibliographic analysis and web-accessible database for global mapping of species and trichothecene toxin chemotypes. *Phytopathology* 112(4)**,** 741-751. doi: 10.1094/PHYTO-06-21-0277-RVW.

Dill-Macky, R., and Jones, R.K. (2000). The effect of previous crop residues and tillage on Fusarium head blight of wheat. *Plant Dis* 84(1)**,** 71-76. doi: 10.1094/PDIS.2000.84.1.71.

European Commission, E.C. (2017). Commission Regulation (EU) No 165/2010 of 26 February 2010 amending Regulation (EC) No 1881/2006 setting maximum levels for certain contaminants in foodstuffs as regards aflatoxins. *Off J Eur Union* 50**,** 8-12.

Gaikpa, D.S., Kessel, B., Presterl, T., Ouzunova, M., Galiano-Carneiro, A.L., Mayer, M., et al. (2021). Exploiting genetic diversity in two European maize landraces for improving Gibberella ear rot resistance using genomic tools. *Theor Appl Genet* 134(3)**,** 793-805. doi: 10.1007/s00122-020-03731-9.

Gaikpa, D.S., and Miedaner, T. (2019). Genomics-assisted breeding for ear rot resistances and reduced mycotoxin contamination in maize: methods, advances and prospects. *Theor Appl Genet* 132(10)**,** 2721-2739. doi: 10.1007/s00122-019-03412-2.

Galiano-Carneiro, A.L., Kessel, B., Presterl, T., Gaikpa, D.S., Kistner, M.B., and Miedaner, T. (2021). Multi-parent QTL mapping reveals stable QTL conferring resistance to Gibberella ear rot in maize. *Euphytica* 217(1). doi: 10.1007/s10681-020-02748-x.

Gilsinger, J., Kong, L., Shen, X., and Ohm, H. (2005). DNA markers associated with low Fusarium head blight incidence and narrow flower opening in wheat. *Theor Appl Genet* 110(7)**,** 1218-1225. doi: 10.1007/s00122-005-1953-4.

Giomi, G.M., Kreff, E.D., Iglesias, J., Fauguel, C.M., Fernandez, M., Oviedo, M.S., et al. (2016). Quantitative trait loci for Fusarium and Gibberella ear rot resistance in Argentinian maize germplasm. *Euphytica* 211(3)**,** 287-294. doi: 10.1007/s10681-016-1725-z.

Grote, U., Fasse, A., Nguyen, T.T., and Erenstein, O. (2021). Food security and the dynamics of wheat and maize value chains in Africa and Asia. *Front Sustain Food Syst* 4**,** 617009. doi: 10.3389/fsufs.2020.617009.

Han, S., Miedaner, T., Utz, H.F., Schipprack, W., Schrag, T.A., and Melchinger, A.E. (2018). Genomic prediction and GWAS of Gibberella ear rot resistance traits in dent and flint lines of a public maize breeding program. *Euphytica* 214(1). doi: 10.1007/s10681-017-2090-2.

Han, S., Utz, H.F., Liu, W., Schrag, T.A., Stange, M., Würschum, T., et al. (2016). Choice of models for QTL mapping with multiple families and design of the training set for prediction of Fusarium resistance traits in maize. *Theor Appl Genet* 129(2)**,** 431-444. doi: 10.1007/s00122-015-2637-3.

Hao, Y., Rasheed, A., Zhu, Z., Wulff, B.B.H., and He, Z. (2020). Harnessing wheat *Fhb1* for Fusarium resistance. *Trends Plant Sci* 25(1)**,** 1-3. doi: https://doi.org/10.1016/j.tplants.2019.10.006.

Hedden, P. (2003). The genes of the green revolution. *Trends Genet* 19(1)**,** 5-9. doi: https://doi.org/10.1016/S0168-9525(02)00009-4.

Herter, C.P., Ebmeyer, E., Kollers, S., Korzun, V., Leiser, W.L., Würschum, T., et al. (2018). *Rht24* reduces height in the winter wheat population 'Solitär × Bussard' without adverse effects on Fusarium head blight infection. *Theor Appl Genet* 131(6)**,** 1263-1272. doi: 10.1007/s00122-018-3076-8.

Jeon, D., Kang, Y., Lee, S., Choi, S., Sung, Y., Lee, T.-H., et al. (2023). Digitalizing breeding in plants: A new trend of next-generation breeding based on genomic prediction. *Front Plant Sci* 14:1092584. doi: https://doi.org/10.3389/fpls.2023.1092584.

Jochum, C.C., Osborne, L.E., and Yuen, G.Y. (2006). Fusarium head blight biological control with *Lysobacter enzymogenes* strain C3. *Biol Control* 39(3)**,** 336-344. doi: https://doi.org/10.1016/j.biocontrol.2006.05.004.

Johns, L.E., Bebber, D.P., Gurr, S.J., and Brown, N.A. (2022). Emerging health threat and cost of Fusarium mycotoxins in European wheat. *Nat Food* 3(12)**,** 1014-1019. doi: 10.1038/s43016-022-00655-z.

Kebebe, A.Z., Reid, L.M., Zhu, X., Wu, J., Woldemariam, T., Voloaca, C., et al. (2015). Relationship between kernel drydown rate and resistance to Gibberella ear rot in maize. *Euphytica* 201(1)**,** 79-88. doi: 10.1007/s10681-014-1185-2.

Kebede, A.Z., Woldemariam, T., Reid, L.M., and Harris, L.J. (2016). Quantitative trait loci mapping for Gibberella ear rot resistance and associated agronomic traits using genotyping-by-sequencing in maize. *Theor Appl Genet* 129(1)**,** 17-29. doi: 10.1007/s00122-015-2600-3.

Khan, M.K., Pandey, A., Athar, T., Choudhary, S., Deval, R., Gezgin, S., et al. (2020). Fusarium head blight in wheat: contemporary status and molecular approaches. *3 Biotech* 10(4)**,** 172. doi: 10.1007/s13205-020-2158-x.

Korte, A., and Farlow, A. (2013). The advantages and limitations of trait analysis with GWAS: a review. *Plant Methods* 9(1)**,** 29. doi: 10.1186/1746-4811-9-29.

Kubo, K., Fujita, M., Kawada, N., Nakajima, T., Nakamura, K., Maejima, H., et al. (2013). Minor differences in anther extrusion affect resistance to Fusarium head blight in wheat. *J Phytopathol* 161(5)**,** 308-314. doi: https://doi.org/10.1111/jph.12060.

Kubo, K., Kawada, N., Fujita, M., Hatta, K., Oda, S., and Nakajima, T. (2010). Effect of cleistogamy on Fusarium head blight resistance in wheat. *Breed Sci* 60(4)**,** 405-411. doi: 10.1270/jsbbs.60.405.

Leslie, J.F., and Summerell, B.A. (2008). *The Fusarium laboratory manual*. John Wiley & Sons.

Li, T., Zhang, D., Zhou, X., Bai, G., Li, L., and Gu, S. (2016). Fusarium head blight resistance loci in a stratified population of wheat landraces and varieties. *Euphytica* 207(3)**,** 551-561. doi: 10.1007/s10681-015-1539-4.

Li, Y., Shi, F., Lin, Z., Robinson, H., Moody, D., Rattey, A., et al. (2022). Benefit of introgression depends on level of genetic trait variation in cereal breeding programmes. *Front Plant Sci* 13**,** 786452. doi: 10.3389/fpls.2022.786452.

Liu, S., Griffey, C.A., Hall, M.D., McKendry, A.L., Chen, J., Brooks, W.S., et al. (2013). Molecular characterization of field resistance to Fusarium head blight in two US soft red winter wheat cultivars. *Theor Appl Genet* 126(10)**,** 2485-2498. doi: 10.1007/s00122-013-2149-y.

Loddo, S., and Gooding, M.J. (2012). Semi-dwarfing (*Rht-B1b*) improves nitrogen-use efficiency in wheat, but not at economically optimal levels of nitrogen availability. *Cereal Res Commun* 40(1)**,** 116-121. doi: 10.1556/CRC.40.2012.1.13.

Löffler, M., Kessel, B., Ouzunova, M., and Miedaner, T. (2010a). Population parameters for resistance to *Fusarium graminearum* and *Fusarium verticillioides* ear rot among large sets of early, mid-late and late maturing European maize (*Zea mays* L.) inbred lines. *Theor Appl Genet* 120(5)**,** 1053-1062. doi: 10.1007/s00122-009-1233-9.

Löffler, M., Kessel, B., Ouzunova, M., and Miedaner, T. (2011). Covariation between line and testcross performance for reduced mycotoxin concentrations in European maize after silk channel inoculation of two Fusarium species. *Theor Appl Genet* 122(5)**,** 925-934. doi: 10.1007/s00122-010-1499-y.

Löffler, M., Miedaner, T., Kessel, B., and Ouzunova, M. (2010b). Mycotoxin accumulation and corresponding ear rot rating in three maturity groups of European maize inoculated

by two Fusarium species. *Euphytica* 174(2)**,** 153-164. doi: 10.1007/s10681-009-0080-8.

Logrieco, A., Battilani, P., Leggieri, M.C., Jiang, Y., Haesaert, G., Lanubile, A., et al. (2021). Perspectives on global mycotoxin issues and management from the Mycokey maize working group. *Plant Dis* 105(3)**,** 525-537. doi: 10.1094/PDIS-06-20-1322-FE.

Logrieco, A., Mulè, G., Moretti, A., and Bottalico, A. (2002). Toxigenic Fusarium species and mycotoxins associated with maize ear rot in Europe. *Eur J Plant Pathol* 108(7)**,** 597-609. doi: 10.1023/A:1020679029993.

Lu, Q., Lillemo, M., Skinnes, H., He, X., Shi, J., Ji, F., et al. (2013). Anther extrusion and plant height are associated with type I resistance to Fusarium head blight in bread wheat line 'Shanghai-3/Catbird'. *Theor Appl Genet* 126(2)**,** 317-334. doi: 10.1007/s00122-012-1981-9.

Machado, F.J., de Barros, A.V., McMaster, N., Schmale, D.G., III, Vaillancourt, L.J., and Del Ponte, E.M. (2022). Aggressiveness and mycotoxin production by *Fusarium meridionale* compared with *F. graminearum* on maize ears and stalks in the field. *Phytopathology* 112(2)**,** 271-277. doi: 10.1094/PHYTO-04-21-0149-R.

Martin, M., Miedaner, T., Dhillon, B.S., Ufermann, U., Kessel, B., Ouzunova, M., et al. (2011). Colocalization of QTL for gibberella ear rot resistance and low mycotoxin contamination in early European maize. *Crop Sci* 51(5)**,** 1935-1945. doi: 10.2135/cropsci2010.11.0664.

Martin, M., Miedaner, T., Schwegler, D.D., Kessel, B., Ouzunova, M., Dhillon, B.S., et al. (2012). Comparative quantitative trait loci mapping for Gibberella ear rot resistance and reduced deoxynivalenol contamination across connected maize populations. *Crop Sci* 52(1)**,** 32-43. doi: 10.2135/cropsci2011.04.0214.

Matarese, F., Sarrocco, S., Gruber, S., Seidl-Seiboth, V., and Vannacci, G. (2012). Biocontrol of Fusarium head blight: interactions between Trichoderma and mycotoxigenic Fusarium. *Microbiology* 158(1)**,** 98-106. doi: https://doi.org/10.1099/mic.0.052639-0.

Mesterházy, Á., Bartók, T., Mirocha, C.G., and Komoróczy, R. (1999). Nature of wheat resistance to Fusarium head blight and the role of deoxynivalenol for breeding. *Plant Breed* 118(2)**,** 97-110. doi: https://doi.org/10.1046/j.1439-0523.1999.118002097.x.

Mesterházy, A., Lemmens, M., and Reid, L.M. (2012). Breeding for resistance to ear rots caused by *Fusarium* spp. in maize - A review. *Plant Breed* 131(1)**,** 1-19. doi: 10.1111/j.1439-0523.2011.01936.x.

Miedaner, T., Boeven, A.L.G.C., Gaikpa, D.S., Kistner, M.B., and Grote, C.P. (2020). Genomics-assisted breeding for quantitative disease resistances in small-grain cereals and maize. *Int J Mol Sci* 21(24)**,** 1-22. doi: 10.3390/ijms21249717.

Miedaner, T., Flamm, C., and Oberforster, M. (2023). The importance of Fusarium head blight resistance in the cereal breeding industry: Case studies from Germany and Austria. *Plant Breed* n/a(n/a). doi: https://doi.org/10.1111/pbr.13098.

Miedaner, T., Herter, C.P., Ebmeyer, E., Kollers, S., and Korzun, V. (2019). Use of non-adapted quantitative trait loci for increasing Fusarium head blight resistance for breeding semi-dwarf wheat. *Plant Breed* 138(2)**,** 140-147. doi: https://doi.org/10.1111/pbr.12683.

Miedaner, T., and Juroszek, P. (2021a). Climate change will influence disease resistance breeding in wheat in Northwestern Europe. *Theor Appl Genet* 134(6)**,** 1771-1785. doi: 10.1007/s00122-021-03807-0.

Miedaner, T., and Juroszek, P. (2021b). Global warming and increasing maize cultivation demand comprehensive efforts in disease and insect resistance breeding in north-western Europe. *Plant Pathol* 70(5)**,** 1032-1046. doi: 10.1111/ppa.13365.

Miedaner, T., Lenhardt, M., Grehl, J., Gruner, P., and Koch, S. (2022). Dwarfing gene *Rht24* does not affect Fusarium head blight resistance in a large European winter wheat diversity panel. *Euphytica* 218(6)**,** 73. doi: 10.1007/s10681-022-03028-6.

Munkvold, G.P. (2003). Epidemiology of Fusarium diseases and their mycotoxins in maize ears. *Eur J Plant Pathol* 109(7)**,** 705-713. doi: 10.1023/A:1026078324268.

Nannuru, V.K.R., Windju, S.S., Belova, T., Dieseth, J.A., Alsheikh, M., Dong, Y., et al. (2022). Genetic architecture of Fusarium head blight disease resistance and associated traits in Nordic spring wheat. *Theor Appl Genet*. doi: 10.1007/s00122-022-04109-9.

Palazzini, J.M., Ramirez, M.L., Torres, A.M., and Chulze, S.N. (2007). Potential biocontrol agents for Fusarium head blight and deoxynivalenol production in wheat. *Crop Prot* 26(11)**,** 1702-1710. doi: https://doi.org/10.1016/j.cropro.2007.03.004.

Pfordt, A., Schiwek, S., Rathgeb, A., Rodemann, C., Bollmann, N., Buchholz, M., et al. (2020). Occurrence, pathogenicity, and mycotoxin production of *Fusarium temperatum* in relation to other Fusarium species on maize in Germany. *Pathogens* 9(11)**,** 1-21. doi: 10.3390/pathogens9110864.

Piepho, H.-P., and Möhring, J. (2007). Computing heritability and selection response from unbalanced plant breeding trials. *Genetics* 177(3)**,** 1881-1888. doi: 10.1534/genetics.107.074229.

Ray, S., Wenner, N.G., Ankoma-Darko, O., Kaye, J.P., Kuldau, G.A., and Ali, J.G. (2022). Cover crop selection affects maize susceptibility to the fungal pathogen *Fusarium verticillioides*. *Pedobiologia* 91-92. doi: 10.1016/j.pedobi.2022.150806.

Raza, M.M., and Bebber, D.P. (2022). Climate change and plant pathogens. *Curr Opin Microbiol* 70**,** 102233. doi: https://doi.org/10.1016/j.mib.2022.102233.

Righetti, L., Bhandari, D.R., Rolli, E., Tortorella, S., Bruni, R., Dall'Asta, C., et al. (2021). Mycotoxin uptake in wheat-Eavesdropping Fusarium presence for priming plant defenses or a trojan horse to weaken them? *Front Plant Sci* 12. doi: https://doi.org/10.3389/fpls.2021.711389.

Ruan, Y., Zhang, W., Knox, R.E., Berraies, S., Campbell, H.L., Ragupathy, R., et al. (2020). Characterization of the genetic architecture for Fusarium head blight resistance in durum wheat: The complex association of resistance, flowering time, and height genes. *Front Plant Sci* 11. doi: 10.3389/fpls.2020.592064.

Schaafsma, A.W., Limay-Rios, V., and Tamburic-Illincic, L. (2008). Mycotoxins and Fusarium species associated with maize ear rot in Ontario, Canada. *Cereal Res Commun* 36**,** 525-527.

Schaafsma, A.W., Tamburic-Ilincic, L., and Reid, L.M. (2006). Fumonisin B1 accumulation and severity of Fusarium ear rot and Gibberella ear rot in food-grade corn hybrids in Ontario after inoculation according to two methods. *Can J Plant Pathol* 28(4)**,** 548-557. doi: 10.1080/07060660609507333.

Schils, R., Olesen, J.E., Kersebaum, K.-C., Rijk, B., Oberforster, M., Kalyada, V., et al. (2018). Cereal yield gaps across Europe. *Eur J Agron* 101**,** 109-120. doi: https://doi.org/10.1016/j.eja.2018.09.003.

Schisler, D.A., Khan, N.I., Boehm, M.J., Lipps, P.E., Slininger, P.J., and Zhang, S. (2006). Selection and evaluation of the potential of choline-metabolizing microbial strains to reduce Fusarium head blight. *Biol Control* 39(3)**,** 497-506. doi: https://doi.org/10.1016/j.biocontrol.2006.08.007.

Schroeder, H.W., and Christensen, J.J. (1963). Factors affecting resistance of wheat to scab caused by Gibberella zeae. *Phytopathology* 53(7, 1)**,** 831-838.

Steiner, B., Buerstmayr, M., Wagner, C., Danler, A., Eshonkulov, B., Ehn, M., et al. (2019). Fine-mapping of the Fusarium head blight resistance QTL *Qfhs.ifa-5A* identifies two resistance QTL associated with anther extrusion. *Theor Appl Genet* 132(7)**,** 2039-2053. doi: 10.1007/s00122-019-03336-x.

Tessmann, E.W., and van Sanford, D.A. (2019). Associations between morphological and FHB traits in a soft red winter wheat population. *Euphytica* 215(11)**,** 189. doi: 10.1007/s10681-019-2509-z.

Tian, X., Wen, W., Xie, L., Fu, L., Xu, D., Fu, C., et al. (2017). Molecular mapping of reduced plant height gene *Rht24* in bread wheat. *Front Plant Sci* 8. doi: https://doi.org/10.3389/fpls.2017.01379.

Tibbs-Cortes, L., Zhang, Z., and Yu, J. (2021). Status and prospects of genome-wide association studies in plants. *Plant Genome* 14(1)**,** e20077. doi: https://doi.org/10.1002/tpg2.20077.

Venske, E., dos Santos, R.S., Farias, D.d.R., Rother, V., da Maia, L.C., Pegoraro, C., et al. (2019). Meta-analysis of the QTLome of Fusarium head blight resistance in bread wheat: Refining the rurrent puzzle. *Front Plant Sci* 10. doi: 10.3389/fpls.2019.00727.

Wachowska, U., and Głowacka, K. (2014). Antagonistic interactions between *Aureobasidium pullulans* and *Fusarium culmorum*, a fungal pathogen of winter wheat. *BioControl* 59(5)**,** 635-645. doi: 10.1007/s10526-014-9596-5.

Wada, N., Ueta, R., Osakabe, Y., and Osakabe, K. (2020). Precision genome editing in plants: state-of-the-art in CRISPR/Cas9-based genome engineering. *BMC Plant Biol* 20(1)**,** 234. doi: 10.1186/s12870-020-02385-5.

Wang, F., Yoshida, H., and Matsuoka, M. (2021). Making the 'Green Revolution' truly green: Improving crop nitrogen use efficiency. *Plant Cell Physiol* 62(6)**,** 942-947. doi: 10.1093/pcp/pcab051.

Wegulo, S.N., Baenziger, P.S., Hernandez Nopsa, J., Bockus, W.W., and Hallen-Adams, H. (2015). Management of Fusarium head blight of wheat and barley. *Crop Prot* 73**,** 100-107. doi: https://doi.org/10.1016/j.cropro.2015.02.025.

Wen, J., Shen, Y., Xing, Y., Wang, Z., Han, S., Li, S., et al. (2020). QTL mapping of resistance to Gibberella ear rot in maize. *Mol Breed* 40(10). doi: 10.1007/s11032-020-01173-1.

Xu, K., He, X., Dreisigacker, S., He, Z., and Singh, P.K. (2020). Anther extrusion and its association with Fusarium head blight in CIMMYT wheat germplasm. *Agronomy* 10(1). doi: 10.3390/agronomy10010047.

Xu, Y., Li, P., Zou, C., Lu, Y., Xie, C., Zhang, X., et al. (2017). Enhancing genetic gain in the era of molecular breeding. *J Exp Bot* 68(11)**,** 2641-2666. doi: 10.1093/jxb/erx135.

Xue, A.G., Chen, Y., Voldeng, H.D., Fedak, G., Savard, M.E., Längle, T., et al. (2014). Concentration and cultivar effects on efficacy of CLO-1 biofungicide in controlling Fusarium head blight of wheat. *Biol Control* 73**,** 2-7. doi: https://doi.org/10.1016/j.biocontrol.2014.02.010.

Yuan, G., Chen, B., Peng, H., Zheng, Q., Li, Y., Xiang, K., et al. (2020). QTL mapping for resistance to ear rot caused by *Fusarium graminearum* using an IBM Syn10 DH population in maize. *Mol Breed* 40(9). doi: 10.1007/s11032-020-01158-0.

Zhang, A., Wang, H., Beyene, Y., Semagn, K., Liu, Y., Cao, S., et al. (2017). Effect of trait heritability, training population size and marker density on genomic prediction accuracy estimation in 22 bi-parental tropical maize populations. *Front Plant Sci* 8.

Zhao, Y., Selvaraj, J.N., Xing, F., Zhou, L., Wang, Y., Song, H., et al. (2014). Antagonistic action of *Bacillus subtilis* strain sg6 on *Fusarium graminearum*. *PLoS One* 9(3)**,** e92486. doi: 10.1371/journal.pone.0092486.

Zhao, Z., Wang, E., Kirkegaard, J.A., and Rebetzke, G.J. (2022). Novel wheat varieties facilitate deep sowing to beat the heat of changing climates. *Nat Clim Chang* 12(3)**,** 291-296. doi: 10.1038/s41558-022-01305-9.

Zhou, G., Li, S., Ma, L., Wang, F., Jiang, F., Sun, Y., et al. (2021). Mapping and validation of a stable quantitative trait locus conferring maize resistance to Gibberella ear rot. *Plant Dis* 105(7). doi: 10.1094/PDIS-11-20-2487-RE.

Zhu, Z., Hao, Y., Mergoum, M., Bai, G., Humphreys, G., Cloutier, S., et al. (2019). Breeding wheat for resistance to Fusarium head blight in the Global North: China, USA, and Canada. *Crop J* 7(6)**,** 730-738. doi: https://doi.org/10.1016/j.cj.2019.06.003.

Please note that the following material is only available in digital form, retrievable via indicated journal links and additionally stored on the CD enclosed with this dissertation:

Chapter 2: Separation of the effects of two reduced height (*Rht*) genes and genomic background to select for less Fusarium head blight of short-strawed winter wheat (*Triticum aestivum* L.) varieties

Table S1: Best linear unbiased estimations (BLUEs) of the eight traits across five environments. Available online at: https://static-content.springer.com/esm/art%3A10.1007%2Fs00122-022-04219-4/MediaObjects/122_2022_4219_MOESM1_ESM.xlsx

Table S6: Significant markers sequences and physical positions of candidate genes. Available online at: https://static-content.springer.com/esm/art%3A10.1007%2Fs00122-022-04219-4/MediaObjects/122_2022_4219_MOESM1_ESM.xlsx

Chapter 3: Meta-analysis and co-expression analysis revealed stable QTL and candidate genes conferring resistances to Fusarium and Gibberella ear rots while reducing mycotoxin contamination in maize

Supplementary File 1: Information recorded on quantitative trait loci (QTL) reported by 15 SNP-based studies on resistance to Fusarium and Gibberella ear rots related traits in maize. QTL highlighted in grey were not included in the meta-analysis. Available online at: https://www.frontiersin.org/articles/10.3389/fpls.2022.1050891/full#supplementary-material

Supplementary File 3: Consensus map. Available online at: https://www.frontiersin.org/articles/10.3389/fpls.2022.1050891/full#supplementary-material

Supplementary File 4: Characterization of meta-QTL (MQTL) identified based on the 15 QTL mapping studies. CI = confidence interval, PVE = phenotypic variance explained, FER = Fusarium ear rot, GER = Gibberella ear rot, SR = silk resistance, KR = kernel resistance, DON = Deoxynivalenol accumulation, FUM = fuminosin accumulation, KDD = kernel dry-down rate, HC = husk coverage. Meta-QTL name referred to *Zea mays* abbreviated as *Zm*, followed by MQTL, the corresponding chromosome, and identification number on the chromosome. Available online at: https://www.frontiersin.org/articles/10.3389/fpls.2022.1050891/full#supplementary-material

Supplementary File 6: Candidate genes mined within major and most refined meta-QTL (MQTL). Available online at: https://www.frontiersin.org/articles/10.3389/fpls.2022.1050891/full#supplementary-material

Supplementary File 7: Expression level in transcripts per million (TPM) of differentially expressed candidate genes (CG) in two maize lines under control conditions and after infection with *Fusarium graminearum*. DAI = days after inoculation, FC = fold change. Available online at: https://www.frontiersin.org/articles/10.3389/fpls.2022.1050891/full#supplementary-material

Supplementary File 8: Annotation and ontology terms and functional category of differentially expressed candidate genes (CG) in both resistant (CO441) and susceptible (B37) lines within meta-QTL (MQTL). Available online at: https://www.frontiersin.org/articles/10.3389/fpls.2022.1050891/full#supplementary-material

Chapter 4: Effectiveness of introgression of resistance loci for Gibberella ear rot from two European flint landraces into adapted elite maize (*Zea mays* L.)

S1 Table: Best linear unbiased estimations (BLUEs) of Gibberella ear rot (GER) severity (back-transformed values, %), days to silking (DS, days), plant height (PH, cm), seed-set (SS, %), and plant vigor (PV) across environments. Doubled haploid (DH) populations were evaluated across two locations, while others lines were evaluated across four environments. Available online at: https://doi.org/10.1371/journal.pone.0292095.s001

Acknowledgements

As the saying goes, "*It takes a village to raise a scholar*." My sincere gratitude go to the countless individuals who have joined me on this academic journey, providing their unwavering support, guidance and encouragement at all time.

First, I would like to express my sincere gratitude to my supervisor apl. Prof. Dr. Thomas Miedaner. Thanks for accepting me as a PhD student and allowing me to join your research group. Thanks for your daily guidance, encouragement and support of all kind. Your attitude to science and attention to details inspired me a lot. You were always available whenever I came for questions and you explained everything patiently and provided new ideas and orientations. Your listening ears and optimism motivated and humbled me a lot. You are the best supervisor ever.

I would also like to thank my 2nd mentor Prof. Dr. Tobias Würschum. Thank you for your support and availability whenever I needed. I extend my gratitude to my 3rd mentor Prof. Dr. Hans-Peter Piepho. Thanks for your support and guidance regarding data analysis using appropriate statistical approaches. My PhD journey would not have been possible without your inputs. In addition, I thank you, Prof. Dr. Hans Peter Maurer for facilitating my work on the servers.

Also, thanks to the technical staffs from the LSA-Research group Rye and LSA-Research group Triticale. Especially, thanks to Silvia Koch, Bärbel Lieberherr, Heike Goßlau, Marlene Warsow, Christian Metzke, Thomas Grafe and Lore Handt for your invaluable support from the Lab to the field. Silvia Koch and Bärbel Lieberherr, I have learnt a lot from your patience, hard-working and high organizational skills for the successful implementation of field trials. Thank you, Heike Goßlau for your help with inoculum production. I also want to thank all the BSc and MSc students who helped me with field inoculation and data collection. Thank you, Sebastian Frank for your availability and assistance. I am grateful!

Thanks to all my colleagues from the State Plant Breeding Institute and the Institute of Plant Breeding. Thanks to Dr. Willmar L. Leiser, Dr. Patrick Thorwarth, Dr. Hans Peter Maurer, apl. Dr. Volker Hahn, Prof. Dr. C. Friedrich H. Longin, apl. Prof. Dr. Thomas Miedaner, Dr. Kim Steige, Prof. Tobias Würschum, Thomas Schmidt and Deter Schmidt. Thanks to Mrs. Kurka and Mrs. Kösling for helping me with administrative matters. Thank you to all PhD students, postdocs, and friends, Dr. Paul Gruner, Dr. Xintian Zhu, Dr. Muhammad Afzal, Dr. Khaoula

EL Hassouni, Dr. Ana Kodisch, Dr. Felix Jähne, Dr. Thea Mi Weiß, Cleo Döttinger, Sandra Roller, Carina Meyenberg, Niharika Rakasi, Che-Wei Chang, and Ali Baturaygil. The time with you was full of unforgettable memories. Thanks to my brother and friend, Dr. David Sewordor Gaikpa for your daily support and encouragement of all kind. You have made so many things easier for me. I am indebted to you!

At the Graduate Academy, I am indebted to Dr. Anja Pohl for her guidance and assistance with my registration and doctoral procedure. Thanks to you, Mrs Alexandra Hawlitschek and Gabriele Kuhn-Giovannini for your assistance and advice during the doctoral procedure. Thanks for always being available. I am grateful!

I express my sincere gratitude to Dr. Bettina Kessel and Dr. Thomas Presterl from KWS SAAT SE & Co. KGaA in Germany for your invaluable support towards the implementation of my research projects. Thanks to all the KWS technical staff in Gondelsheim for your availability and contribution to field trials. Thanks to Mrs. Dorothee Seyfang and Dr. Oyiga Benedict Chijioke for all your support. Your availability for my field trials helped me at lot.

My sincere gratitude to Deutscher Akademischer Austauschdienst (DAAD) for the financial support during my doctoral studies in Germany. Thanks to ST32 DAAD staff, particularly Mrs. Susanne Wohlleben and my contact person Mr. Alexander Thym for all your support.

I would also like to extend my gratitude to my scientific father, Prof. Dr. Enoch Achigan-Dako Head of the Laboratory of Genetics, Horticulture and Seed Science of the University of Abomey-Calavi, Benin. My scientific journey started back in 2014 with you. You are always there, providing support, advice and encouragement. Thanks for your unwavering belief in my potential. Without you, I would not have come this far. Thank you for always reminding me to keep the light on. I am grateful for everything Prof!

Last, but not least, I want to thank my family who supported and encouraged me a lot. Anyone who made this journey would know that family and close relatives are the ones who endured the most. Thanks to you Mom and Dad. I am grateful to my wife, Eunice Awoudo for always supporting and understanding me all the time. Thanks to my brothers, Hervé and Samuel for your support of all kind. May God bless us!

Curriculum vitae

Name:	Félicien Akohoue
Date and place of birth:	01st January 1992 in Kemondji, Benin

Education

10/2020 – Present:	Doctor of Philosophy, Option: Plant Breeding State Plant Breeding Institute (720), University of Hohenheim, Stuttgart, Germany
02/2018 – 04/2019:	Master of Science, Option: Plant Breeding School of Agricultural, Earth and Environmental Sciences, University of KwaZulu-Natal, South Africa
12/2015 – 12/2016:	Master of Science, Option: Crop Science Faculty of Agronomic Sciences, University of Abomey-Calavi, Benin
12/2011 – 01/2015:	Bachelor of Science, Option: Crop Science Faculty of Agronomic Sciences, University of Abomey-Calavi, Benin

Work Experience

02/2020 – Present:	Doctoral Researcher on maize and wheat Rye research group, State Plant Breeding Institute (720), University of Hohenheim, Stuttgart, Germany
02/2019 – 12/2020:	Project Manager: Amplification of agro-ecological transition (AGRO-ECO) R&D project involving the University of Abomey-Calavi (Benin), University Nazi Boni (Burkina Faso), Catholic University of Louvain (Belgium), University of Liège (Belgium) and six farmers and non-governmental organizations based in Burkina Faso and Benin

12/2016 – 01/2019:	Research Associate Laboratory of Genetics, Horticulture and Seed Science (http://gbios-uac.org/), University of Abomey-Calavi, Benin.
02/2016 – 07/2016:	Assistant Teacher, Crop Science Agricultural High School of Medji, Ministry of Secondary and Technical Schools, and Professional training, Benin
02/2015 – 12/2016:	Field Technician Laboratory of Genetics, Horticulture and Seed Science (http://gbios-uac.org/), University of Abomey-Calavi, Benin

Conference

04/2022:	Conference on "Advances in disease control and resistance breeding of agricultural crops". April 11-12th 2022. Fulda, Germany
10/2019:	Maiden Conference of the African Plant Breeders Association, October 23-25th, 2019. University of Ghana, Accra. One oral presentation.
09/2019:	Seventh Colloquium of Sciences, Technologies and Cultures: Oral presentation, September 16-21st, 2019. University of Abomey-Calavi, Benin. Two oral presentations.
09/2017:	Sixth Colloquium of Sciences, Technologies and Cultures: Oral presentation, September 25-30th, 2017. University of Abomey-Calavi, Benin. One oral presentation.

Fellowships, Grants

2020:	Deutscher Akademischer Austaschdienst (DAAD) Doctoral Programm scholarship for my doctoral studies at the University of Hohenheim, Germany

2017:	Intra Africa Mobility MSc scholarship (Enhancing training and research mobility for novel crops breeding in Africa (MoBreed, www.mobreed.com), University of KwaZulu-Natal, South Africa
2017:	BecA-ILRI, Integrated Genomic Service and Support (IGSS) research grant, Biosciences Eastern and Central Africa (BecA), International Livestock Research Institute (ILRI), Nairobi, Kenya
2014:	New Alliance Trust Ltd. Small research grant for my Bachelor's research activities
2011:	Benin Government scholarship for Bachelor studies at the University of Abomey-Calavi

Hohenheim, 13th May 2023

Félicien Akohoue

Annex 3

Declaration in lieu of an oath on independent work

according to Sec. 18(3) sentence 5 of the University of Hohenheim's Doctoral Regulations for the Faculties of Agricultural Sciences, Natural Sciences, and Business, Economics and Social Sciences

1. The dissertation submitted on the topic

Improving host resistance to Fusarium head blight in wheat (Triticum aestivum L.) and Gibberella ear rot in maize (Zea mays L.)

is work done independently by me.

2. I only used the sources and aids listed and did not make use of any impermissible assistance from third parties. In particular, I marked all content taken word-for-word or paraphrased from other works.

3. I did not use the assistance of a commercial doctoral placement or advising agency.

4. I am aware of the importance of the declaration in lieu of oath and the criminal consequences of false or incomplete declarations in lieu of oath.

I confirm that the declaration above is correct. I declare in lieu of oath that I have declared only the truth to the best of my knowledge and have not omitted anything.

Hohenheim, 19 May 2023

Place, Date

Signature